KWAME NKRUMAH UNIVERSITY OF SCIENCE AND TECHNOLOGY, KUMASI, GHANA

ASSESSMENT OF URBAN GROWTH EFFECT ON THE FORMATION AND INTENSIFICATION OF URBAN HEAT ISLANDS IN SEKONDI-TAKORADI METROPOLIS OF GHANA

BY

ERNEST BINEY

(MPHIL. GEOGRAPHIC INFORMATION SYSTEMS)

A THESIS SUBMITTED TO THE DEPARTMENT OF CIVIL ENGINEERING, COLLEGE OF ENGINEERING

IN PARTIAL FULFILLMENT OF THE REQUIREMENTS OF THE DEGREE OF

DOCTOR OF PHILOSOPHY

IN

CLIMATE CHANGE AND LAND USE

October, 2024

DECLARATION

I, Ernest Biney hereby declare that this Ph.D. thesis is my work, and to the best of my knowledge, it contains no material previously published by another nor material that has been accepted for the award of any other degree of the university except where due acknowledgment has been made.

Ernest Biney

…….. ……..……...

(PG6992921) Signature Date

Certified by:

Prof. Eric K. Forkuo

…….. ……..……...

(Supervisor) Signature Date

Prof. Michael Poku-Boansi

…..……... ...……..……...

(Supervisor) Signature Date

Prof. Richard Akwasi Buamah

..……..... ..…….....

(Head of Department) Signature Date

ABSTRACT

The prevalence of industries as well as the presence of the harbour and airport, and the upsurge in economic activities due to the oil discovery have made Sekondi-Takoradi one of the preferred cities for many people and migrants. As a result, the number of urban dwellers has increased, and this by effect, has been met by an increasing transformation of the land use land cover (LULC) into built-up, sprawl-like growth and a direct influence on temperature rise. Previous studies have not established enough evidence on land use and land cover changes in the metropolis and the influence of urban growth on the development of urban heat islands (UHIs) in the metropolis remains understudied. For this reason, this study assessed the effect of urban growth on the formation and intensification of urban heat islands in Sekondi-Takoradi. Multi-source datasets such as remote sensing data (Landsat images), referenced data, and vector data served as the basis for evaluating the spatiotemporal dynamics of land use and land cover, urban sprawl, and urban heat island within the metropolis. The supervised random forest technique was utilized to map the land cover changes whereas Geospatial techniques and spatial metrics such as Annual Urban Expansion Rate (AEUR), Urban Expansion Intensity Index (UEII), Landscape metrics, Shannon, and relative entropy were used to evaluate the spatio-temporal pattern of urban growth in the Sekondi-Takoradi metropolis. Furthermore, the spectral indices, elevation, some proximity factors, land surface temperature (LST), and urban thermal field variance index (UTFVI) were used to analyze the development of urban heat Islands and its intensification by urban growth or urban expansion as well as investigate temperature variations across the metropolis. Results from the changes in land use land cover showed a substantial increase in built-up by 63.08 km^2 (32.91%) and a decrease in vegetation and water by 60.99 km^2 (31.82%) and 2.08 km^2 (1.09%) respectively. Projections for 2030 indicate further changes with water areas decreasing to 1.21 km2 (0.63 %), vegetation diminishing to 95.31 km^2 (49.73 %), and built-up areas expanding to 95.14 km^2 (49.64 %). This shows the rate at which the metropolis is becoming urbanized and raises concern about the adverse effects the metropolis may experience if urban expansion is not properly monitored and controlled. Also, the urban expansion analysis, specifically, the urban intensity index revealed that the metropolis expanded from a slow speed (0.34) to a very high speed (2.58), highlighting the high susceptibility of the area to experiencing urban sprawl. The presence of sprawling characteristics was confirmed throughout the application of landscape metrics which revealed a greater degree of fragmentation in the landscape. Additionally, the results from Shannon and

relative entropy computations, which respectively ranged from 2.17 to 2.47 and 0.76 to 0.87 revealed that the metropolis has been sprawling throughout the study period and this would cause significant changes in the land cover composition of the metropolis and potentially impede the achievement of Sustainable Development Goal 11. Unfortunately, the effect of this dramatic land use change and urban sprawl led to a 3.1°C rise in mean LST and a 19.38 km^2 expansion of areas affected by the UHI effect. The UTFVI analysis further indicated a 33.63 km^2 increase in the worst ecological zone due to the temperature rise. Statistical analysis between LST, NDVI, NDWI, and NDBI revealed significant variability in explaining the intensity of LST and UHI in the metropolis over the study period. In addition to the spectral indices, elevation, and proximity factors significantly contributed to the temperature variation across the study area. Hence, provided valuable insight into the intensification of LST and UHI in the metropolis. This study equips city authorities and urban planners with the fundamental knowledge needed to prepare a sustainable development plan that alleviates adverse effects of urban growth and elevated temperature-related issues. Also, the findings contribute to global efforts to promote more livable and climate-resilient urban environments and highlight the significance of spatial modeling in environmental management and urban planning. Lastly, the combined use of remote sensing, GIS, and other supplementary datasets has proven to be efficient for evaluating the impact of urban growth on the formation and intensification of urban heat islands.

Keywords: Urban growth, Sekondi-Takoradi; Landsat images,; Shannon and relative entropy, Land use and land cover; Random Forest; Spectral Indices; Urban Thermal Field Variance Index (UTFVI); Land Surface Temperature (LST); Urban Heat Island (UHI); Spatial Factors

TABLE OF CONTENT

LIST OF TABLES

LIST OF FIGURES

LIST OF ACRONYMS AND ABBREVIATIONS

AEUR	Annual Urban Expansion Rate
AIC	Akaike Information Criterion
ASTER	Advanced Spaceborne Thermal Emission and Reflection Radiometer
AVHRR	Advanced Very High Resolution Radiometer
CBD	Central Business District
DEM	Digital Elevation Model
EEI	Ecological Evaluation Index
ETM	Enhanced Thematic Mapper
FAO	Food and Agricultural Organization
FCC	False Colour Combination
GIS	Geographic Information Systems
GPHA	Ghana Port and Harbour Authority
GPS	Global Positioning System
GWR	Geographically Weighted Regression
IPCC	Intergovernmental Panel on Climate Change
LPI	Largest Patch Index
LST	Land Surface Temperature
LUC	Land Use Cover
LULC	Land use land cover
LULCC	Land Use Land Cover Chanage
MC	Markov Chain
MIR	Mid-Infrared
MNDWI	Modified Normalized Difference Water Index
MODIS	Moderate Resolution Imaging Spectroradiometer
MOLUSCE	Modules for Land Use Change Evaluation
NDBI	Normalized Difference Built-up Index
NDBI	Normalized Difference Built-up Index
NDVI	Normalized Difference Vegetation Index
NIR	Near Infrared
NP	Number of Patch
OA	Overall Accuracy
OLS	Ordinary Least Square
PD	Patch Density
PHC	Population and Housing Census
QGIS	Quantum Geographic Information System
RF	Random Forest
SCP	Semi-automatic classification plugin
SDG	Sustainable Development Goal
SLC	Scan Line Corrector
STMA	Sekondi Takoradi Metropolis Assembly

SUHI	Surface Urban Heat Island
SVM	Support Vector Machine
TIRS	Thermal Infrared Sensor
TLA	Total Land Area
UEII	Urban Expansion Intensity index
UHI	Urban Heat Island
UNICEF	United Nations International Children's Emergency Fund.
USGS	United States Geological Survey
UTFVI	Urban Thermal Field Variance Intensity
UTM	Universal Transverse Mercator
VIF	Variance Inflation Factor
WHO	World Health Organization
WUDAPT	World Urban Database and Access Portal Tool

ACKNOWLEDGMENT

First and foremost, I would like to express my profound gratitude to the Almighty God whose Grace and Mercies have seen me through this programme. I am also grateful to my supervisory team, Prof. Eric K. Forkuo, Prof. Michael Poku-Boansi, Dr. Kwame O. Hackman, Dr. Michael Thiel, Dr. Yaw Mensah Asare, for their constructive feedback, suggestions, continuous guidance, encouragement, and invaluable insights throughout my research. Their input and expertise have significantly enhanced the quality of this research and brought it to completion.

My sincere thanks go to my colleagues and friends, whose discussions, advice, and moral support have been a source of strength during this journey. A special thank you to Daniel Buston Yankey, Albert Elikplim Agbenorhevi, Honeygift Nimako, and Ernestina Annan, for always being available to help me navigate through challenging times. I would also like to acknowledge the Federal Ministry of Education and Research (BMBF) and the West African Science Centre on Climate Change and Adapted Land Use (WASCAL)-KNUST for providing me with the resources, facilities, and a conducive environment for research. My appreciation extends to the administrative and technical staff, whose assistance was greatly appreciated. To my family, I owe an immeasurable debt of gratitude for their unconditional love, patience, and support throughout this process. To my parents and uncle, Madam Agnes Harris, Mr. Dominic Biney, and Mr. Justice Harris, thank you for always believing in me. Lastly, I dedicate this thesis to my siblings Mary Biney, Charlotte Biney, Dominic Biney, and Agnes Harris, whose inspiration and encouragement have motivated me to achieve this milestone.

CHAPTER 1: GENERAL INTRODUCTION

1.1 Background

Urban growth is a complex and evolving phenomenon typically characterized by changes in population, societal structures, governance, and economic development. Viana et al. (2019), defines urban growth as the expansion of areas covered by urban development. Urban growth is closely connected to changes in the landscape, but, urban growth pertains specifically to the increase in the size of urban regions, while landscape transformation involves multiple forms of fragmentation, including the diminishment of non-urban areas. This makes Anande & Park (2021), assert that urban growth should be understood both as a pattern, representing the spatial arrangement of an urban area at a specific point in time, and as a process, reflecting how the spatial organization of urban areas evolves (Ankrah et al., 2024). The term urban sprawl is also often used interchangeably with urban growth, despite having conceptual meanings (Amponsah et al., 2022). Urban growth resulting from unregulated or haphazard development is referred to as urban sprawl. This phenomenon is often viewed negatively, as it tends to exacerbate various urban challenges including land degradation, water and air pollution, all of which have detrimental effects on human health (Viana et al., 2019).

One potential approach to facilitating urban growth is by urban expansion or urban extension, therefore, a sharp rise in urban population drives the swift expansion of urban areas (Rana & Sarkar, 2021) and this massively affects the environment, especially, in the case of unplanned urbanization. Unregulated and accelerated urban development worldwide has led to significant alterations in environmental ecological processes, heightening the susceptibility of urban regions to environmental challenges (Afriyanie et al., 2018**)**. As a result of rapid urban growth most cities experience population increase pressure which causes urban sprawl (Rana & Sarkar, 2021**).** According to Shao et al. (2021), one of the main causes of the excessive rate of urban sprawl is the global increase in urban population. The global urban population has increased from 1 billion in 1960 to 4.4 billion in 2020 (United Nations, 2020). Currently, more than 55% of people on Earth reside in cities, and estimates indicate that by 2050, this percentage will rise to 68% (Klein & Anderegg, 2021). This projected urban growth rate is anticipated to be significantly greater in developing nations compared to developed nations and raises concerns about sustainable development, especially in the era of climate change (Anande & Park, 2021; Satterthwaite et al.,

2020). In Africa, over half of the urban population resides in low-lying coastal regions (Nieves et al., 2020), and between 2000 and 2030, population growth in developing nations is projected to double whereas urban areas are expected to triple.

In Ghana, the increasing growth in population coupled with unplanned developmental activities has resulted in urbanization with poor urban planning. Ghana's population in the year 1957 was 6 million and it increased to 18 million in the year 1996 (Ghana Statistical Service, 2014). In the year 2010, Ghana's population increased a little above 24 million and the number of urban dwellers also doubled (Ghana Statistical Service, 2021). The alarming rate of population growth, especially in the major cities in Ghana calls for an increase in the demand for land for urban dwellers. Unfortunately, this growth is not commensurate with its urban planning and land demand in the cities. As a result, people turn to settle in the outlying areas or boundaries of the major cities where basic facilities are not available. Ablo et al. (2020), opines that an increase in urban population brings changes that improve society. However, a society's improvement depends on good management of available land resources because land is an essential resource that aids in the sustenance of man; therefore, it is important to ensure that proper regulations apply to the use of land.

Recently, the structures of major cities in Ghana are changing rapidly and this stems from the changes in the urban environment caused by the high rate of urbanization. The increasing transformation in urban trends directly affects urban land use and this also changes the land use pattern of urban areas (Abass et al., 2020). Moreover, land tenure system and uncontrolled physical development are partly causing land use change in Ghana (Doe et al., 2022). Congestion and unlawful settlements, for instance, negatively alter the development of urban areas. The recent threatening trend of development in cities like Accra, Kumasi, and Sekondi-Takoradi, for instance, calls for a review of the land tenure system especially with the framework used (Asibey, et al., 2023). Over the past three decades, Sekondi-Takoradi has had an increase in its urban population (Ghana Statistical Service, 2021; Ghana Statistical Service, 2014). The growth in its population has led to changes in its land use as well as increased economic development. In the bid to provide land for the growing population, many vegetative lands are disappearing to be converted into urban uses. Lands that were previously overlaid with vegetation are now being turned into roads and buildings.

The World Health Organization (WHO), in 1961, introduced four fundamental principles for the living environment: safety, health, convenience, and comfort. However, the safety component is now mostly threatened by climate change, especially with extreme climate change. This is making many countries pay attention to the safety and health of the human environment (Ding et al., 2021). Regrettably, the growth of urban areas presents numerous challenges, such as rising air pollution, unmanaged urban sprawl, and the demand for greater efficiency in transportation, fuel, and energy use. Simultaneously, the urban landscape would undergo drastic transformation to accommodate the increasing population, hence, increasing the vulnerability of people to adverse climate change impacts (Anande & Park, 2021). Although urban centers serve as hubs for socio-economic development, the land use processes cause most urban centers to be susceptible to environmental disasters (Liu et al., 2020).

Studies have shown that urban growth brings about higher temperatures in urban areas than in the surrounding rural areas (Abass et al., 2020), a phenomenon known as the urban heat island (UHI) effect. This arises primarily from land cover changes, where natural vegetative areas are replaced by built-up and impervious surfaces (Borges et al., 2022). The increase in built-up, for instance, reduces vegetation cover and adds more impervious and heat-absorbing surfaces which trap more heat thereby raising the temperature in urban areas and making it warmer than its rural surroundings (Surawar & Kotharkar, 2017). A key indicator of the urban heat island effect is the Land Surface Temperature (LST) and it is defined as the radiative temperature of the Earth's surface, measured from the perspective of the remote sensor. The effects of the Urban Heat Island (UHI) phenomenon encompass Dehydration, mortality (heat stroke), increased energy demand, higher levels of pollution, high emission of carbon monoxide, formation of harmful smog, etc. (Afriyanie et al., 2018**)**. The trend of urbanization and the creation of UHI may also be connected to the increased extremes of rainfall in recent decades (Lima et al., 2018). The Intergovernmental Panel on Climate Change (IPCC) Fifth Assessment Report highlights that the rise in greenhouse gas concentrations will result in various climate-related impacts. Unfortunately, urban centers majorly produce these greenhouse gases due to rapid urbanization. In West Africa, the key effects are increased temperatures, sea level rise, and altered precipitation patterns (Ilori & Ajayi, 2020). The rise in temperature contributes to sea level elevation through the melting of polar ice caps and thermal expansion, making coastal regions in West African cities particularly susceptible to the adverse effects of climate change (Salimi & Al-ghamdi, 2020). Climate change denotes the

alteration of global and regional climate systems, especially evident from the mid-20th century onwards, primarily driven by increased carbon dioxide levels from fossil fuel consumption (Salimi & Al-ghamdi, 2020). Urban growth significantly influences climate change and climate change also affects urban areas (Hasan et al., 2019). Over the years, the intricate interplay between human activities and the environment has prompted urban centers to adopt comprehensive sustainable development strategies aimed at addressing the impacts of urban heat island warming and urban growth effect. This issue has emerged as a critical concern requiring coordinated efforts from policymakers and interdisciplinary experts to equip cities for future challenges. According to projections by the Intergovernmental Panel on Climate Change (IPCC), climate change is intensifying in both frequency and severity, underscoring the urgency for action (Birkmann et al., 2022; Hasan et al., 2019).

The urban environment can be accurately mapped and examined using remote sensing (RS) and geographic information systems (GIS) (Hasan et al.,2023; Rana & Sarkar 2021). The integration of RS and GIS in detecting urban land use change has widely proven to be an effective tool (Dhanaraj & Angadi, 2022). Satellite, which is a remote sensing tool, for instance, can amass multi-temporal data which can be processed into useful information for monitoring urban land changes and growth. On the other hand, GIS provides a convenient way for inputting, manipulating, analyzing, and showing spatially digital data from several sources that are useful for monitoring and assessing the pattern and impact of urban growth over different periods. Pramanik & Punia (2020), used satellite images to assess changes in the city of Delhi. From their research, information from satellites was found to be efficiently useful for urban development and sustainable environment. Sarif & Gupta (2021), used GIS to examine urban sprawl and land cover changes in Udupi Mangalore. Moreover, mapping urban growth helps to show where land development is occurring, identifies where the natural resources are being threatened by the growth, and helps to predict the pattern of urban growth (Sarif & Gupta, 2021; Shikary and Rudra 2020). According to Sumari et al. (2020), effective assessment of urban growth can be done via the combined application of geospatial techniques and spatial metrics. This makes RS and GIS effective for detecting and analyzing urban growth (Al-Kafy et al., 2020). Additionally, RS and GIS have played a crucial role in determining the thermal variation influenced by urban growth (Jahan & Rahman, 2021).

1.2 Problem Statement

Sekondi-Takoradi serves as a major economic and political center for both the Western Region and the nation. A report by the Sekondi-Takoradi Metropolitan Assembly (STMA) shows that the metropolis is experiencing a sharp rise increase in socioeconomic activities with several infrastructural projects taking place in the hospitality, health, residential, commercial, industrial, and educational sectors of the city (Mensah et al., 2019; STMA, 2022). This increase became phenomenal in 2010 after the discovery of oil in commercial quantities in Ghana where Sekondi-Takoradi is the closest major city to the oil field (Mensah et al., 2018). For instance, in 2000, the metropolis had a population of about 360,000. Following the discovery and commercial exploitation of oil in 2010, the population grew to about 560,000. By 2017, it had increased to 700,000, with a growth rate of 3.2%, surpassing the national growth of 2.7% (Ghana Statistical Service, 2021; Service, 2014). Within that same year, the completion of the Takoradi Port expansion converted about 60,000 hectares of arable or vegetative lands into impervious surfaces (GPHA, 2016). In 2020, the spatial development unit of the metropolis highlighted a significant transformation in the physical landscape due to the pressure on land for development caused by the rising population (Mensah et al., 2019; STMA, 2022). These changes impact the city's sustainability and contribute to environmental problems such as Urban Heat Island.

According to Aduah & Baffoe (2013), if changes in urban areas are not properly handled, they can result in many social, economic, and environmental tragedies like loss of biodiversity, congestion, pollution, flooding, landslides, heat waves, drought, and low crop yield, and difficulty in getting safe water which destruct the sustainable development of urban lands. Since the establishment of the Sekondi-Takoradi harbour, the metropolis has been a business hub for major local, national, and international organizations. Therefore, any disaster in Sekondi-Takoradi will have a roll-over effect on the national economy and to some extent the global economy. For instance, the increase in temperature in Central Europe led to a loss of 45 billion work hours in 2018. This affected the economy of central Europe as productivity was significantly affected (Filho et al., 2021). Research work by Dankwa (2018), over the southern part of Ghana suggests that the coastal part of Ghana is becoming warmer compared with the north. The study further revealed that surface temperature will continue to rise by the end of the mid-21st century in the major cities in Ghana. This development will put the major cities at risk of experiencing environmental problems like urban heat islands and so needs to be addressed (Mensah et al., 2019). It is against this background that

this research aims to assess the effect of urban growth on the intensification of urban heat islands in the Sekondi-Takoradi metropolis.

1.3 Knowledge Gap

First, Landsat images have been used in land use land cover studies of the metropolis (Kumi-Boateng et al., 2015; Aduah & Baffoe, 2013). Unfortunately, previous studies extensively concentrated on the application of parametric classifiers mostly the maximum likelihood classifier (Aduah & Baffoe, 2013; Kumi-Boateng et al., 2015; Mensah et al., 2018). This study addresses the existing knowledge gap and enhances the scientific contributions to the literature by employing a machine learning technique, specifically the random forests classifier, for satellite image classification.

Second, previous studies on urban growth in Sekondi-Takoradi have not examined the direction-wise urban growth pattern. This is crucial in comprehending the local causative growth factors of the metropolis and also captures the different characteristics of urban growth since urban expansion does not occur uniformly in all directions of a city (Roy & Kasemi, 2022). Third, to the best of the researcher's knowledge, the only study on urban heat islands carried out in the Sekondi-Takoradi metropolis was conducted by Kumi-Bsoateng & Stemn, (2015). Unfortunately, the analysis only spanned a brief period of 17 (1991-2008), satellite data was limited to only Landsat 5 and 7, and lacked information on the extent, intensity, and magnitude of UHI which is covered extensively in this study. Also, using the urban thermal field variance index (UTFVI) to measure the thermal comfort level of the metropolis was not addressed in the works of Kumi-Boateng & Stemn, (2015). Even taking Ghana as a whole, less attention has been given to the application of UTFVI in UHI studies.

Also, the interplay of various spatial influencing factors results in distinct thermal patterns and archetypes within the urban environment. Unfortunately, previous studies, especially in Ghana and within the study area have focused only on how land cover affects LST and UHIs (Buo et al., 2021; Frimpong et al., 2023; Kursah, 2023; Osei et al., 2023; Stemn & Kumi, 2020). No studies have been conducted on the spatial influencing factors of LST such as proximity to roads, waterbodies, Central business district (CBD), digital elevation model (DEM) as well as land use land cover, and spectral indices effects on LST and UHI. Therefore, this study addresses the research gap by incorporating UTFVI to analyze UHI and provides information on the extent, intensity, and

magnitude of UHI which is lacking. It also investigates the significant differences in surface temperature potentially influenced by the spatial factors within the different archetypes of the study area—a dimension often overlooked in previous research.

This study addresses the research gap by incorporating UTFVI to analyze UHI and provides information on the extent, intensity, and magnitude of UHI which is lacking. Fourth, NDVI was the only spectral indices utilized in the study of LST by Kumi-Boateng & Stemn, (2015) and they did not employ Ordinary Least Squares (OLS) regression or Geographically Weighted Regression (GWR) to model the relationship between LST, NDVI, and NDBI, a limitation consistent with earlier research. This research addresses this gap by incorporating both OLS and GWR to establish the relationships among LST, NDVI, and NDBI. This approach is innovative within the existing literature, particularly in the context of Ghana and specifically in the Sekondi-Takoradi metropolis.

1.4 Research Objectives

This study aims to assess the effect of urban growth on the formation and intensification of heat islands in the Sekondi-Takoradi metropolis. Specifically, the research seeks to:

1. To determine the spatio-temporal dynamics of land use land cover in the metropolis and forecast future trends of LULC.
2. To quantify the intensity of urban expansion and its degree of dispersion and compaction over the study period.
3. To examine the influence of urban growth on urban heat islands in the metropolis.

1.5 Research Questions

1. What are the spatio-temporal dynamics of land use and land cover in the metropolis, and how can future trends of LULC be forecasted?
2. What is the intensity of urban expansion and the degree of dispersion and compaction over the study period?
3. How has urban growth influenced the urban heat island warming within the metropolis from 1991 to 2023?

1.6 Significance of the study

Studies on urban growth are always critical to the globe irrespective of their spatial scale due to the impact it has on the environment. In developing countries where urbanization and

vulnerabilities to adverse effects of urban growth such as urban heat islands are increasing, there is limited literature on studies based on the effect of urban growth especially on the formation and intensification of urban heat islands, due to the constraints of data availability, research, and technological capacities. Therefore, in many urban centers, the question of formation and intensification of heat islands to the dynamics of urban growth is not adequately answered. Urban growth has significant ecological, social, and economic ramifications. According to Taloor et al. (2024), urban growth brings about deforestation, changes in hydrological patterns, and biodiversity loss. These changes also have repercussions for human health, economic activities, and susceptibility to natural disasters, underscoring the complex relationship between urban growth and sustainability. Identifying and effectively managing these implications is crucial for informed land management policies, which aim to strike a balance between development and environmental protection.

With evidence showing that climate extremes will increase in the future, it is essential to analyze changes in urban space in Ghana (Danso et al., 2020; Kendon et al., 2019). This need becomes more pressing especially when one considers that Sekondi-Takoradi is witnessing rapid growth and urbanization, which will continue to increase in future years. Though challenges of urban growth keep increasing in Ghana, most empirical studies are directed at addressing problems in the national capital, Accra, and little has been done on the assessment of urban growth effect in the metropolis using geospatial techniques. For instance, the Central Business District of the Sekondi-Takoradi Metropolis has become congested with no open vegetation space making it susceptible to severe thermal conditions. Therefore, research on the metropolis is timely as it brings to the fore the effects of urban growth and contributes to the increasing understanding of the causal relationship between urban growth and urban heat island effect. It contributes valuable knowledge to urban planners and policymakers in dealing effectively with the challenges of urban growth and heat islands. Serving as a valuable reference for policymakers and stakeholders, the research supports effective spatial planning, management practices, and future land utilization in the metropolis. The outcome of this study is poised to advance existing knowledge and contribute to the growth and development of urban areas not only in Ghana but also in other developing cities across the tropics.

1.7 Structure of the thesis report

The research is structured into seven chapters. Chapter one focuses on the background of the study, the problem statement, research objectives and questions, the knowledge gap, the significance of the study, and the organization of the study. Chapter two provides a comprehensive literature review pertinent to the research, structured around key thematic areas and sectioned into relevant themes. Chapters three, four, and five address the study's three main research objectives, each written in manuscript format. Chapter six presents a general discussion of the entire study, while chapter seven provides the conclusions and recommendations of the study.

CHAPTER 2: LITERATURE REVIEW

2.1 Introduction

This chapter provides a review of the contextual arguments and analysis of the pertinent literature on urban growth, land use land cover, geospatial techniques, and urban heat islands to aid in the comprehension of the assessment of urban growth effect on the formation and intensification of urban heat islands in the Sekondi-Takoradi Metropolis of Ghana. For analytical ease, this chapter is structured under broad and sub-headings and has been done from a global perspective to a local perspective.

2.2 Urban

From the Latin word "urbs" comes the word urban; the term urban is mostly used interchangeably to refer to a city or town without a proper distinction between a city and a town (Cobbinah and Amoako, 2014). This is because the demographic and geographical definition for classifying a place as a city or a town differs across the world. For instance, Denmark and Sweden consider a settlement of more than 200 people as a town, while Australia and Canada use a minimum of 1,000 people to refer to as a town. In the case of a city, France and Israel consider a minimum population of 15,000 as a city. In contrast, USA and Mexico have set a minimum of 2,500 people compared to Japan which states that cities should have at least 30,000 people. A town may have characteristics of a city but the population and size will be smaller than a city. Towns are not densely populated and have less diversity of ethnicities. Conversely, a city is an area with dense settlements over a larger geographical location and with high population density. In cities, there are diverse people of different languages, religion, and race and their economies are bigger than towns (World Atlas, 2019).

According to (UNICEF, 2012) the definition of "Urban" differs from one country to another and this makes direct comparison and having a general definition difficult. Defining urban areas is mostly agreed on by governments at the national level. Countries with a lower population may call some towns urban irrespective of the population (Mathur, 2019). For instance, in Albania, towns and other industrial centres with a population of more than 400 are termed urban while in Germany, communes with a population density higher than or equal to 150 people per square kilometer are also termed urban areas. In the Netherlands, towns with 20000 or more inhabitants are classified as urban areas. In Finland, settlements with more than 200 population, where houses are distanced

by 200m are term urban (Dijkstra et al., 2022). With this background of disparities, the United Nations (UN) therefore, proposes a national-level definition for setting urban areas rather than standardized ones (Patterson et al, 2017; Dijkstra et al., 2022). However, the setting up of urban areas consists of several elements that should be adapted and applied (Norell, 2017). According to UNICEF, (2012), the following criteria should be considered when defining urban areas: administrative or political criteria, the size of the population, economic function, population density, and the availability of urban features (Othow, 2017). The World Vision (2016), asserts that in a wider manner, urban areas can be defined based on population density, concentration of administrative and infrastructures, and various forms of livelihood and income creation activities. Therefore, if an area has some of these features, it can be regarded as urban. In most cases, urban places have a population density higher than rural centers and they are delineated by municipal boundaries and administrative structures.

In Ghana, an urban area is any settlement that has a population of five thousand or more population (Ghana Statistical Service, 2014). Although the statistical definition makes it easier to determine which areas in Ghana can be grouped as urban, its simplistic nature does not provide an excellent basis for comparison because two localities with the same population size may be engaged in different types of socio-economic activities (Ghana Statistical Service, 2014). Perhaps it is as a result of this weakness that some countries do not use population size alone to determine their urban localities. Economic activity mainly engaged in by the majority of the population is considered a factor when classifying urban localities. For instance, where the majority of the required population size is involved in secondary economic functions, it can be termed as urban. The function each settlement performs could be used as a basis for urban classification. Settlements whose function is mainly non-agricultural could be considered as urban while the settlement that operates largely as agricultural economies could be presumed as rural. The availability of basic social facilities or amenities such as health facilities, energy, and educational facilities are also important in the classification of localities as urban. Amanfu (2017) asserts that urban areas are towns whose areas are densely settled into their fringes. In urban areas, there is the provision of high-order services with its populace largely engaged in commercial and industrial services. Based on the view of Tamakloe (2017) and Ghana Statistical Service, (2021), the Sekondi-Takoradi metropolis can be classified as urban.

2.3 Urban Theory and Modelling

In describing the growth pattern of cities and land use, different models have been developed to explain urban development and changes in land use. According to Asamoah (2010), many of the urban models were designed to show the growth pattern of land in the early industrial cities of the developed countries. The generalized nature of these models makes them less accurate in describing land use patterns in all cities. It has been criticized that most of these models are suitable for cities in the United States of America than for cities in other nations, especially in developing countries (Danso-Wiredu, 2020). Again, the models are being criticized for their static nature and their failure for not describing the process by which changes occur in the land use (Kora et al., 2024). However, the generalized explanation of the models provides a useful understanding of how land is used within the city. Below is an explanation of the Concentric Zone Model, Sector Model Multiple Nuclei Model, and Exploitative model of urban land use.

2.3.1 Concentric Zone Model

This model was put forward by Ernest Burgess to explain the growth and structure of a city. The theory hypothesized that cities evolve and expand concentrically by grouping functional zones of the city's land use into a series of land use rings centered on the Central Business District (CBD) (Danso-Wiredu, 2020). When a city is growing, it expands from the center to the overlying areas. Expansion of cities creates interaction among people in terms of economic, social, and political organization and these bring a rapid outward expansion from the concentric zone. Chicago is an example of this concentric zone model and in Ghana, Sunyani is a perfect example of a concentric zone model.

With the concentric zone model, there are five concentric zones. These are Commercial Center, Zone of Transition, Working Class Residence, Middle- or Higher-Class Residence, and Commuter zone (Mohammed et al, 2014; Danso-Wiredu, 2020). Commercial Center, is found in the middle part of the city and is the innermost ring of the concentric zone model. This zone is characterized by a lot of economic, commercial, civic, and social activities. Also, being the center of economic activities makes its accessibility possible from various directions and attracts a large number of people. The thorough use of land and the influx of people and businesses at the commercial center make the demand for land or rent higher. This explains how expansion begins to spread from the core to the outer zone. The second zone which is the zone of transition is mostly occupied by slums

and some industries. This zone is characterized by low-income households, rough neighborhoods, and other social deviances (Mohammed et al, 2014). The third type of zone is the working class. It is close to places of economic activities that mostly extend into the outward rings. The nearness of this zone to the transition zone influences the quality of life by reflecting the adverse effect of industrial pollution and cultural impact of slums on this zone. Middle- or higher-class residence occupies the outer rings of the working class and this is the fourth zone of the concentric zone model. It is also called the residential zone. Health facilities, sanitation, proper transportation, and better facilities and features of quality of life are found in the residential zone, but there is a high commuting cost attached to these facilities (Kowalczyk, 2020). On the further side of the residential zone or high-class residence is the fifth zone called the Commuter zone. This zone encompasses small towns, villages, and cities where people daily travel to the commercial centers for reason of employment but they reside in little towns and villages. Commuter zone is found in suburbs and satellite towns (Mohammed et al, 2014).

Burgess' concentric zone model in the early years provided a good explanation of the internal structure and a guide to the understanding of the pattern of city development. However, the model is mostly centered on Chicago cities and cities of North America and it has no explanation for the growth of cities in the developing countries. In light of this, Homer Hoyt asserts that cities do not grow in a complete circle; they are mostly distorted by topographic features and major transport. Again, the model did not take into consideration the endogenous forces that affect the structural growth of a city, but based its assumption on only invasion and succession (Shun et al., 2020). Also, the concentric model has been criticized for the assumption that the more the income the distant a household may be located from the center.

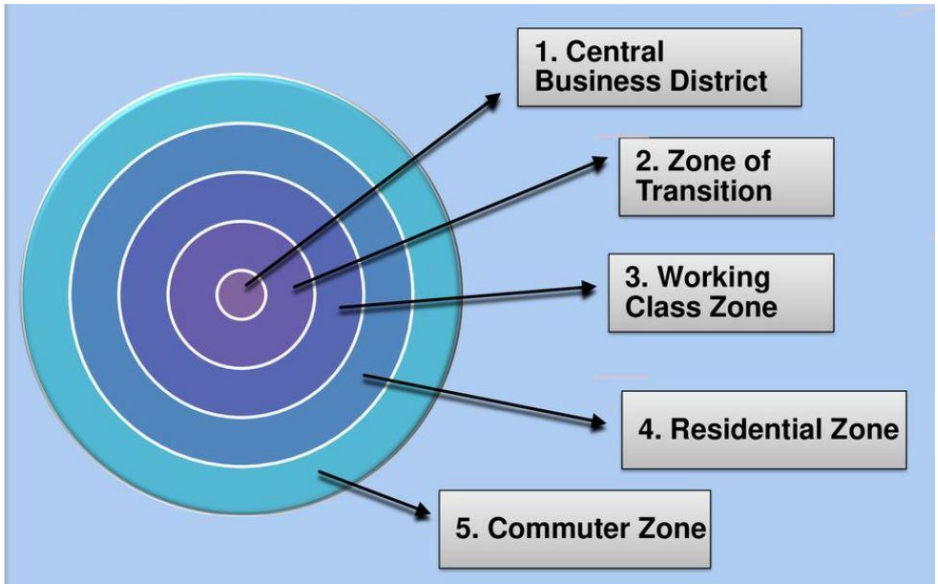

Figure 2.1: Concentric Zone Model. Source: Burgess Model (1925)

2.3.2 The Sector Model

As an improvement upon the Concentric Zone Model, Homer Hoyt in 1939 came up with the sector model (Danso-Wiredu, 2020). This model emphasizes residential rents and transportation routes development and it theorizes that rent differs from one sector to another. Homer's theory was an outcome of empirical studies carried out in American cities where he found out that places with costly rent are found in a sector or more of the city. According to Antipova & Antipova, (2018), the sector model suggests how cities would grow in a wedge-shaped pattern along major transportation routes that extend from the central business district. Thus, a fast-travelling route into the urban centre would over time attract settlement along the travelling route. The sector model also has a central business district (CBD) and outward expansion as a common concept of the concentric zone model (Saravia & Pinho, 2017). However, it takes into account direction and distance as factors in determining residential allocation. The sector model is simply a modified concentric model that looks at the impact of transportation routes on accessibility and land value (Mohammed et al, 2014).

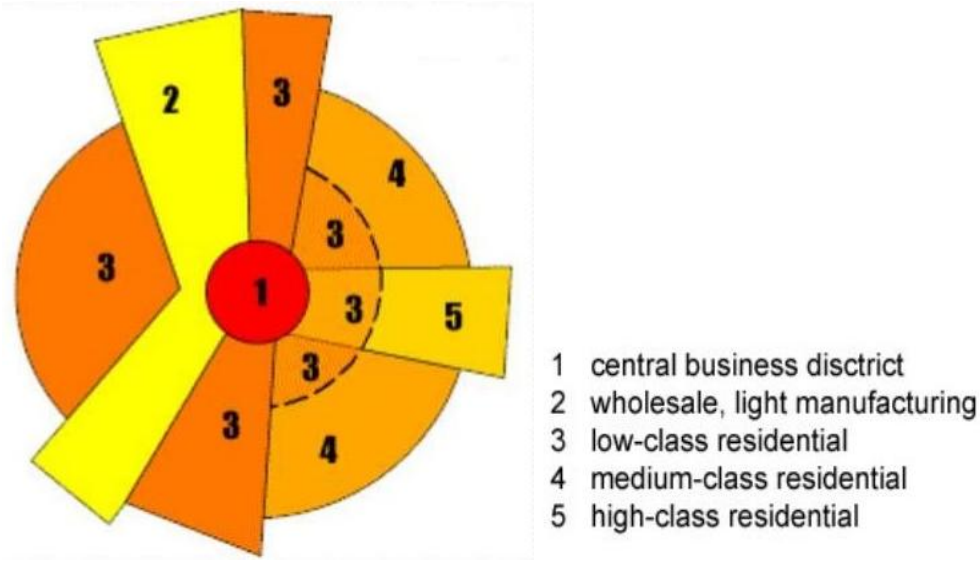

Figure 2.2: Sector model. Source: internal structure of cities (2018)

2.3.3 The Multi Nuclei Model

The Multiple nuclei model was developed by Chauncy Harris and Edward L. Ullaman in 1945. It was developed on the belief that cities are not homocentric, instead, they have mini-centers that help in the development of a city (Offong, 2020). Thus, the growth of cities is said to occur around several distinct nuclei or mini-centers. These mini-centers developed exclusively either through the distinct activities they offered or by similar activities grouped in the area. Unlike the concentric zone and sector model, multiple nuclei hold that a city does not develop around a central business district (CBD) but, in a group of mini-centers. The model again argues that cities with suburbs that grow into a substantial size operate as mini business districts which further serve as mini-centers along which a pattern of land use is formed (Mohammed et al, 2014). This model (Figure 2.3) is fractured into; central business, wholesale or light manufacturing, low-income residential, medium-income-residential, high-income residential, heavy industry, outlying business, residential suburb, and industrial suburb (Danso-Wiredu et al., 2020).

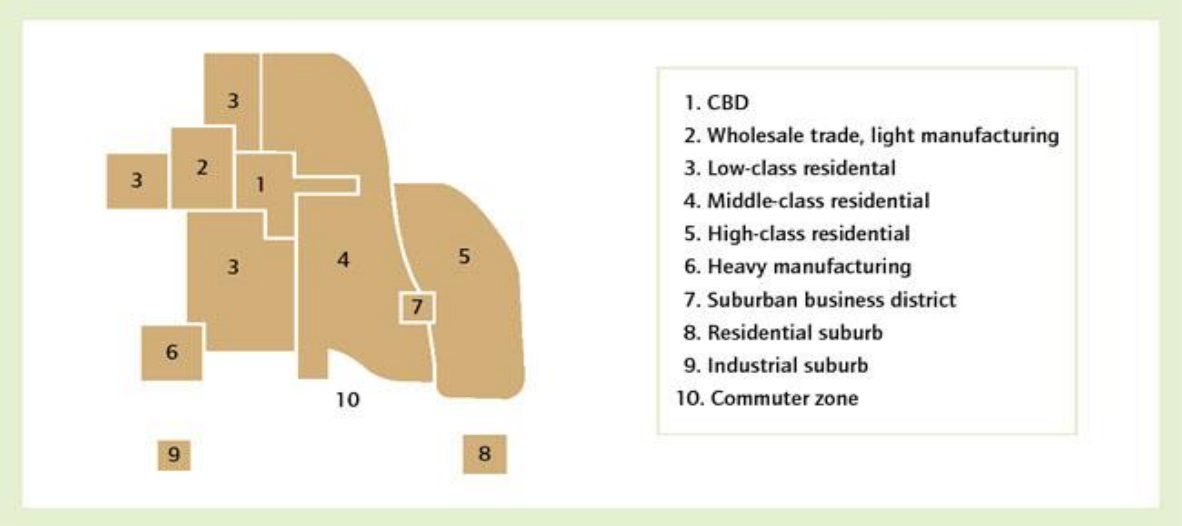

Figure 2.3: The Multiple Nuclei Model. Source: internal structure of cities (2018).

2.3.4 Exploitative Model

With the exploitative model, a city is partitioned into three semicircle zones based on ownership of resources and payment capability (Figure 2.4). The model demonstrates the transfer of money from the core of the city to outlying zones through to the wealthy urban areas. There are three semi-circular concentric zones proposed by the model, namely: the city of death, the city of need, and the city of superfluity (Mohammed et al, 2014). From the exploitative model, the city of death lies at the core of the city and it is characterized by exploitation from the two semi-circular concentric zones. The poor mostly live in this zone and they are exploited through payment of "Machine tax and Death tax". When workers are paid less than what they are due, the surplus income is seen as machine tax. Death tax is also paid by the poor residents in the form of higher food prices, high renting or housing prices, and higher service. The city of need lies between the city of death and the city of superfluity (Mohammed et al, 2014) and is exploited by businesses through the payment of "Machine tax". The outermost part of the exploitative model is the city of superfluity. This zone is inhabited by the affluent and is less in number compared to the population of the other two cities. Despite the small number of the affluent, they control the distribution of resources and affect governmental or administrative decisions. The picture of exploitation and problems occurring within the core of the city is presented by the exploitative model. Due to the exploited system within the core of the city, the inhabitants of the inner city have less acquisition

and development and few job opportunities. They are undermined by the payment of more taxes which affects their development.

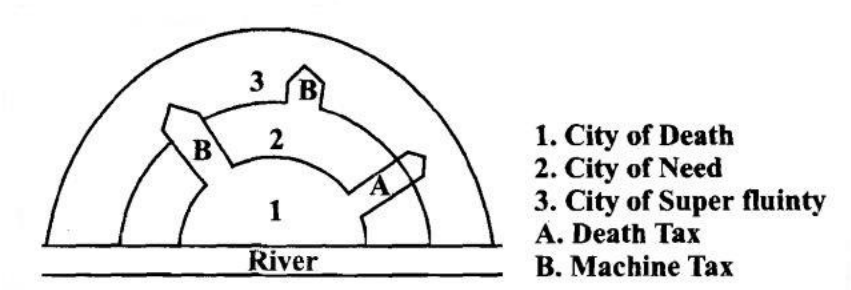

Figure 2.4: The Exploitative Model

2.4 The Concept of Urban Sprawl

In recent decades, urban sprawl has become a topic of concern in both public and academic discussions (Asibey et al., 2024). According to Chettry (2023), due to the changes urban sprawl brings to the earth's surface and its associated problems, urban sprawl has become a subject of importance in world environmental studies. The use of the term urban sprawl has created diverse meanings which often brings confusion and misunderstanding. Therefore, it is important to have a detailed and wide understanding of the concept of urban sprawl before one can do any empirical analysis of it (Viana et al., 2019). The lack of clarity in defining urban sprawl makes Karakayaci (2016) assert that describing urban sprawl is more appropriate than defining it.

Steurer & Bayr (2020) points out various reasons that make defining urban sprawl difficult. First, the term is used in public and political debate and scientific contexts. Second, many scientific disciplines employ the term in a manner that is different for each field. Third, the broad nature of the term brings about ambiguity and misinterpretation. Fourth, the causes, effects, and indicators of sprawl are mostly confused. Fifth, no clear distinction is made between terms such as urban growth, and suburban development. Lastly, no specific method exists for measuring sprawl to some degree due to no generally accepted definition. During the national conference in 1937 in the United States of America, Earl Darper first used the term “sprawl”. Sprawl was explained as an unartistic and wasteful form of settlement (Hatab et al., 2019). According to Dabie (2015), city planners refer to sprawl as a wasteful type of urban growth. Mohammadian et al. (2017) defined urban sprawl as an extension of a city into peripheral and suburban areas which has a low density, single-use, and scattered development in a monocentric urban structure. Resnik (2010) defines

urban sprawl as an uncontrolled pattern of development that occurs around a city's boundary, commonly found in industrialized areas (Ismael, 2021). Though no generally accepted standardized definition of urban sprawl exists, it is commonly seen as a haphazard and overly expansion of urban areas (Cho et al., 2021).

There are agents responsible for the occurrence of urban sprawl and these factors, according to Amoako and Abass et al. (2018), lead to growth in a particular direction. Urban sprawl in developed countries has been caused by globalization, industrialization, and the dominance of capitalist ideology(Amponsah et al., 2022) In developing countries, urban sprawl is mostly caused by inappropriate government policies on land and housing, migration from rural to urban centers, and low- and middle-income household's ability to afford land at the urban fringes (Mohammadian et al., 2017). Research works on urban sprawl in some developing countries like South Africa, Ethiopia, Nigeria, India and Eritrea reported that population, migration, and economic growth are important factors causing urban sprawl (Kantakumar et al., 2016; Abudu et al., 2019). Moreover, built-up density, built-up growth rate, economic growth rate, accessibility, and urban infrastructure seem to drive urban sprawl (Manesha et al., 2021).

Siedentop and Fina (2012) interpret that there are two explanations for the causes of urban sprawl: the first explanation is the demand for urban land. This is driven by household, public, and industrial demand for land. But factors such as income, wealth transportation which serve as determinants of location choice are made after assessing the cost and utility effect. The second cause is specific regulation patterns. Construction of road networks and local basic infrastructures, as substantial subsidies for low-density and suburban forms of living encourage urban sprawl. Population growth, industrialization, dominance of automobiles, transportation system, industrialization, and commercial activities have been identified by some researchers as characteristics and causes of urban sprawl (Karakayaci, 2016; Sinha, 2018).

These causes are explained further in this section. Migration and natural increase in population are two population growth factors in urban areas, which bring about a high population growth rate leading to urban sprawl. The presence of infrastructural facilities and job opportunities at urban centers attracts people from several places, especially from rural areas and from some urban centers that lack certain infrastructural facilities and job opportunities to the urban centers where

these facilities and employment opportunities are available (Mohammadian et al., 2017). This leads to an increase in the population of urban centers. Also, improved healthcare facilities at the urban center have helped to reduce mortality and morbidity rates and contributed to a high birth rate. This, coupled with rural-urban migration brings about an increase in the population growth rate, thereby propelling the growth of a city. Ineffective urban planning and management at the expense of high population growth in the urban center leads to unaesthetic spatial expansion in all directions at the city's fringes (Ayambire et al., 2019; Sui & Lu, 2021).

According to Manesha et al. (2021), population growth and rise in household income increases the demand for housing and a greater number of houses are available and affordable at the fringes. He explained that land prices reduce with distance far away from the urban center due to the demand for accessibility into the central business district (CBD). Also, people choose where to reside in the urban area by trading off low housing costs against transportation costs. Where housing cost is greater than the cost of transportation, households will move away from the central business district. This causes expansion to take place at the fringes of the urban area. Good transportation systems are believed to be a major contributing factor for growing and expanding cities (Pradhan et al., 2017). Transportation routes make cities easily accessible and open to outlying areas. The expansion of cities that goes with lower transportation costs, as well as the chance to enjoy the advantages of living in a city makes it easier to live away from the urban centers. Lower transportation cost enables people to travel longer distances at a lower price which encourages suburban living (Geshkov, 2015) (Asibey et al., 2024). According to Sinha, (2018), urban sprawl in the twentieth century was mainly caused by automobiles.

The establishment of industries attracts people from all walks of life in search of job opportunities (Davis & Golden, 2017). As industries are established, commercial and service centers that have specialized functions spring up and this expands the area into a larger area. Industrial set-up requires large space for operation, therefore, the transition into an industrialized economy demands land for residential, industrial, and commercial purposes (Wei & Wei, 2018). Due to the low value of land and its availability at the fringes, they become a preferred choice for housing and industrial development. In addition to the fundamental causes discussed above, Bhatta (2010) identifies speculation and expectation of land appreciation, physical geography, demand for more living

space, development and property cost, road width, and developmental policies as contributing sources of urban sprawl.

2.5 Urbanization in Ghana

Cobbinah & Erdiaw-Kwasie (2018) defined urbanization as a change from a rural society into an urban society where the population in the urban society increases during a particular year. According to Osawe & Ojeifo (2019), urbanization results from developments of social, political, and economic factors which lead to the increase of people in urban centres and the growth of larger cities, hence changing the land use and transforming it from a rural to an urban setting. Songsore (2020) also states that urbanization is the process by which an activity or activities attract people to concentrate in a specified area within a short period. This process leads to rapid development and brings changes to the region or area such as an increase in the size of the area, population, and human activities within a given time. Songsore (2020) and Asamoah (2010) consider population as an important factor in the definition of urbanization and this makes Owusu & Yankson (2017) simply define urbanization as the growing concentration of urban inhabitants. It is a continuous process that is seen as an indicator of how traditional rural economies are changing into modern industrial economies (Dhali et al., 2019). Though urbanization helps in a city's development, it can be a fatal flaw in a city's growth strategy especially when its growth is not properly monitored and planned. Growth has significant consequences and necessitates the improvement of facilities and infrastructure; thus, it is imperative to identify areas of concern using growth drivers that are unique to the city and prioritize the development scenario per those findings (Siddiqui et al., 2018).

Urbanization can impact positively and negatively. One of such advantages is the market potential and opportunity of the population. Due to its variety and increasing number of available shops and markets, urban dwellers have the opportunity to choose from which market or shop to buy. Also, the prevalence of shops and markets brings competition in attracting consumers, therefore, it is difficult to monopolize prices to attract customers. On the negative side, traffic jams, lack of jobs, and housing may be experienced in an urbanized area. The congestion of people makes movement very difficult as compared to the rural areas where the population is small in number. Also, the influx of migrants into the urban areas in search of jobs is higher than the number of jobs and housing available. Urban areas may provide a variety of accommodations to their populace, but in many cities, poor housing facilities are leading to homeless people (Ofori, 2020). Like most

African countries such as South Africa, Egypt, Libya Nigeria, etc. Ghana is experiencing rapid urbanization. The increasing rate of urbanization in Ghana is fueled by migration of people from rural to urban centers, natural increases in urban centers, and the changing of rural areas to urban when they attained the standard criteria of five thousand population according to Ghana's definition of an urban center (Ghana Statistical Service, 2014). In explaining the process of urbanization in Ghana, some researchers have categorized Ghana's urban development into three phases; namely, the Precolonial, colonial, and post-colonial periods (Ghana Statistical Service, 2014).

During the precolonial period, urban life was a characteristic of the people living in Sub-Sahara Africa. According to Songsore (2020) and Marian (2014), sub-Saharan Africa had its civilization in which religion served as the foundation for possible transformation and development of towns. As a result of the river Niger, Islamic civilization gained ground with many Saharan empires in the early centuries. Gambaga, Nalerigu, Yendi, and Wa are some settlements that evolved as seats of government and trading centers in the 11th and 16th centuries during trade with Western Sudan. Also, Larabanga, Walewale, Lawra, and Savelugu, at the same time developed as commercial centers. Towns like Kumasi, Begho, and Salaga, however, developed inland (Songsore, 2020). In the mid-15th century, European traders started arriving at the coast of West Africa. Among the European traders were the Portuguese merchants, the British, and the French. The arrival of these European merchants shifted economic activities from the northern savannah areas to the coastal areas. This led to the development of strings of towns along the coast (Songsore, 2020). Also, a complex set of middle towns was developed to connect the sources of raw materials in the hinterland to the colonial castles and forts. Kumasi, for instance, is one of the middle towns which was used by European merchants. These activities began a redistribution of Ghana's spatial arrangement bringing about a new urban system from the European coast trade. European trade was carried out by middlemen and merchants who acted as agents between the Europeans and hinterland cities. This medium of trading brought up settlements of towns around these trading centers along the coast and in the middle and hinterlands of Ghana. This period marked the first phase of urban development hence the beginning of urbanization (Ghana Statistical Service, 2014). Colonialism, which was Ghana's second phase of urbanization under British administration, during the 20th century, was marked by improvement in economic, educational, and social development. This development was not uniform but biased, since investment and development

were concentrated in regions with natural resources such as cash crops, timber, gold mines, and areas close to the coast. As a result, development in the southern part of the country was higher compared to the northern part of the country.

In view of this, Cobbinah et al. (2019) opine that the spatial economy of the country was formed by two main structures. One is the center-periphery structure. Under this structure, all forest belts that produced raw materials had a center where production was concentrated and Kumasi is an example of the center of this system. The second type of growth structure was the import-export activities of the coastal towns especially in Sekondi-Takoradi and Accra. These towns had much control of the modern infrastructure in the country and this led to a population increase in these towns. The development of Ghana's colonial towns started as operational towns purposed to aid the extraction of raw materials. Also, in a bid to help these commercial towns, a transportation network was developed to link the coastal towns to the hinterland where they acquired raw materials (Amoah et al., 2019). This aided in the growth of some urban centers. For example, from 1911 to 1921, Accra's population of 38,000 increased to 200,000 by the 1940s (Ghana Statistical Service, 2010) Around that time, Kumasi had a good yield in cocoa production causing its population to increase to 70,000. Furthermore, when the colonial administrators moved to live in Ghana, their well-being and even the education of their wards became a priority of concern; therefore, a rudimentary local government was established to provide for the needs of its people (Ghana Statistical Service, 2010). This made Governor Sir Gordon Guggisberg come up with the infrastructure Development plan. The plan led to the setting up of schools, colleges, and health facilities making towns that had these educational and health infrastructures become urbanized within a short period and this boosted the process of urbanization (Ghana Statistical Service, 2014). According to the Ghana Statistical Service (2014), the strategies of development were focused on industrialization, economic diversification, modernization, and transforming the economy to suit the local culture. Due to the heavy dependence on raw materials during the colonial era, some towns like Sekondi-Takoradi, Kumasi, and Accra had infrastructures that supported the development and growth of modern industries and markets after independence.

The post-independence development strategies aimed at industrializing these urban centers, so capital investment was made in urban centers to cause growth that will ripple to affect various economic sectors and the rural areas (Ghana Statistical Service, 2010). Unluckily, the

developmental strategies for transforming the economy were unsuccessful, and not much regional development and spatial integration were achieved (Owusu & Yankson, 2017). Owusu (2015), however, states that government policies and decentralization are contributing factors that led to the growth and increasing number of urban centers across the nation. Ghana's increasing urbanization is due to its high rate of natural increase and internal migration (Ghana Statistical Service, 2014). The high rate of rural-urban migration at the early stage of urbanization which was a dominant factor was mainly the reason for the differences in the level of development between the urban and the rural areas. For years, internal migration has led to the redistribution of Ghana's population and this redistribution is uneven throughout the nation. For instance, the southern part of the nation due to its socio-economic opportunities and growth has had a lot of people migrate there compared to the northern part of the country. This has made regions with less socio-economic growth experience out-migration (Ghana Statistical Service, 2014).

Table 2.1: Population by region from 1960 to 2021.

	Region	Population (2021)	Population (2010)	Population (2000)	Population 1984	Population 1970	Population 1960	Percent of total (2021)
1	Greater Accra	5,455,692	4,010,054	2,905,726	1,431,099	903,447	541,933	17.69%
2	Ashanti	5,440,463	4,780,380	3,612,950	2,090,100	1,481,698	1,109,133	17.64%
3	Eastern	2,925,653	2,633,154	2,106,696	1,680,890	1,209,828	1,044,080	9.49%
4	Central	2,859,821	2,201,863	1,593,823	1,142,335	890,135	751,392	9.28%
5	Northern	2,310,939	2,479,461	1,820,806	1,164,583	727,618	531,573	7.50%
6	Western	2,060,585	2,376,021	1,924,577	1,157,807	770,087	626,155	6.68%
7	Volta	1,659,040	2,118,252	1,635,421	1,211,907	947,268	777,285	5.38%
8	Upper East	1,301,226	1,046,545	920,089	772,744	542,858	468,638	4.22%
9	Bono (Brong-Ahafo)	1,208,649	2,310,983	1,815,408	1,206,608	766,509	587,920	3.92%
10	Bono East	1,203,400	Brong Ahafo	Brong Ahafo	Brong Ahafo	Brong Ahafo	Brong Ahafo	3.90%
11	Upper West	901,502	702,110	576,583	438,008	319,865	288,706	2.92%
12	Western North	880,921	Western	Western	western	Western	Western	2.86%
13	Oti	747,248	Volta	Volta	Volta	volta	Volta	2.42%
14	North East	658,946	Northern	Northern	Northern	Northern	Northern	2.14%
15	Savannah	653,266	Northern	Northern	Northern	Northern	Northern	2.12%
16	Ahafo	564,668	Brong-Ahafo	Brong-Ahafo	Brong-Ahafo	Brong Ahafo	Brong Ahafo	1.83%
17	Total	30,832,019	24,658,823	18,912,079	12,296,081	8,559,313	6,726,815	100%

Source: Ghana Statistical Service (2021).

Before the 2021 population census, Ghana had 10 regions and as shown in Table 2.1, there was an increase in the population of all the regions from 1960 to 2010 the regions in Ghana. The creation of new regions on 27 December 2018 from some old regions namely; Western, Volta, Northern, and Brong-Ahafo increased the number of regions to 16 and this ostensibly reduced the population of the regions that new regions were birthed from. The increasing number of people in a region tells of the rate of urbanization, since in Ghana, reaching a minimum number of 5000 population qualifies a locality to become urban. Also, in Ghana, the discovery and utilization of natural resources contributes to internal migration. Thus, when new resources are identified and put into

use, it attracts migrants from several places due to the economic prospects and the livelihood opportunities it brings. For instance, the oil discovery in the Western Region has attracted migrants from other regions, making the Western region have a positive net in-migration in the year 2010 among four other regions (Ghana Statistical Service, 2014). However, since 1970, the natural increase in urban centers has played an important role in addition to migration. According to (Owusu & Yankson, 2017), a report from the Ghana Statistical Service showed that, although in 1988 the rural areas had a high fertility level of about 15%, the establishment of modern health facilities in the urban towns brought about a lower mortality and morbidity rate which led to an increase in population in these urban centers. The relationship between births and deaths affects how the population in a locality naturally grows, especially when births far exceed deaths, to attain the minimum population requirement to become an urban town. In Ghana, regional variations exist in births and deaths, so by using the differences in births and deaths, a region could become urbanized earlier or later than another. Though there has been a decline in Ghana's population growth rate compared with previous census, Ghana's population is growing or is constantly increasing (Ghana Statistical Service, 2021). This eventually increases the trends of urbanization in the country as shown in Table 2.2.

Table 2.2: Trend of urbanization (1921-2021)

Year	Total Population	Percentage Urbanized	Urban Population	No. of Urban Settlement
1921	2,296,400	7.8	179,244	-
1931	3,160,386	9.4	297,322	-
1948	4,118,459	12.9	570,597	41
1960	6,726,815	23.1	1,551,174	98
1970	8,559,313	28.9	2,472,456	135
1984	12,296,081	32.0	3,938,614	203
2000	18,912,079	43.8	8,278,636	364
2010	24,658,823	51.0	12,545,229	636
2021	30,832,019	56.7	17,472,530	1523

Source: Ghana Statistcal Service, (2021).

Table 2.2 shows an increase in the number of urban settlements due to the constant increase in the total population. In 1921, the total population contributed to 7.8 % urbanization and, therefore increased to 56.7% in the year the year 2021, showing how fast Ghana is becoming urbanized. The National Development Planning Commission (2020) asserts that effective urban planning and efficient management practices need to be developed for Ghana to properly enjoy the benefits of urbanization as seen in most developed and some Asian countries (Adei, 2020). The reason is that

urbanization in Ghana is commonly characterized by high unemployment rate, increased environmental degradation, increased crime rates, and poor housing provision. These negative characteristics make it difficult to fully enjoy the benefits of urbanization in Ghana. Hence, effective management and urban planning need to be adopted.

2.6 URBAN LAND USE AND LAND COVER CHANGES

Throughout history, the Earth's surface has changed at various spatial and temporal scales. These alterations occur over both short and extended periods and are driven by natural phenomena as well as human activities (Singh et al., 2018). Natural events such as droughts, flooding, earthquakes, and volcanic eruptions significantly impact the Earth's land surface (Roberts, 2019). However, the predominant alterations in land cover are primarily attributed to human activities (Mariano et al., 2018). Singh et al. (2018) notes that the rate of human-induced modifications to the Earth's land surface in recent years is indeed alarming.

In the definition of Nnaji et al. (2016) land cover refers to the natural vegetative cover types that characterize a particular area, and land use refers to human direct actions that alter the land cover. Similar to the definition of Hussain et al. (2022), land cover (LC) refers to the physical features on the earth's surface while land use (LU) is the change in land cover as a result of human actions. Forest, mountain, and water are examples of land cover, and roads and urban infrastructure are land use examples (Hussain et al., 2022). Hasan et al. (2020) also assert that land cover is the physical and biological cover over the earth's surface. These physical and biological cover include water, vegetation, and human structures (Briassoulis, 2020; Appiah, 2017). According to Houdon et al, (2014) and Appiah (2017), the vegetation type of land surface was originally what was used to refer to land cover but the subsequent expansion of the concept of land cover over the years has included human structures such as building and physical aspect of the environment into its definition. This makes Chilagane (2017) opine that in defining land cover in its technical and strict sense, emphasis should be laid on vegetation and artificial or man-made features. Land use, however, is defined by the Food and Agricultural Organization-FAO (1995) cited by Briassoulis (2020) as the human activities that directly affect the land through the means of using its resources. Thus, land use is the purpose for which land is used by humans. This definition is similar to Nedd et al. (2021) definition which states that land uses are the reasons to which man utilizes the land. In simple terms, Garcia et al, (2010) explain land cover as the natural physical surface not related

to human activities, while land use is how the land is utilized by transforming the natural environment into built-up. At the knowledge level, it is easy to differentiate land use from land cover but in practice, the available data makes the distinction unclear and this makes it difficult to explain either of them (Appiah, 2017).

Land use and land cover change (LULCC) is generally used to mean the alterations humans bring to the earth's surface. It also refers to the transformation in a given land cover or land use type (Briassoulis, 2020). Currently, the magnitude of LULC changes is unprecedentedly causing significant alteration to the ecosystem (Appiah, 2017). This is evident by the increasing changing of vegetative lands into impervious surfaces, decreasing surface permeability, and increasing the occurrence of urban heat and drought. Unfortunately, these changes are fueling climate change which impacts both man and wildlife (Shamsudeen et al., 2022). Although, globally, these changes predominantly occur in metropolitan areas, they are increasingly problematic in developing countries (Appiah, 2017).

UN-HABITAT (2020) reported that more than (50%) half of the global population currently resides in urban areas and this makes urban landscapes the fastest-growing land cover type (Zhongming et al., 2020). According to Kumar et al. (2018), the global population is forecasted to surge from 6.8 billion in 2009 to 9.1 billion by the year 2050 while urban population is expected to increase from 3.4 billion in 2009 to 6.3 billion by 2050. As people living in the urban centers increase, the peripheries are sought as a refuge from congestion and issues arising from overcrowding. (Dabie, 2015; Kumar et al, 2018; Mariwah et al., 2017). This distorts the land cover pattern at the fringes due to the pressure and the modification it undergoes. In developing nations, urban expansion adversely impacts agricultural areas which are critical determinants of determining land use land cover change (Dabie, 2015).

2.6.1 Land Use and Land Cover in Sekondi-Takoradi Metropolis

According to Kumi-Boateng (2015) and Mensah (2018), Sekondi-Takoradi is experiencing unprecedented alterations in its land cover. These changes are fueled by the increase in population and pressure on land demand for development purposes. For instance, the increase in economic activities, the harbor, and the discovery of oil have attracted lots of industries and migrants to the metropolis (Abdul-Kareem et al., 2021; Mensah et al., 2018b). Unfortunately, these industries and migrants require space for residential, industrial, and commercial purposes. Therefore, have

brought changes to the land cover of the metropolis (Alqattan et al., 2019; Yankson et al., 2017). In 1970, the population of the metropolis was 135,760, 559,548 in 2010, and then 734,645 in 2021 (Fiave, 2017; Ghana Statistical Service, 2014; Ghana Statistical Service, 2021). This proves there has been an increase in the city's urban population and would potentially affect the land cover as stated by (Mohanta & Sharma (2017)**.** According to Mohanta & Sharma (2017)**,** population growth, urbanization, and industrialization transform the land surface and atmospheric components which are largely responsible for the trends of climate change. Haldar & Majumder (2022) also assert that environmental problems like water pollution, greenhouse gas emission, air pollution, and urban heat island are caused by urbanization and industrialization along with rapid changes in land use land cover.

2.7 Urban Heat Islands

The urban environments can be viewed as resources and limitations for its dwellers. In cities of developing countries like Ghana, the increasing changes in pervious surfaces to impervious surfaces have altered the thermal conditions and led to the rise of heat waves (Saha et al., 2021). Urbanization brought on by changes in land cover affects the meteorological characteristics of an area by increasing air temperature, increasing relative humidity, decreasing rainfall, and increasing energy demand. These changes cause urban heat island (UHI) phenomenon (Naim & Kafy, 2021) which has recently emerged as one of the important results of rapid urbanization (Saha et al., 2021). UHI occurs when the urban areas have temperatures significantly higher than their surrounding rural areas and this is mostly caused by anthropogenic activities on land surface (Mansour et al., 2022a)**.** UHI causes changes in the urban microclimate like evapotranspiration, water vapor, solar radiation absorption, atmospheric temperature, land surface temperature, and air pollutant concentration which have an immediate impact on human health. Consequently, comprehending the dynamics of UHI over an urban environment forms an integral component of sustainable urban planning (Mohanta & Sharma, 2017)**.** The main causes of UHI include the conversion of natural and semi-natural land cover into built-ups, discharge of heat from vehicles and industries, construction materials, and urban geometry (Saha et al., 2021). UHI can be assessed either based on air temperature or based on land surface temperature.

In this study, Urban Heat Island (UHI) was assessed based on land surface temperature (LST) (Saha et al., 2021a). Previously, discrete data of near-surface air temperature was used to calculate

the UHI intensity. Now, with the advent of thermal remote sensing LST is frequently used (Mohanta & Sharma, 2017). According to Worku et al. (2021), LST, which is the radiative land surface skin temperature varies greatly due to the thermal characteristics of the land surface features. For instance, in places where the vegetative cover is altered to built-up, the thermal properties also change and this causes temperature to rise above the surrounding areas. Based on this, Shamsudeen et al. (2022) opines that LST determines the surface air temperature and is an essential factor that affects the distribution of energy between vegetation and the ground.

Numerous studies in different cities of the world show that an increase in impervious surfaces causes urban heat island (Worku et al., 2021). Bokaie et al. (2016) and Pal and Ziaul (2017) assert that the conversion of vegetated surfaces to impermeable surfaces is the cause of the rising land surface temperature (LST). Therefore, rural areas with less impervious surface area record lower temperatures than metropolitan areas (Naim & Kafy, 2021). Also, Naim & Kafy (2021), discovered that whereas vegetation and waterbodies exhibit a modest LST, built-up areas increase urban temperature(Naim & Kafy, 2021). Apart from land use land cover, elevation, and other topographic features are factors that affect land surface temperature. In the studies of Worku et al. (2021), it was concluded that topographic factors such as height, slope, and aspect caused a significant spatial variation in land surface temperature over the mountain regions in northeastern China. A report by the IPCC (2018) reveals that the global mean LST of 0.87 observed from 2006 to 2015 is higher than what it was between 1850 and 1990. However, it is predicted that LST in metropolitan areas will rise further globally (Saha et al., 2021a). As a result of this, the United Nations (2018) predicted that by 2050, 68% of the world's population will be affected by UH (Mansour et al., 2022a). This will affect the developmental process of the urban areas. Hence, for effective planning and management of urban areas, it is essential to examine the impact of urbanization or landscape on Land Surface Temperature (Shamsudeen et al., 2022).

2.7.1 Impact of Urban Heat Islands

According to literature, the impact of UHI can be categorized broadly into two groups: positive and negative or adverse effects. Unfortunately, the significant threat UHI poses to the quality of life in society makes a lot of studies focus on the adverse effect or negative effects of UHI (Traore et al., 2021). These negative effects, according to Deilami (2017), are themed under health, environment, and economics.

The earlier studies on UHI carried out by Clarke (1972) in New York, revealed that the sustained heat stress caused many deaths. This made Buechley et al. (1972) correlate heat islands to death to indicate that excessive heat increases mortality. Investigations in Lyon and Chicago revealed staggering death tolls during heat waves, with 14,800 and 700 deaths recorded in 2003 and 1995, respectively (Piracha & Chaudhary, 2022). Likewise, Darlington et al. (2017) established a significant connection between heat-related mortality and UHI in Shanghai. Furthermore, Taylor et al. (2015) found that most old people and those with respiratory diseases in London were vulnerable to excessive heat-related mortality. Other health-related effects of UHIs are general discomfort, heatstroke, sunburn, dehydration, and respiratory difficulties (Darlington et al., 2017; Faisal et al., 2021; Nimish et al., 2020; Saha et al., 2021; Traore et al., 2021; Ullah et al., 2022; Viju et al., 2023). Saha et al. (2021) revealed that extreme heat stress can lead to conditions such as heat strokes, heat cramps, and heat rashes. Filho et al. (2021) reported that the increased discomfort and heat problems associated with UHI are evident in the form of dehydration, higher mortality and morbidity cases and exhaustion.

Studies have also uncovered environmental challenges associated with urban heat islands (UHIs), including weather fluctuations, ecosystem pollution, and energy-related emissions. Regarding weather, research indicates that UHI exacerbates smog formation, alters precipitation patterns, and elevates humidity levels (Frimpong, 2022; Stemn & Kumi, 2020). Another significant concern linked to UHIs is thermal pollution of water bodies, endangering aquatic fauna. Experiments demonstrate that rainwater temperature increases significantly from 21°C to 35°C upon contact with pavement surfaces before eventually reaching rivers and streams, posing detrimental effects on their ecosystems. Furthermore, during the hot season, the demand for cooler environments escalates energy consumption (Choudhury et al., 2023). This increases greenhouse gases and other air pollutants driven by the utilization of fossil fuels to meet the energy needs of consumers (EPA, 2016). Other environmental impacts include habitat loss, depletion of fresh water, and high levels of air pollution (Darlington et al., 2017). Urban Heat Islands (UHIs) also exert numerous adverse effects on the economy of cities. For instance, in 2018, about 45 billion working hours were reported to have been lost to the rising temperatures in the Netherlands. Therefore, as working hours directly correlate with productivity and economic growth, a loss in labour hours is a loss in economic growth (Filho et al., 2021).

Further, Deilami, (2017) revealed that reducing the average temperature by -16.78 to -15.78°C in cities like Sacramento, Salt Lake City, and Baton Rouge could result in annual savings of approximately $26 million. Also, millions of dollars are expended annually on medical expenses for individuals suffering from respiratory issues attributed to heat-related problems across the United States (Wondmagegn et al., 2019). All these have a serious tow on the economy of a city. Despite the manifold disadvantages associated with UHI, Filho et al, (2021) recognize certain benefits for cities situated in high-latitude areas. The UHI effect contributes to warmer weather experiences during cold seasons. Additionally, UHI leads to reduced energy consumption during colder periods in urban areas compared to non-urban areas, thus offsetting the exceptionally high energy usage during warmer seasons in urban locales.

2.7.2 Relationship between UHI and its indicators

Mostly, the land cover types that are used as explanatory variables for the UHI are vegetation, waterbody, and built-up or impervious surfaces. These land cover classes have been observed from literature as either having a positive or negative correlation with UHI. For instance, there is a consensus that water and vegetation have a negative correlation with UHI whereas built-up or impervious surfaces have a positive relationship with UHI. From the work of Haldar & Majumder (2022), it was found that normalized difference built-up index and LST showed a positive correlation whereas a negative relation existed between LST, normalized difference vegetation index (NDVI), and modified normalized difference water index (MNDWI). Also, Ullah et al. (2022) found NDVI had a negative relationship with LST while NDBI had a positive correlation with NDBI. Similarly, Balew & Korme (2020) used linear regression to statistically analyze the relationship between LST, NDVI and NDBI. The result showed that LST had a positive relationship with NDBI and a negative relationship was observed between LST and NDVI.

2.8 Application of Remote Sensing (GIS) and Geographic Information Systems (GIS) in Urban Growth and Urban Heat Islands

Globally, modernized techniques such as Remote Sensing (RS), and Geographic Information Systems (GIS) are being used by researchers and urban planners in areas such as land use land cover, urban growth, and urban heat islands (Gašparović, 2020**;** Liu et al., 2015). “Geographic Information System (GIS) is a system designed to capture, store, manipulate, analyze, manage, and present all types of geographical data” (Kuria et al., 2019). On the other hand, Lillesand et al.

(2015) defined remote sensing as getting information about a phenomenon without having physical contact with the phenomenon. Using a traditional survey approach to determine changes in a geospatial phenomenon, especially of a larger area is difficult, expensive and time-consuming. This, in most cases, introduces lots of errors that affect the accuracy and reliability of results (Elagouz et al., 2020). Therefore, when conducting studies, for instance, on land cover change over a larger area and of different periods, it is prudent to use a technique that can provide a more accurate and reliable measurement and can effectively provide an up-to-date change in land use land cover (Elagouz et al., 2020). Satellite imageries are mostly used in studying the changes in urban land use land cover and the examination of urban land use land cover involves the use of multi-temporal images to ascertain the alterations in land use caused by human activities and by environmental factors (Singh, 2017). Remotely sensed satellite images obtained from platforms like Landsat, Sentinel, Aster, etc. serve as a foundation for studying land cover changes, urban growth, and UHI.

2.8.1 Remote Sensing and GIS Application to Land Use Land Cover and Urban Growth

GIS and RS have been used in several sectors of development such as mapping and management of natural resources, urban and regional planning, environmental management, transportation planning, and land use management studies. According to Watershed et al. (2022), RS and GIS techniques are popular methods for creating LULC maps of a region with sufficient accuracy. These methods help users assess the spatiotemporal changes in the geospatial phenomenon under investigation to adopt necessary actions and manage natural resources sustainably. In the area of urban growth, remote sensing data makes it suitable to map spatio-temporal dynamics of impervious surfaces at coarse, medium to high resolutions (Mohanta & Sharma, 2017). RS and GIS have helped in monitoring, predicting and measuring the pattern, direction and growth in built-up, thereby, leading to a better understanding of urban growth.

A lot of studies have been conducted on urban growth and land use land cover using GIS and remote sensing. For example, Qi lv et al. (2015), used Synthetic Aperture Radar data to study urban land use and land cover classification in the northern Greater Toronto Area (GTA), Ontario, Canada. In Bangladesh, Haque and Basak, (2016) used remote sensing and GIS to conduct a spatio-temporal study on Tanguar Haor to determine changes in land cover over 30 years from 1980-2010. In India, Ghosh et al. (2023) used GIS and remote sensing data to study land use and land

cover classification in the urban city of Burdwan. Ghaderi & Rahbani (2020) employed remote sensing and GIS in assessing urban growth in Bandar Abbas City, Iran. In Egypt, Mohammadian et al. (2017) employed remote sensing and GIS to evaluate changes in land use and to measure urban sprawl in the city of Qom. Mohan (2023) also used remote sensing and GIS to investigate the dynamics of urbanization on green cover in the city of Delhi, India.

2.8.2 Remote Sensing and GIS Application to Land Surface Temperature (LST)

The study of urban thermal environments at varied spatial and temporal resolutions is made possible through the use of multi-temporal thermal remote sensing as it can measure the land surface temperature (Mansour et al., 2022a). This has made monitoring LST gain more attention in recent years due to their effect on the urban environment. Accordingly, thermal satellite sensors range in resolution from low resolution, such as the Moderate Resolution Imaging Spectroradiometer (MODIS) and Advanced Very High Resolution Radiometer (AVHRR); to medium resolution, such as the Landsat Thematic Mapper (TM), Enhanced Thematic Mapper Plus (ETM+), Enhanced Thematic Mapper Plus (ETM+), and Operational Land Imager (OLI)/ Thermal Infrared Sensor (TIRS); and Advanced Spaceborne Thermal Emission and Reflection Radiometer (ASTER) has been used in retrieving thermal information used for LST (Balew & Korme, 2020).

Previously, remote sensing data such as AVHRR and MODIS data were used largely for regional LST estimations (Naim & Kafy, 2021). However, Landsat images have been extensively employed in retrieving LST at local, regional, and global scales due to their relatively consistent global coverage with appropriate spatial, spectral, and temporal resolution when compared to MODIS and AVHRR (Mohanta & Sharma, 2017). For instance, Al Kafy et al. (2020) and Sahak (2022) employed Landsat TM and ETM+ data to estimate the LST on a small scale. Abouel-Magd et al. (2016) used multi-temporal Landsat data to study the UHIs over Cairo and showed that urban growth increased the creation of UHIs. Additionally, Roupioz et al. (2018) also investigated the feasibility of using satellite data (Landsat) to assess UHIs based on LST and emissivity measurements from various thermal-infrared (TIR) data sources. To achieve a reliable LST calculation, Naim and Kafy (2021) recommended using images with a resolution less than 200m and this has made Landsat images commonly used in the monitoring of LST and UHI.

The efficiency and adaptability of RS and GIS make it possible to be employed in urban climate studies and this has made it easier to conduct studies on the relationship between urbanization and

urban heat islands in diverse ways (Mohanta & Sharma, 2017). For instance, Mishra et al. (2020) and Yang et al. (2017) used remote sensing data and the Temperature-Vegetation Index to examine the effects of land cover changes on the LST (Naim & Kafy, 2021). Xiao et al. (2018) used regression models to investigate the reactions of land cover classes to land surface temperature at different places at varying scales. Kim and Brown (2021) assessed the relationship between land cover change and Surface urban Heat Intensity (SUHI). Kedia et al. (2021) used the Index Based Built-up Index (IBI) to investigate the relationship between the LST and urban built-up of Istanbul.

2.9 Forecasting land use change and urban growth

Besides knowing and understanding the drivers of land use land cover and urban growth, it is essential to also comprehend the process of growth through an analytical framework eligible for including the existing scenario and enabling the projection of the future scenario. According to Siddiqui et al. (2018), an efficient way of understanding the spatial process of urban growth is by modeling, hence, an increasing demand for explicit spatial land use change and urban growth models has led to the development of modelling approaches for forecasting urban growth and land use changes. These modelling approaches are founded on either agent that leads the simulation process or founded on data acquired from the land cover and its changes over a period (Addae, 2019). Modelling methods such as Evolutionary models, Expert systems models, Multi-agent models, Cellular Automata, Principal Component Analysis, Markov Chain, Artificial Neural Networks, Agent-Based Model, Statistical Models, Rule-Based Models, Logistic Regression, Sleuth, and Analytical Hierarchy Processes are used to quantify, and project urban growth (Dhali et al., 2019). Of these models, the commonest type of models for forecasting land use changes and urban growth are Cellular Automata (CA), Markovian Models and the hybrid model known as CA-Markov (Rui, 2013;Wangyel et al., 2021).

2.9.1 Cellular Automata (CA)

Ulan and Neuman introduced the concept of Cellular Automata (CA) in 1940 and it is a non-continuous time-dependent system that uses simple decision rules to simulate complex spatial processes. (Mosammam et al., 2017). Cellular Automata models stress neighbour effects and change the interaction between agents of land use cells. The application of cellular automata to simulate land use change considers environmental factors, economic factors, technological factors, comprehensive policy, human factors, and historical records of land use data (Chilagane, 2017).

The CA model consists of five main elements: (a) the lattice, which is the space in which cells exist; (b) the cell state, which is one of an unlimited number of states; (c) the neighbourhood, which is made up of cells that are close to a certain cell. (d) the transition rule, which determines the condition of the cell in the following period depending on its current state and surroundings. (d) Temporal space: The time steps in which the cell evolves. The CA model can be expressed mathematically using equation (2.1)

$$S(t, t+1) = f(S(t), N) \quad \ldots (2.1)$$

where S is the set of limited and discrete cellular states, N is the Cellular field, t and t + 1 indicate the different times, and f is the transformation rule of cellular states in local space (Gidey et al., 2017; Nath et al., 2023).

2.9.2. Markov chain analysis (MC)

This model was invented in 1906 by Andrei Andreyevich Markov. The fundamental tenet of the Markov chain model is that any spatial position (pixel) and any change in a nearby pixel can be explained by the present state (Abudu et al., 2019). According to Tariq et al. (2022), the model assumes that the state at some point in the future (t+1) can be expressed as a function of the current state (t), meaning, the present change only determines the future change. The result of Markov Chain is a transition probability matrix between two time periods (t1 and t2), and this does not only explain the possibility of changing from one state to another but helps to forecast how the state of a land cover or class will be in future (Mosammam et al., 2017; Tariq et al., 2022). In this model, space is discrete and its randomly determined process functions mainly on probabilities. The Markov chain is expressed mathematically in equation (2.2).

$$P(X_{t+n} = X_{t+n} | X_t = X_t) = P(X_n = X_{t+1} | X_0 = X_t); n = 0,1,2, \ldots \quad (2.2)$$

Where; P is the Markov Chain transition matrix; X, the sequence of length; n, the prediction duration; t and x, the new state of X after a specific time (Abudu et al., 2019). Satya, (2020) explains also that, Markov model is based on the formation of Markov random process system for forecasting and optimal control method. This model treats land use change as a randomly determined process by assuming that the changes between classes of land use are almost constant from one period to another. It is mostly used in predicting geographical features or characteristics with no delayed effect and this has of late become a crucial prediction method in geographic

research (Satya, 2020). According to Mosammam et al. (2017), the Markov chain is limited by a lack of the spatial dimension so it cannot identify the occurrences of spatial distribution within each LULC category. Also, it does not take into account the spatial distribution of information inside each class and the likelihood of transition between landscape states is not uniform (Wangyel et al., 2021; Mosammam et al., 2017). Therefore, it can provide the appropriate magnitude, but not the appropriate direction (Mohammadian et al., 2017). These shortcomings are lessened by using CA-Markov model.

2.9.3 CA-Markov Model

The CA-Markov model integrates the Cellular Automata model with the Markov chain model. According to Mosammam et al. (2017), this model was created to overcome the spatial dimension constraint of Markov Chains and is commonly used in simulating LULC and urban growth due to its efficiency and effectiveness proven in numerous studies by researchers. For instance, Wangyel et al. (2021) asserts that CA-Markov has the potential to simulate and forecast spatial changes in complex land use systems and outperforms regression-based models. The fundamental tenet of the CA-Markov model is that the current state of a cell depends on the neighbouring cell's present state. This underpins the dynamics of change events based on proximity, which makes it more likely for regions to change to a different class when they are closer to existing areas of the same class (Gidey et al., 2017). A key feature of CA-Markov is the use of transition rules to predict complex dynamic spatial and temporal patterns. The model has been used effectively in several scientific studies to project future distribution of LULC (Gidey et al., 2017). Tariq et al. (2022) simulated land use dynamics of Peshawar, Pakistan using CA-Markov chain model. Mosammam et al. (2017) used the CA-Markov model in IDRISI Selva to simulate LULC change and model urban growth in Qom City. Wangyel et al. (2021) used CA-Markov model to carry out a geospatial analysis of Bhutan's Thimphu city by predicting the changes in land use for the year 2050. Lu et al. (2017) explored the potential impact of climate change on urban growth in London using cellular automata-based Markov chain model. This study thus employed the CA and Markov chain models in conjunction to predict the future probabilities of LULC dynamics.

2.10 Shannon Entropy Model

In spatial planning, mapping and quantification are regarded as key components of urban growth (Manesha et al., 2021). According to Bhatta et al. (2010), the multi-dimensional aspect of urban growth calls for a variety of scales to measure the growth effect. With the use of GIS techniques and Satellite data, researchers have become interested in mapping and quantifying urban growth using a variety of mathematical and statistical methodologies (Dhali et al., 2019). This has made Shannon entropy a commonly used statistical method in measuring urban growth among other methods like land absorption rate, and Moran I spatial indices (Dhali et al., 2019; Roy & Kasemi, 2021). The Shannon entropy model is commonly used to ascertain the spatial dispersion or concentration of a city (Dhali et al., 2019). The value ranges from 0 to log(n) where values closer to 0 indicate compaction and entropy values closer to log(n) show dispersion or sprawling (Bhatta et al., 2010). It has been observed in several studies as an efficient method for measuring growth when combined with GIS and remote sensing techniques (Albert & Yiran, 2021; Antalyn & Weerasinghe, 2020; Cengiz, Görmüş, & Oguz, 2022; Pradhan, 2017; Roy & Kasemi, 2021; Steurer & Bayr, 2020b). Pursuant to Chong (2017), Shannon entropy is less sensitively linked to the changing areal measurement issues where results may change due to factors such as the size, shape and the number of zones. For the past years, many fields have applied the mathematical communication theory known as Shannon's entropy in urban studies due to its mathematical ability to estimate unplanned urban growth. This model was used to measure urban spatial patterns and expansion of urban growth as it is capable of determining the spatial distribution of a geographical phenomenon. Within a GIS framework, this model makes it possible to evaluate urban sprawl and analyze disparities in urban patterns.

CHAPTER 3: DETERMINE THE SPATIO-TEMPORAL DYNAMICS OF LAND USE LAND COVER IN THE METROPOLIS AND FORECAST FUTURE TRENDS OF LULC

ABSTRACT

Sekondi-Takoradi is the most urbanized metropolis in the Western region of Ghana. Over the past two decades, it has experienced rapid shifts in both population density and land cover. Unfortunately, these transformations have significantly altered the natural landscape and expanded urban coverage. Previous studies have not established enough evidence on land use and land cover changes in the metropolis. For this reason, this study examined the existence, rate, and spatial distribution of land use and land cover as well as the future changes in land cover in the metropolis. Landsat imagery spanning from 1991, 2009, 2016, to 2023 provided the basis for evaluating the spatiotemporal dynamics of land use and cover within the metropolis. The Random Forest Classification algorithm was employed to categorize the images into three distinct classes: water, vegetation, and built-up areas. Analysis revealed a rapid growth in built-up areas by 63.08 km² (32.91%), accompanied by a decrease in vegetation and water coverage by 60.99 km² (31.82%) and 2.08 km² (1.09%) respectively. This highlights the accelerating urbanization trend, emphasizing the critical need for vigilant monitoring and controlled urban expansion to mitigate potential adverse effects. Projections for 2030 indicate further changes with water areas decreasing to 1.21 km² (0.63%), vegetation diminishing to 95.31 km² (49.73%), and built-up areas expanding to 95.14 km² (49.64%). This signifies a significant shift towards built-up areas, altering the metropolis' land cover composition and potentially impeding the achievement of Sustainable Development Goal 11. Understanding these changes in land use and land cover holds significant value for policymakers, enabling them to effectively monitor and safeguard natural resources.

Keywords: Land use and land cover; Landsat images; Geospatial techniques; Land compositions; Random Forest; Sustainable development goals.

3.1 Introduction

Globally, more than 70% of the changes that occur on the land surface are human-induced (Younes et al., 2023). Unfortunately, these changes, especially the conversion of vegetation and waterbodies to built-up areas have little chance of being restored to their former cover (Mohammadian et al., 2017). As a result, the decision to put land to a particular use must be carefully assessed before any action is taken to avoid manifold dire implications (Obodai et al., 2019). According to Ramadan & Effat (2021), and Krishnaveni & Anil (2022), anthropogenic activities that bring changes in the land use land cover are mostly fueled by population growth and increasing economic activities. Currently, the world's population stands at 8 billion with an annual growth rate of 1.11% (Thambawita et al., 2023). About 55% of the world's population resides in urban areas and this figure is estimated to increase to 68% by 2050 (Abass et al., 2022; Rainey et al., 2021). Also, urban cities with a population exceeding 1 million are expected to increase from 512 to 662 cities by 2030. This growth will force the acquisition of more land and accelerate competition in land use (Younes et al., 2023). Land use reflects human activities such as the use of land for different purposes whereas land cover refers to the physical condition or the biophysical state of the earth's surface (Frimpong, 2015). The actions of people in their environment directly affect the land cover, i.e. land use may lead to land cover change (Phong, 2004). Therefore, Aduah & Baffoe (2013) argue that when transformations in urban areas are not adequately managed they can lead to numerous social, economic, and environmental problems.

Africa, for instance, is experiencing a high rate of urban growth, but it is characterized by unplanned urbanization which is shown in the imbalance between the level of urbanization and its economic and industrial growth (Getu & Bhat, 2021). Despite urban areas occupying a relatively small portion of land size compared to other land cover types, the swift expansion of urban areas around the world, especially in Africa, is causing transformations in the land cover classes such as vegetation, farmland, forests, wetlands, and waterbodies (Alijani et al., 2020; Alqadhi et al., 2021; Han et al., 2015; Varghese & Singh, 2016). Krishnaveni & Anil (2022) further assert that in developing countries, urban development and land cover changes are often driven by a combination of socioeconomic, environmental, and institutional factors. These factors regrettably cause significant challenges such as informal settlements and slums, inadequate infrastructure, lack of adequate housing, land degradation, inequality and social exclusion, and climate change vulnerability (Mukherjee & Singh, 2020; Saha et al., 2021).

In Ghana, urban expansion primarily involves extensive and unrestricted outward growth, often at the expense of other land cover types (Frimpong et al., 2022; Nyamekye et al., 2020). From 1975 to 2010, Ghana witnessed a significant increase in its urban areas from 2560 km^2 to 3830 km^2 (Doe et al., 2022). Unfortunately, this rapid urbanization has led to the conversion of various land cover into residential and industrial areas. A report by the Sekondi-Takoradi Metropolitan Assembly (STMA), asserts that the metropolis is experiencing a surge in socio-economic activities, with multiple infrastructural projects across various sectors (STMA, 2011, 2013 & 2019; Mensah et al., 2019**)**. This increase intensified after the 2010 oil discovery in Ghana, drawing a notable influx of people and a surge in real estate activity (Fiave, 2017; Mensah et al., 2019). In this regard, between 2010 and 2013, the spatial development planning unit of Sekondi-Takoradi emphasized the changing landscape due to development pressures (Alqattan et al., 2019; Fiave, 2017; Mensah et al., 2019; STMA, 2013; Vinh & Nguyen, 2019). These changes pose challenges to the city's sustainability, conflicting with global development goals, particularly target 11.3 of SDG 11 (United Nations, 2015). Research work by Biney & Boakye (2021) and Mensah et al. (2019) revealed that the metropolis is experiencing an excessive increase in built-up and a rise in impervious surfaces. Such high levels of impervious surfaces are not recommended in sustainable cities due to their runoff potential, limited infiltration capacity, and low reflection of solar radiation. In this light, Aduah & Baffoe (2013) assert that if changes in urban areas are not properly handled, they can result in tragedies that will affect both the livelihood of urban dwellers and the sustainable development of urban lands. Fortunately, Sekondi-Takoradi is a business hub for local, national, and international organizations, therefore, any disaster in this area would have ripple effects on Ghana's economy.

Land use and land cover change (LULCC) can be monitored with the help of different geospatial techniques. Geographic Information Systems (GIS) and Remote Sensing (RS) have emerged as widely employed geospatial techniques for detecting changes in land use and land cover (Alqadhi et al., 2021; Frimpong et al., 2022; Hackman et al., 2020; Juma et al., 2022; Manesha et al., 2021; Tariq et al., 2022; Wangyel et al., 2021). For instance, through the analysis of satellite images, land cover transformations have been measured effectively and accurately compared to the traditional survey method (Shao et al., 2021). This viewpoint is supported by Dissanayake (2020), Hasan et al. (2023), and Rana & Sarkar (2021) as their studies demonstrated that using remote sensing and GIS to analyze the rate of land cover transformation is a time-efficient and cost-

effective method. In recent times, addressing the potential future LULC changes has gained international attention, therefore, various spatiotemporal prediction models have been developed to forecast land use and land cover changes (LULCC) (Satya, 2020). Among these, the Cellular Automata Markov Chain (CA-MC) model has been widely employed in spatio-temporal dynamic modeling for land-use change analysis because it serves as a reliable tool for predicting future LULC changes and is particularly effective for forecasting future LULC scenarios (Anom & Harisuseno, 2023; Doe et al., 2022; Gharaibeh et al., 2020; Rangarajan, 2022). In this context, GIS and remote sensing techniques were used to analyze the dynamics of land use and land cover of Sekondi-Takoradi Metropolis, and the CA-MC model was utilized to predict the future LULC for the year 2030.

This study will contribute to elucidating the increasing concerns of land cover changes in the Metropolis, and the negative consequences it has incurred over the study years. Therefore, city planners and policymakers will gain a comprehensive understanding of the multifaceted aspects and spatio-temporal dynamics of land use and land cover which will enable them to allocate resources efficiently and implement effective infrastructure management strategies accordingly. Also, the approach employed in this study can be used to evaluate urban growth in other cities in Ghana or other developing nations with comparable conditions. The extent to which this study area's land use and land cover has been studied in terms of its pattern, magnitude, rate, and spatiotemporal characteristics as well as its effects on the other LULC categories is lacking. It is against this background that this study aims to analyze the dynamics and future projection of land use land cover in the metropolis over the past 32 years (from 1991 to 2023).

3.2 Materials and Methods

The study's methodology has been sub-sectioned into 1. Study area (Figure 3.1) 2. Materials: Dataset used and Software 3. Method: this includes image pre-processing, selection of training and validation, image classification, accuracy assessment, and land use and land cover change analysis (Figure 4.3).

3.2.1 Study area

The Sekondi-Takoradi metropolis or the study area is situation at between latitude 4° 52' 30" N and 5° 04' 00" N and longitudes 1° 37' 00" W and 1° 52' 30"W. It serves as the administrative

capital of the western region and has with a land size of about 191.7 km^2. As of 2021, the population of the metropolis stood at 734,645 with 96.1% of the population living in urban areas and 3.9% living in rural areas (Ghana Statistical Service, 2021). This shows a significant number of people live in urban areas (Dadzie-Paintsil & Mensah, 2022; Ghana Statistical Service, 2010). Major industries and companies in the metropolis include oil and Gas, shipping and maritime service, mining and mineral processing, manufacturing and industrial processing, agriculture and agro-processing, construction and real estate, tourism and hospitality, and financial and business Services (Aduah & Mantey, 2023; Mensah et al., 2019). The Whin and Kansaworodo rivers are the only principal rivers of the metropolis and it experience two distinct rainfall seasons yearly. The minor season starts from August to November and the major season starts from April to July. From December to March is the dry season with a mean annual temperature of 22^{0}C. A pictorial description of the study area can be seen in Figure 3.1.

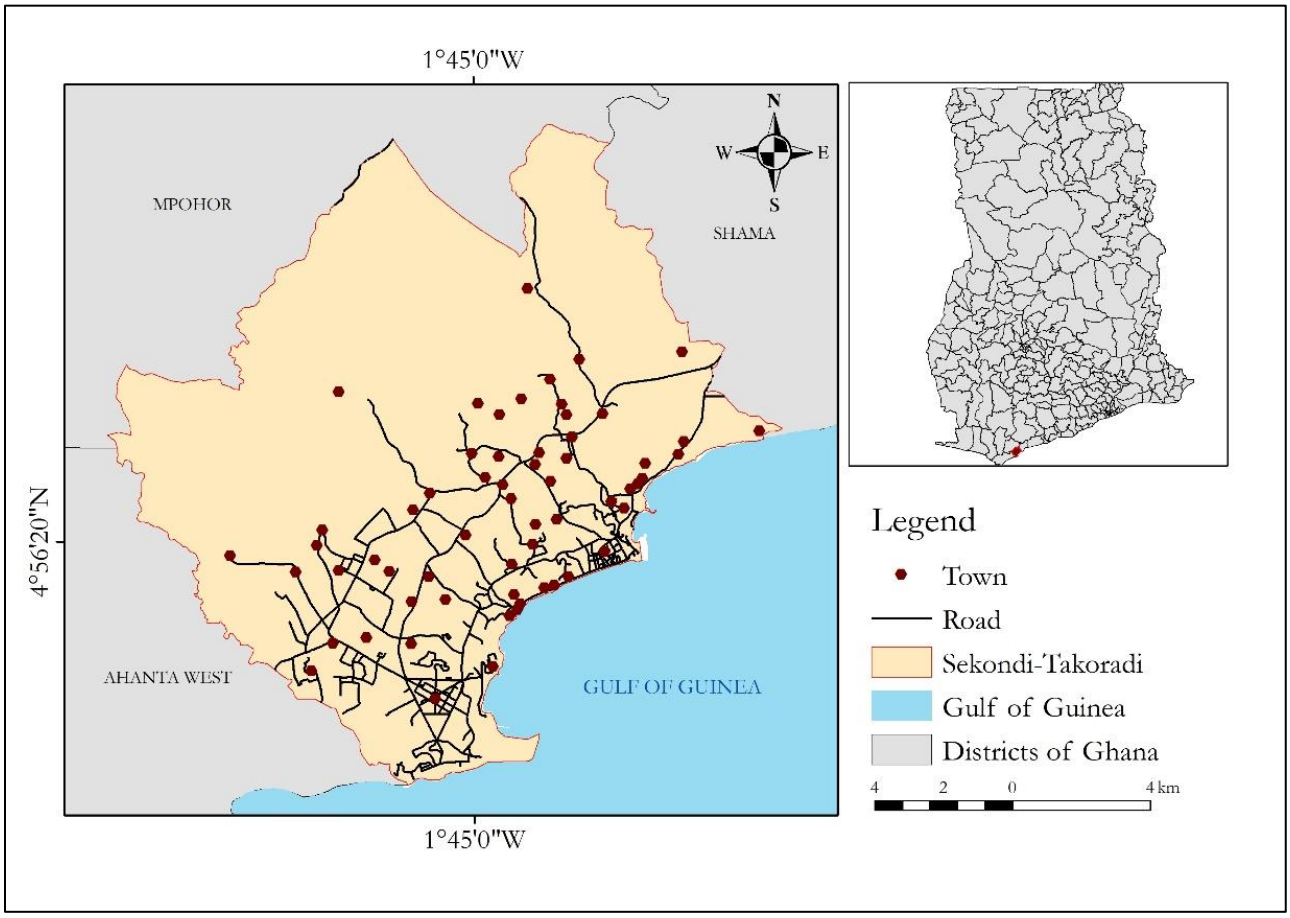

Figure 3.1: Map of the study area.

3.2.2 Datasets Used and Software

The data used for the study is shown in Table 3.1. They are categorized into Landsat images and referenced data. The Landsat images utilized in this study were downloaded from the United States Geological Survey (USGS) Earth Explorer and with a criterion of images having less than 10% cloud cover. The collection 2 level-1 Landsat images were chosen for the study because they have the best image quality in terms of radiometric consistency and atmospheric correction, and these images are surface reflectance data with meta-data and per-pixel quality information, therefore, considered suitable for time-series processing analysis (Kombate et al., 2022)**.** The study area falls within path 194 and row 057 of the Worldwide Reference System (WRS2). Given the study's extensive scope, the Landsat images were obtained from different Landsat sensors (Table 3.1). The Scanline errors in the 2009 and 2016 Landsat 7 ETM+ images (Figure 3.2) were rectified through a gap-filling process in Quantum Geographic Information System (QGIS.3.22). Moreover, the images were acquired in the same season for each year to prevent extreme differences in the reflectance dataset. Four images were used for the study to have a better understanding of how the land cover has changed over the years, however, the inconsistency in the image intervals was due to the lack of data with a cloud cover of less than 10%. Reference data were gathered from a variety of sources (Table 3.1). Google Earth images, GPS points, and land cover maps were used in training and assessing the accuracy of the classification. Using the stratified random sampling technique, 1,200 Ground Control Points (GCPs) were selected. Out of these, 840 (70%) were allocated for training, while the remaining 360 (30%) were set aside for validation.

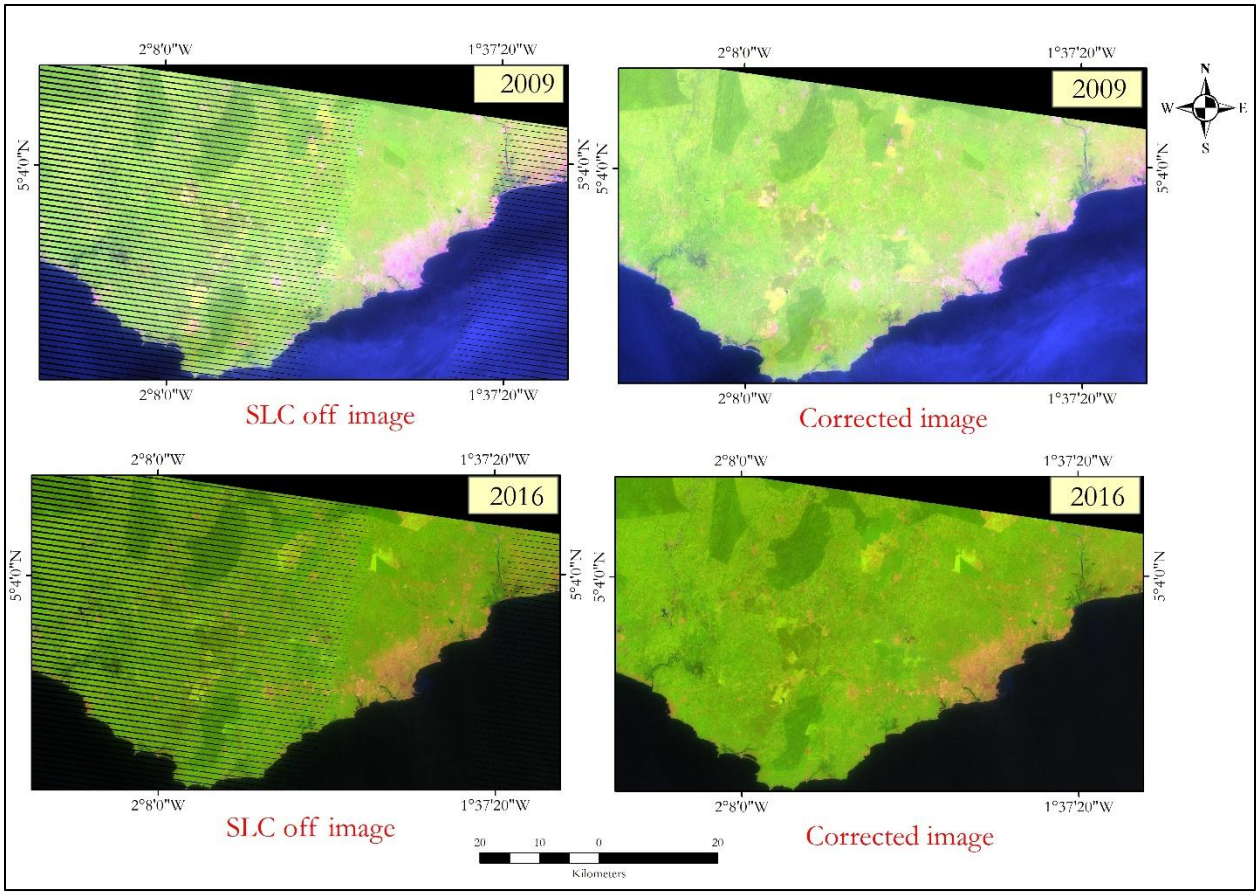

Figure 3.2: SLC off and corrected image of Landsat 7.

The Landsat images were pre-processed and processed using several software such as Google Earth Engine, QGIS, and ArcGIS Pro. The QGIS and Google Earth engine were used specifically to pre-process, classify, and assess the accuracy of the satellite images. ArcGIS Pro was used to produce all classified and output maps whereas the generation of change maps, transitional probability, and modelling and predicting future changes in the land cover was done using QGIS.

Table 3.1: Dataset used for the study.

Landsat image	Resolution	Date acquired	Source	No. of bands
Landsat TM	30m	01-1-1991	USGS	7
Landsat ETM+	30m	01-2-2009	USGS	8
Landsat ETM+	30m	06-1-2016	USGS	8
Landsat OLI/TRIS	30m	01-1-2023	USGS	11
Reference data				
Google Earth images		1991, 2009, 2016 and 2023	Google earth explorer	
Land cover maps		1991, 2009,2016	Forestry Department, Ghana	
Spatial variables (DEM, Slope, Proximity to road and city centre)	30m		USGS/Survey Department	

3.2.3 Methods

Quantifying changes in land cover through the use of remote sensing and geographic information systems entails a series of activities and intricate processes. This is because if the processing of multi-temporal images is not properly carried out to obtain precise and accurate information, significant changes will not be detected and proper analysis cannot be done. The method employed in this study is primarily categorized into four stages. These stages are Image Pre-processing, Image classification, Change Detection, and Modelling and Prediction of land cover change. A flow chart outlining the study's approach is shown in Figure 3.3.

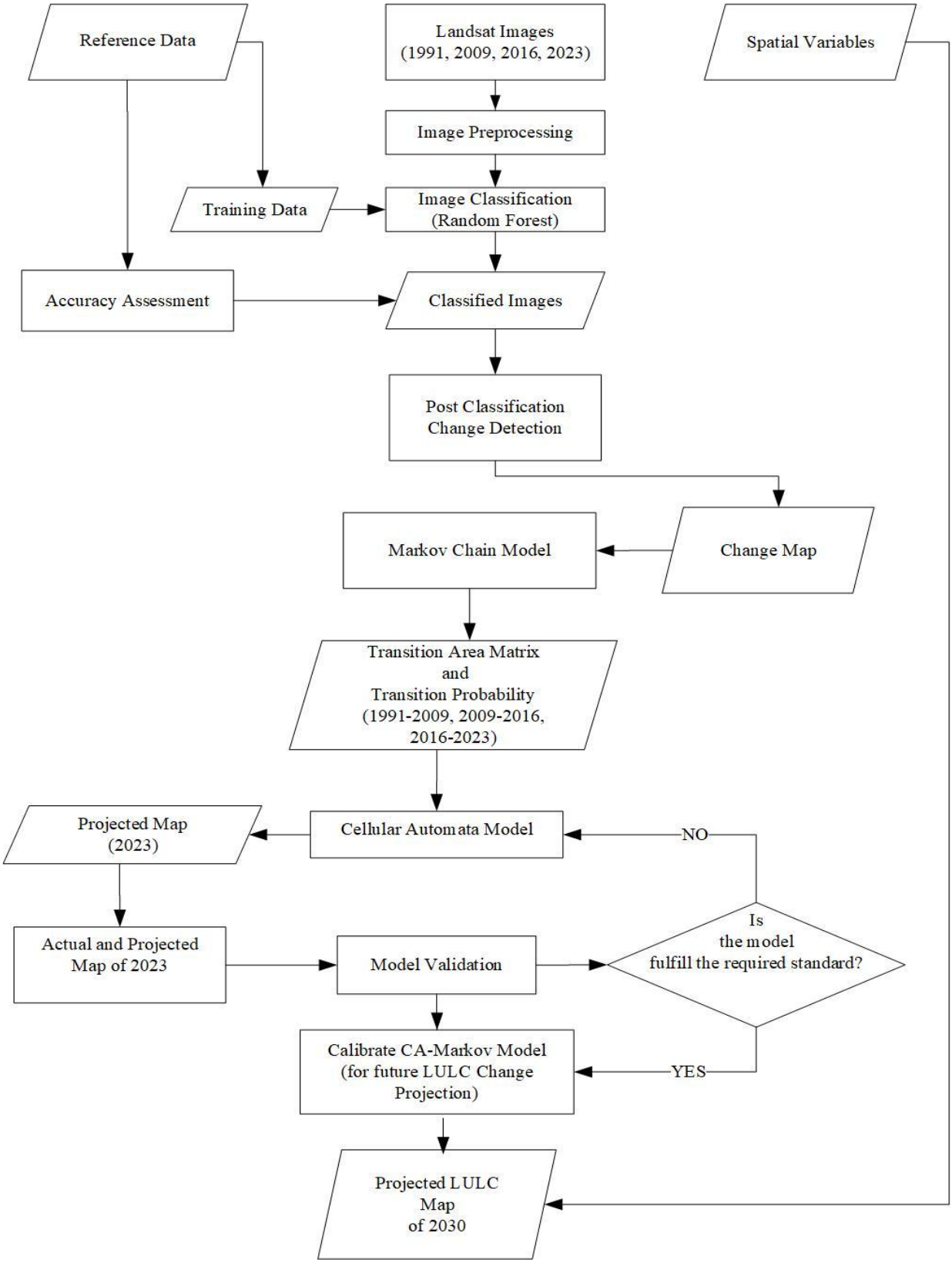

Figure 3.3: Methodological flowchart of the study.

3.2.3.1 Image Pre-processing

Satellite images need to be pre-processed to correct any errors caused by atmospheric influence, earth curvature, and sensor effects before image classification and change detection can be done efficiently (Gašparović, 2020). The image pre-processing that was conducted in this study were geometric corrections, radiometric corrections, and image band stacking. The acquired Landsat images were geometrically corrected from source and geo-referenced to 1984 World Geodetic System Universal Transverse Mercator Zone 30 North Projection (UTM '84 zone 30N). However, to ensure uniformity in the size and position of the acquired images, image-to-image registration was performed in QGIS using 2023 Landsat image as the reference image and then were reprojected to UTM '84 zone 30N (Abudu et al., 2019). With the image-to-image registration, the Nearest-Neighbour re-sampling approach was employed due to its ability to keep the pixel values of the source image. According to Anwar et al. (2022), errors that affect the quality of digital numbers of satellite images can be improved by radiometric correction. Radiometric correction is a crucial step in the preparation of satellite imagery since classification is done using radiometric values (Gašparović, 2020)**.** The radiometric correction performed on the images was carried out in QGIS by using the Semi-Automatic Classification (SCP) plugin. The bands of the Landsat images used in this study range from 1 to 11. These bands were combined to form a multi-colour band and displayed in different colour band combinations. Selecting the best band combination helps to better understand the features of the satellite image because band combination can extract specific and meaningful information from the image (Anwar et al., 2022). A False Colour Composite (FCC) was used to identify the land cover classes on the images for classification. The FCC was chosen because it produced distinct spectral signatures for easy identification of land cover classes such as water, vegetation, and Build-up which is needed for analysis (Abass et al., 2018).

3.2.3.2 Image Classification

One of the most important steps in extracting important information from satellite images is image classification (Saha et al., 2021). Image classification is the process of obtaining information by grouping all pixels in an image to have a set of classes (Saha et al., 2021b). In this study, the classification was done by first acquiring training samples, creating training sites, and employing the supervised classification technique. There are several supervised classification techniques available (Gašparović, 2020), but the study used the random forest supervised classification method to classify the images because it yields results with excellent accuracies and can work

efficiently on large datasets with higher noise levels (Kombate et al., 2022; Ullah et al., 2022) This has been proven in the works of Fernández-Delgado (2014) who evaluated 179 relevant classifiers from 17 families using 121 datasets and found random Forest to be the best classifier. Also, Random Forest is useful in calculating important information about errors, variable importance, and data outliers. Such information can be used to assess the performance of the model and make changes to the training data if necessary (Horning, 2010). The training samples were acquired from Google Earth images and GPS coordinates during field visits. In line with the objective of the study, the study area was classified into three classes, as explained in Table 3.2.

Table 3.2: A land cover classification scheme.

LAND COVER CLASS	EXPLANATION
Water	This includes the rivers, streams, and lakes, inland water in the study area.
Vegetation	This includes natural plants, trees, and green spaces.
Built-up or Settlement	This includes built-up areas or areas covered by made-made structures, impervious surfaces, residential areas, industrial areas, and commercial areas, paved areas, roads.

Source: Modified from Anderson Classification system, (1980).

3.2.3.3 Accuracy assessment

After pre-processing and image classification, the process of determining the accuracy of the classified images was carried out. This process is crucial because classification with inaccuracies will misguide the analysis of land use land cover (Othow et al., 2017; Mosammam et al., 2017). In this study, a validation dataset was used to assess the performance of the classified images. The validation dataset was obtained from high-resolution satellite images such as the Google Earth and from field surveys. Since the validation dataset used to assess the accuracy of the classification must be collected in the same period as the classified data (Gašparović, 2020), the study used a validation dataset that corresponded to the exact years of the classified images. The points for validation were randomly selected over the study area with samples for each class not less than 100 points. A total random point of three hundred for each year was extracted to perform the accuracy assessment. Using the confusion matrix, the accuracy of the classification results was assessed (Foody, 2020). Various measures such as overall accuracy, kappa coefficient, user's and producer's accuracy were computed from the confusion matrix (Abudu et al., 2019; García-álvarez

et al., 2022). The accuracy assessment parameters used in the classification accuracy can be expressed mathematically in the following equations (3.1 to 3.4) (Shamsudeen et al., 2022).

$$\text{User Accuracy} = \frac{\text{Number of correctly classified pixels in each category}}{\text{Total number of classified pixels in that category (the row total)}} \times 100 \quad (3.1)$$

$$\text{Producer Accuracy} = \frac{\text{Number of correctly classified pixels in eacg category}}{\text{Total number of classified pixels in that category (the column total)}} \times 100 \quad (3.2)$$

$$\text{Overall Accuracy} = \frac{\text{Total number of correctly classified pixels (Diagonal)}}{\text{Total number of reference pixels}} \times 100 \quad (3.3)$$

$$\text{Kappa Coefficient} = \frac{(\text{TS} \times \text{TCS} -) - \sum(\text{Column Total} \times \text{Row Total})}{\text{TS2} - \sum(\text{Column Total} \times \text{Row Total})} \times 100 \quad (3.4)$$

Where TS is the Total number of samples and TCS is the Total number of correctly classified samples.

3.2.3.4 Change Detection

Change detection is the process of identifying the differences in the condition of an object observed at various time intervals. Thus, it determines how much of an object has changed over a period. In this study, post-classification change detection was used to analyze the changes in the land cover (Elagouz et al., 2020). The rationale for employing post-classification change detection is that it offers detailed information regarding alterations in class cover relative to other classes, including the location, magnitude, and quantity of the change. (Alijani et al., 2020; Mensah et al., 2019; Stemn & Agyapong, 2014). This, according to Asare et al. (2023), makes it possible to have a change matrix, which helps to track any change in pixel between two time periods to ascertain the trade-offs between the classes. Based on the classified images, the post-classification change detection was conducted in QGIS. This involved computing the change statistics and generating change maps for the time steps (1991-2009, 2009-2016, 2016-2023, and 1991-2023) to determine changes that have occurred within the metropolis. Also, as part of the post-classification change detection, the annual rate of change and percentage annual rate of change was computed using

equations (3.5) and (3.6) respectively (Getu et al., 2021; Hussain et al., 2022; Deribew, 2020; Frimpong et al., 2022; Nath et al., 2023).

$$A_r = \left(\frac{A_2 - A_1}{T}\right) \quad (3.5)$$

Where A_r is the annual rate of change, A_2 is the current area of land use and land cover type in km^2, A_1 is the initial area of land cover type in km^2 and T= time interval between initial year (A_1) and the current year (A_2).

$$C = \left[\left(\frac{F-I}{I}\right) * \left(\frac{1}{T}\right)\right] * 100 \quad (3.6)$$

Where "C" is the percentage annual rate of change, "F "is the final year, "I" is the initial year, and "T" is the time period (interval) between the final year and the initial year.

3.2.3.5 Change transition and Prediction of land use and land cover

In this study, the cross-tabulation matrix was used to determine the growth and changes between all land use and land cover maps. According to Abdullahi & Pradhan (2017), the output of cross-tabulation can be in four types, namely: 1. cross-classification image, 2. full cross-tabulation table, 3. both cross-classification image and cross-tabulation table and 4. image similarity data only. To have a cross-tabulation table and cross-classification image, output type 3 was chosen for this study. Using the MOLUSCE matrix module in QGIS, four cross-tabulation tables from the classified maps 1991-2009, 2009-2016, 2016-2023, and 1991-2023 were produced for this study. Within the tabulation table, the elements in the diagonal positions represent classes that have not changed, whereas the off-diagonals represent classes that have changed. The horizontal elements indicate classes in a later time period (second year), while the vertical elements indicate classes in an earlier time period (first year). The last rows and columns of the tables are the total of each row and column and they indicate either a loss or gain for the various classes or land use categories. Growth occurs when there is a positive value and loss occurs when there is a negative value. According to Boakye et al., (2019), a predicted land cover type can be computed by the cellular automata predicting model. For the projection of land cover maps, the Modules for Land Use Change Evaluation (MOLUSCE) plugin software in QGIS was used to project future land use and land cover maps of 2030. Researchers such as Zaki et al. (2022**)**, Asare et al. (2023), Gaur & Rajendra (2023), Alqadhi et al. (2021), Satya et al. (2020), and Issiako et al. (2022) have used MOLUSCE to forecast future land use and land cover maps. The model parameters used in the

MOLUSCE for the simulation are Iteration rate: 1000, Learning rate: 0.001, Momentum: 0.02, Neighbourhood: 10px, Hidden layer: 10, and model iteration was set at 14 (Alqadhi et al., 2021; Khwarahm, 2021; Rangarajan, 2022).

3.3 Results and Discussion

3.3.1 Classified land use and land cover maps

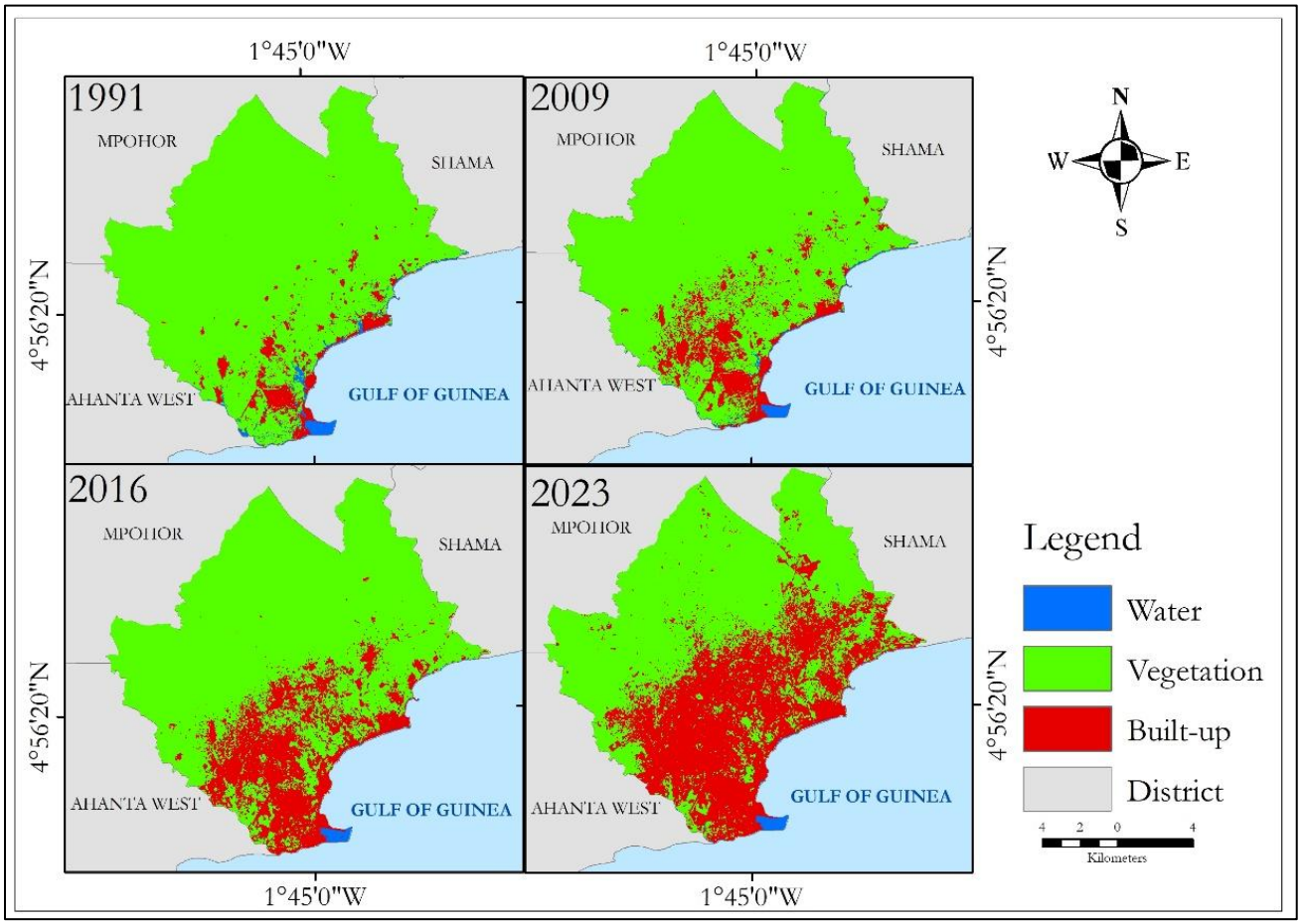

Figure 3.4**:** land use and land cover (LULC) maps from 1991 to 2023.

By visual interpretation of Figure 3.4, built-up areas increased significantly throughout the study periods while water and vegetation decreased over the years. A detailed statistical account of Figure 3.4 which comprises the total land area, area, and percentage cover of each class for the various years is presented in Table 3.3.

Table 3.3: Area statistics of land cover classes from 1991 to 2023

Class	1991		2009		2016		2023	
	Area (km^2)	(%)	Area (km^2)	(%)	Area (km^2)	(%)	Area (km^2)	(%)
Water	3.38	1.77	2.21	1.16	1.03	0.54	1.30	0.68
Vegetation	177.72	92.72	167.32	87.29	151.66	79.13	116.73	60.90
Built up	10.56	5.51	22.13	11.55	38.98	20.33	73.63	38.42
Total	**191.66**	**100**	**191.66**	**100**	**191.66**	**100**	**191.66**	**100**

From Table 3.3, the total area coverage of water in the year 1991 was 3.38 km^2 (1.77%) and it decreased to 2.21 km^2 (1.16%) in 2009. This decrease in water further decreased to 1.03 km^2 (0.54%) in 2016 but later increased in 2023 to 1.30 km^2 (0.68%). The water body decreased by 1.17 km^2 (0.61%) from 1991-2009, again decreased by 1.18 km^2 (0.67%) during 2009-2016, and then increased by 0.23 km^2 (0.14%) during 2016-2023 (Table 3.4). The decrease in water during the periods of 1991-2009 and 2009-2009 can be attributed to a substantial increase in infrastructural development or build-up (Fiave, 2017; Kumi-Boateng & Stemn, 2015; Mensah et al., 2019). This result corroborates the assertions of Mosammam et al. (2017) and Wangyel et al. (2021) that the expansion of built-up can have detrimental implications on the area coverage of water, especially, if not properly monitored. However, the increase in water was due to the consecutive flooding incidents that occurred in the years 2019, 2021, 2022, and 2023. In those years mentioned, several flood-prone areas experienced inundation. For instance, the Wetlands near New Takoradi and the Aboadze thermal plant, and areas near the Whin River experienced inundation as the banks of the river were breached, hence, leading to the submersion of numerous hectares of diverse land cover (Dadzie-Paintsil & Mensah, 2022). In General, the area of water was reduced by 2.08 (1.09%) between 1991 and 2023 as a result of the conversion to other land use and land cover classes primarily built-up as indicated in Figure 3.4 and Table 3.3. This suggests that people have encroached upon water areas for construction purposes. These waterways are often filled with sand and prepared for building and other construction activities. In the study of Aduah & Baffoe (2013), it was revealed that the waterways and waterbodies within the metropolis were being converted into built-up areas. Additionally, Dadzie-Paintsil & Mensah (2022) revealed that residents in communities such as New Takoradi, Kojokrom, Buabakrom, and Whindo in the

metropolis have encroached upon portions of the water bodies. A notable example is the Anankori River, where certain tributaries have been obstructed and filled with boulders to facilitate the transportation of quarry materials via heavy-duty trucks (Aklorbortu, 2019; Biney & Boakye, 2021). The state of these water bodies and channels compared to the 1990s signifies a high rate of encroachment and conversion into built-up which will deprive the metropolis of enjoying the benefits associated with water conservation (Danso & Addo, 2018).

Area coverage of vegetation in 1991 was 177.72 km^2 (92.72%) and this reduced to 167.32 km^2 (87.29%) in 2009. As witnessed in the previous year (2009), vegetation continued to decrease to 151.66 km^2 (79.13%) in 2016 and to 116.73 km^2 (60.90%) in 2023 (Table 3.3). Throughout the entire timeframe, the area occupied by the vegetation class continuously reduced. It experienced a reduction of 10.40 km^2 (5.43%) from 1991 to 2009, followed by a further decrease of 15.66 km^2 (8.16%) between 2009 and 2016. Subsequently, there was an additional decline of 34.93 km^2 (18.23%) between 2009 and 2023 (Table 3.4). Overall, from 1991 to 2023, the vegetation class consistently decreased, by 60.99 km^2 (31.82%) which is mainly due to the transformation of vegetation to built-up as seen in Figure 3.4. This outcome is in agreement with the notion that when the urban area is expanding the vegetation class becomes the prime target (Appiah, 2016; Daata et al., 2021). According to the Ghana Statistical Service (2015), the Sekondi-Takoradi metropolis has experienced a significant influx of migrants since 1991. This population growth has exerted pressure on the available green spaces, leading to the conversion of lands within and beyond the urban fringe for various purposes. A study conducted by Mensah et al. (2018) on urban green spaces in Sekondi-Takoradi revealed ongoing building projects at different stages of construction encroaching upon vegetative land and semi-natural green spaces. Within the metropolis, the Monkey Hill Nature Reserve, and the Whin Estuary, serve as prominent examples of semi-natural urban green spaces. These semi-natural green spaces are currently facing rapid encroachment due to population pressure, and so, pose a significant risk of diminishing the benefits such as preserving biodiversity, acting as carbon sinks, and supporting eco-tourism derived from these spaces. Further, the Independent Oil and Gas Information Centre (2017) revealed that about 49,000 people working in the oil and banking sectors are seeking for housing within the metropolis. This substantial demand for housing has incentivized landowners, predominantly chiefs and family members, to sell off green spaces to capitalize on the lucrative housing market (Yalley and Ofori-Darko, 2012). This situation aligns with the social disruption theory, which posits that the

discovery of oil precipitates the disintegration of societal systems (Ennis et al., 2013). In the case of the metropolis, this disruption is manifested through the loss of farmlands and the depletion of green spaces (Mensah et al., 2018b). In the same vein, the 2010-2013 Spatial Development Plan of the metropolis ascribes the swift decline of green spaces to infrastructure development, which has been partially influenced by the emergence of the oil industries (Mensah et al., 2019; STMA, 2013).

With the Built-up class, its area coverage in 1991 was 10.56 km^2 (5.51%), which then increased to 22.13 km^2 (11.55%) in 2009. It further expanded to 38.98 km^2 (20.33%) in 2016 and finally increased to 73.63 km^2 (38.42%) in 2023 (Table 3.3). Based on the analyses of land cover changes over time, it is evident that built-up consistently increased. Between 1991 and 2009, the built-up area expanded by 11.57 km^2 (6.04%), followed by a substantial increase of 16.85 km^2 (8.78%) between 2009 and 2016, and a significant growth of 34.65 km^2 (18.09%) from 2016 to 2023 (Table 3.4). Generally, from the period of 1991 to 2023, built-up expanded by 63.07 km^2 (32.1%). An explanation for this can be attributed to the increasing demand for land for various constructional purposes driven by population growth. and the upsurge in economic activities, which are partially connected to the oil discovery. This correlation has been emphasized by Ghana Statistical Service (2021) and is also supported by the works of Aduah & Mantey, (2023) and Dadzie-Paintsil & Mensah (2022). Before the oil discovery, the population of the metropolis in 2000 was 359,363. However, following the oil discovery, the population increased to 559, 548 in 2010 (Ghana Statistical Service, 2012). This surge in population was accompanied by migrants seeking employment opportunities as well as a corresponding rise in land demand for residential, commercial, and industrial purposes (Fiave, 2017) leading to the conversion of various land cover types into built-up. According to Mensah et al. (2019), the heightened demand for land for housing, especially, in 2011 led to a prompt intervention by real estate developers, and this birthed out the construction of housing projects like the Takoradi oil village and the King City to accommodate the growing population. Further, most establishments in the hospitality sector especially hotels had facelifts and expanded their facilities to accommodate more guests, while new establishments also emerged to meet the needs of affluent expatriates from the oil industry who relocated to the city (Biney & Boakye, 2021). Moreover, in 2010, the Urban Road initiated a plan to develop alternative routes and to expand existing single-lane roads into double-lane roads in the city. This led to the construction of the Kansaworado bypass. However, the construction of this bypass converted land

cover types into impermeable surfaces (Fiave, 2017; STMA, 2010). Also, the expansion of the Takoradi port, which commenced in November 2014 according to the Ghana Ports and Harbour (GPHA), affected approximately 53,000 hectares of arable land in New Takoradi and Poase (GPHA, 2016). These developments have contributed to the expansion of built-up areas.

Table 3.4: Trend of LULC Changes from 1991 to 2023.

A. Class	**1991 (km^2)**	**2009 (km^2)**	**Change (km^2)**	**1991 (%)**	**2009 (%)**	**Change (%)**
Water	3.38	2.21	-1.17	1.77	1.16	-0.61
Vegetation	177.72	167.32	-10.40	92.72	87.29	-5.43
Built-up	10.56	22.13	11.57	5.51	11.55	6.04
B. Class	**2009 (km^2)**	**2016 (km^2)**	**Change (km^2)**	**2009 (%)**	**2016 (%)**	**Change (%)**
Water	2.21	1.03	-1.18	1.16	0.54	-0.62
Vegetation	167.32	151.66	-15.66	87.29	79.13	-8.16
Built-up	22.13	38.98	16.85	11.55	20.33	8.78
C. Class	**2016 (km^2)**	**2023 (km^2)**	**Change (km^2)**	**2016 (%)**	**2023 (%)**	**Change (%)**
Water	1.03	1.30	0.27	0.54	0.68	0.14
Vegetation	151.66	116.73	-34.93	79.13	60.90	-18.23
Built-up	38.98	73.63	34.65	20.33	38.42	18.09
D. Class	**1991 (km^2)**	**2023 (km^2)**	**Change (km^2)**	**1991 (%)**	**2023 (%)**	**Change (%)**
Water	3.38	1.30	-2.08	1.77	0.68	-1.09
Vegetation	177.72	116.73	-60.99	92.72	60.90	-31.82
Built-up	10.56	73.63	63.07	5.51	38.42	32.91

The data presented in Table 3.3 and Table 3.4 demonstrate significant changes in land use and land cover classes. These changes, according to the annual rate of change (Figure 3.5), show that between 1991 and 2009, water and vegetation decreased annually by 0.06 km^2 and 0.58 km^2 respectively. However, an increased annual rate of change was observed in built-up by 0.64 km^2 within the same period. Between 2009 and 2016, there was a decline of 0.17 km^2 in water and 2.23

km^2 in vegetation each year, while built-up areas increased by 2.4 km^2 annually. Moreover, from the period 2016-2023, water and built-up increased annually by 0.04 km^2 and by 4.95 km^2 respectively whereas vegetation decreased by an annual rate of 4.99 km^2. Over the entire study period, water decreased annually by 0.06 km^2, vegetation decreased by 1.91 km^2, and built-up increased by 1.97 km^2 annually (Figure 3.5).

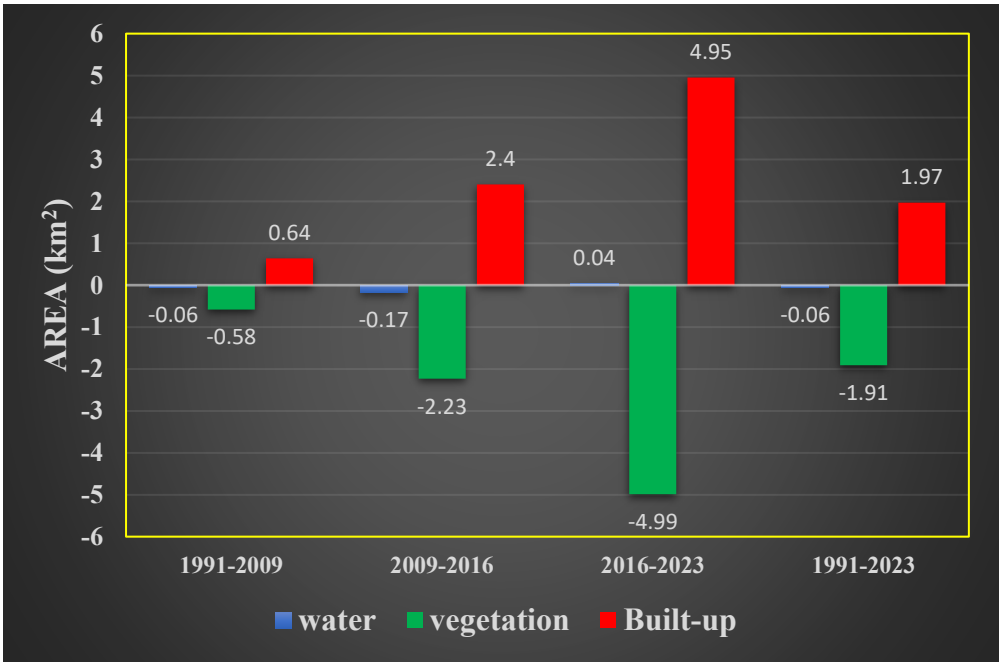

Figure 3.5: Annual rate of change from 1991 and 2023.

3.3.2 Accuracy assessment of LULC classification

To assess the accuracy of the classified images, the error matrix and Kappa statistic were employed (Krishnaveni & Anil, 2022). It was observed from Table 3.5 that an overall accuracy of 96.00% was obtained for the year 2023. Correspondingly, the overall accuracy for the year 2016 was 94.67%, 2009 was 90.67%, and that of 1991 was 87.67%. A Kappa coefficient of 0.82 was attained for 1991, 0.86 for 2009, 0.92 for 2016, and 0.94 for 2023. It is worth noting that the overall accuracy values presented in Table 3.5 exceeded the minimum 80% accuracy standard proposed by Siddiqui et al. (2018), Sarica et al. (2021), and Krishnaveni & Anil (2022). Therefore, the classification results can be used for further computation and analysis specifically, change detection analysis.

Table 3.5: Assessment of classification accuracy

Year	Producer's Accuracy			User's Accuracy			Overall Accuracy (%)	Kappa Coefficient
	Water	Vegetation	Built-up	Water	Vegetation	Built-up		
1991	88.66	86.41	88.00	86.00	89.00	88.00	***87.67***	***0.82***
2009	91.84	87.74	92.71	90.00	93.00	100	***90.67***	***0.86***
2016	94.06	93.20	96.88	95.00	96.00	93.00	***94.67***	***0.92***
2023	96.04	94.23	97.89	97.00	98.00	93.00	***96.00***	***0.94***

3.3.3 Transition probability

To gain deeper insights into the transformations that have occurred in the Sekondi-Takoradi Metropolis between 1991 and 2023, the change detection matrices depicted in Table 3.6 as well as the map of the transition matrices in Figure 3.6 provided a comprehensive breakdown of the LULC categories within the metropolis. From Table 3.6, the columns represent the land cover classes of the later date and the rows indicate the land cover classes of the earlier date. The diagonal elements of the transition matrices show the classes that have not changed between the earlier dates and the later dates. However, the off-diagonals of the transition matrices indicate changes that have occurred in the classes from the earlier dates to the later dates.

Table 3.6: Transition area matrices of various LULC from 1991 to 2023.

		2009			
	LULC Class	**Water (km^2)**	**Vegetation (km^2)**	**Built-up (km^2)**	**Total of 1991**
1991	Water	**1.40**	1.17	0.81	**3.38**
	Vegetation	0.75	**164.75**	12.22	**177.72**
	Built-up	0.06	1.40	**9.10**	**10.56**
	Total of 2009	**2.21**	**167.32**	**22.13**	
	Net change	***-1.17***	***-10.41***	**11.57**	
	Total unchanged	***175.25 (91.43%)***			
		2016			
	LULC Class	**Water (km^2)**	**Vegetation (km^2)**	**Built-up (km^2)**	**Total of 2009**
2009	Water	**0.99**	0.79	0.43	**2.21**
	Vegetation	0.01	**149.08**	18.24	**167.32**
	Built-up	0.03	1.79	**20.31**	**22.13**
	Total of 2016	**1.03**	**151.66**	**38.98**	
	Net change	***-1.18***	***-15.67***	***16.85***	
	Total unchanged	***170.38 (88.89%)***			
		2023			
	LULC Class	**Water (km^2)**	**Vegetation (km^2)**	**Built-up (km^2)**	**Total of 2016**
2016	Water	**0.99**	0.00	0.04	**1.03**
	Vegetation	0.10	**116.02**	35.54	**151.66**
	Built-up	0.21	0.71	**38.05**	**38.98**
	Total of 2023	**1.30**	**116.73**	**73.63**	
	Net change	***0.27***	***-34.93***	***34.66***	
	Total unchanged	***155.06 (80.90%)***			
		2023			
	LULC Class	**Water (km^2)**	**Vegetation (km^2)**	**Built-up (km^2)**	**Total of 1991**
1991	Water	**1.19**	0.58	1.61	**3.38**
	Vegetation	0.08	**115.93**	61.71	**177.2**
	Built-up	0.03	0.22	**10.31**	**10.56**
	Total of 2023	**1.30**	**116.73**	**73.63**	
	Net change	***-2.08***	***-60.99***	***63.08***	
	Total unchanged	***127.42(66.48%)***			

Between 1991 and 2009, it can be observed from Table 3.6 that 1.40 km^2, 164.75 km^2, and 9.10 km^2 of water, vegetation, and built-up respectively did not change. These unchanged classes covered a total of 175.25 km^2 (91.43%) while the classes that changed covered a total of 16.41 km^2 (8.56%). Of the transition that occurred among the land cover classes, the conversion from vegetation to built-up was the highest with an area of 12.22 km^2 while the conversion from built-

up to water had the least transition of 0.06 km^2. The increasing change in vegetation to built-up is by dint of increasing anthropogenic activities that occurred through the infrastructural development. This is proven in Table 3.6 where the rise in built-up at a rate of 11.57 km^2 was substantially from 10.41 km^2 decrease in vegetation and 1.17 km^2 loss in water.

From 2009 to 2016, the total land cover classes that remained unchanged covered an area of 170.38 km^2 (88.89%), and the total land cover types that changed occupied an area of 21.26 km^2 (11.10%). The unchanged area, in contrast to the transitional phase between 1991 and 2009 experienced a reduction of 4.87 km^2. Of the transitions that occurred among the land cover classes, the conversion from vegetation to built-up was the highest with an area of 18.24 km^2 while the conversion from vegetation to water had the least transition of 0.01 km^2. Lastly, the significant increase in built-up at a rate of 16.85 km^2 was mostly from 15.67 km^2 decrease in vegetation and 1.18 km^2 marginal decline in water. Between 2016 and 2023, the total land use classes that remained unchanged was 155.06 km^2 (80.90%) while the total area of classes that changed was 36.60 km^2 (19.10%). The unchanged area, when compared to the transition period of 2009 and 2016, decreased by 15.32 km^2 (Table 3.6). Further, amid the transitions observed from the period 2016 to 2023, the conversion from vegetation to built-up was the highest with an area of 35.54 km^2 while the conversion from water to vegetation was the lowest with no change. Notably, water and built-up respectively increased by 0.27 km^2 and 34.66 km^2 and this was at the drastic decline in vegetation by 34.93 km^2 (Table 3.6). From the result, vegetative land has been increasingly converted to built-up and this is a visible indication of degradation of vegetation quality.

Generally, between 1991 and 2023, the total land use classes that remained unchanged was 127.42 km^2 (66.48%) while the total area of classes that changed was 64.24 km^2 (33.52%) (Table 3.6). Further, amid the transitions observed from the period between 1991 and 2023, the conversion from vegetation to built-up was the highest with an area of 61.71 km^2 while the conversion from built-up to water was the lowest with an area of 0.03 km^2. Remarkably, built-up increased by 63.08 km^2 and this was at the considerable decline in vegetation by 60.99 km^2. This analysis underscores the increasing trend of converting vegetative land into built-up areas, highlighting a visible degradation in vegetation quality.

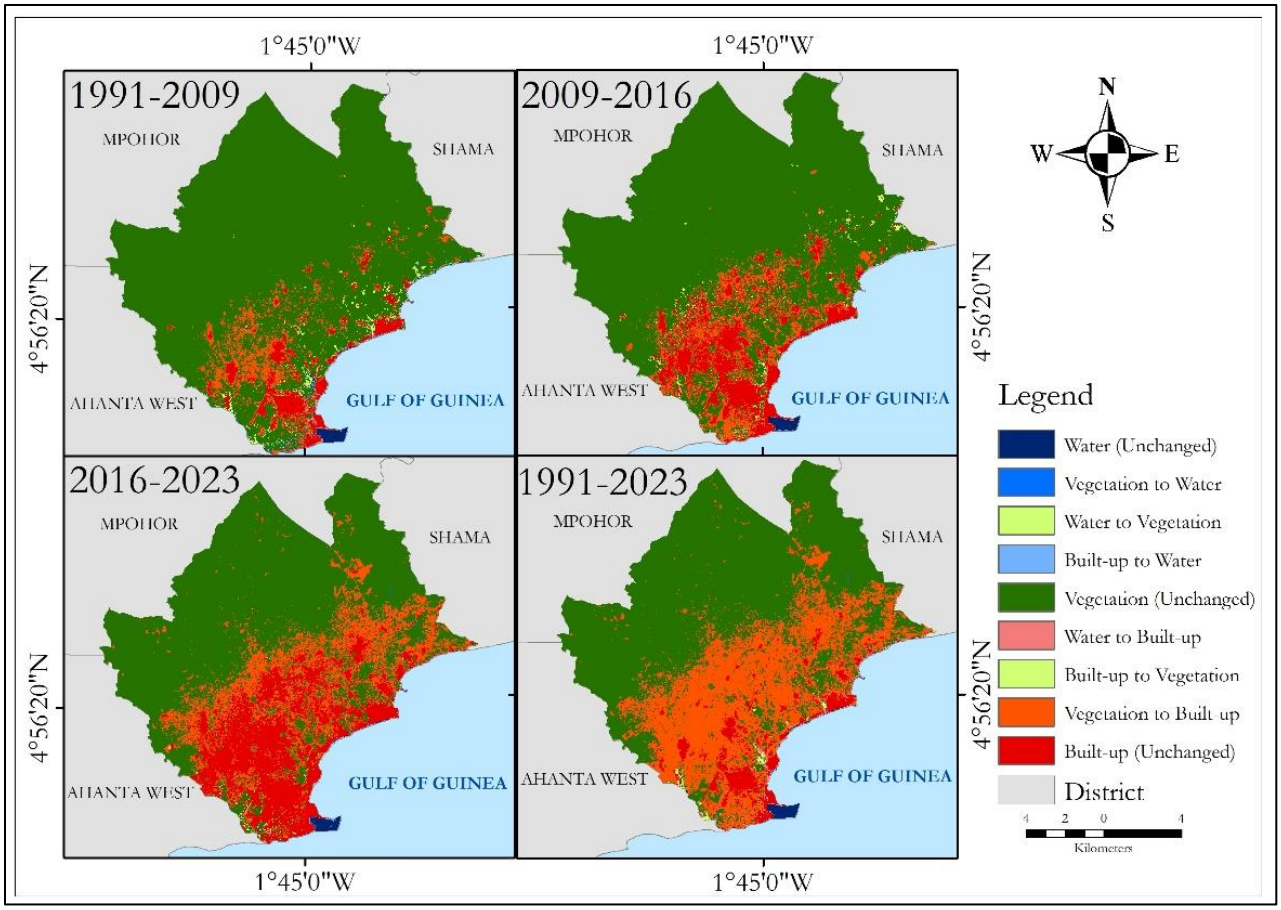

Figure 3.6: Map of transition matrices.

3.3.4 Spatial variables

After thoroughly analyzing the land use and growth pattern of the metropolis, factors that influence changes in land cover and urban growth were assessed. According to Aduah et al. (2020), how land is used in the Sekondi-Takoradi Metropolis and its surrounding areas is significantly influenced by some spatial variables such as elevation, slope, proximity to roads, and proximity to the Central business district (CBD) as depicted in Figure 3.7.

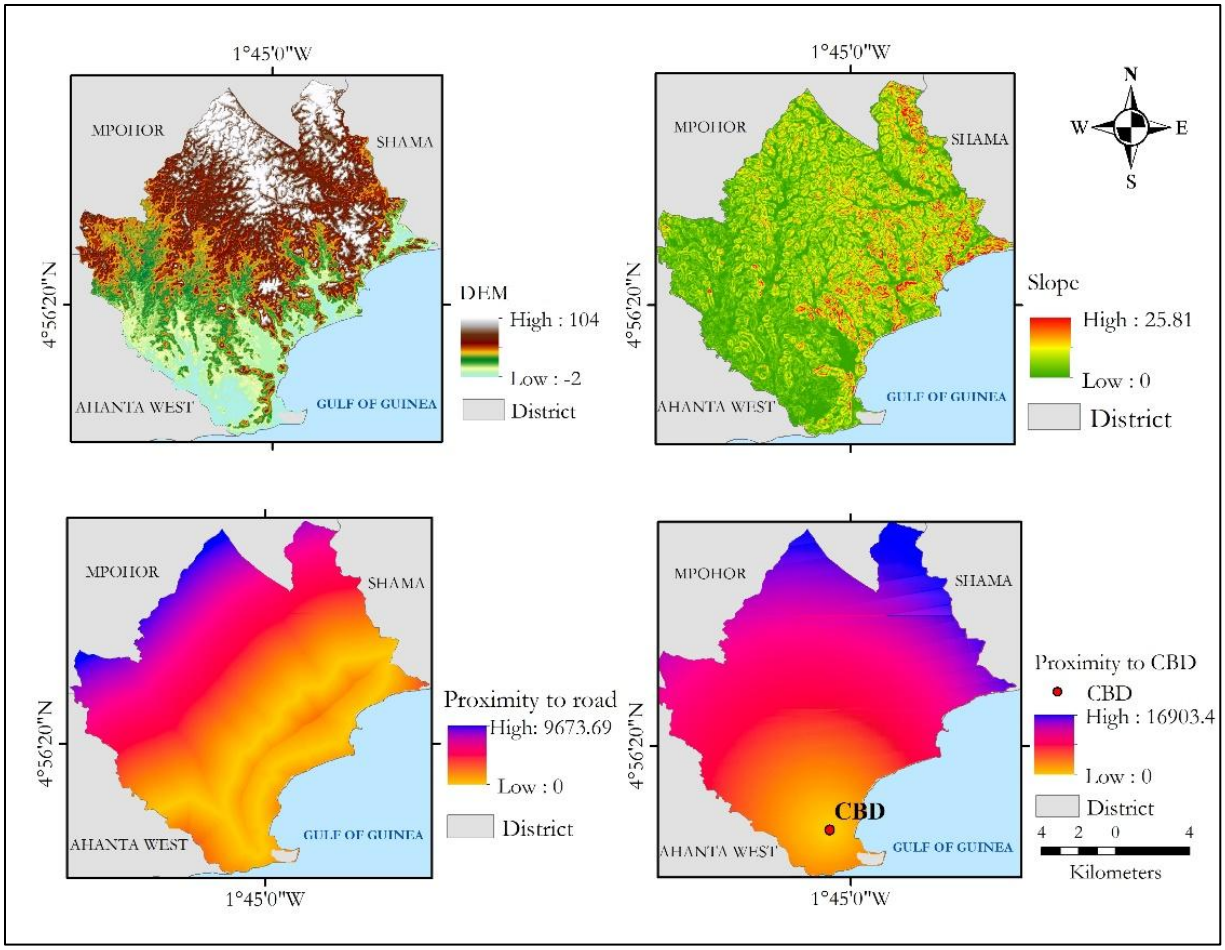

Figure 3.7**:** spatial variables Elevation(a), Slope(b), Proximity to major roads (c), Proximity to CBD (d).

To facilitate meaningful comparisons within the same range, the continuous raster maps were normalized using the minimum-maximum linear transformation technique (Siddiqui et al., 2018), as depicted in Figure 3.8.

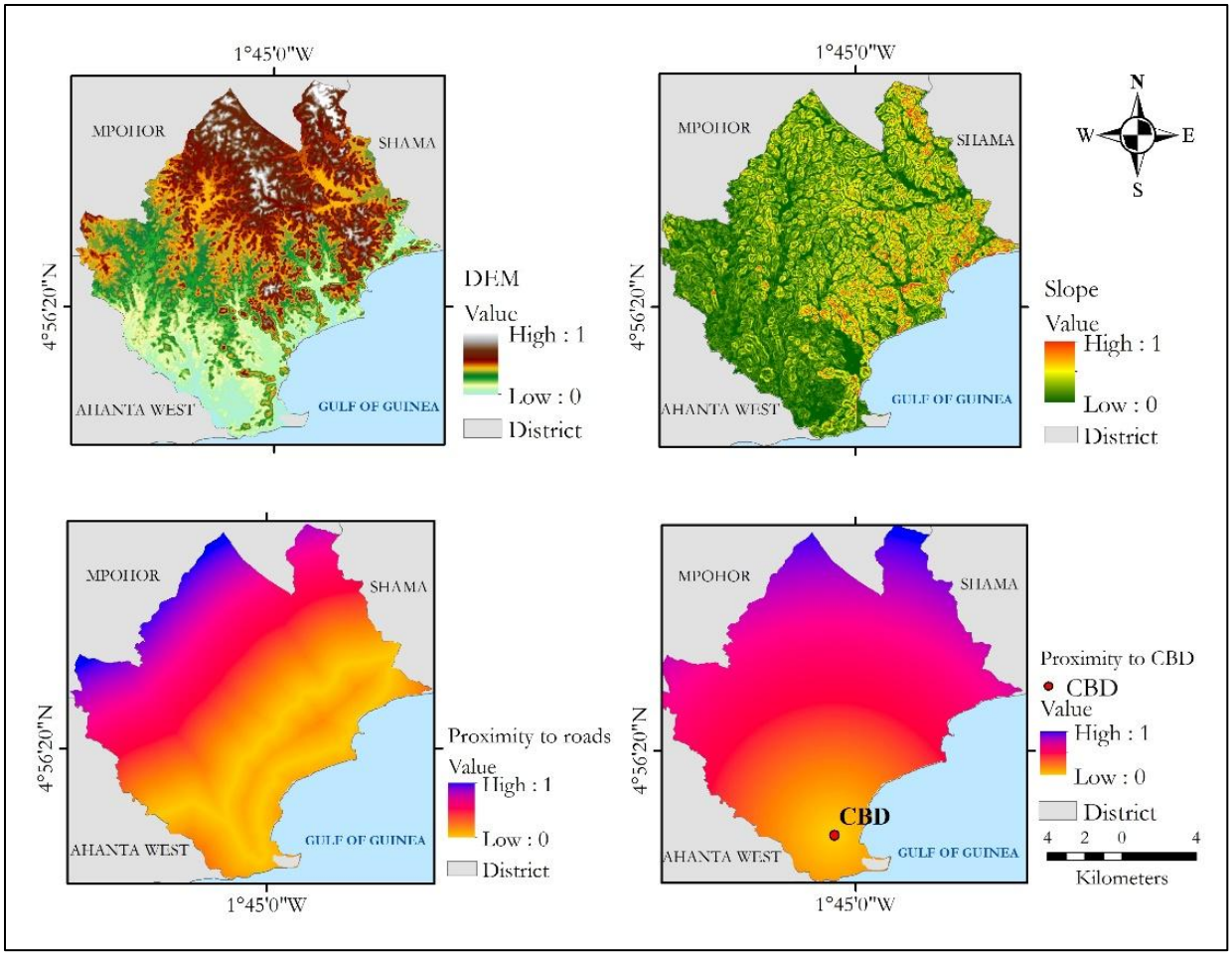

Figure 3.8**:** Normalized spatial variables Elevation(a), Slope(b), Proximity to major roads (c), Proximity to CBD (d).

3.3.5 Simulation and projection of land use and land cover map

To forecast the future trend of land use and land cover in the study area, first, the 2009 and 2016 images were used to stimulate 2023 classified images by employing the cellular automated-based approach as shown in Figure 3.9. Based on the stimulated 2023 classified image, water covered an area of 1.29 km^2 (0.67%), vegetation covered a land size of 118.02 km^2 (61.58%), and Built-up had an area of 71.35 km^2 (37.23%) (Table 3.7). Comparing the area statistics of the simulated 2023 classified images to the actual 2023 classified image in Table 3.8, the area of water reduced by 0.01 Km^2, vegetation reduced by 1.29 km^2, and built-up increased by 2.28 km^2. From Table 3.7, the stimulated 2023 classified image significantly modelled the actual 2023 classified image with

less than 2% variations which are insignificant according to Rana & Sarkar (2021). Therefore, the stimulated image was closely related to the actual 2023 image.

Table 3.7: Area statistics of simulated 2023 and actual 2023 land use and land cover.

Simulated 2023 LULC			Actual 2023 LULC			Difference (A-S)
Class	**Area (km^2)**	**%**	**Class**	**Area (km^2)**	**%**	**Area (km^2)**
Water	1.29	0.67	Water	1.30	0.68	-0.01
Vegetation	118.02	61.58	Vegetation	116.73	60.90	-1.29
Built-up	71.35	37.23	Built-up	73.63	38.42	+2.28
Total	**191.66**	**100**	**Total**	**191.66**	**100**	

S = Stimulated 2023 LULC and A = Actual 2023 LULC

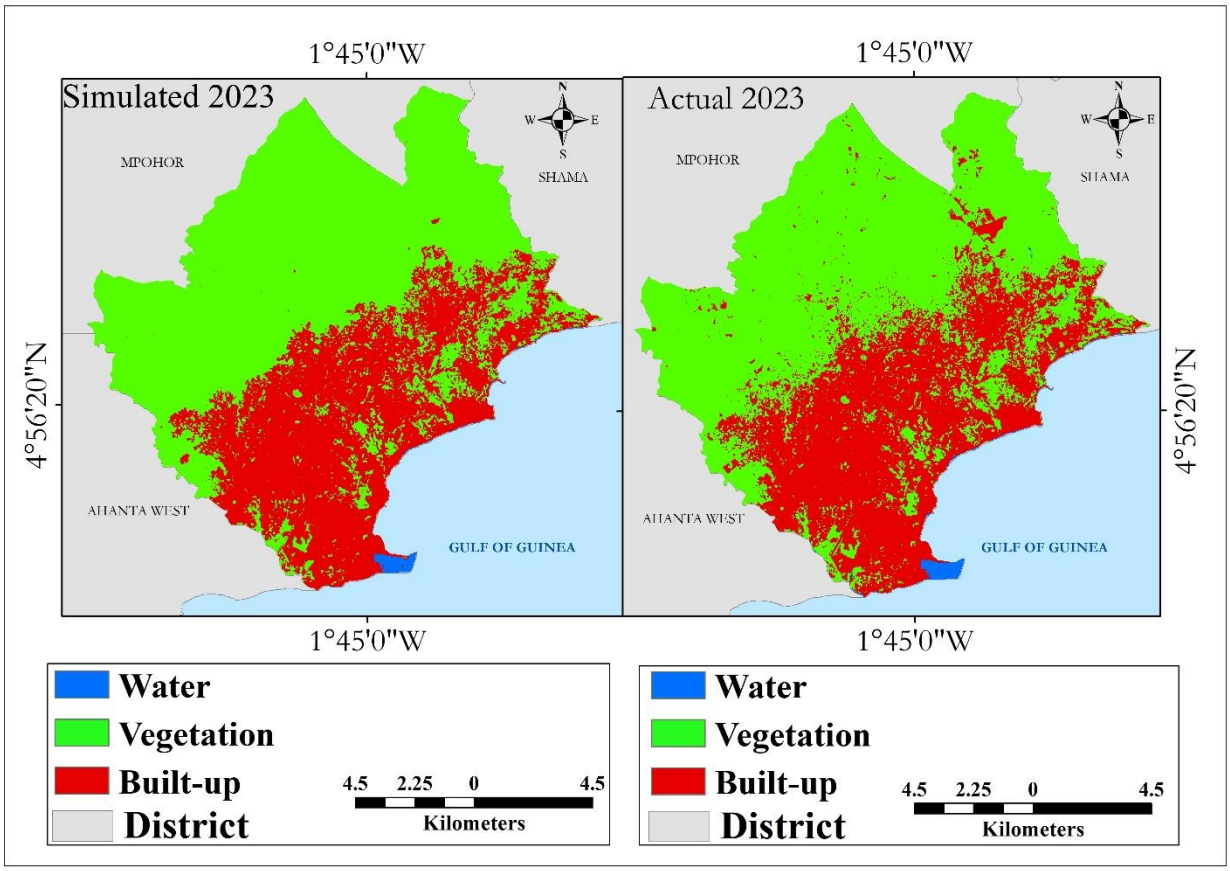

Figure 3.9: Simulated and Actual 2023 land use and land cover map.

According to Satya et al. (2020), predicting land use and land cover is deemed reliable only when it is validated against the existing data. Therefore, the simulated 2023 image was validated with the actual classified 2023 image in Figures 3.4 and 3.9. To determine the accuracy of the simulated

2023 image, four kappa statistics parameters namely; percent correctness, kappa location, kappa histogram, and overall kappa were computed (Table 3.8).

Table 3.8: Kappa index for simulated 2023 LULC with actual 2023 as reference.

Parameters	Value
Kappa (overall)	0.86
Kappa (histogram)	0.87
Kappa (location)	0.94
% of correctness	89.88

Kappa (location) is used to assess the simulation's capacity to detect location while Kappa (overall) is used to assess the overall performance of the simulation (Satya et al., 2020). Kappa coefficient of 0 means no agreement exists between simulated and actual images whereas 1 means a perfect agreement. From Table 3.8, there exists a significant agreement between the simulated and actual 2023 LULC and that the model is good and reliable for projecting future land use and land cover of 2030. As the validation yielded a good agreement—where the accuracy parameters were above 80%—the same process was used to project 2030 land use and land cover. The projected 2030 land use and land cover is shown in Figure 3.10 with its area statistics in Table 3.9.

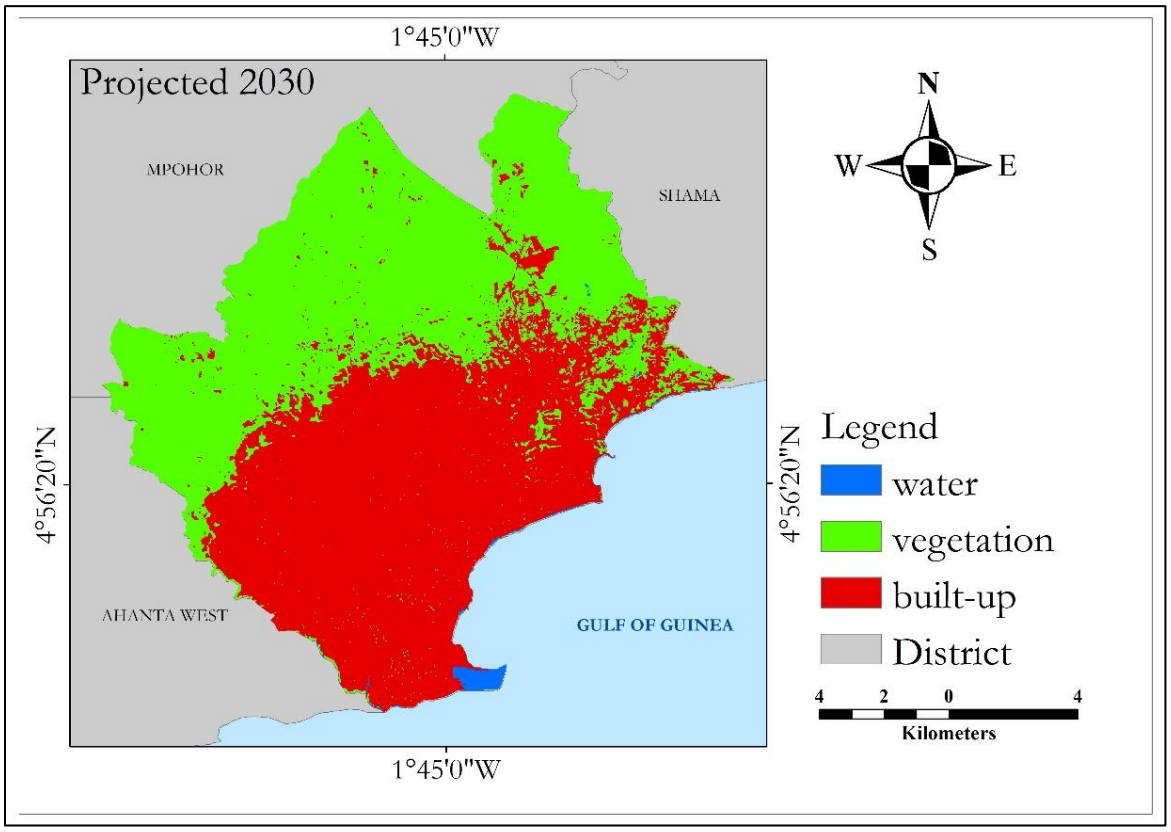

Figure 3.10: Projected LULC map of 2030.

The selection of the year 2030 for projecting land use and land cover changes aligns with the strategic pursuit of target 11.3 of the eleventh Sustainable Development Goal (SDG) (Andersson et al., 2016; Shao et al., 2021; UN, 2017). According to Figure 3.10, water is expected to decrease to 1.21 km^2 (0.63%), vegetation is expected to 95.31 km^2 (49.73%) and built-up will go up to 95.14 km^2 (49.64%) (Table 3.9). The output of Figure 3.10 shows that a significant conversion of other classes to built-up will mostly take place in the Western and South-Western parts of the metropolis. The western part of the metropolis borders the Ahanta West district (Figure 3.1; Mensah et al., 2019), and the operational sites of most oil companies in the Ahanta West district are also closer to the Western and South-western parts of the metropolis (Mensah et al., 2019). Therefore, these operational sites of oil companies serve as a pull factor for settlement and infrastructural development which may be a reason for the higher conversion of other classes into built-up at the Western and the South-western parts of the metropolis. Moreover, in the South-western part of the metropolis is located the Takoradi airport, market circle, the Takoradi Harbour, companies, and the central business district. These infrastructural developments and places are mostly known for their influence on population increase which brings increasing demand for land for residential, industrial, and commercial purposes (Vinh & Nguyen, 2019; Yankson et al., 2017). The projected pattern of built-up rapidly converting significant land covers like vegetation and water aligns with findings from various urbanization studies conducted in developing countries (Abudu et al., 2019; Asare et al., 2023; Hackman et al., 2020; Krishnaveni & Anil, 2022; Tariq et al., 2022). Therefore, for the metropolis to circumvent the irreversible challenges experienced by many cities, due to the increase in built-up, the metropolis must transition from its current business model and swiftly embrace an ecosystem-based approach to urban development as suggested by Wangyel et al. (2021).

Table 3.9: Area statistics of Projected 2030 land use and land cover.

Class	**Area (km^2)**	**%**
Water	1.21	0.63
Vegetation	95.31	49.73
Built-up	95.14	49.64
Total	**191.66**	**100**

Lastly, in assessing how different the projected 2030 map will be from the classified 2023 map, it was revealed that water and vegetation will respectively decrease by 0.09 km^2 and 21.42 km^2 while built-up will increase by 21.51 km^2. The decrease in water and vegetation will occur at an annual rate of 0.01 km^2 and 3.06 km^2 whereas built-up will increase annually at a rate of 3.07 km^2 (Table 10). This means the metropolis is becoming more urbanized and will continue in the development of new infrastructures as evidenced in Table 3.9. However, as indicated by Abudu et al. (2019), the metropolis must attain a sustainable balance that can manage infrastructure development, population growth, and environmental preservation as it expands because the increase in impervious surfaces at the expense of natural vegetation, water, and proper planning makes a city or an urban area susceptible to urban flooding and urban heat which affect the quality and survival of life in the urban environmental (Doe et al., 2022; Hussain et al., 2022).

Table 3.10: Change detection between 2023 LULC and Predicted 2030.

LULC Class	2023 (km^2)	2030 (km^2)	Area (km^2)	Percentage Change (%)	Annual change rate (km^2)
Water	1.30	1.21	-0.09	-6.92	-0.01
Vegetation	116.73	95.31	-21.42	-18.35	-3.06
Built-up	73.63	95.14	21.51	29.21	3.07

3.4 Discussion

Studies on land use land cover (LULC) have been carried out at the local, regional, and global levels. Unfortunately, many of these studies have focused on developed countries with few studies addressing developing countries (Hussain et al., 2022). This study examined the spatio-temporal dynamics of land use and land cover in the metropolis and projected future LULC trends.

Using the random forest classification technique, the classification accuracy exceeded the 80% threshold recommended by Tarawally et al. (2019) as acceptable for classification using a medium-resolution dataset. In comparison with studies of Kumi-Boateng & Stemn (2015) and Mensah et al. (2019) that used maximum likelihood for image classification, the accuracies of this study were higher. This can be attributed to the classifier's robustness to outliers and inherent design capabilities. Moreover, Chowdhury (2024) concludes that the random forest technique performs better compared to other classifiers. As the above-cited works have proven random forest to be a better classifier than the traditional techniques, it is urged that attention should be given to

its use in image classification. Analysis of the post-classification LULC revealed a significant increase in built-up and a decline in vegetation and water over the study period. This indicates a growing human impact in the metropolis through urban development and infrastructure expansion. According to Aduah et al. (2020), land use in the metropolis is predominantly geared toward built-up areas, corroborating the observed increase in built-up as identified by this study over the past 32 years. Environmental and governmental agencies within the metropolis have the mandate to prevent encroachment into unauthorized areas and protect the natural reserves of the city. However, the LULC analysis revealed trends that appear misaligned with these mandates, suggesting the potential ineffectiveness of these agencies in fulfilling their roles, which may contribute to the uncontrolled nature of physical land development in the area.

In Ghana, much of the substantial growth in urban built-up areas is driven by population growth (Addae, 2019) and increased economic activities (Mensah et al., 2019). The case of the metropolis serves as evidence as its population increased from 360,000 in 2000 to 560,000 in 2010 (Ghana Statistical Service, 2021; Ghana Statistical Service, 2014). This surge in population can be attributed to the oil discovery of oil in 2007 and increased socio-economic activities which made the metropolis a point of attraction for migrants and industries, and a business hub for local, national, and international companies (Dadzie-Paintsil & Mensah, 2022; Fiave, 2017) Unfortunately, these industries and migrants require land for residential and industrial purposes, causing an increased demand for housing, rising land conversion for built-up areas, and increased settlement at the city's peripheries where land prices are comparatively cheaper (Addae, 2019; Mensah et al., 2019). Additionally, from the projected LULC, built-up is expected to increase while other land covers are expected to further decrease. Reducing vegetation and increasing impervious surfaces can lead to an increase in CO_2 emissions (Kafy et al., 2022). A study by Juma et al. (2022) revealed that changes in LULC, specifically the expansion of built-up areas and reduction in vegetation, increase an area's vulnerability to flooding and heat islands, and ultimately affect the quality and quantity of water resources. As noted by Larbi (2023), implementing appropriate measures to control improper buildings can mitigate climate change-related risks such as floods and heat.

The outlook of future LULC trends not only provides evidence of rapid urbanization but also offers important information and guidance to city planners and authorities on where to anticipate growth

or change as well as aid them in prioritizing development efforts (Addae, 2019). This would help alleviate slum and informal settlement occurrences in the metropolis. Land use land cover (LULC) is a critical element that can aid decision-makers in developing effective plans for achieving sustainable development (Larbi, 2023). For instance, the significant loss in vegetation and water identified in this study is valuable information for developing indicators to monitor relevant CO_2 emission goals under SDG 13 and urban resilience indicators under goals SDG 11.

3.5 Conclusion

The study employed Landsat images to examine the dynamics of land use and land cover within the Sekondi-Takoradi metropolis from 1991 to 2023. Through the use of the random forest classification method, the Landsat images were classified images into three categories. Notably, the most significant class conversion observed during this period was the depletion of vegetation, with a substantial portion of 60.99 km^2 converted into built-up land. The study, further showed that the metropolis has expanded its sphere of influence greatly to the south and south-western boundary by annexing nearby towns and communities over the last three decades. The methodology employed in this study can be adapted to assess changes in the land cover in other metropolises in Ghana or similar developing countries. Understanding the changes in land use and land cover is vital for achieving the Sustainable Development Goal of creating inclusive, safe, resilient, and sustainable urban environments. Decision-makers, urban planners, and policymakers can leverage these findings to address inadequately enforced land-use regulations and develop effective plans, strategies, and policies to optimize resource and infrastructure allocation. However, to enhance the accuracy of the findings, further research is needed to encompass other aspects of urban sprawl dynamics, such as its various drivers and a landscape metrics analysis in different directions.

3.6 Publication

The objective of this work has been published with the title below in the Scientific African Journal of Elsevier.

A comprehensive analysis and future projection of land use and land cover dynamics in a fast-growing city: A case study of Sekondi-Takoradi metropolis, Ghana

Biney, E., Forkuo, E. K., Poku-Boansi, M., Asare, Y. M., Hackman, K. O., Yankey, D. B., Agbenorhevi, A. E., & Annan, E. (2024). A comprehensive analysis and future projection of land use and land cover dynamics in a fast-growing city: A case study of Sekondi-Takoradi metropolis, Ghana. *Scientific African*, *24*(February), e02207. https://doi.org/10.1016/j.sciaf.2024.e02207

CHAPTER 4: QUANTIFY THE INTENSITY OF URBAN EXPANSION AND ITS DEGREE OF DISPERSION AND COMPACTION OVER THE STUDY PERIOD

ABSTRACT

The upsurge in economic activities and urban dwellers has stimulated sprawl-like growth in the Sekondi-Takoradi metropolis. This study used Landsat imageries and spatial metrics such as Shannon entropy and relative entropy, Urban Expansion Intensity Index (UEII), Annual Urban Expansion Rate ($AUER_i$), and landscape metrics to quantify the intensity of urban expansion and its degree of dispersion and compaction over the study period. Analysis of the study revealed an increase in built-up by 63.07 km^2 while the urban expansion intensity Index (UEII) and annual urban expansion rate ($AUER_i$) values of 6.26% and 4.70% respectively revealed the metropolis is expanding at a high speed which indicates the high susceptibility of experiencing urban sprawl. The presence of sprawling characteristics was confirmed throughout the application of landscape metrics which revealed a greater degree of fragmentation in the landscape. Further, the Shannon and relative entropy result (which ranged from 2.17 to 2.47 and 0.76 to 0.87) showed that the metropolis has been expanding by dispersion from 1991 to 2023. Consequently, this has resulted in substantial changes in the land cover patterns of the metropolis. This study provides valuable insights into the spatial dynamics of the metropolis, which will guide policymakers in addressing the environmental challenges associated with urban expansion.

Keywords: Urban sprawl; Sekondi-Takoradi; Shannon's entropy; Landsat; Geospatial techniques; urban expansion intensity index.

4.1 Introduction

Given how advanced and connected the world has become, the global urban population has increased rapidly from 1 billion in 1960 to 4.4 billion in 2020 (Friedrich, 2021; Tariq, Yan, et al., 2022) and estimated to increase to 68% by 2050 (Rainey et al., 2021; United Nations, 2020). According to Østby (2016), a bulk of the estimated urban population growth will take place in Africa and Asia, and this calls for proper planning to accommodate the growing population (Anande & Park, 2021; Satterthwaite et al., 2020). This is because if transformations occurring in urban areas are not adequately managed, they can lead to numerous social, economic, and environmental problems (Aduah & Baffoe, 2013; United Nations, 2019). Globally, industrialization has contributed significantly to transforming rural areas into urban areas, a process known as urbanization. Unfortunately, urbanization adversely results in land cover transformation, primarily marked by an increase in built-up and impervious surfaces (Chettry, 2022). This makes Surya et al. (2021) asserts that urbanization is intricately linked with urban sprawl by acting as a catalyst for urban sprawl.

Urban sprawl refers to the dispersion of built-up commonly marked by low-density development, unregulated, and spontaneous growth (Akubia & Bruns, 2019; Feng & Gauthier, 2021). It is characterized by haphazard and random low-density patterns of urban growth, leading to inefficient resource utilization (Kamruzzaman et al., 2018). The term urban sprawl is often used interchangeably with urban growth despite having different conceptual meanings (Viana et al., 2019). Urban growth resulting from unregulated or haphazard development is referred to as urban sprawl. This phenomenon is often viewed negatively, as it tends to exacerbate various urban challenges, including land degradation, and water and air pollution, all of which have detrimental effects on human health (Viana et al., 2019). The sprawl phenomenon, according to the concentric[1] zone theory occurs when cities expand uncontrollably by extending their concentric land use zones outwards from Central Business District (CBD). Research by Getu et al. (2021) and Shao et al. (2021) highlight that urban sprawl is primarily exacerbated by rapid population and socioeconomic

[1] Details of the concentric zone theory as well as other sprawl theories such as Von Thünen, Central Place, Sector, Multi Nuclei Bid–Rent are presented in Pradhan (2017).

development, and its occurrence in both developed and developing countries has made it an issue of global concern.

In Africa, over half of the urban population resides in low-lying coastal regions (Nieves et al., 2020), and between 2000 and 2030, population growth in developing nations is projected to double whereas urban areas are expected to triple. Regardless of the challenges of urban growth currently observed, Tarawally et al. (2019) posit a continuous increase even after 2100. The occurrence of urban sprawl in both developed and developing countries has made it an issue of global concern. In developed nations, urban sprawl becomes worse after reaching saturation levels of urbanization. However, most developing countries, at the beginning of urbanization are predisposed to sprawl at an exacerbated scale due to high population growth and densities, characterized by inadequate basic amenities and infrastructure, unlike the developed countries where the saturated level of urbanization is fueled by industrialization, technological support, and a prosperous economy (Krishnaveni & Anil, 2022).

In Ghana, most people are currently living in urban areas and this is due to the alarming rise in its population from 6 million in 1975 to 32 million in 2021 (Ghana Statistical Service, 2021). Unfortunately, rapid urbanization is not commensurate with proper urban planning in most cities. As a result, people tend to settle in places that do not conform to the spatial plan of the city (Frimpong et al., 2022; Nyamekye et al., 2020). This has massively affected the urban environment as it leads to significant transformation in environmental ecological processes and heightens the susceptibility of urban regions to environmental challenges (Afriyanie et al., 2018). Ineffective and under-resourced planning agencies, challenges related to land title acquisition, and the complexities of the land tenure system have significantly contributed to Ghana's environmental challenges (Albert & Yiran, 2021). However, Buo et al. (2021) assert that the transition to democratic governance, the adoption of the 1992 Constitution and Ghana's open-door policy toward capital investment, and the free movement of people within the West African region have further contributed to and accelerated the urbanization process in Ghana. According to the Ghana Statistical Service (2021), the high rate of urbanization is changing the structures of major cities in Ghana. This increasing transformation in urban areas directly affects urban land use and also changes the land use pattern (Abass et al., 2022). Over the past thirty years, the Sekondi-Takoradi metropolis has undergone significant transformation, intensifying the existing pressures and

environmental challenges faced by its residents. This transformation is reflected in the rising influx of migrants seeking employment, the high conversion rate of undeveloped areas into built environments for residential and commercial use, and the continuous population growth (Alqattan et al., 2019; Fiave, 2017**).** For instance, before the oil discovery in 2000, the metropolis had a population of about 360,000. However, after commercial oil exploitation started in 2010, the population stood at about 560,000 (Fiave, 2017) and in 2017, the metropolis had a growth rate (of 3.2%) which was higher than the national growth rate (Mensah et al., 2019**)**. The increase in the urban population during that time brought a corresponding increase in the demand for land for various purposes. As a result, pressure was put on land availability and this brought drastic changes to the land use pattern and land cover characteristics within the metropolis (Stemn & Agyapong, 2014; Mensah et al., 2019). Further, research by Tarawally et al. (2019) revealed that rapid urbanization leads to significant environmental impacts such as natural resources depletion, deterioration of air quality due to the burning of fossil fuels and the increased use of vehicles emitting carbon monoxide, increased carbon dioxide emissions, poor water quality, inadequate sewage and waste management systems, and a major loss of biodiversity. Besides the benefits such as improvement in service provision, rapid urbanization and population growth negatively affect the environment (Tarawally et al., 2019). Therefore, the sustainability of an urban area is mostly threatened. Understanding the spatio-temporal dynamics of urban growth is essential for effective assessment and monitoring of environmental consequences. This knowledge provides critical evidence to guide the future expansion of cities in Ghana, ensuring well-informed urban planning and sustainable development. Given Ghana's current economic instability and slow growth, the country cannot afford to overlook the potential negative effects of inadequate comprehension of spatial growth patterns and their socio-economic implications. Accurate and up-to-date information on growth patterns is crucial for ensuring the sustainable development of cities in Ghana. This can be achieved through the integrated application of GIS, RS, and Spatial metrics.

Geographic Information Systems (GIS) and Remote Sensing (RS) have been widely acknowledged as effective and cost-efficient tools for analyzing urban growth and changes in land use and land cover compared to conventional survey techniques (Shao et al., 2021). This viewpoint is validated by Hasan et al. (2023) and Rana & Sarkar (2021) as their studies showed that employing GIS and remote sensing are cost-effective and time-efficient methods to quantitatively analyze urban sprawl. Shikary & Rudra (2020) highlighted that effective assessment of urban sprawl requires

using efficient techniques to comprehend the present state and pattern of urban expansion. This, according to Sumari et al. (2020), can be achieved through the combined application of geospatial techniques and spatial metrics such as Shannon's entropy urban expansion intensity index, and landscape metrics. Shannon's entropy quantifies the degree of compactness or dispersion of a geospatial element (Deribew, 2020; Ibrahim et al., 2019) while landscape metrics are valuable for quantifying and measuring the spatial characteristics of the landscape. The application of landscape and Shannon's entropy have aided in comprehending the trend and pattern of urban growth occurrence across the urban space (Shikary & Rudra, 2020) and this makes them valuable methods for quantifying and monitoring urban sprawl. Unfortunately, earlier studies of urban growth in the metropolis have not employed landscape metrics in their analysis. Additionally, urban growth in the metropolis has not been examined in its direction-wise pattern of growth which is important in understanding the local causative patterns of growth and identifying areas with significant land development. According to (Wolff & Wiechman, 2018), factors influencing growth can differ across regions, therefore there is a need for location-specific analysis of urban growth. The location and environmental conditions of the metropolis are key factors that likely shape its spatial and temporal growth patterns, making them important subjects for investigation (Tarawally et al., 2019). Further, there is a global initiative to provide comprehensive data on urban areas through the World Urban Database and Access Portal Tool (WUDAPT) (Mushore et al., 2023). Given Africa's limited representation in WUDAPT, recent studies on Sekondi-Takoradi will make a significant contribution from Ghana. Lastly, the approach employed in this study can be used to evaluate urban growth in other cities in Ghana or other developing nations with comparable conditions. Also, knowledge from this study will enable city planners and policymakers to gain a comprehensive understanding of the multifaceted aspects and spatio-temporal dynamics of urban sprawl, which will enable them to allocate resources efficiently and implement effective infrastructure management strategies accordingly. Therefore, using remotely sensed data, GIS, Urban expansion Intensity Index, landscape metrics, and Shannon's entropy model, the objective of the study is to examine to quantify the intensity of urban expansion and its degree of dispersion and compaction using Landsat images from 1991 to 2023.

4.2 Materials and Methods

The materials and methods used in the study are detailed in the subsequent subsections.

4.2.1 Study area

Sekondi-Takoradi Metropolis (Figure 4.1) is situated in the Western region of Ghana and lies between Latitude 4° 52' 30" N and 5° 04' 00" N, as well as Longitudes 1° 37' 00" W and 1° 52' 30" W. The metropolis has an area of approximately 191.7 km^2. It shares borders with Wassa East District to the North, the Gulf of Guinea to the South, Shama District to the East, and Ahanta West District to the West. By 2010, the metropolis had a population of 559,548 (PHC, 2010). However, by 2021, the population increased to 734,645 (Dadzie-Paintsil & Mensah, 2022). This proves that a large number of the people living within the metropolis live in urban areas. Sekondi-Takoradi was chosen because it serves as the hub for economic and political activities for the Western Region and the nation at large. However, the extent to which this study area's urban growth has been studied in terms of its pattern, magnitude, rate, and spatiotemporal characteristics as well as its effects on the other LULC categories remains insufficient, especially in an era where its rate of urbanization makes it the third urbanized metropolis in Ghana.

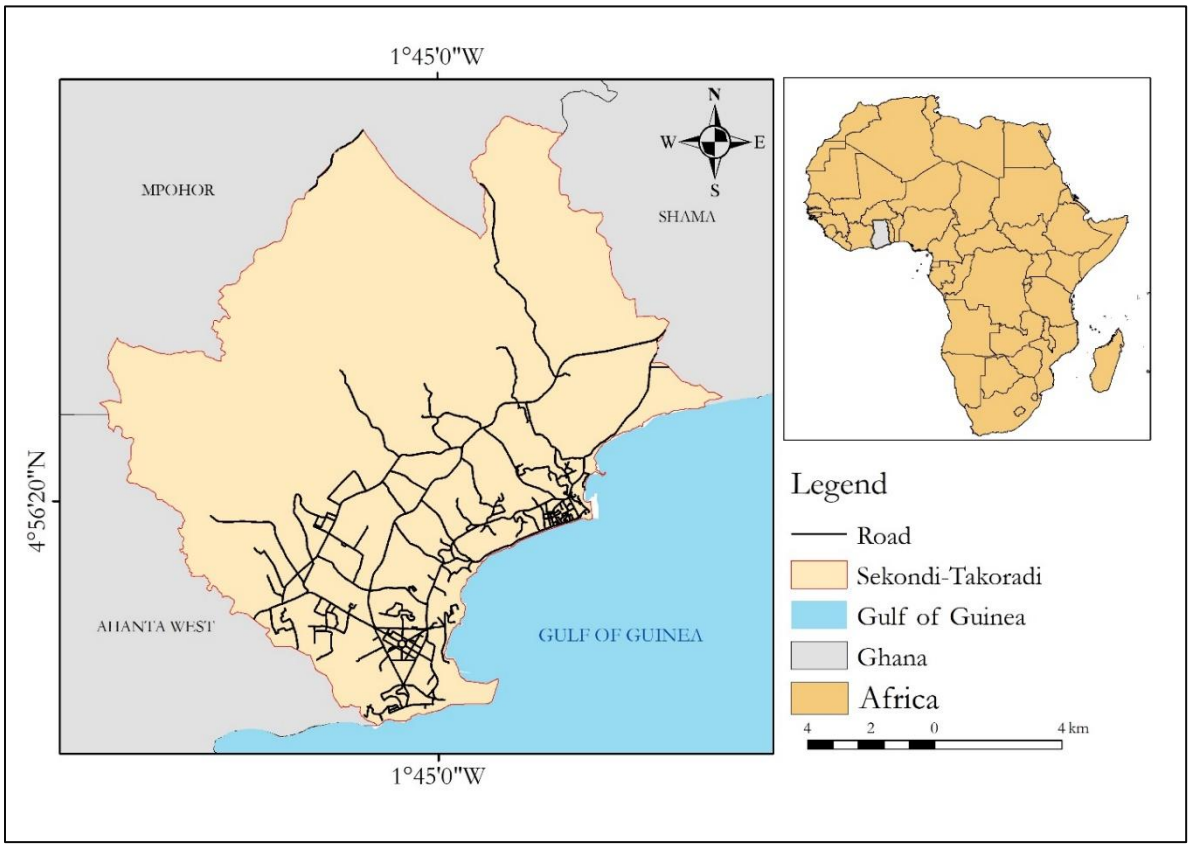

Figure 4.1: Map of the study area.

4.2.2 Datasets Used and Software

Table 1 displays the data used for the study. The irregularity in the image intervals stemmed from insufficient data with less than 10% cloud cover. The pre-processing and processing of the Landsat images employed various software such as ArcGIS Pro, Google Earth Engine, and QGIS. Specifically, the QGIS and Google Earth Engine were used for pre-processing, classification, accuracy assessment, and creating transitional probability. ArcGIS Pro was utilized to generate all classified maps and output maps.

Table 4.1: Dataset used for the study.

Satellite Data	Resolution	Date Acquired	Source	No. of bands
Landsat TM	30m	01/01/1991	USGS	7
Landsat ETM+	30m	01/02/2009	USGS	8
Landsat ETM+	30m	01/01/2016	USGS	8
Landsat OLI/TRIS	30m	01/01/2023	USGS	11
Reference data				
Google Earth images		1991,2009, 2016 and 2023	Google earth explorer	

4.2.3 Methods

According to Getu and Bhat (2021), detecting significant changes in multi-temporal images involves a series of activities and complex processes to obtain precise and accurate information. Therefore, the following processes as outlined in Figure 4.2 and elaborated in the subsequent sub-sections were carried out for this study.

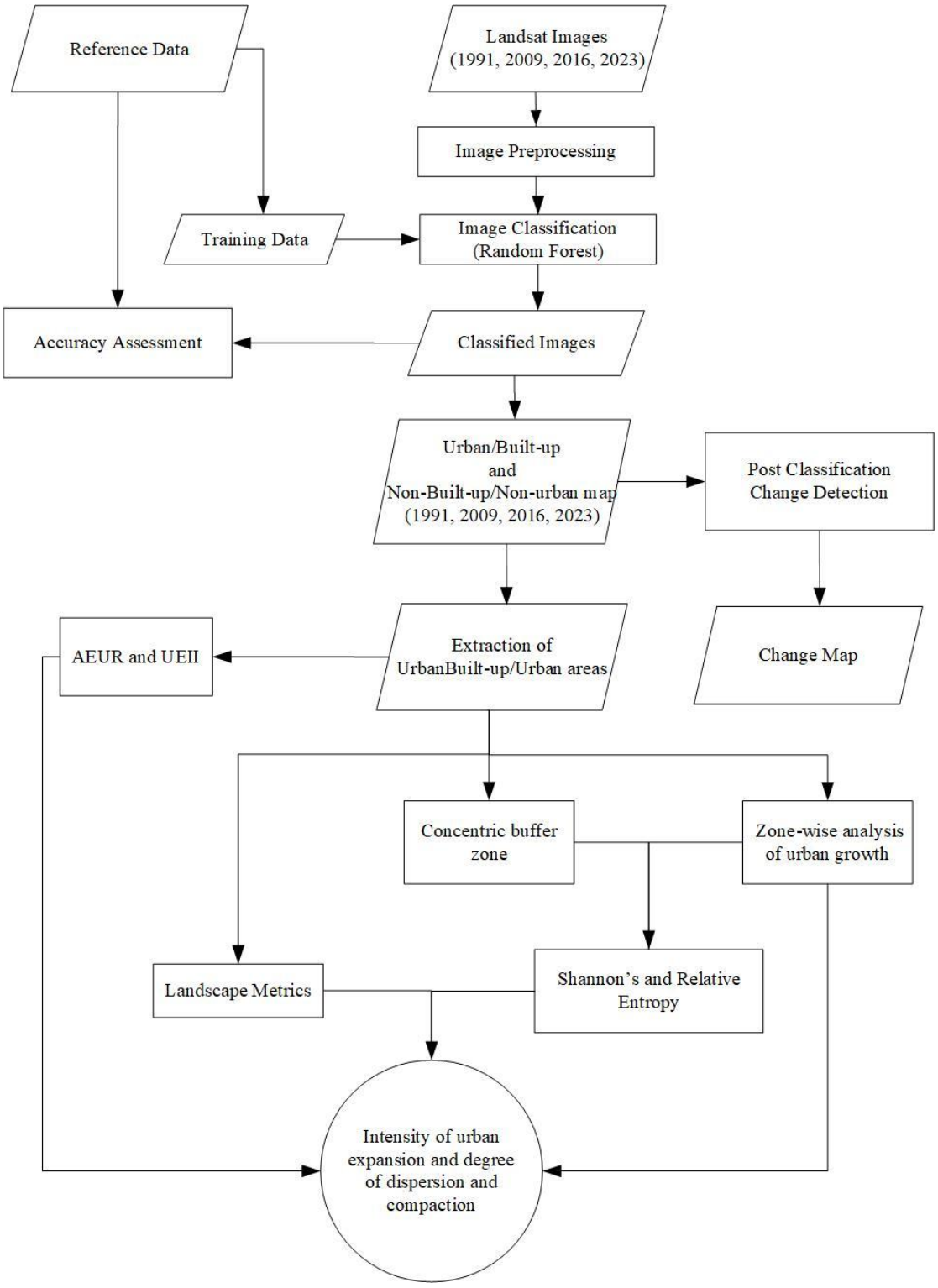

Figure 4.2: Methodological flowchart.

4.2.3.1 Image Pre-processing

Before image classification can be done efficiently, a satellite image needs to be preprocessed to correct any error encountered during its imaging (Gašparović, 2020). Geometric and Radiometric corrections and image band staking were the pre-processing types conducted in this study. The obtained Landsat images were geometrically corrected from the source. However, to maintain consistency in both the size and positioning of the obtained images, image-to-image registration was conducted in QGIS. The 2023 Landsat image served as the base image for this process, followed by reprojection to UTM ’84 zone 30N (Abudu et al., 2019). According to Anwar et al. (2022), errors that affect the quality of digital numbers of satellite images can be improved by radiometric correction. The Semi-Automatic Classification (SCP) plugin in QGIS was used to radiometrically correct the images and then band stacked to form composite bands which could be visualized in different color combinations. According to Abass et al. (2018), False Colour Composite (FCC) produces distinct spectral signatures for easy identification of land color classes. Therefore, this study used FCC to identify the land cover classes.

4.2.3.2 Image Classification

Image classification is the process of obtaining information by grouping all pixels in an image to have a set of classes (Saha et al., 2021b). The supervised classification technique was used in this study to categorize the images into their appropriate classes after training samples and signature classes had been established. Based on the objectives of the study and employing an acceptable categorization method, the study area was classified into non-built-up and built-up (Table 4.2).

Table 4.2: Description of the land cover classes.

CLASS	Description
Non-Built-up	Waterbodies and vegetative areas.
Built-up	These include paved areas, impervious surfaces, roads, bare lands, residential areas, areas covered by man-made structures, and commercial areas.

Like many research, this study employed a supervised technique in classifying the images. The supervised classification is based on the concept of using samples with known identities to categorize pixels with unknown identities (Anwar et al., 2022). Specifically, Random Forest (RF)

supervised classification method was used to classify the images. This supervised classification technique was chosen because it generates higher classification accuracy even when applied to data with higher noise levels compared to other classifiers like Support Vector Machine (SVM), Classification, and Regression Trees (Hidalgo-García & Arco-Díaz, 2022; Xiang et al., 2022)**.** This has been proven in the works of Fernández-Delgado (2014) who evaluated 179 relevant classifiers from 17 families using 121 datasets and found random forest to be the best classifier. Additionally, RF can manage missing values, and categorical and unbalanced data- a capacity that is not present in SVM (Haas, 2013).

4.2.3.3 Accuracy assessment

Land use land cover classification with inaccuracies affects the genuineness of the analysis (Mohammadian et al., 2017), therefore, to prevent such a situation, an accuracy assessment needs to be performed. In this study, the confusion matrix was used to assess the performance of the classified images (Foody, 2020). Various measures such as overall accuracy (*OA*), kappa coefficient (*K*), user's (*UA*), and producer's accuracy (*PA*) that are directly used as indicators of either overall accuracy assessment or individual class assessment were computed from the confusion matrix. The accuracy assessment parameters used in the classification accuracy can be expressed mathematically in the following equations (4.1 to 4.4) (Shamsudeen et al., 2022)**.**

$$\mathrm{UA} = \frac{\text{Number of correctly classified pixels in each category}}{\text{Total number of classified pixels in that category}} \times 100 \quad (4.1)$$

$$\mathrm{PA} = \frac{\text{Number of correctly classified pixels in eacg category}}{\text{Total number of classified pixels in that category}} \times 100 \quad (4.2)$$

$$\mathrm{OA} = \frac{\text{Total number of correctly classified pixels}}{\text{Total number of reference pixels}} \times 100 \quad (4.3)$$

$$K = \frac{\mathbf{N}\sum_{\mathbf{i=1}}^{\mathbf{r}} \mathbf{x_{ii}} - \sum_{\mathbf{i=1}}^{\mathbf{r}} (\mathbf{x_{i+}} \times \mathbf{x_{+i}})}{\mathbf{N^2} - \sum_{\mathbf{i=1}}^{\mathbf{r}} (\mathbf{x_{i+}} \times \mathbf{x_{+i}})} \quad (4.4)$$

Where N is the total number of samples in the matrix, r corresponds to the number of the rows in the matrix, x_{ii} is the number in row I and column i, x_{+i} is the total for row i, and x_{i+} is the total for column i.

4.2.3.4 Change Detection

In this study, post-classification change detection was used because it gives detailed information about changes that take place from one class to another. These changes make it possible to create a change matrix that aids in tracking pixel changes over two time periods to determine the trade-offs between the classes (Alijani et al., 2020; Asare et al., 2023). Also, the annual rate of change and percentage annual rate of change were computed using equations (4.5) and (4.6) respectively as part of the post-classification change detection (Deribew, 2020b).

$$A_r = \left(\frac{A_2 - A_1}{T}\right) \quad (4.5)$$

Where A_r is the annual rate of change, A_2 is the current area of land use land cover type in km^2 and A_1 is the initial area of land cover type in km^2, and T= time interval between the initial year (A_1) and the current year (A_2).

$$C = \left[\left(\frac{F-I}{I}\right) * \left(\frac{1}{T}\right)\right] * 100 \quad (4.6)$$

Where "C" is the percentage annual rate of change, "F "is the final year, "I" is the initial year, and "T" is the time period (interval) between the final year and the initial year.

4.2.3.5 Urban Expansion Measurement

To assess the rate and intensity of urban expansion throughout the study period, the Annual Urban Expansion Rate (AUER), and Expansion Intensity Index (UEII) were utilized (Akubia & Bruns, 2019). The Annual Urban Expansion Rate (AUER) quantifies the average annual rate of built-up area of the study area between two time periods. This index was computed using equation (4.7) as expressed by Akubia & Bruns (2019).

$$\text{Annual Urban Expansion Rate } (AUER_i) = \left[\left(\frac{ULA_i^{t_2}}{ULA_i^{t_1}}\right)^{\frac{1}{t_2 - t_1}} - 1\right] \times 100 \quad (4.7)$$

From equation (4.7), $AUER_i$ is the Annual Urban Expansion Rate; $ULA_i^{t_2}$ and $ULA_i^{t_1}$ are the area of urban built-up land at current period (t_2) and previous period (t_1).

The Urban Expansion Intensity Index (UEII) "quantifies the degree of differentiation in urban expansion and depicts the proportion of urban expansion within a spatial unit concerning the total study area and study duration" (Alam et al., 2023). According to Akubia & Bruns (2019), UEII

shows the potential and future direction of urban expansion and determines the speed or intensity of urban land use change across different periods. This index is expressed in equation (4.8) (Akubia & Bruns, 2019; Alam et al., 2023)

$$\text{Urban Expansion Intensity Index (UEII)} = \left(\frac{ULA_i^{t_2} - ULA_i^{t_1}}{TLA \times \Delta t}\right) \times 100 \qquad (4.8)$$

where UEII is the Urban Expansion Intensity Index, $ULA_i^{t_2}$ and $ULA_i^{t_1}$ are the built-up areas at (current period (t_2) and previous period(t_1) times t_2 and t_1, respectively, and TLA is the total land area within the study area and Δt is the difference between the previous and the current period (i.e., $t_2 - t_1$). The benchmark values for interpreting UEII outputs are as follows: <0.28 indicates very slow expansion, 0.28–0.59 denotes slow expansion, 0.5–1.05 signifies medium-speed expansion, 1.05–1.92 represents high-speed expansion, and >1.92 indicates very high-speed expansion (Akubia & Bruns, 2019).

4.2.3.6 Landscape Metrics Measurement

Describing, analyzing, and modeling the form of an urban area are critical components in urban growth studies which can be achieved by the application of landscape metrics (Krishnaveni & Anil Kumar, 2022). Landscape metrics have been demonstrated to effectively quantify and analyze the composition and configuration of urban landscapes. The composition refers to the variety and affluence of its elements whereas configuration refers to the positioning, structure, and arrangement of these elements (Li et al., 2022). Mondal & Gavsker (2024) defined landscape as a diversified land area made up of several unique features or patches. In urban areas, the landscape changes due to natural patches becoming fragmented and eventually combining with built-up areas to produce larger urban centers. Therefore, employing landscape metrics incorporating landscape metrics with RS to analyze and describe the structure and patterns of the landscape provides a more comprehensive understanding of urban processes (Cengiz, Görmüş, & Oğuz, 2022). According to Barman et al. (2024), landscape metrics are employed to gain a thorough comprehension of urban landscapes. This understanding is essential for the effective and sustainable management of urban environments as it helps to clarify the complexities of urban areas, facilitating better planning and decision-making for sustainable development. This study employed class-level metrics encompassing the Class Area (CA), Number of Urban Patches (NP), Patch Density (PD), Largest Patch Index (LPI), Edge Density (ED), and Fractal dimension (Table

4.3) to investigate the dynamic landscape patterns of the metropolis using the R open-source software.

Table 4.3: Description of the selected spatial landscape metrics.

Landscape metrics	unit	Explanation	formula	Range
Class Area (CA)	hectares	CA is the total patch area of a particular class	$CA = \sum_{j=1}^{n} a_{ij}\left(\frac{1}{10{,}000}\right)$ a_{ij} is area(m^2) of patch ij; n_i is number of patch types (class)	Ca> 0, without limit
Number of Patches (NP)		The overall built-up patches within the landscape	NP = b_i where b_i is the number of patches of built-up	NP ≥1
Edge density (ED)	Meter/hectare (m/ha)	The total length of all built-up edges in a given landscape area.	$ED = \frac{E}{A}(10{,}000)$ Where A denotes the total area of the landscape (in square meters); E denotes the total length of edge of built-up class (in meters) in the landscape.	$ED \geq 0, without\ limit$
Patch Density (PD)	Number/100 ha	The proportion of the total number of patches of built-up to the landscape total area.	$PD = \frac{n_i}{A}(10{,}000)(100)$ Where n_i is the number of patches in the built-up class; A is the total landscape.	$PD \geq 0, without\ limit$
Fractal Dimension	None	This metric assesses patch complexity or shape based on the size within the landscape	$FRAC = \frac{2\ln(0.25p_{ij})}{\ln a_{ij}}$	1≤FRAC≤2
Largest Patch Index (LPI)	percent	The proportion of the largest built-up patch in the landscape relative to the total landscape area	$LPI = \frac{\max_{j=1}^{n}(a_{ij})}{A}(100)$ where a_{ij} is the area of built-up batch (ij); A is the total landscape area	$0 < LPI \leq 100$

4.2.3.7 Measurement of Urban Sprawl

As urban expansion does not occur uniformly in all directions (Roy & Kasemi, 2022), the study area was divided into 4 zones: Northeast (NE), Southwest (SW), Northwest (NW), and Southeast (SE) with 90-degree gaps in a clockwise direction (Figure 4.9. and Table 4.9). These zones were delineated by using the Central Business District as the center point or city center. Each zone was further divided into concentric zones or circles at 1 km intervals or radius from the city center. This segmentation aimed to assess the extent and growth rate of each zone and to gain insights into the local factors influencing growth in specific sectors. Zonal analysis helps to identify the factors causing urbanization as well as determine specific locations undergoing different degrees of urban development. Furthermore, this analysis, enables city administrators to comprehend the dynamics of urbanization which is crucial for implementing suitable infrastructure and providing essential amenities (Ramachandra et al., 2015).

4.3 Results and Discussion

4.3.1 Classified land use land cover

By visual interpretation, the metropolis showed signs of growth from the central business district, along the coastal corridor, and along the main roads that link the metropolis to other cities. The Western and the Southern-Western part of the study, clearly have experienced significant growth (Figure 4.3). This type of urban growth can be seen in some coastal cities in Ghana such as Cape Coast and Accra (Service, 2021) and it can be explained by the fact that a city's main road network, the presence of seaport and airport have a significant impact on its population density (Hackman et al., 2020) which is the case in the western and southern parts of the metropolis. A statistical analysis of Figure 4.3 is presented in Table 4.4.

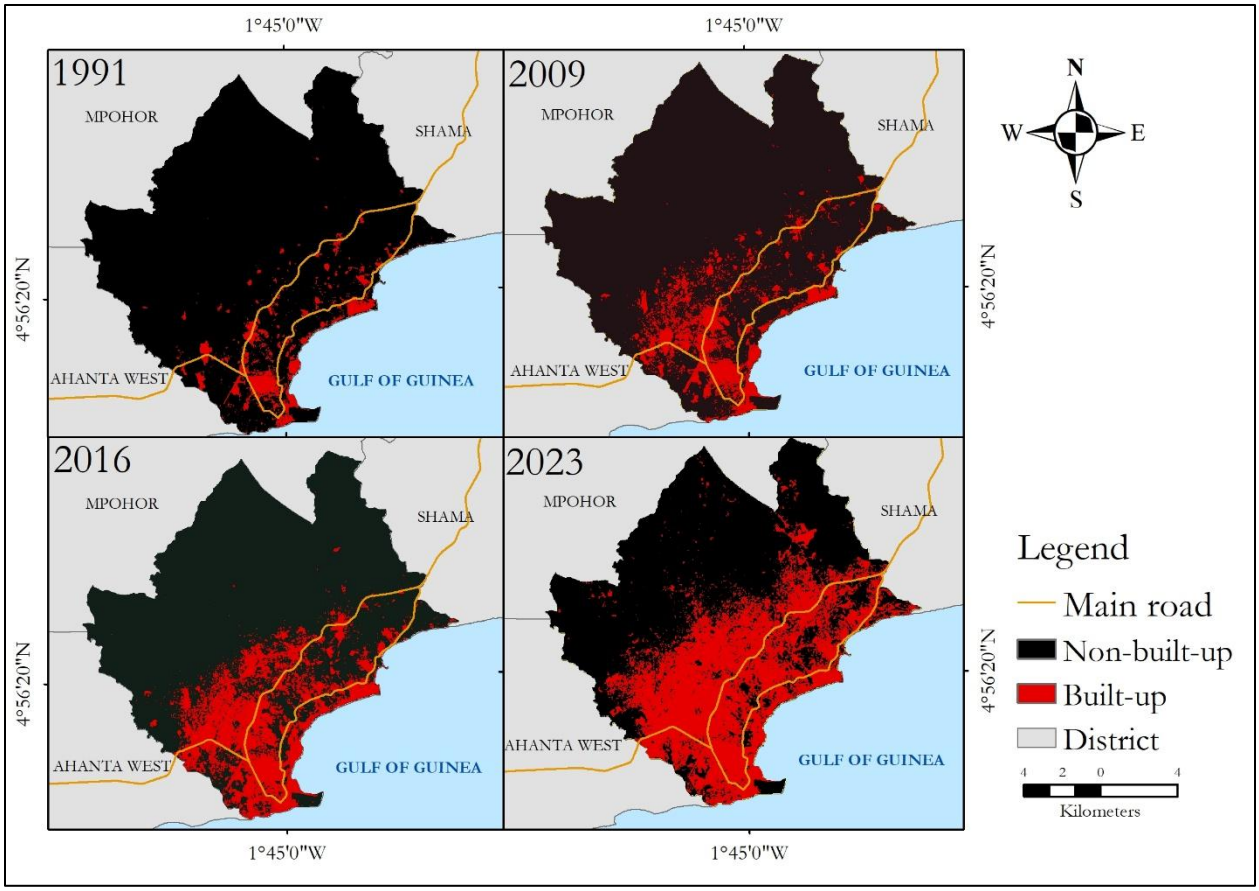

Figure 4.3: Map of Built-up and Non-built-up.

Table 4.4: Statistics of classes from 1991 to 2023.

Year	Total Area (km^2)	Non-Built-up (km^2)	Non-Built-up (%)	Built-up (km^2)	Built-up (%)	Change in Built-up (km^2)	Change in Built-up (%)
1991	191.66	181.10	94.49	10.56	5.51	-	-
2009	191.66	169.53	88.45	22.13	11.55	11.57	6.04
2016	191.66	152.68	79.66	38.98	20.33	16.85	8.79
2023	191.66	118.03	61.58	73.63	38.42	34.65	18.08

From Table 4.4, built-up increased significantly throughout the study period at the expense of a drastic decline in the area of non-built-up. This suggests a significant urban expansion in the study area and reflects a shift in land use from natural or undeveloped spaces to developed or urbanized areas. The increase in built-up, as a consequence of the persistent decrease in non-built-up, could be attributed to the increasing demand for land for constructional purposes influenced by

population growth and an increase in economic activities that are largely linked to the oil discovery (Fiave, 2017; Mensah et al., 2019). This correlation is highlighted in the 2021 Population and Housing Census of Ghana (Service, 2021) and is further substantiated by Dadzie-Paintsil & Mensah (2022). Predating the oil discovery, 359,363 people lived in the metropolis. Following the oil discovery, the population grew to 559, 548 in 2010 (Service, 2014). The population surge coincided with an increase in the demand for land for residential, commercial, and industrial purposes, resulting in the transformation of diverse land cover into built-up areas (Fiave, 2017). Figure 4.3 supports the claim of Fiave (2017) as population data from the United Nations World Population Prospect (2023) concurrently corresponds to the increase in built-up over the study period.

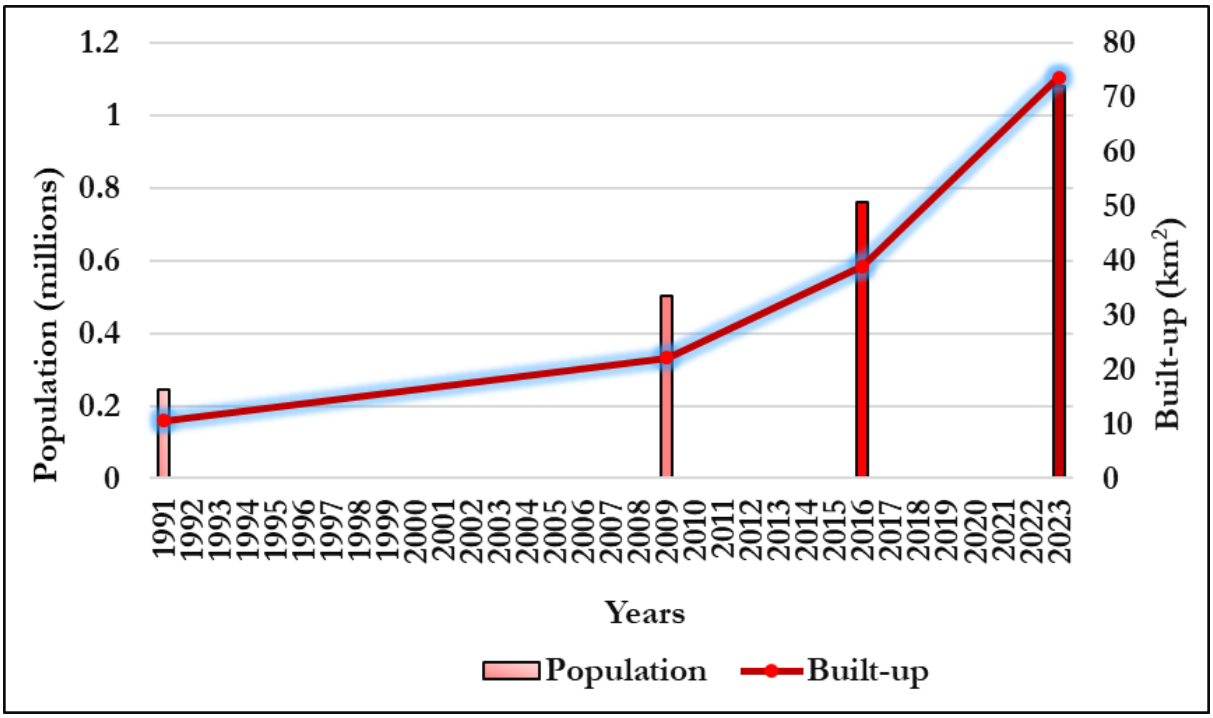

Figure 4.4: The pattern of population growth and expansion of built-up areas.

Further analysis of Figure 4.4 revealed that although population and built-up were increasing, built-up was higher than population which signifies that more spaces are being used in the metropolis (Figure, 4.5). This, according to Dadzie-Paintsil & Mensah (2022), Danso & Addo (2016), and STMA (2022) can be attributed to the architectural style in the metropolis which is predominantly characterized by horizontal expansion of houses which claims more space instead of vertical expansion of houses (Frimpong et al., 2023). In a study by Buo et al. (2021), it was

found that the cities of Kumasi and Accra expanded at a rate faster than their population growth which reflects the inefficient land use in addressing the housing deficits in these urban areas. Moreover, contributing to the horizontal spread of built-up is the higher social status and prominence most societies in Ghana attached to owning a house (Kpienbaareh et al., 2019).

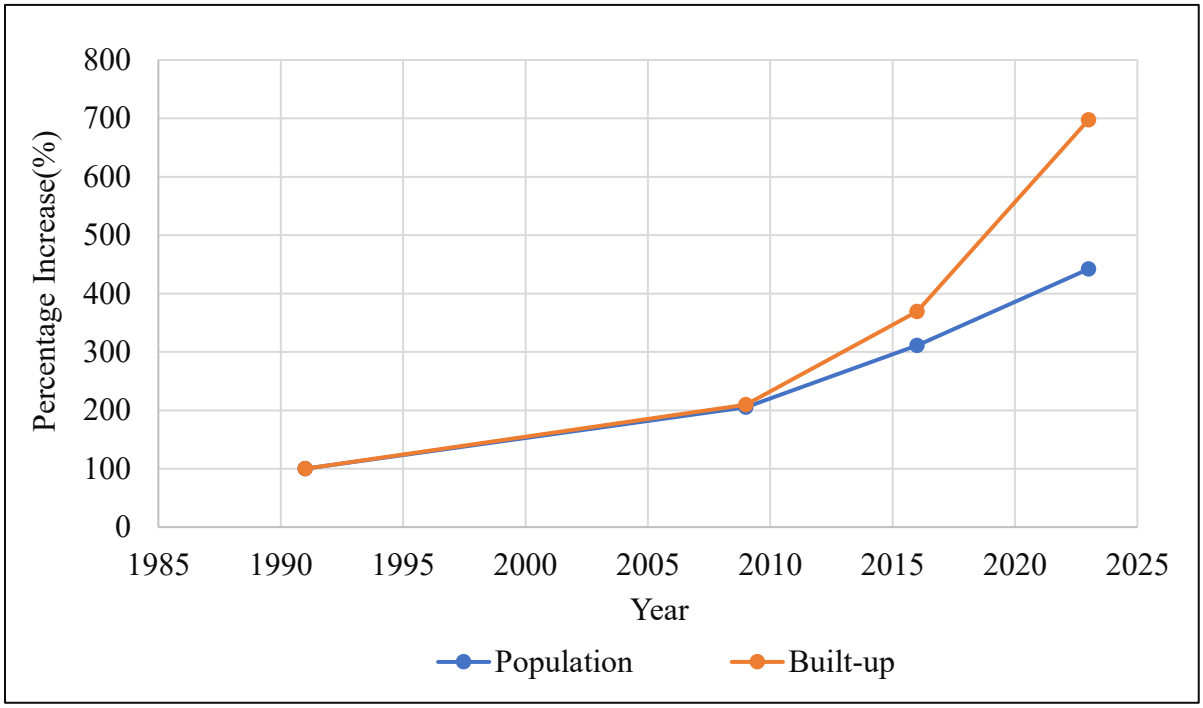

Figure 4.5: Percentage increase in population and Built-up.

According to Mensah et al., (2019), the demand for housing, particularly in 2011, prompted immediate action from real estate developers, resulting in the initiation of housing projects such as the Takoradi Oil Village and King City to accommodate the expanding population. Additionally, many establishments within the hospitality sector underwent renovations and expanded their facilities to take in more guests while new establishments sprang up to cater to the needs and address the accommodation requirements of high-income expatriates from the oil industry who moved to the metropolis (Biney & Boakye, 2021). Furthermore, from 2011 to 2016, the construction of the N1 road and the dualization of single roads to enhance transportation infrastructure transformed several hectares of diverse land cover into impermeable surfaces (Mensah et al., 2019). Currently, the construction of the Kwame Nkrumah interchange which began in 2020 as well as the expansion of the road from the Paa Grant roundabout to Sekondi has

claimed several vegetative land and wetlands lands (Annim, 2023). Lastly, during the Takoradi Port development in 2016, approximately 530 km^2 of cultivated land was transformed into impermeable surfaces (GPHA, 2016). These developments have played a crucial role in the expanding built-up areas in the metropolis.

Studies by Aduah & Baffoe (2013) revealed that waterways that are a non-built-up component are being converted into built-up. These waterways are frequently filled with sand and prepped for building and other construction activities. A notable case is the Anankori River where boulders have been used to fill several of its tributaries to allow tipper vehicles to transport sand and stones from the river (Biney & Boakye, 2021; Mensah et al., 2018a). Currently, the condition of these waterways and waterbodies compared to their state in the 1990s indicates a significant rate of encroachment and conversion into built-up areas. Hence, depriving the metropolis of the benefits that come with water conversation (Danso & Addo, 2018). This is consistent with the claims of Mohammadian (2017) and Wangyel et al. (2021) that the growth of built-up areas can negatively affect areas covered by water if they are not efficiently monitored. Furthermore, the decline in the non-built-up area aligns with the notion that vegetation mostly suffers losses when a city is expanding (Appiah, 2016; Biney et al., 2022; Daata et al., 2021). The Ghana Statistical Service (2014) reports that since 1991 there has been a notable migration wave into the Sekondi-Takoradi metropolitan. Due to the pressure that the population surge has placed on the existing green spaces, private estate developers and individuals have begun to convert lands both within and outside of the urban perimeter. The significant changes in the cover classes presented in Table 4.4 occurred at an increasing annual rate for built-up and a decreasing annual rate for non-built-up (Figure 4.6). Throughout the study period, built-up increased while non-built-up declined by 1.97 km^2 annually.

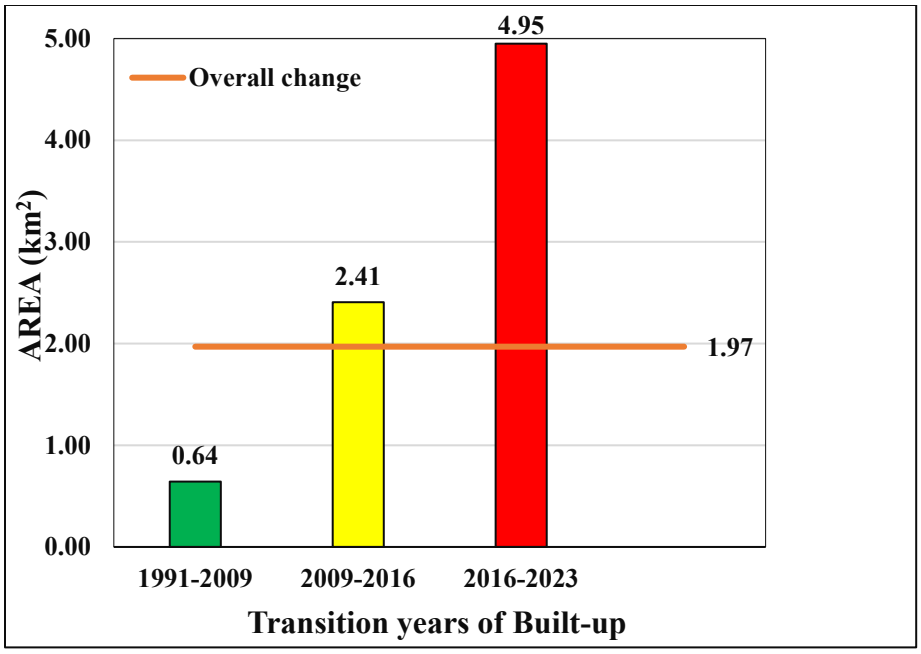

Figure 4.6: Annual rate of change from 1991 and 2023.

4.3.2 Accuracy Assessment of LULC Classification

Obeng et al. (2023) asserts that image classification with kappa values higher than 0.7 and an overall accuracy of 85% is indicative of quality classification. The accuracy values presented in Table 4.5 exceeded the minimum accuracy standard proposed by Obeng et al. (2023). Therefore, the classification results were used in further computation and analysis specifically, change detection analysis.

Table 4.5: Classification accuracy.

Year	Producer's Accuracy		User's Accuracy		Overall Accuracy (%)	Kappa Coefficient
	Non-built-up	Built-up	Non-Built-up	Built-up		
1991	92.69	90.68	90.89	94.60	***92.69***	***0.85***
2009	98.31	90.76	86.63	98.88	***93.62***	***0.87***
2016	94.95	93.56	92.25	95.83	***94.18***	***0.88***
2023	97.58	93.22	93.25	97.57	***95.36***	***0.91***

4.3.4 Built-up density of concentric ring buffer

The built-up images were fragmented into seventeen concentric zones at an interval of 1km between the zones, starting from the city center (Figure 4.7). This division was done to assess sprawl for the various years and to aid in defining the direction of urban land growth (Verma et al., 2021).

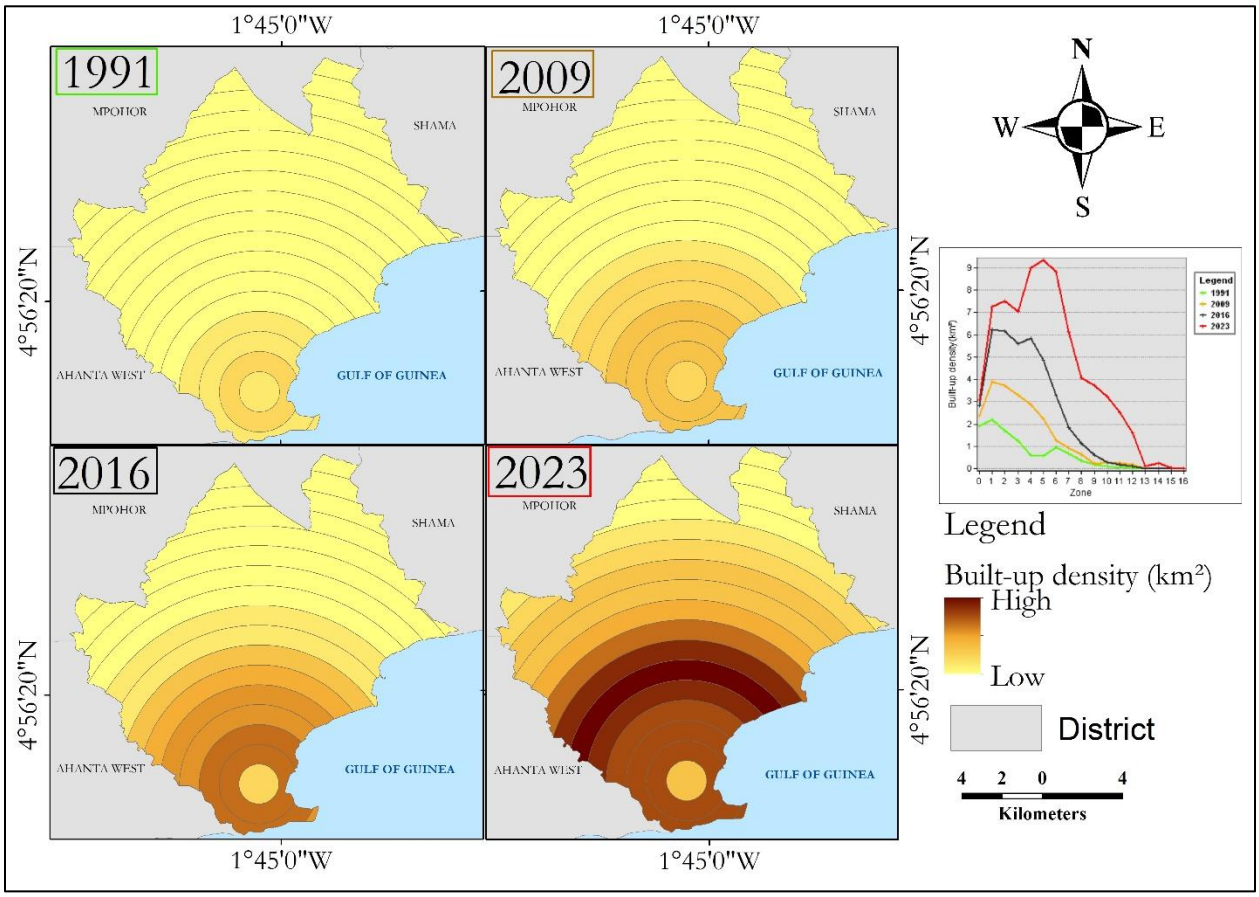

Figure 4.7: Built-up density map.

It can be seen in Figure 4.7 that there was an irregular increase and decrease in the built-up density in all the zones for the various years. This could be explained by the existence of various pull factors during the time of urban growth (Agenda, 2013; Doe et al., 2022). However, comparing the values in each zone to the zones of the subsequent years, an increasing trend was observed among the various years which signifies an increase in urban development. From the city center to about the 7th zone, built-up density was relatively high for all years but mostly decreased as it extended further from the 7th Zone. This means built-up has expanded into the fringes of the metropolis and as pointed out by Krishnaveni & Anil (2022) and Mensah et al. (2019), it will bring

several adverse implications like the loss of vegetative cover and green spaces, increased infrastructure costs (Rainey et al., 2021), increased carbon emissions (Feng & Gauthier, 2021; Frimpong et al., 2022), increased traffic congestion (Mukherjee & Singh, 2020), increase energy consumption (Hackman et al., 2020), and decrease social cohesion (Mohammadian, 2017).

4.3.5 Urban Expansion Analysis

From Table 4.6 there was a consistent increase in both $AUER_i$ and UEII values throughout the study period. These values, especially the UEII, occurred in three levels: slow-speed, high-speed, and very high-speed expansion. This reveals how the metropolis expanded from a slow speed to a very high speed. Hence, indicates a high susceptibility of the area to experiencing urban sprawl.

Table 4.6: Measurement of urban expansion.

Time step	**$AUER_i$ (%)**	**UEII (%)**
1991-2009	4.20	0.34
2009-2016	8.42	1.26
2016-2023	9.51	2.58
1991-2023	6.26	4.70

Overall, the metropolis expanded at a very high speed (4.70%) and this aligns with the study of Akubia and Bruns (2019) where Adenta municipal expanded at a very high speed (5.98%) and also similar to the work of Alam et al. (2023) where the Khulna metropolis expanded at the rate of 6.76%.

4.3.6 Measurement of landscape dynamics through landscape metrics analysis

From Table 4.7, the study area experienced a consistent increase in edge density throughout the study period. This revealed an increase in the total edge length of built-up patches and fragmentation, indicating a sprawling effect on built-up expansion. Likewise, the substantial rise in the NP indicated substantial fragmentation of the landscape which suggests the creation of smaller isolated regions through the development of new built-up areas. Additionally, CA increased nearly fourfold over the past 32 years. Between 1991 and 2009, the built-up area increased by 1157 hectares, followed by a dramatic increase of 1685 hectares between 2009 and 2023, and to 3465 hectares increase from 2016 to 2023.

Further, the rise in Patch density (PD) throughout the study period also revealed more isolated built-up patches in the landscape. According to Krishnaveni & Anil Kumar, (2022), increasing isolated patches of built-up signifies high urban scatter. The fractal dimension showed an increase from 1991 to 2016 and decreased slightly in 2023 (Table 4.7). For the Fractal dimension, a simple and regular shape is indicated by values less than 1 while a complex and irregular patch shape is signified by values more than 1 (Barman et al. 2024; Cengiz et al. 2022). Though there was a fluctuation in the fractal dimension, the values were closer to 2 (more than 1) which indicates more irregular patterns in the landscape potentially due to dispersed urban development, as noted by (Manesha et al.,2022). In summary, the landscape dynamics of the study area revealed growing fragmentation, ongoing expansion of built-up patches, and unregulated urban growth. Analyzing patterns of landscape provides profound comprehension into the dynamics of urban growth within the metropolis and this insight can support city authorities, urban planners, and local governments in making informed decisions to promote environmentally sustainable urban development.

Table 4.7: Landscape metrics of built-up class over the study period.

Year	PD	ED	Fractal dimension	LPI	(CA)	NP
1991	2.624	15.411	1.354	1.279	1056	503
2009	3.892	33.773	1.413	6.540	2213	941
2016	3.746	40.957	1.420	17.054	3898	718
2023	4.909	54.050	1.413	36.138	7363	746

4.3.7 Quantification of dispersion and compaction using shannon and relative entropy

According to Cengiz et al. (2022), the growth of urban areas predominantly relies on the transformation of various Land Use Land Cover (LULC) categories. Therefore, it is crucial to evaluate the pattern of LULC to comprehend the dynamics within the land cover classes that contribute to urban growth. One effective method for conducting this evaluation is through the application of spatial metrics such as the Shannon and relative entropy. From Table 4.8, the entropy values showed an irregular pattern despite the relatively high entropy values for the various years. By examining the Shannon and relative entropy values of the various timesteps against the thresholds, it was evident that all the years had values greater than the thresholds which according to Krishnaveni & Anil (2022), denotes dispersion taking place in all the years. This dispersion, per Buo et al. (2021), can be attributed to factors such as ineffective and under-resourced planning

agencies, challenges related to land title acquisition, and the complexities of the land tenure system which are key drivers of urban sprawl in Ghana. Kleemann et al., (2017) also assert that laxity in zoning regulations, and the desire for people to live outside the city center as a result of high rent costs, heavy traffic, and increased pollution have influenced the dispersed distribution of the metropolis. The lowest entropy occurred in 1991 while the highest entropy was recorded in 2023 (Table 4.8). This finding reveals that in 2023, the city exhibited a greater degree of sprawl than in other years. The reason for the significant dispersion in 2023 could be explained by the increasing infrastructural construction at the fringes of the city (Mensah et al., 2019; Service, 2021).

Table 4.8: Shannon and relative entropy.

Year	**Built-up (km^2)**	**Shannon entropy**	**Relative entropy**
1991	10.56	2.17	0.76
2009	22.13	2.27	0.80
2016	38.98	2.20	0.77
2023	73.63	2.47	0.87
Maximum entropy	-	2.83	1
Threshold	-	1.42	0.5

Additionally, although the metropolis has been sprawling, the rate of sprawl is not uniform. The changes in entropy show that dispersion was highest between 2016 and 2023 and lowest between 1991 and 2009 (Figure 4.8). This indicates that rapid development and significant outward growth of urban areas occurred between 2016 and 2023. Unfortunately, the significant disparities in the entropy values over the thirty-two (32) years will make it difficult to achieve goal 11 of the sustainable development goals (SDGs) and also threaten the existence of other land cover classes in the metropolis (Dijkstra et al., 2022). From the study of Kleemann et al. (2017), ineffective land use planning does only contributes to increased land fragmentation but is also an indicator of climate change risk. It is recommended that the metropolis should implement stringent land use regulations and prioritize sustainable urban development practices. This will align the metropolis to Target 11.3 of the sustainable development goal 11 of making human settlements safe, sustainable, and resilient (Larbi, 2023).

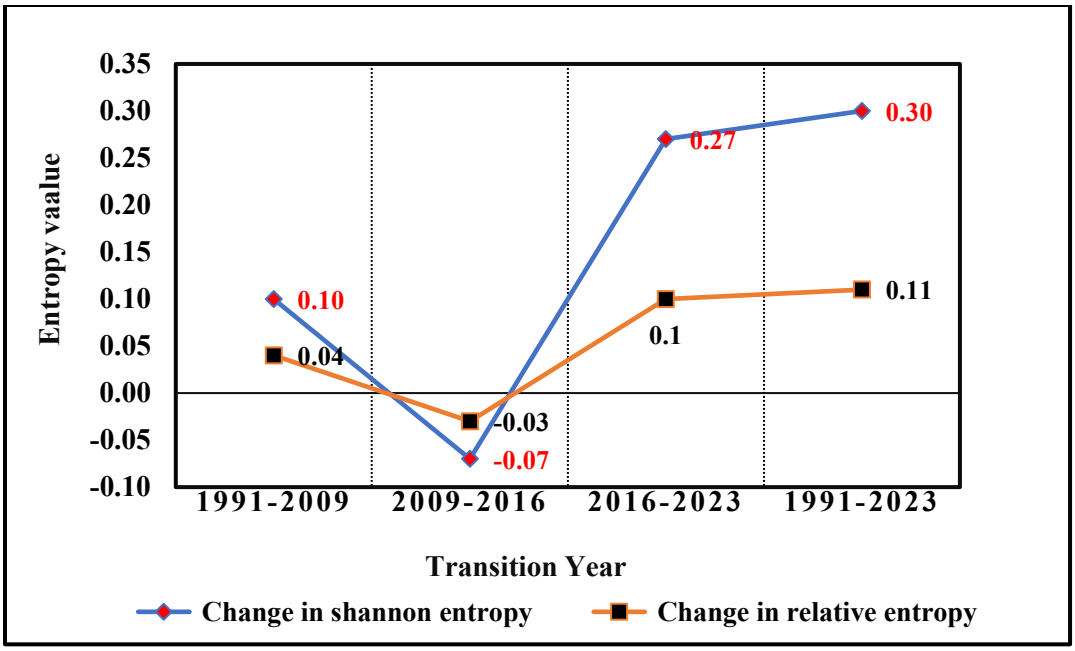

Figure. 4.8: Change in entropy.

4.3.7 Zone-wise analysis of urban growth

According to Wei & Ewing (2018), urbanization often unfolds unevenly across an urban space therefore, it is important to determine areas with significant land development to aid policymakers, urban planners, and environmental managers to make informed decisions that promote balanced, sustainable, and equitable urban growth. The direction-based zone or zone-wise can effectively capture areas with significant land development, and characteristics of urban growth and provide a comprehensive understanding of urban growth (Oztruk, 2017). In this study, areas of significant land development, and their degree of compaction and dispersion were computed at the zone-wise level (Table 4.9 and Figure 4.9) The zonal gradient analysis revealed that throughout the study period, significant land development occurred mostly in the NE part of the study while low land development occurred at the SE part of the metropolis. Apart from the availability of land and its relatively lower price at the NE, some pull factors like Takoradi Technical University, the presence of secondary schools, companies, teachers and nursing training colleges, regional offices, companies, district and regional hospitals, harbour have contributed to the significant land development. In contrast to NE, land development at SE is due to the higher land prices and limited land resources despite its proximity to the central business district. This finding aligns with the study of Dewa et al. (2022) where the unequal development in various parts of the Semarang Metropolitan Region was attributed to land prices and availability.

Table 4.9: Zone-wise distribution of built-up and its Shannon and Relative entropy.

Quadrant	**Built-up (km^2)**							
	1991	**2009**	**2016**	**2023**	**1991-2009**	**2009-2016**	**2016-2023**	**1991-2023**
SW	0.96	1.49	3.44	3.84	0.53	1.95	0.40	2.88
SE	1.62	2.42	3.09	3.25	0.81	0.67	0.16	1.64
NE	4.87	7.42	15.13	36.61	2.55	7.71	21.48	31.74
NW	3.12	10.80	17.32	29.93	7.68	6.52	12.61	26.81
Total	***10.56***	***22.13***	***38.98***	***73.63***	***11.58***	***16.85***	***34.64***	**63.07**
Quadrant	**Shannon entropy**				**Relative entropy**			
	1991	**2009**	**2016**	**2023**	**1991**	**2009**	**2016**	**2023**
SW	1.12	1.11	1.11	1.12	0.39	0.39	0.39	0.40
SE	1.05	1.04	1.02	0.98	0.37	0.37	0.36	0.35
NE	2.32	2.43	2.32	2.50	0.82	0.86	0.82	0.88
NW	1.68	1.78	1.80	2.07	0.59	0.63	0.63	0.73
Threshold	1.42	1.42	1.42	1.42	0.5	0.5	0.5	0.5

Further, the Shannon and relational entropy revealed a concentrated distribution at the SW and SE parts of the metropolis while a dispersed distribution occurred at the NE and NW parts (Table 4.9). With more spread-out urban areas, the costs of building and maintaining roads, water supply, electricity, and public transportation systems can increase significantly (Shao et al, 2021). This makes the provision of efficient public services more difficult and expensive and could indicate future challenges in maintaining balanced urban development across the metropolis (Gielen et al., 2021). City planners and authorities should focus on smart growth policies that direct new developments to areas that are already serviced by infrastructure, encourage more compaction, and update zoning regulations to limit excessive land consumption (Angelidou, 2018; Amponsah et al., 2022).

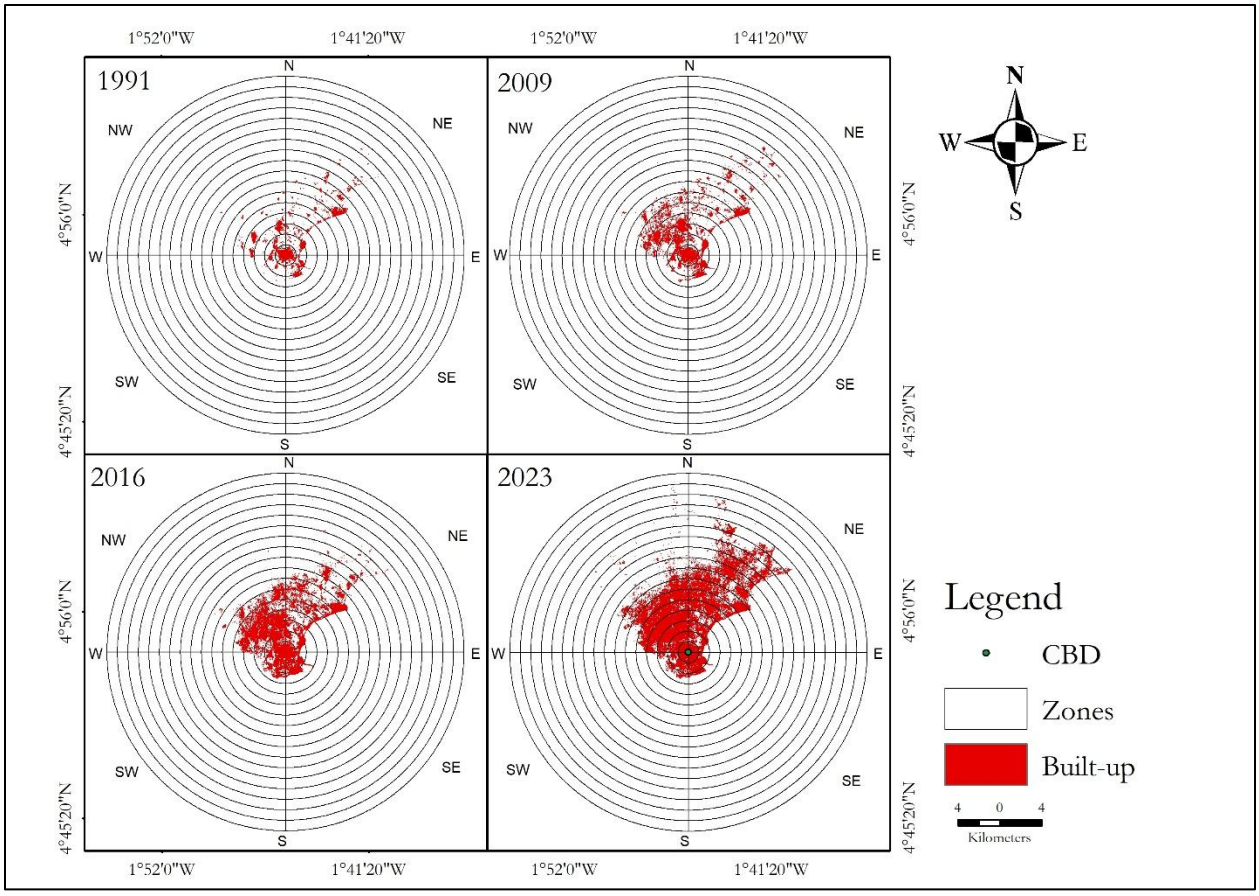

Figure 4.9: Zone-wise distribution of built-up.

4.4 Discussion

This study used Landsat images and statistical metrics to examine the intensity of urban expansion and its degree of dispersion and compaction for 32 years in the Sekondi-Takoradi metropolis. From the change detection analysis, the significant increase in built-up areas revealed a substantial shift from natural or undeveloped space to an urbanized area. The intensive modification of and encroachment into non-built-up areas is causing rapid urban growth in Sekondi-Takoradi (STMA, 2022). Mensah et al. (2018) reported that significant green space depletion in the metropolis is progressively causing landscape degradation. This would seriously threaten the metropolis's eco-environmental quality and livability (Dhali et al., 2019b). Notably, the western and southern parts of the study experienced this significant growth due to the presence of the seaport, airport, central business district, and the main road network which have a significant impact on population density (Hackman et al., 2020). Moreover, the study found that the expansion of urban areas outpaced population growth, reflecting inefficient land use likely due to the architectural style favoring

horizontal spread and the social value placed on house ownership. In a study by Buo et al. (2021), Kumasi and Accra also expanded faster than their population growth, corroborating the findings of this study.

In addition, the analysis of urban expansion indices revealed a marked increase in the intensity of urban expansion throughout the study period. The UEII and AUER demonstrated a rapid rate of urban expansion, indicating a high occurrence of urban sprawl within the metropolitan area. These findings are consistent with the research conducted by Acheampong et al. (2017) and Mondal & Gavsker (2024). These researchers identified variations in the occurrence of built-up development to various urban expansion indices within the Greater Kumasi of Ghana and Asansol City in West Bengal, respectively. Although urban growth is a complex process, landscape metrics make it simple to assess and quantify the dynamics and patterns of urban growth. The increase in metrics values (ED, PD, ED, FRAC, and NP) revealed the metropolis is experiencing fragmentation as a result of the creation of new patches. Similar studies by Getu & Bhat (2021) in Bahir Dar City and by Krishnaveni & Anil Kumar, (2022) in Kochi City, Kerala India also observed an increase in the metrics values and fragmentation in the landscape which was attributed to the development of new patches mostly at the fringes of the study areas. Although the study differs in terms of study length and overall area, the increases in values of spatial metrics were equally highly substantial when compared to other studies by Barman et al. (2024), Cengiz et al. (2022), Getu & Bhat (2021), Krishnaveni & Anil Kumar (2022), and Mondal & Gavsker (2024). Hence, supports that the metropolis experienced rapid urban sprawl or dispersion. The evaluation of Shannon and relative entropy values revealed a slight variability in urban growth over the study period. These entropy values surpassed the established threshold, signifying a dispersed distribution of built-up over the study period. Similarly, Mondal & Gavsker (2024) reported entropy values exceeding the defined limits for the Asansol city in India with Shannon values ranging from 1.65 to 1.76. Likewise, Roy & Kasemi (2021) observed an increase in the entropy values for Raiganj municipality in India during the period 1991 to 2019. According to Dewa et al. (2022), dispersed urban growth causes unsustainable patterns of development throughout a city. In this light, Dhali et al. (2019) opines that dispersed urban growth makes it more costly and logistically difficult to provide infrastructure and services like public transportation, water, sewage, and roadways. Also, biodiversity loss, agricultural land loss, and environmental degradation may be the outcomes of increased land usage and sprawling of built-up into natural regions. Given that urbanization is not uniformly distributed

across the study due to varying push and pull factors shown by the zone-wise analysis, a one-size-fits-all policy for the metropolis cannot be accurately and effectively applied across all aspects of the area (Dadras et al., 2015). As a result, this study advocates for effective urban growth management strategies that take into account the varying levels of urbanization and promote smart and compact development within the metropolis.

4.5 Conclusion

Understanding the configuration of urban sprawl is vital in creating an inclusive, safe, resilient, and sustainable urban environment. This study employed Landsat images and spatial metrics to assess urban sprawl in Sekondi-Takoradi metropolis from 1991 to 2023. Through the use of the supervised random forest classification algorithm, the images were classified into two classes which were aimed at examining the growth pattern of the metropolis. Change detection results over the 32 years revealed a 63.07 km^2 increase in built-up while the AEUR and UEII values indicated a rapid expansion of built-up with the most pronounced expansion occurring between 2016 and 2023. The analysis of the landscape metrics revealed an increasing fragmentation, complexity, and an irregular pattern in the landscape potentially due to dispersed urban development. Using Shannon's and relative entropy to quantify the degree of dispersion and compaction, it was observed that the study area started sprawling as early as 1991. The extent of sprawl primarily increased from the city center towards the northeast and northwest directions leading to the annexation of adjacent communities. However, the study was limited by the following challenges. First, there were discrepancies in the acquisition dates of the satellite images due to issues of cloud cover. A more robust analysis and conclusion could be made if the images had the same time interval. Second, due to the spatial resolution of the Landsat images, changes that occur on small scales cannot be effectively identified. These challenges should be taken into account for future studies. Despite these challenges, the findings remain valuable for city authorities and urban planners. The critical areas of unplanned urban expansion highlighted by the study serve as a useful guide for urban planners and city authorities to implement strategies for sustainable land management, especially at the fringes of the city that are likely to become impermeable surfaces. It also emphasizes the importance of finding appropriate urban development sites within the city to prevent future unregulated and disorganized urban growth. Therefore, by quantifying the intensity of urban expansion, determining the degree of dispersion and compaction, and identifying the difficulties brought on by unregulated dispersed growth, this

study provides a foundation for attaining sustainable urban development. Finally, the methodology employed in this study could be adapted to evaluate urban sprawl in other metropolises in Ghana or similar developing countries.

4.6 Publication

The objective of this work has been published with the title below in the African Geographical Review of Taylor & Francis.

AFRICAN GEOGRAPHICAL REVIEW
https://doi.org/10.1080/19376812.2024.2334726

Geospatial assessment of urban sprawl in Sekondi-Takoradi Metropolis, Ghana from 1991 to 2023

Ernest Biney[a,b], Eric Kwabena Forkuo[a,b], Michael Poku-Boansi[c] and Yaw Mensah Asare[b]

[a]WASCAL Graduate Research Programme on Climate Change and Land Use, Department of Civil Engineering, Kwame Nkrumah University of Science and Technology, Kumasi, Ghana; [b]Department of Geomatic Engineering, Kwame Nkrumah University of Science and Technology, Kumasi, Ghana; [c]Department of Planning, Nkrumah University of Science and Technology, Kumasi, Ghana

Biney, E., Forkuo, E. K., Poku-boansi, M., & Mensah, Y. (2024). Geospatial assessment of urban sprawl in Sekondi- Takoradi Metropolis , Ghana from 1991 to 2023. *African Geographical Review*, *00*(00), 1–18. https://doi.org/10.1080/19376812.2024.2334726

CHAPTER 5: EXAMINE THE INFLUENCE OF URBAN GROWTH ON URBAN HEAT ISLANDS IN THE METROPOLIS

ABSTRACT

The rapid urbanization in Sekondi-Takoradi, Ghana has significantly transformed the land cover, resulting in the proliferation of impervious surfaces and a decline in vegetation. However, the influence of this urban growth on the development of urban heat islands (UHIs) in the metropolis remains understudied. This study aimed to fill this research gap by employing Landsat images to explore the influence of urban growth on urban heat islands in the metropolis from 1991 to 2023. The supervised random forest technique was utilized to map the land cover changes. Furthermore, the computed normalized difference built-up index (NDBI), normalized difference vegetation index (NDVI), normalized difference water index (NDWI), elevation, proximity factors, land surface temperature (LST), and urban thermal field variance index (UTFVI) were used to analyze the influence of urban expansion on UHIs. The findings revealed a 63.07 km^2 increase in built-up areas and a 60.99 km^2 decrease in vegetation cover during the study period. This dramatic land use change led to a 3.1°C rise in mean LST and a 19.38 km^2 expansion of areas affected by the UHI effect. The UTFVI analysis further indicated a 33.63 km^2 increase in the worst ecological zone due to the temperature rise. Statistical analysis between LST, NDVI, NDWI, and NDBI revealed significant variability in explaining the intensity of LST and UHI in the metropolis over the study period. In addition to the spectral indices, elevation, and proximity factors significantly contributed to the temperature variation across the study area. Hence, provided valuable insight into the intensification of LST and UHI in the metropolis. The study equips city authorities and planners with the fundamental knowledge needed to prepare a sustainable development plan that alleviates adverse effects of urban growth and elevated temperature-related issues. Also, the findings contribute to the global efforts in promoting more livable and climate-resilient urban environments.

Keywords: Normalized Difference Vegetation Index (NDVI); Urban Thermal Field Variance Index (UTFVI); Sekondi-Takoradi; Land Surface Temperature (LST); Urban Heat Island (UHI); Normalized Difference Built-up index (NDBI); Spatial factors, Normalized Difference Water Index.

5.1. Introduction

Over the past few decades, the world has experienced speedy urban growth with the majority of this increase taking place in developing nations, particularly in Africa. Unfortunately, this speedy urban growth is significantly changing the land cover and the biophysical environment into impervious surfaces (Huang et al., 2020). According to Kumi-Boateng and Stemn (2015), urban growth is recognized as a major and enduring type of land use land cover change with ecological consequences, and the extent to which it has increased is correlated with population growth and economic development. Halder & Bandyopadhyay (2021) also pointed out that urban growth alters the natural landscape by replacing it with impermeable surfaces which significantly impacts local weather and climate. The localized climate of urban areas is affected as they undergo urbanization (Golestani et al., 2024). Per the research of Jumari et al. (2023), there has been a global increase in the surface temperature by 1.53 ℃ due to the drastic rise in urbanization. Rapid urbanization significantly impacts the thermal environments of cities by transforming the natural surfaces into built-up areas (Moisa & Gemeda, 2022). Negesse et al. (2024) noted that the most noticeable effect of rapid urbanization on climate is an increase in temperature. Urban areas have a higher tendency to absorb solar radiation and retain heat due to the presence of artificial structures and impervious materials like buildings, asphalt, paved surfaces, and metals. These materials store heat during the day and release it at night due to their greater thermal conductivity and capacity (Gyimah et al., 2023). Therefore, a dense concentration of these artificial structures coupled with a lack of green spaces creates "islands" with elevated temperatures (Belenok, 2021). Dutta (2022) and Sekertekin & Bonafoni (2020) assert that replacing natural cover types with impermeable materials modifies the surface energy balance of the earth and subsequently increases land surface temperature[2] (LST). This causes a warmer climate in urban areas than the surrounding rural environment, bringing about a phenomenon known as urban heat island (UHI) (Rami et al., 2023).

Mostly, UHI areas exhibit higher LST (Taloor et al., 2024)**.** Urban geometry, construction materials, and changes in land cover are the main causes of UHI (Taloor et al., 2024). The presence of dark materials and heat-absorbing impermeable surfaces make UHI predominant in built-up

[2] LST refers to the radiant energy emitted at a maximum distance of 1.2m above the earth's surface from diverse materials that absorb and release heat (Gyimah et al., 2023).

areas (Choudhury et al., 2023). Potentially, the rise in UHI leads to changes in precipitation patterns, increased demand for energy and air conditioners, and elevated pollution levels which contribute to global warming and negatively impact environmental quality (Chatterjee & Gupta, 2021). Zhao et al. (2016) noted that a significant UHI effect affects the comfort and health of urban residents and impedes further improvements in the quality of life and the city's development. In light of this, the United Nations (2018) predicts that by 2050 the trend of LST and dangerous pollutants in urban air will affect about 68% of the global population (Al-Kafy et al., 2020). Several research studies have established thermal comfort indicators to quantify the impact of UHI intensity (Mohammad et al., 2022). Due to the strong correlation of the urban thermal field variance index (UTFVI) with LST, it has become the preferred and most used index for the ecological assessment of the urban environment (Guha et al., 2018). Also, UTFVI does not require parameter datasets like humidity and wind speed, which are demanded by other comfort indicators but are not readily accessible in high spatial resolution for most areas including the study area. Importantly, the UTFVI has been examined with Landsat data and shown satisfactory results (Guha et al., 2018; Kursah, 2023).

Throughout the preceding years, Ghana has witnessed substantial expansion in its urban populace. For instance, from 1931 to 2010, the urban population increased from 9.4% to 50% (Wemegah et al., 2020) and today, approximately 15.5 million out of the 30 million Ghanaian population which represents 58% reside in urban centers (Niel, 2023; Ghana Statistical Service, 2021). Also, there has been an increase in Ghana's urban centers to 212 urban centers. (Africapolis, 2023; Ghana Statistical Service, 2021). This evidence of urban growth is rapidly changing the land use land cover pattern in Ghana into built-up and has brought changes in the hydrological services (Negesse et al., 2024). According to Jumari et al. (2023), a contributory factor to the climate change phenomenon is the transformations in land use land cover. Sadly, Sekondi-Takoradi, which is one of Ghana's urbanized metropolises in the western region is no exception to the increasing loss of land cover to built-up. Mensah et al. (2019) characterized the metropolis as a city of infrastructural development after noticing a surge in its construction activities. According to the Ghana Statistical Service (2021), the urbanization rate in the metropolis was approximately 61.8% as of 2021 which represents a significant increase from the urbanization rate of 36.4% in 1984. The prime cause of rapid urban growth in the metropolis is due to the concentration of economic activities and industries within the metropolis (Service, 2014). As of 2021, cement and concrete made up 75.7%

of the construction materials used in the metropolis for outer walls while wood made up 4.7% of the main construction materials for outer walls. Also, the main construction materials for roofs within the metropolis were metal sheets (56.9%), slate or Asbestos (25.0%), and cement or concrete (12.3%). These building materials are mostly impermeable and have significant heat retention capacity which influences the natural ecology and local climate ecology of an area. Additionally, the growth of the metropolis has also led to increasing use of automobiles which is an influencing factor in causing high temperatures in the metropolis (Ghana Statistical Service, 2021). In 2022, the developmental planning unit stressed that the ongoing constructions in the metropolis have warranted an increased number of machineries to transport materials. Hence, it leads to a substantial increase in both traffic and air pollution (STMA, 2022) which contributes significantly to the rise in the temperature and thermal discomfort in urban areas (Filho, 2021; Mansour, 2022). As urbanization and anthropogenic heat-generating activities continue at a rapid rate with no proper mitigating measures, it is expected that heat islands will worsen (Belenok et al., 2021).

UHI can be measured using either remote sensing or ground-based datasets. According to Kursah (2023), traditional methods or ground-based weather stations encounter issues such as inconsistent data coverage, changes in instruments and sites, and the absence of pixel-based data. These limitations restrict the use of data from weather stations, hence making satellite remote sensing datasets the preferred. The large temporal and spatial datasets coverage from remote sensing satellites facilitates comprehensive spatial analysis. They make it possible to accurately and precisely retrieve the surface temperature of each pixel and can track variations in surface temperature at all levels (Frimpong, 2022). Furthermore, since temperature is a continuous variable, relying on a limited number of discrete measurements is insufficient for accurately estimating surface temperatures (Buo et al., 2021). The application of remote sensing (RS) and Geographic Information Systems (GIS) technologies has witnessed significant growth in assessing LULC changes and LST variations in urban areas. These technologies have garnered considerable interest in studying ecosystem transformations, biodiversity, and global climate patterns (Jahan & Rahman, 2021). Traditional methods of change detection in LULC scenarios and direct field visits for LST monitoring are resource-intensive, time-consuming, and susceptible to errors. However, by integrating RS and GIS technologies, it becomes more efficient to evaluate, monitor, and model changes in LULC, urban growth, and UHI (Al-Kafy et al., 2020; Jahan & Rahman, 2021).

Extensive studies have utilized RS and GIS to discern the thermal characteristics of urban surfaces and establish connections between the various LULC classes and the LST in various ways. For instance, Wemegah et al. (2020) evaluated the phenomenon of urban heat island effect in the Greater Accra region using land cover types, thermal data, and daily observed minimum and maximum temperature data. Stemn and Kumi (2020) used land surface temperature to model heat-related conditions in the Wassa West mining area of Ghana. Jahan & Rahman, (2021) used remote sensing and GIS to simulate surface temperature under climate change scenarios. Huda & Al (2021) employed remote sensing and statistical techniques to evaluate the relationship between temperature and land cover in Chattogram City. Kumi-Boateng & Stemn (2015) integrated RS and GIS to evaluate the impact of rapid urban growth on surface temperature. By combining GIS with RS, this study carried out a thorough evaluation of UHI warming in the Sekondi-Takoradi Metropolis.

In some regions of Ghana, especially in the Greater Accra region, UHI has been extensively addressed (Gyimah et al., 2023; Wemegah et al., 2020). However, to the best of the researcher's knowledge, the only study on urban heat islands carried out in the Sekondi-Takoradi metropolis was conducted by Kumi-Boateng & Stemn (2015). Kumi-Boateng & Stemn (2015) examined the impact of urban expansion on the thermal environment in the Sekondi-Takoradi metropolis, but the analysis only spanned a brief period of 17 (1991-2008), data was limited to only Landsat 5 and 7 and lacked information on the extent, intensity and magnitude of UHI which is covered extensively in this study. Also, using the UTFVI to measure the thermal comfort level of the metropolis was not addressed in the works of Kumi-Boateng & Stemn (2015). Even taking Ghana as a whole, less attention has been given to the application of UTFVI in UHI studies. Also, the interplay of various spatial influencing factors results in distinct thermal patterns and archetypes within the urban environment. Unfortunately, previous studies, especially in Ghana and within the study area have focused only on how land cover affects LST and UHIs (Buo et al., 2021; Frimpong et al., 2023; Kursah, 2023; Osei et al., 2023; Stemn & Kumi, 2020). No studies have been conducted on the spatial influencing factors of LST such as proximity to roads, waterbodies, Central business district (CBD), digital elevation model (DEM) as well as land use land cover, and spectral indices effects on LST and UHI. Therefore, this study addresses the research gap by incorporating UTFVI to analyze UHI and provides information on the extent, intensity, and magnitude of UHI which is lacking. It also investigates the significant differences in surface

temperature potentially influenced by the spatial factors within the different archetypes of the study area—a dimension often overlooked in previous research. Furthermore, Guha et al. (2018) demonstrated that LST corresponds variably with seasons and surface cover, so, it cannot accurately and universally depict the same situation everywhere. This stems from the fact that every city has a distinctive nature and their complex interplay of factors affects LST. As a result, Kursah (2023) has explicitly emphasized the need for location-specific studies on LST to develop a comprehensive universal understanding of how urban growth influences heat patterns. In addition, Golestani et al. (2024) emphasize that there are variations in the intensity of heat island effects from one city to another. Therefore, understanding these variations is very important for gaining a total comprehension of UHI. Achieving this research objective offers valuable insights for urban planners and city authorities, equipping them with the essential knowledge to develop sustainable development plans that mitigate the adverse effects of urban growth and elevated temperatures in the Sekondi-Takoradi metropolis. Furthermore, the findings contribute to global efforts to create more livable and climate-resilient urban environments.

5.2 Materials and Methods

The following subsections discuss the materials and methods (Figure 5.1 and 5.5) employed in the study.

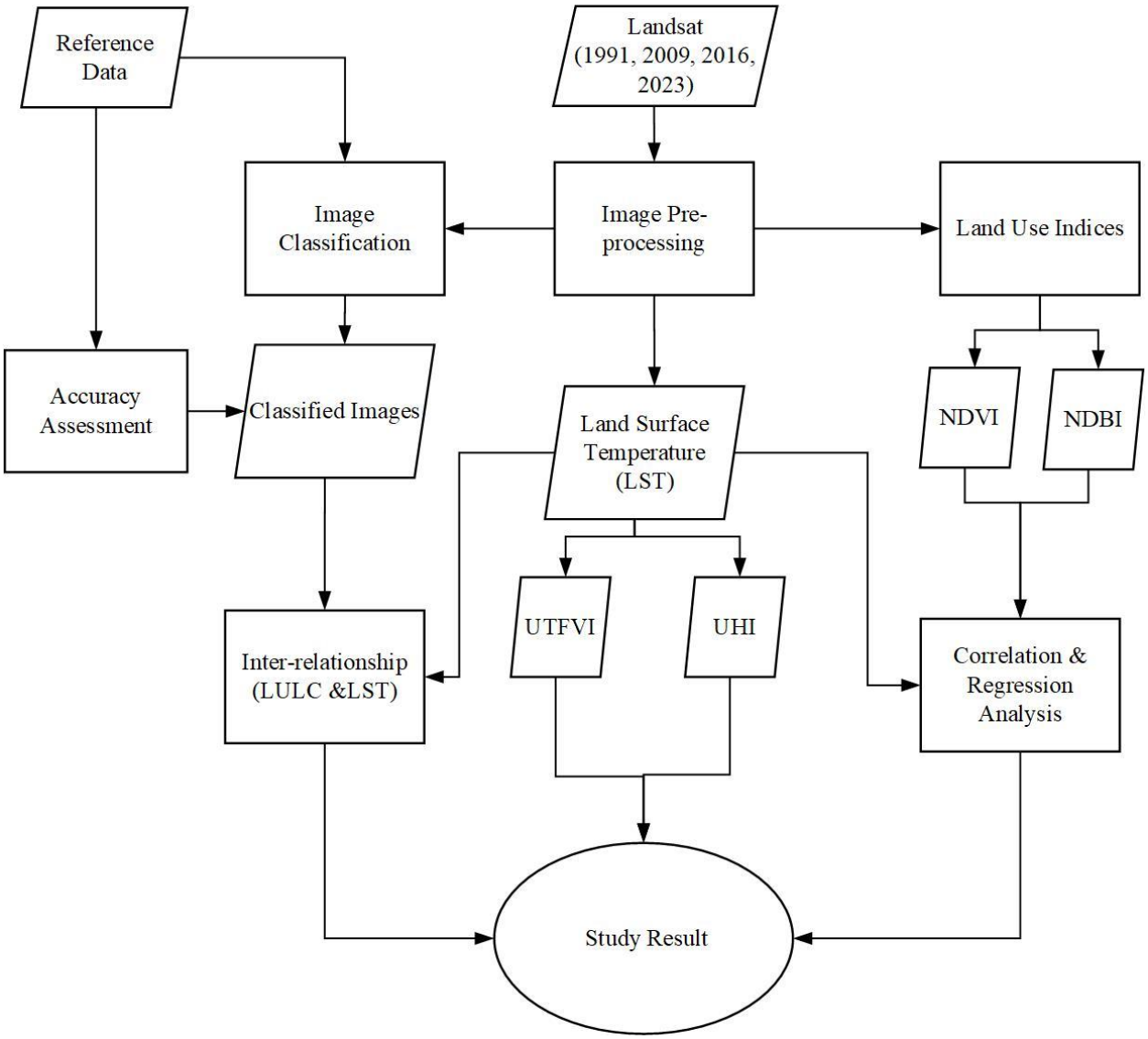

Figure 5.1: Methodical workflow.

5.2.1 Study Area

As illustrated in Figure 2, Sekondi-Takoradi is located at latitude 4° 52′ 30″ N and 5 °04′ 00″ N and longitudes 1° 37′ 00″ W and 1° 52′ 30″W. It is the administrative hub for the western region of Ghana with a land area of 191.7 km^2. 96.1% of the population in the metropolis resides in urban areas, while 3.9% resides in rural areas. This demonstrates that a significant portion of the city residents reside in urban regions (Chatwin and Arku, 2018). Due to the role of the metropolis as a commercial and industrial hub, it draws immigrants from all walks of life. Several important businesses such as the wood and plywood industries, shipbuilding, railway repair, and the oil industry can be found in the metropolis (Mensah et al., 2019). It has an equatorial climate and an

average yearly temperature of 22°C. Rainfall in the metropolis occurs in two distinct seasons: the major season starts from March to July and the minor season lasts from August to November. According to Aduah et al., (2020), the average annual rainfall is 1380 mm or 122 rainy days. The study area was chosen because it hosts various construction enterprises and industries. These enterprises and industries engage in burning fossil fuels for manufacturing, energy production, industrial processes, and transportation which are key contributors to elevated temperatures. Increasing temperatures are significant contributors to global warming. Therefore, it is imperative to conduct LST and UHI analysis to effectively monitor the temperature dynamics in Sekondi-Takoradi. Also, vegetation, which acts as a heat sink for the metropolis is massively degrading and this renders the metropolis vulnerable to severe thermal conditions (STMA, 2022).

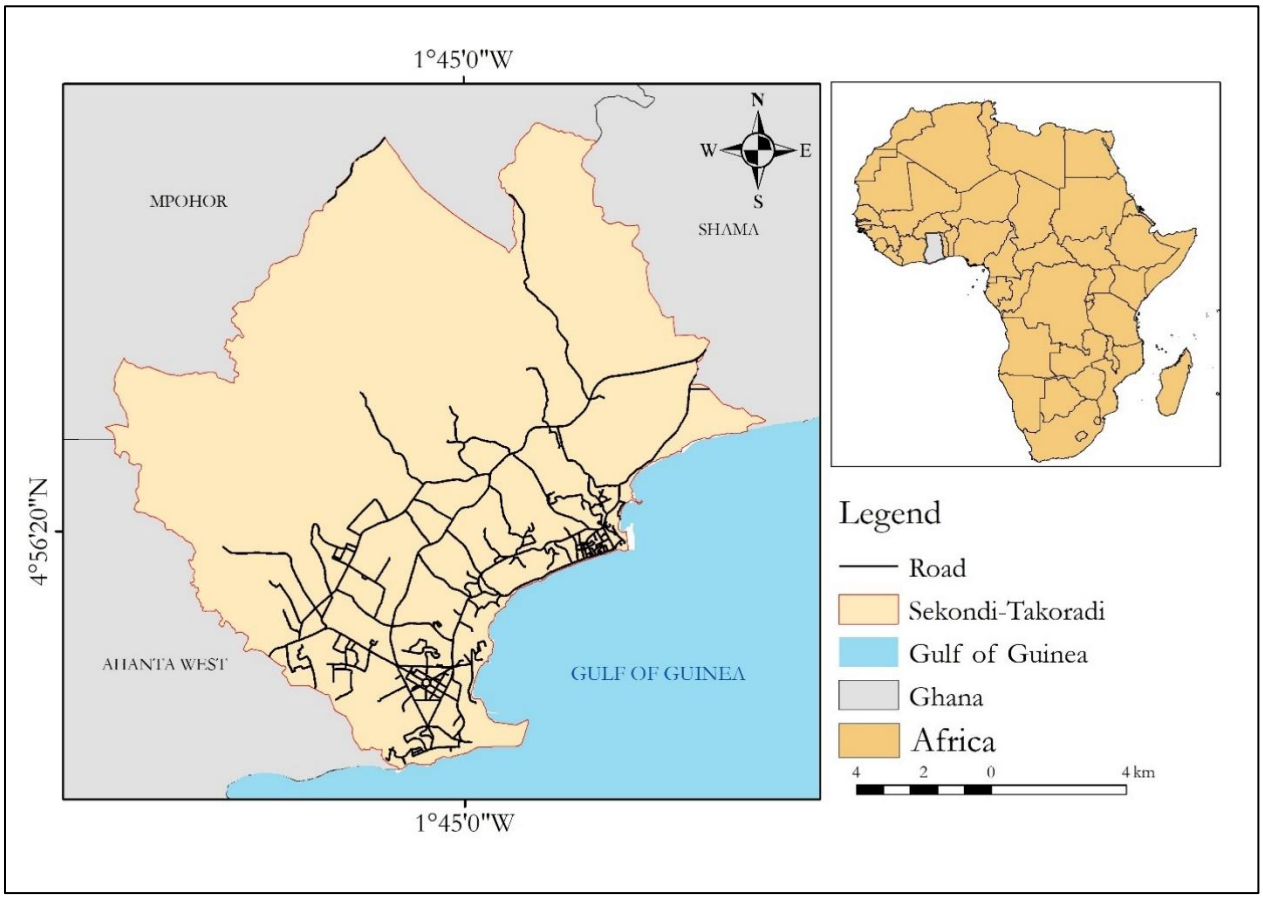

Figure 5.2: study area.

5.2 Dataset used

Four Landsat images spanning from 1991 to 2023 were used to conduct this study (Table 5.1). To avoid the problem of phenology which can affect the accuracies of the study as well as limit the impact of the different seasons on land surface changes, the images were chosen at the same season. Additionally, GPS data obtained during the field survey and other vector data were employed in this study. Details of the Landsat images and other datasets employed are presented in Table 5.1.

Table 5.1: Dataset used

Sensor	Source	Path/Row	Resolution	Acquisition date
Landsat 5	USGS earthexplorer	194/57	30m	01/01/1991
Landsat 7	USGS earthexplorer	194/57	30m	01/02/2009
Landsat 7	USGS earthexplorer	194/57	30m	06/01/2016
Landsat 8	USGS earthexplorer	194/57	30m	01/01/2023
GPS data	Field survey	NA	3m	
Shapefile and other vector data	Survey Department of Lands Commission	NA NA	NA	

Not Applicable=NA

5.3 Methods

This section concisely describes the analysis undertaken for the study as shown in Figure 5.1 and Figure 5.5

5.3.1 Image pre-processing and classification

Satellite images are commonly affected by distortions during the process of imaging and so need to be corrected before any further processing and analysis can be applied (Sarif et al., 2020). In this study, radiometric and geometric corrections were applied to the acquired Landsat images using QGIS software. Several classification algorithms such as the maximum likelihood classifier (MLC), support vector machine (SVM), and random forest (RF) have been used in mapping out land cover types. The supervised random forest method was used to classify the images into three classes (Table 5.2). This algorithm was chosen due to its enhanced ability to handle outliers and data noise (Asif et al., 2023), superior performance with multi-dimensional datasets from various sources, faster processing time, and higher accuracy compared to classifiers like Maximum Likelihood, Support Vector Machine, and Kernel Neural Network (Lukas et al., 2023). Furthermore, the random forest can manage missing values, categorical, and unbalanced data—

capabilities not present in SVM (Hidalgo-García & Arco-Díaz, 2022; Xiang et al., 2022). According to Blay & Abunyuwah (2024), satellite images are high-dimensional data and can be effectively classified and regressed using the Random Forest algorithm. By bootstrapping and aggregating ensembled votes to form classification and regress trees, the RF excels at differentiating and classifying multi-source remote sensing and geographic data, Hence it produces accurate results and robust findings (Tassi & Vizzari, 2020). Additionally, the resampling process in RF is not influenced by weighting, therefore, RF is insensitive to noise and overfitting (Blay & Abunyuwah, 2024). Most machine-learning algorithms suffer from the Hughes phenomenon, unlike the RF which effectively addresses the Hughes phenomenon due to its two-dimensional randomness along with its ability to achieve accurate classification results with a relatively small number of supervised training samples (Zhao et al., 2024). Lastly, the reliable outcomes of RF classification have made many studies recognize it as an effective land use land cover classifier (Sarif et al., 2020).

Table 5.2: Description of class types.

Class type	Description
Water	This includes the rivers, streams, and lakes, inland water in the study area.
Vegetation	This includes natural plants, trees, and green spaces.
Built-up	This includes built-up areas or areas covered by made-made structures, impervious surfaces, residential areas, industrial areas, and commercial areas, paved areas, roads.

5.3.2 Accuracy Assessment

According to Khwarahm et al. (2021), classified images must be assessed for reliability after a classification process. This is because misclassified images will have a negative influence on the outcome of a study (Wangyel et al., 2021). Using reference data, the classified images were assessed for their accuracy. The stratified random sampling point technique was used to sample 300 points for each classified image to create an error matrix. The error matrix is a composition of Producer accuracy (PA), User accuracy (UA), Overall accuracy, (OA), and Kappa coefficients (KC). Equations (5.1)- (5.4) were respectively used to estimate PA, UA, OA, and KC (Khan et al., 2022; Shamsudeen et al., 2022). The ArcGIS 10.5 was used to perform the accuracy assessments

$$\text{Overall accuracy} = \frac{\text{Total number of correctly classified pixels}}{\text{Total number of reference pixels}} \times 100 \qquad (5.1)$$

$$\text{User accuracy} = \frac{\text{Corrected classified pixels in each class}}{\text{Total classified pixel in that class (row total)}} \times 100 \quad (5.2)$$

$$\text{Producer accuracy} = \frac{\text{Corrected classified pixels in each class}}{\text{Total classified pixel in that class (the column total)}} \times 100 \quad (5.3)$$

$$\text{kappa Coefficient} = \frac{(\text{total accuracy} - \text{random accuracy})}{(1 - \text{random accuracy})} \quad (5.4)$$

5.3.3 Spectral indices

Three distinct indices related to land use were estimated. These indices are the normalized difference vegetation index (NDVI), and normalized difference built-up index (NDBI). NDVI is an essential indicator of urban climate (Sarif et al., 2020). It is widely used to assess the quantity and health of vegetation in an area. Its values range from +1 to -1, with large positive values representing vegetation, negative values indicating water, and 0 denotes built-up or bare land (Guha, 2021). Using equation (5.5), the NDVI of the study area was computed (Shamsudeen et al., 2022).

$$\text{NDVI} = \frac{\text{NIR} - \text{RED}}{\text{NIR} + \text{RED}} \quad (5.5)$$

Where NIR denotes Near-Infrared.

NDBI is also commonly used to retrieve information about the imperviousness of an area. It also ranges between the values +1 to -1 where water, vegetation, and built-up are denoted respectively by zero, negative, and positive values. As an important indicator of urban climate, the NDBI was computed using equation (5.6) (Sarif et al., 2020; Shamsudeen et al., 2022).

$$\text{NDBI} = \frac{\text{MIR} - \text{NIR}}{\text{MIR} + \text{NIR}} \quad (5.6)$$

Where MIR denotes mid-infrared and NIR denotes Near-Infrared.

Lastly, NDWI is used to identify and map open-water surfaces as well as assess the level of turbidity in water bodies (Das & Angadi, 2020). The NDWI index ranges from − 1 to +1. (with values greater than 0 typically representing water bodies, while values less than 0 indicate non-water areas (Ahmed & Kranthi, 2018). Equation (5.7), as expressed by Badasa et al. (2022) was used to derive the NDWI for the study

$$\text{NDWI} = \frac{\text{Green}-\text{NIR}}{\text{Green}+\text{NIR}} \quad (5.7)$$

5.3.4. Derivation of land surface temperature (LST)

According to Al-Kafy et al. (2020), the thermal bands of Landsat store temperature data as digital numbers. Therefore, using the thermal bands of various Landsat imageries, the surface temperature can be determined. Band 6 is the thermal band for Landsat 5 and 7 whereas bands 10 and 11 are the thermal bands for Landsat 8 (Huda & Al, 2021). Concerning the thermal band of Landsat 8, Al-khakani (2023) recommended using band 10 for land surface temperature estimation due to the considerable uncertainties associated with band 11. Following this recommendation, this study adopted band 10 and band 6 for the LST estimation. The derivation of LST from Landsat 5 and 7 followed a 3-step process (Figure 5.3) while LST from Landsat 8 was obtained using a 5-step process (Figure 5.4). These steps are widely known and efficiently used to determine LST (Gyimah et al., 2023).

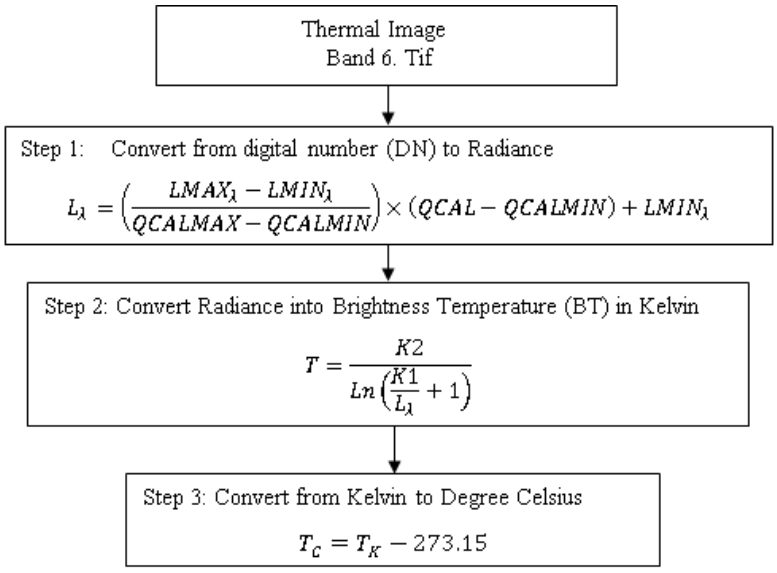

Figure 5.3: A 3-step method for deriving LST from Landsat 5 and 7

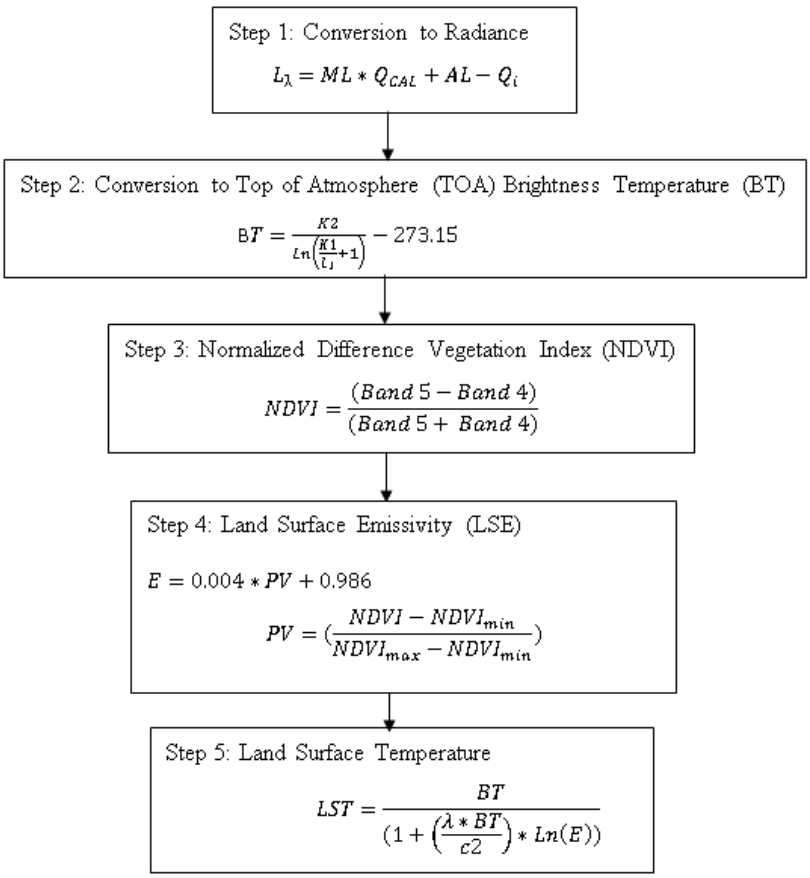

Figure 5.4: A 5-step method for deriving LST from Landsat 8.

5.3.5 Mapping out Urban Heat Islands (UHIs) and Urban Thermal Field Variance (UTFVI)

The UHI zones were determined by applying the following equations (Guha, 2017; Osei et al., 2023).

$LST > \mu + 0.5 * \delta$ referred to UHI zones (5.8)

$0 < LST \leq \mu + 0.5 * \delta$ referred to non UHI zones (5.9)

where μ represents the mean and δ represents the standard deviation of the LST. To quantitatively explain the UHI sensitivity, UTFVI, as expressed in equation (5.10) was applied (Huda & Al, 2021; Wemegah et al., 2020).

$$UTFVI = \frac{T_s - T_m}{T_s} \quad (5.10)$$

Where T_s denotes the LST of the area, T_m is the average LST. Based on the UTFVI, the study area was further divided into six distinct classes (Guha, 2021; Wemegah et al., 2020). These UTFVI

classes are matched with an ecological evaluation index (EEI) (Table 5.3). The ecological evaluation index is a metric that measures the influence of urban thermals on urban ecological life (Huda & Al, 2021).

Table 5.3: Threshold values of UTFVI and its ecological evaluation index (EEI).

UTFVI range	UHI Effect type	EEI
<0	None	Excellent
0-0.005	Weak	Good
0.005-0.010	Middle	Normal
0.010-0.015	Strong	Bad
0.015-0.020	Stronger	Worse
>0.020	Strongest	Worst

5.3.6 Regression analysis using Ordinary Least Square Regression (OLS) and Geographically Weighted Regression (GWR)

In this study, the OLS Regression and GWR were used to examine the connections between LST, NDVI, and NDBI. The ordinary Least Square (OLS) model has widely been used to determine the association between dependent and independent variables. According to Frimpong et al. (2023), although OLS regression is a straightforward model, it fails to account for spatial autocorrelation and spatial non-stationarity (Frimpong et al., 2023). In the case of spatial autocorrelation, the value of a variable at a given location is influenced by the value of the same variable surrounding it (Deilami, 2017). For instance, a location suffers higher temperatures if multiple high-temperature zones border it. On the other hand, the spatial non-stationarity explains the variations between dependent and independent variables over spaces. Consequently, OLS-estimated parameters are averaged over the area of interest instead of being specific within an area. These limitations severely reduce the model's effectiveness and generalizability of the result. Equation (5.11) expresses the formula of OLS:

$$y = \beta_0 + \sum_{j=1}^{n} \beta_j x_i + \varepsilon \quad (5.11)$$

Where y is the dependent variable and x_i is the independent variables; n is the number of independent variables, β_0 and β_j are the intercept and coefficient respectively; e is the error (Mirchooli et al., 2020).

The drawbacks of OLS are addressed by the Geographically Weighted Regression (Zhou et al., 2019). GWR is a linear regression model used to model relationships that change in space. It builds unique equations for every element in the dataset, accounting for the dependent and independent variables of every target feature (Wheeler, 2021). GWR takes into account the location data connected to every sampled point. It enhances forecasts and provides a better understanding of the local variance in the independent variables (Frimpong, 2022). In GWR, the bandwidth controls the size and extent of the neighborhood. There are two types of bandwidths: adaptive and fixed. Fixed kernel local regression is suitable for small datasets that are evenly distributed across space. Conversely, adaptive kernel regression performs well with dense datasets that have an uneven spatial distribution (Mirchooli et al., 2020). Equation (5.12) expresses the GWR model

$$y_i = \beta_{i0} + \sum_{k=1}^{p} \beta_{ik} x_{ik} + \varepsilon_i \qquad (5.12)$$

The dependent variable at location i is represented by yi, the Kth independent variable at location i is represented by x_{ik}, the local regression coefficient for the Kth independent variable at location i is indicated by β_{ik}, the intercept parameter at location i is represented by β_{i0}, and the random disturbance at location $\boldsymbol{\upsilon}$ is represented by εi (Deilami, 2017; Mirchooli et al., 2020).

Jaber (2020) used OLS to examine the relationship between human population distribution and LST in areas with different climatic classifications. Tariq et al. (2022) determined the relationship between seasonal air temperature and MODIS-derived LST in Pakistan by employing GWR, simple regression, and geostatistical interpolation models. Global-based (OLS) and local-based (GWR) analyses were employed to explore the relationship between LST, land cover, and population growth in ten Chinese megacities (Liu et al., 2020). Siddique et al. (2023) identified urban heat island (UHI) areas in Beijing and determined the correlation between LST, LUC, NDVI, and BUI based on GWR. In this study, the ArcGIS 10.8 software was used to conduct the analyses of the OLS and GWR. Essential criteria such as the adjusted R-squared (R^2) and Corrected Akaike Information Criterion (AICc), where a higher adjusted R^2 value and a lower AIC indicate superior model performance were used to evaluate the efficiency of the OLS and GWR.

Additionally, other efficiency criteria (see Appendix 2) were used to evaluate the robustness of the model.

5.3.7 Spatial Influencing Factors of LST within the Archetypes Influence

According to Feng et al., (2019), urban archetypes exhibit varying temperatures due to the significant influence of spatial influencing factors. The spatial factors outlined in Table 5.4 were chosen according to their influence on surface temperature as reported by the literature. Using the vector data (Table 5.1), the Euclidean distance tool in ArcGIS 10.8 was used to generate the proximity factors, elevation, and spectral indices. These spatial variables were assessed for their significance on LST using the generalized additive model (GAM). The significant variables were then normalized using the minimum and maximum linear transformation techniques to ensure consistency across different scales and units. The normalized data was further subjected to Principal Component Analysis (PCA) to reduce dimensionality and identify significant components for analysis. Using the component of the PCA, the K-means unsupervised classification was applied to group pixels into six distinct classes. The K-means algorithm was chosen for its efficiency in processing large datasets, its ability to minimize intra-cluster variance and maximize inter-cluster differences, and its adaptability to multi-dimensional data, making it suitable for geospatial applications (Kanani-sadat et al., 2019). The six distinct classes were extracted and characterized according to the composition of the influence variables of LST. Multi-point sampling was then performed to extract the LST values for each class, enabling statistical analysis. A normality test, specifically the Kolmogorov-Smirnov test, was conducted to assess whether the residuals of the LST values followed a normal distribution. Since the residuals failed the normality test, the Kruskal-Wallis test, a non-parametric method, was applied to determine the statistical significance of differences in LST among the classes.

Table 5.4: Description of spatial factor of LST employed in the study

Variables	Explanation to LST	Literature
Normalized Difference Vegetation Index (NDVI)	Regions with higher NDVI values generally exhibit more significant cooling effects due to increased plant transpiration. Areas with little or no vegetation tend to store more heat leading to higher surface temperatures.	(Das & Angadi, 2020; A. Mondal et al., 2021; Thapa, 2017)
Normalized Difference Built-up Index (NDBI)	Built-up areas characterized by a high NDBI value effectively contribute to a rise in temperature.	(Guha et al., 2018; Taloor et al., 2024; Ullah et al., 2022)
Normalized Difference Water Index (NDWI)	High NDWI is associated with water abundance and cooler surface temperatures while Low NDWI indicates water scarcity, and urban expansion which causes higher surface temperature	(Guha & Govil, 2021; Taloor et al., 2021; Chanyal & Purohit, 2024)
Digital Elevation Model (DEM)	High-altitude areas are cooler due to thinner atmosphere and reduced ability to trap heat. Temperature typically decreases with increasing altitude at an average lapse rate of about 6.5°C per 1,000 meters.	(Danniswari et al., 2022; Kuang et al., 2015; Njoku & Tenenbaum, 2022;Thapa, 2017)
Proximity Road	Roads are a key component of urban infrastructure and can directly and indirectly affect surface temperature due to their physical, material, and functional characteristics. Roads often lead to vegetation clearance, eliminating the cooling effect provided by plants through shading and evapotranspiration.	(Feng et al., 2019;Liu et al., 2020 Nath et al., 2020)
Proximity to Central Business District (CBD)	Proximity to the Central Business District (CBD) strongly influences Land Surface Temperature (LST) due to the dense urban environment, infrastructure, and human activities typical of these areas. The CBD is often a hotspot for the Urban Heat Island (UHI) effect	(Choudhury et al., 2019; Feng et al., 2019; Yu et al., 2019)
Proximity to waterbodies	Water bodies moderate temperatures through high heat capacity and facilitate evaporation which absorbs heat from the surrounding environment leading to a cooling effect.	(Guha & Govil, 2021; Taloor et al., 2021; Chanyal & Purohit, 2024)

Following this, the mean temperature for each class was calculated and linked to the influencing variables to interpret the relationship between land use characteristics and LST. Finally, the influence of these spatial variables on temperature variations within the archetypes was examined

to provide insights into the role of urbanization in shaping surface temperature patterns. These steps are graphically outlined in Figure 5.5

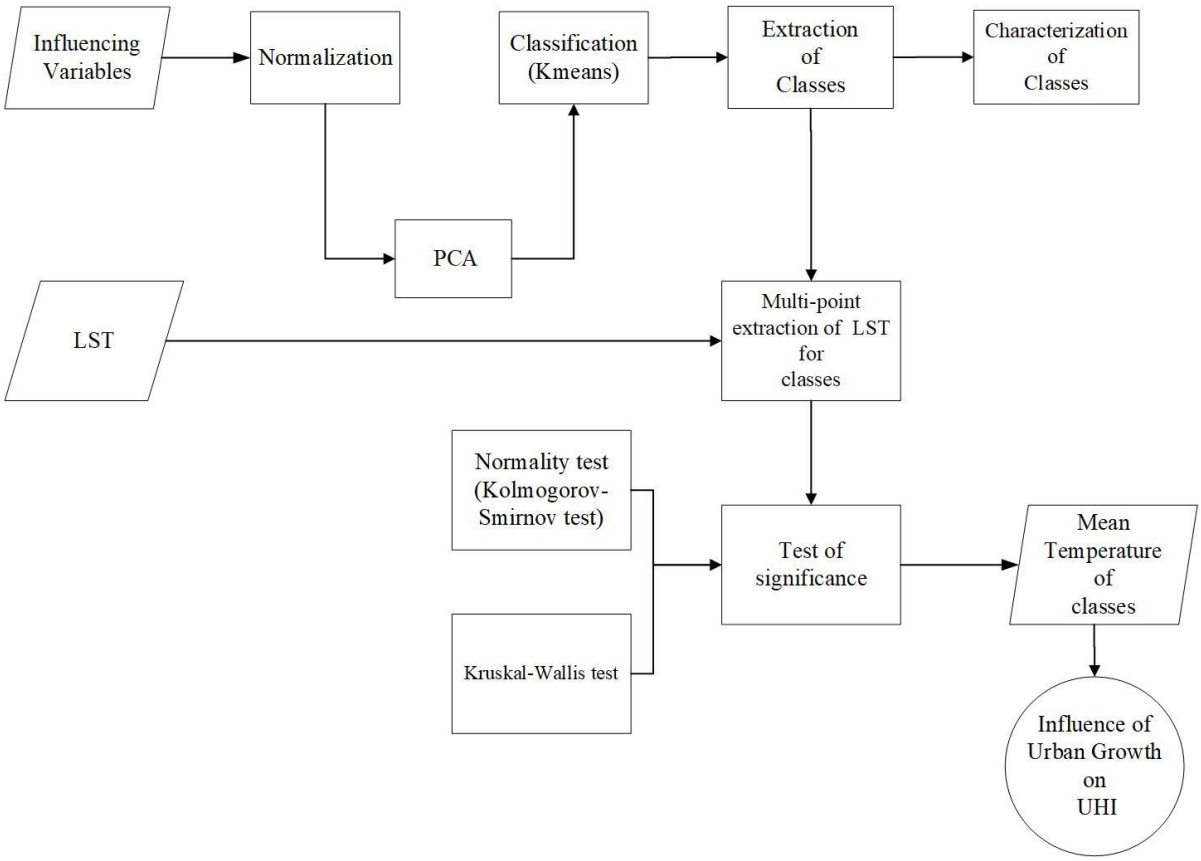

Figure 5.5: The influence of spatial variables on urban archetypes' temperature variations.

5.4. Result and discussion

The results of the analysis conducted in this study are thoroughly presented and discussed in sub-themes under this section.

5.4.1 Land use land cover classification and accuracy assessment

Observing from Figure 5.6, a significant transformation can be seen in the land use land cover pattern of the study area over the period. These changes are statistically detailed in Table 5.5.

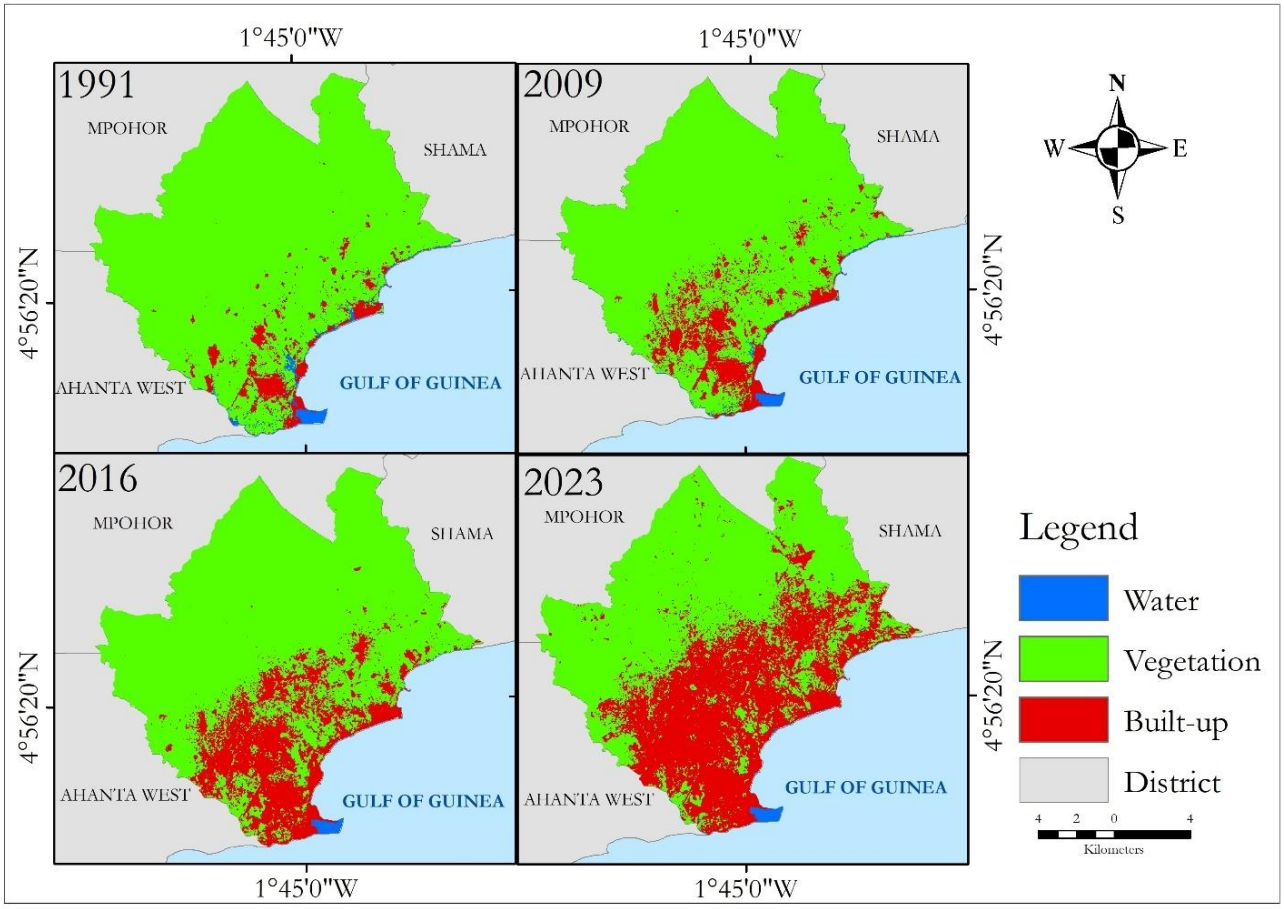

Figure 5.6: LULC map from 1991 to 2023.

Water displayed a dynamic and contrasting pattern across the four-time steps. From 1991 to 2016, water declined drastically by 2.3 km^2 but increased slightly by 0.27 km^2 between 2016 and 2023 (Table 5.5). The decline in water is possibly due to the expansion of built-up (Table 5.5), a shift in hydrological dynamics, and sedimentation (Saleem et al., 2024). According to Mensah et al. (2019), the reduction of water could be explained by the significant decrease in the water retention capacity in watershed and wetland areas due to land degradation and loss of vegetation as seen in Table 5.5. In addition, Muruganandam (2023) expresses that the reduction in water level can be attributed to climate change as it causes changes in rainfall patterns and hydrological cycles. This has been proven in the works of (Huber, 2024) as climate change has led to the depletion of glaciers, consequently affecting water availability directly or indirectly. However, the slight increase in water could be attributed to the occurrence of floods and natural changes in water level (Biney, Forkuo, Poku-Boansi, Asare, et al., 2024). The cumulative decrease in water over the study period indicates the dynamic nature of aquatic ecosystems in the metropolis and its vulnerability

to changes in the environment. Vegetation experienced a continuous decline in its coverage throughout the time steps of the study period. From Table 5.5, a substantial reduction of 10.4 km^2 occurred between 1991 and 2009 and a decrease of 15.66 km^2 and 34.93 km^2 from 2009 to 2016 and 2016 to 2023 respectively. These changes are explained mainly by built-up expansion (Table 5.5), and other factors such as deforestation (Dadzie-Paintsil & Mensah, 2022), ecological changes, and land use practices (Tasantab, 2019). According to Negesse et al. (2024), a sizable portion of vegetation is consumed by built-up during urban expansion. For instance, the growing need for housing has been cited as the reason for the vegetative cover reduction in Addis Ababa. Turning vegetated land into impermeable surfaces reduces surface moisture, alters energy flow, and affects the energy balance, which could raise an area's surface temperature (Ullah et al., 2024). Although the rate of reduction has not been uniform, the significant overall decline of 60.99 km^2 indicates the intricate relationship between urbanization, land management, and environmental conversation (Nyamekye, 2020; Younes, 2023). The spatial coverage of built-up progressively expanded throughout the study period at a cumulative amount of 63.07 km^2. This consistent growth reflects developmental initiatives, urbanization trends, migration patterns, and population growth in the metropolis (Saleem et al., 2024). Among the transitional years, a significant surge of 34.65 km^2 was observed between 2016 and 2023, which highlights the increasing conversion of natural space into built-up spaces and the concurrent infrastructure development in the metropolis. Hence, indicates the rate at which the metropolis is becoming urbanized and the possible presence of unplanned built-up. As a result, Khan et al. (2022), recommend the implementation of strategies and initiatives that will check unauthorized urban growth and inappropriate conversion of natural space or water and vegetation into built-up. The rise in built-up at the cost of other land covers is in line with the work of Asare et al. (2023), Biney & Boakye (2021), and Wemegah et al. (2020). Generally, the analysis of the land use land cover revealed a persistent expansion in built-up, a slight fluctuation in water, and a significant decrease in vegetation. These changes reflect the complex interplay of urbanization, economic development, environmental conservation, and natural land dynamics in the metropolis over the study period.

Table 5.5: Area coverage of land cover classes.

	km²				%			
LULC	1991	2009	2016	2023	1991	2009	2016	2023
Vegetation	177.72	167.32	151.66	116.73	92.72	87.29	79.13	60.90
Built-up	10.56	22.13	38.98	73.63	5.51	11.55	20.33	38.42
Water	3.38	2.21	1.03	1.30	1.77	1.16	0.54	0.68
Total	191.66	191.66	191.66	191.66	100	100	100	100

5.4. 2 Accuracy Assessment

According to Obeng et al. (2023), image classification is considered reliable for analysis if its overall accuracy is above 85% and kappa statistics is above 0.7. From Table 5.6, the accuracy values were above the standardized criteria proposed by Obeng et al. (2023).

Table 5.6: Accuracy assessment result.

Class	**User Accuracy**				**Producer Accuracy**			
	1991	2009	2016	2023	1991	2009	2016	2023
Water	86.00	90.00	95.00	97.00	88.66	91.84	94.06	96.04
Vegetation	89.00	93.00	96.00	98.00	86.41	87.74	93.20	94.23
Built-up	88.00	100	93.00	93.00	88.00	92.71	96.88	97.89
Overall accuracy (%)	87.67	90.67	94.67	96.00				
Kappa Coefficient	0.82	0.86	0.92	0.94				

5.4.3 Analysis of land use indices

From Figure 5.7, the highest NDVI value was recorded in 1991 while the lowest NDVI value was recorded in 2009. According to Badasa et al. (2022) and Haldar & Majumder (2022), NDVI values close to +1 suggest the possibility of dense green vegetation, while values approaching zero indicate the likelihood of urbanized areas. A negative NDVI values indicate the likelihood of water presence. From Figure 5.7, although most of the NDVI values are positive, they are closer to zero than +1, indicating significant urbanization in the metropolis. Consequently, built-up areas have expanded considerably in the metropolis over the studied period

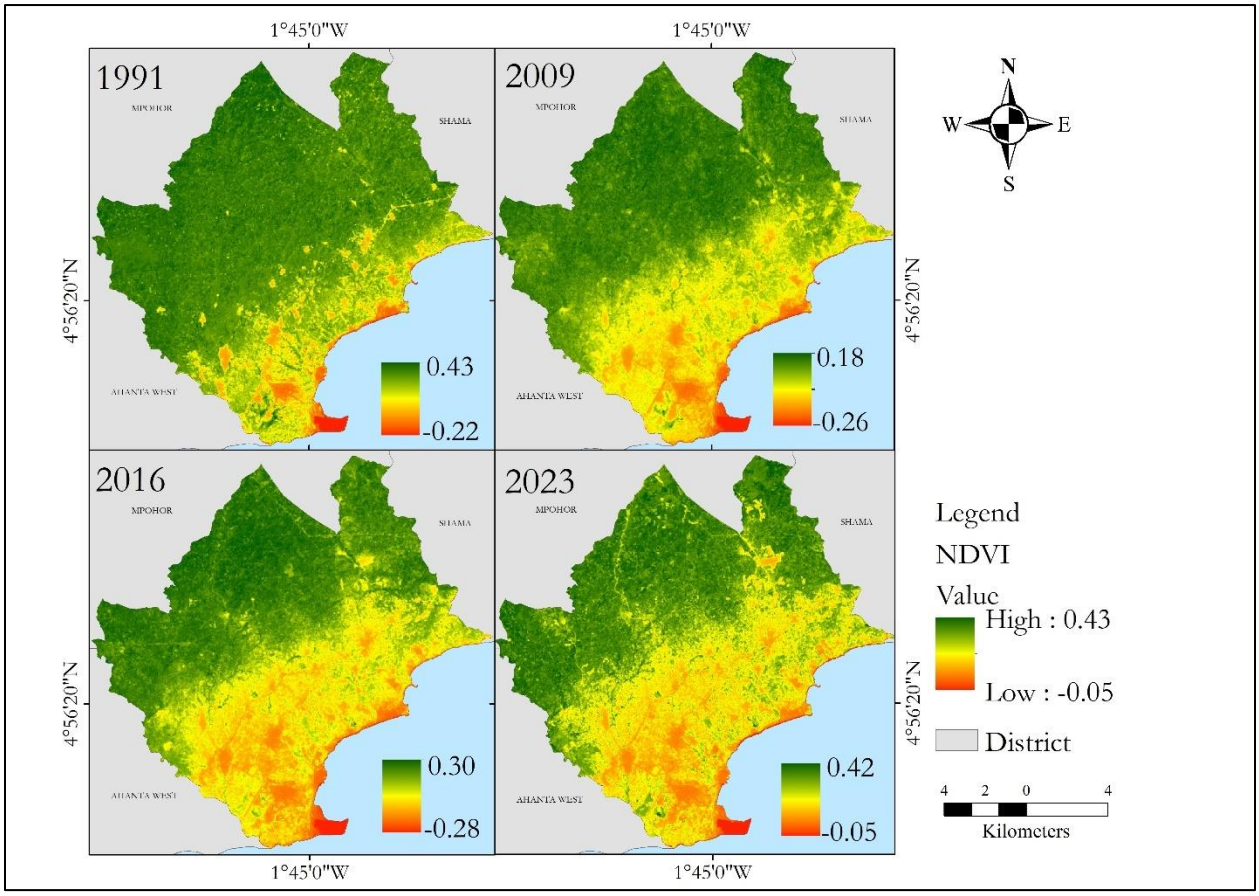

Figure 5.7: NDVI map.

NDBI, however, revealed a persistent increase throughout the study period (Figure 5.8). At each time point, the highest NDBI values were consistently observed in the southern-western and central regions of the study area, attributed to the presence of densely built-up areas. Conversely, the lowest NDBI values were identified in the northern and eastern areas due to the prevalence of high-density vegetation cover. This observed rise in NDBI values demonstrates a positive association with elevated LST readings, implying a direct correlation between the density of built-up areas and surface temperature as illustrated in Figure 5.9.

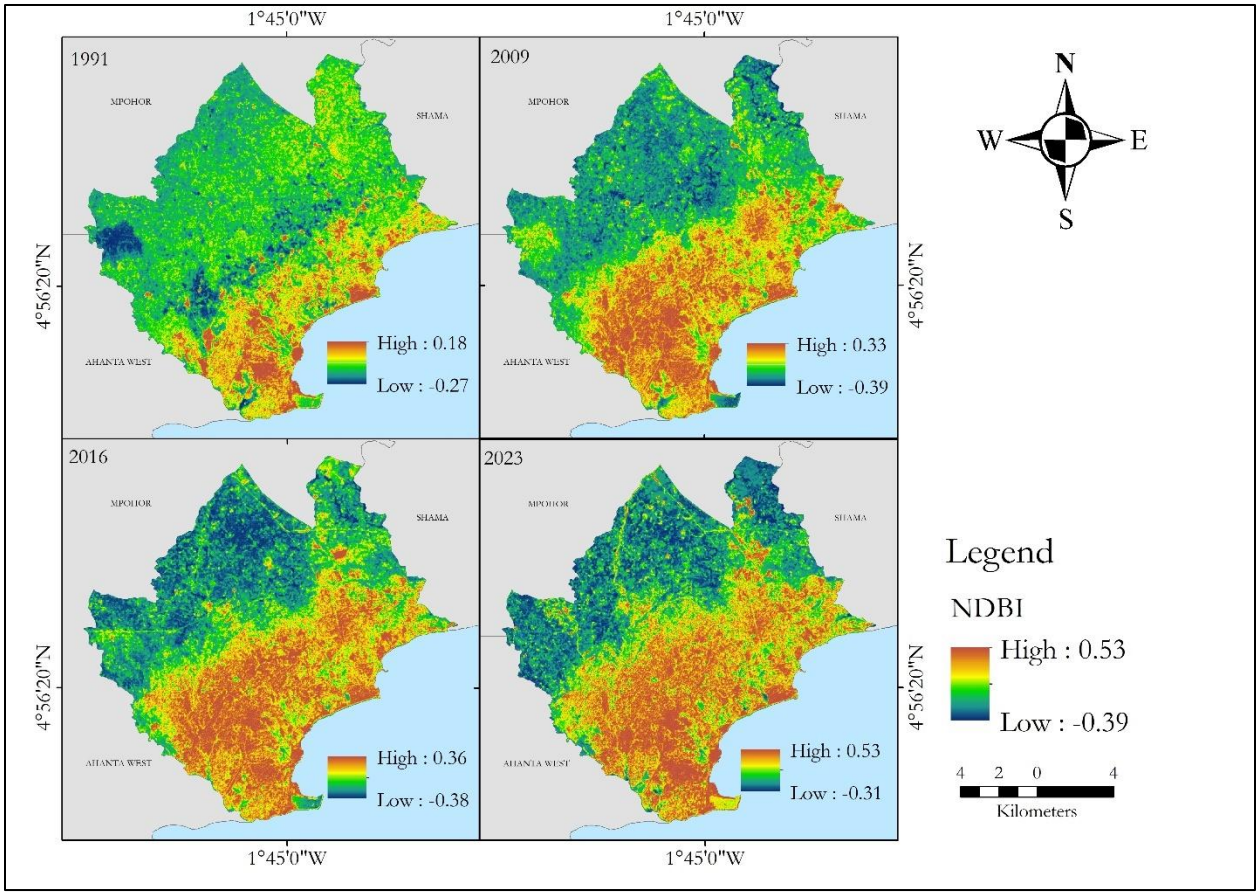

Figure 5.8: NDBI map.

5.4.5 Analysis of land surface temperature (LST)

Advanced remote sensing methods and thermal sensors have facilitated convenient observation and measurement of land surface temperature which was previously challenging to perceive with real eyes (Frimpong et al., 2022). Therefore, by using thermal bands from Landsat imagery, LST for the years 1991, 2009, 2016, and 2023 was assessed (Figure 5.9). These maps were color-symbolized with shades ranging from yellow to dark brown to represent low to high temperatures. By visually comparing the LST maps, it is evident that areas with high LST have expanded over the years, signifying an increase in high-temperature areas by 2023. Also, low temperatures were recorded in the northern part due to the presence of significant vegetation cover. The southern and central regions had high temperatures due to the increase in built-up and reduced vegetation. Thus, the varying land cover across the study area influenced the surface temperatures. This outcome is consistent with the findings of Negesse et al. (2024) who found that the patterns in land surface temperature were closely correlated with the thermal properties of different land cover.

Additionally, Ullah et al. (2024) revealed that differences in surface illumination due to irregular landscapes also influence the variability in LST. Hence, landscape structure, land cover, urban sprawl, and geographic features have been identified as some influencing factors of LST (Ullah et al., 2024; Ghanbari et al., 2023).

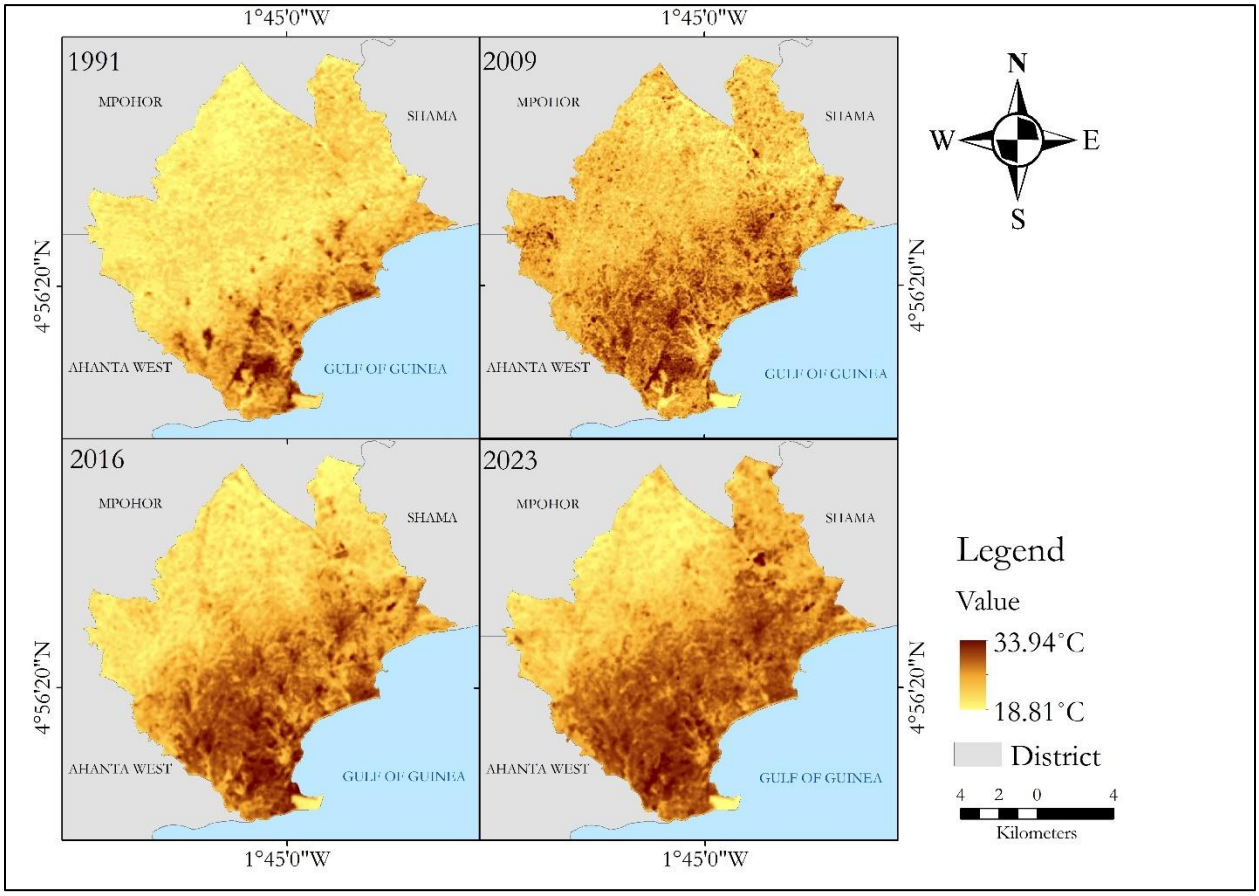

Figure 5.9: LST map of the metropolis.

Statistically, the mean LST showed variations over the years (Figure 5.10). It increased by 3.1°C over the entire period and this indicates that the mean LST increased by 1.03°C every 10 years. This increase of 3.1°C is in line with the predictions made by Rasul et al. (2012) which indicates a global increase in land surface temperature by 1.40 °C to 5.80 °C by the 21st century. Similarly, the IPCC prediction of an increase in global surface warming between 1.1°C and 6.4 °C along with increasing heat waves and hot extremes by the 21st century aligns with this study's findings (Aflaki et al., 2017). Moreover, the mean values are close to the annual average temperature range of 22°C to 28°C (Kursah, 2023b). Stemn & Kumi (2020), also, reported an increase in the mean LST in the Wassa West Mining area from 1990 to 2020. Further, the increase in the minimum and

maximum LST by 1.4 °C and 4.3°C, respectively is closely linked to the decline in vegetation and water, driven by the expansion of built-up areas within the metropolis (Aduah et al., 2020; Badasa et al., 2022). However, Badasa et al. (2022) assert that surface temperature is expected to increase due to global warming.

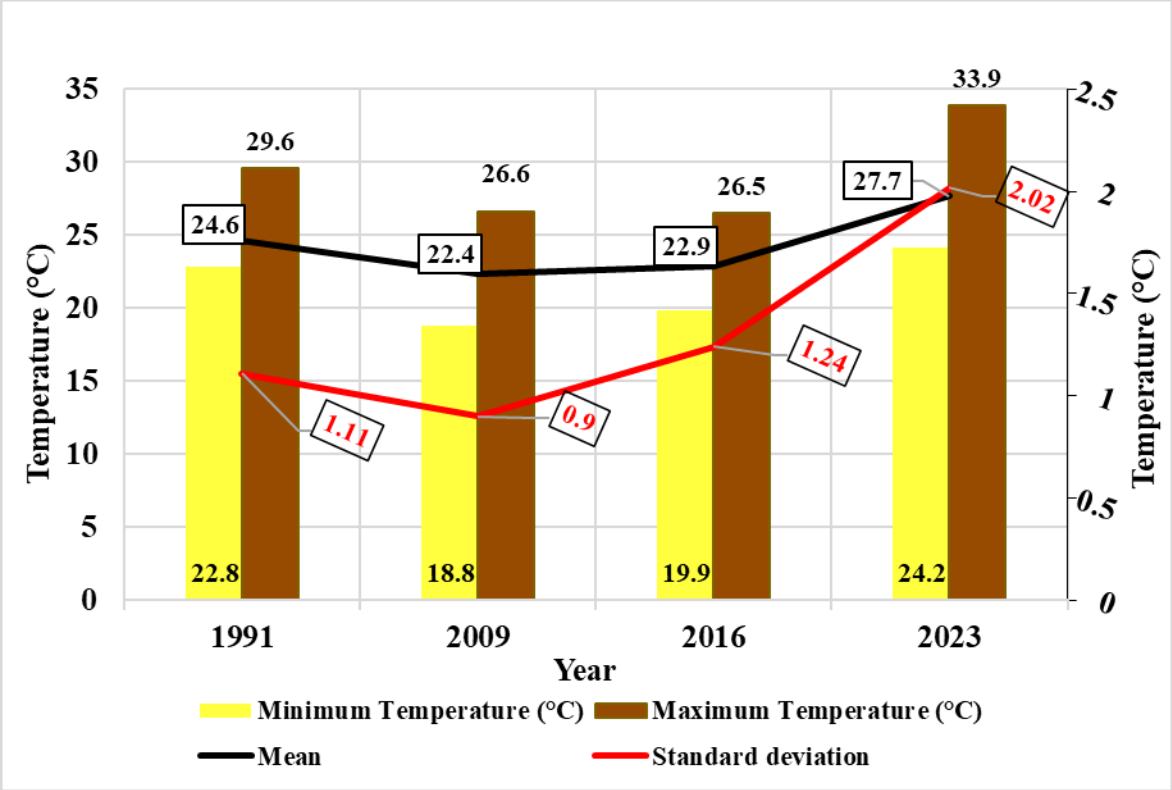

Figure 5.10: Graphical analysis of LST trends.

5.4.6 Area distribution of LST over the study period.

The LST for the various years was broadly categorized into low-temperature class (18-21°C and 21-24°C) and high-temperature class (24-27°C, 27-30°C, and >30°C) and the area of the classes computed (Table 5.7). This categorization assessed the geographical disparity and distribution (area-based distribution) of the research area in various temperature zones. LST in 1991 occupied an area of 54.27 km^2 for the low-temperature class whereas the high-temperature class occupied an area of 137.39 km^2. In 2009, the low-temperature class occupied an area of 184.66 km^2 and the high-temperature class occupied an area of 5.96 km^2. Further, in the year 2016, the low surface temperature class covered an area of 148.69 km^2 and the high-temperature class also increased to 42.24 km^2. Ultimately, in the year 2023, the surface temperature occurred within three classes.

However, there existed significant differences in the type of class and the respective area covered by each temperature class. All temperature values for 2023 fell within the high-temperature class with extreme temperatures (>30°C) recorded only in 2023. This observed phenomenon substantiates the temporal increase in LST in the study area over time and would pose significant challenges to the metropolis. Addressing these challenges demands urgent consideration from local authorities, urban planners, and policymakers, as emphasized in the works of Badasa et al. (2022) and Stemn & Kumi (2020).

Table 5.7: The areas associated with LST class.

Year	**Total Area (km^2)**	**LST classes in km^2 and %**				
		18-21 °C ***(1)***	***21-24*** °C ***(2)***	***24-27*** °C ***(3)***	***27-30*** °C ***(4)***	***>30*** °C ***(5)***
1991	191.66	0.00(0.00)	54.27 (28.31)	130.68(68.18)	6.71(3.50)	0.00(0.00)
2009	191.66	5.96 (3.11)	178.70(93.24)	7.00(3.65)	0.00(0.00)	0.00(0.00)
2016	191.66	14.69(7.67)	134(70.20)	42.42(22.13)	0.00(0.00)	0.00(0.00)
2023	191.66	0.00(0.00)	0.00(0.00)	82.24(42.91)	76.69(40.01)	32.73(17.08)

5.4.7 UHI and UTFVI

The UTFVI and areas with and without UHI effects are statistically highlighted in Table 5.8. From 1991 to 2023, the UHI threshold rose considerably by 13.55°C. This was accompanied by a 10.14% increase in areas with UHI effects, at the expense of areas without UHI effects. These findings align with the research results of Wemegah et al. (2020), Huda & Al (2021), and Siddique et al. (2023) in the cities of Accra, Chattogram, and Beijing respectively. As noted by Kursah (2023), increased UHI can directly induce physiological stress in humans and accelerate the risks of morbidity and mortality for the population.

Table 5.8: UHI Statistics and Corresponding Ecological Effects.

Year	Mean (μ)	Standard deviation (δ)	Threshold (°C) (μ + 0.5 × δ)	Non-UHI (0 < LST ≤ μ+ 0.5δ)		UHI (LST> μ + 0.5δ)	
				Area (km^2)	Area (%)	Area (km^2)	Area (%)
1991	24.6	1.11	25.16	141.25	73.70	50.45	26.30
2009	22.4	0.9	22.85	141.66	73.91	50.00	26.09
2016	22.9	1.24	23.52	118.17	61.66	73.49	38.34
2023	27.7	2.02	38.71	121.82	63.56	69.83	36.44

UTFVI	Area (km^2)				Area (%)				UHI Effect	EEI
	1991	2009	2016	2023	1991	2009	2016	2023		
<0.000	128.45	105.17	97.28	89.34	67.02	54.88	46.61	50.76	None	Excellent
0.000- 0.005	0.00	0.00	3.19	4.04	0.00	0.00	2.11	1.66	Weak	Good
0.005-0.010	0.00	19.35	3.34	4.29	0.00	10.10	2.24	1.74	Middle	Normal
0.010-0.015	12.80	0.00	3.42	4.62	6.68	0.00	2.41	1.78	Strong	Bad
0.015-0.20	0.00	0.00	3.56	5.34	0.00	0.00	2.78	1.86	Stronger	Worse
> 0.020	50.40	67.13	80.86	84.03	26.30	35.03	43.85	42.19	strongest	Worst

Further, the UTFVI values revealed a decrease in the excellent zone from 67.02% in 1991 to 50.76% in 2023 (Table 5.8). This zone consists of areas where water and green spaces are abundant. Mainly, the northern pockets of the central and southern parts experienced excellent thermal conditions. This aligns with the findings of Guha (2021) which indicated that regions with high levels of vegetation and water bodies experienced excellent thermal conditions. Conversely, 26.30% of the study area categorized under "worst zone" in 1991 increased to 42.19% in 2023. This category is primarily characterized by impervious surfaces and urban development. Despite the closeness of the study area to the coastline where the sea breeze would typically provide cooling effects, they showed high UTFVI. This demonstrates how anthropogenic activities have a greater influence on the study's thermal environment than natural forces. It also aligns with the finding that human activities have a greater impact on the formation of UHI than natural factors (Kikon et al., 2023). For instance, the fishing communities and the harbor experienced the worst thermal conditions due to the high rate of heat-generating activities such as smoking of fish, burning fossil fuels, and pollution emissions from the cement factory, vehicles, and anchored vessels at the port. These activities have the potential to trap returning radiation, warming the

surfaces and increasing the mean Land Surface Temperature (LST) (Guha et al., 2018). In view of this, Kursah (2023) suggests using afforestation techniques to turn urban areas into green or eco-friendly spaces. Guha (2021) revealed that zones with excellent thermal comfort increased after the implementation of mitigation programmes in Raipur City. The "normal" thermal condition is observed in patches surrounding the areas exhibiting excellent thermal conditions, while, the bad, and worse, conditions are prevalent in proximity to areas marked by extensive built-up. These findings indicate a growing vulnerability of the study area to extreme heat conditions and a clear deterioration in the thermal comfort of the area. Hence, the study area is progressively becoming susceptible to severe thermal conditions which adversely affect ecological life, therefore, there is an urgent need for appropriate mitigation measures. This outcome is consistent with the research findings of Kikon et al. (2023) and Guha (2021) where extreme categories of thermal comfort index increased in areas with UHI.

5.4.8 Correlation analysis of LST with spectral indices

A correlation analysis was employed to examine the relationship between LST, NDBI, and NDVI. The analysis revealed a consistent positive correlation between LST and NDBI (Figure 5.11) with a corresponding correlation coefficient (r) of 0.82 for 1991, 0.83 for 2009, 0.88 for 2016, and 0.90 for 2023. This temporal pattern suggests that the influence of built-up areas, as proxied by NDBI, on temperature patterns has become progressively more substantial. Also, the strong correlation between NDBI and LST highlights the significant impact of urbanized areas on surface temperature fluctuations, positioning them as primary drivers of the UHI phenomenon. In Istanbul, Koc et al. (2019) identified a positive association between NDBI and LST.

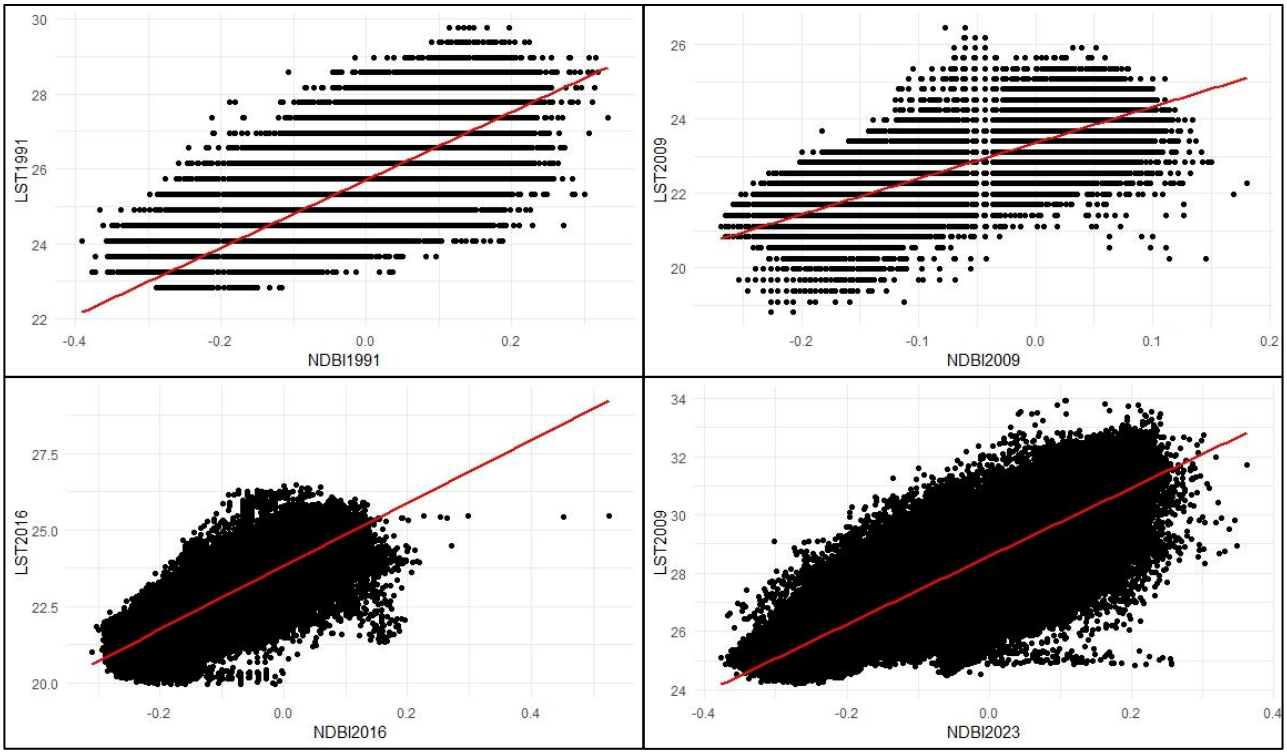

Figure 5.11: correlation between LST and NDBI.

However, a contrasting relationship was revealed between LST and NDVI across the years (Figure 5.12). The correlation illustrated an inverse relationship between LST and NDVI (Figure 5.12) with a corresponding correlation coefficient (r) of -0.80 for 1991, -0.66 for 2009, -0.81 for 2016, and -0.87 for 2023. This strong negative relationship also indicates the influence of vegetation on temperature patterns and aligns with the study of Kikon et al (2023). In summary, over the years, a positive correlation was observed between NDBI and LST while a negative correlation was observed between NDVI and LST. The direct correlation between NDBI and LST confirms the recognized concept that built-up areas contribute to elevated surface temperatures while the inverse relationship between NDVI, and LST supports the established understanding that denser vegetation leads to cooler surfaces through shading, higher albedo and evapotranspiration (Cevik & Cetin, 2023; Choudhury et al., 2023; Huang et al., 2024; A. Mondal et al., 2021; Mukherjee & Singh, 2020; Stemn & Kumi, 2020).

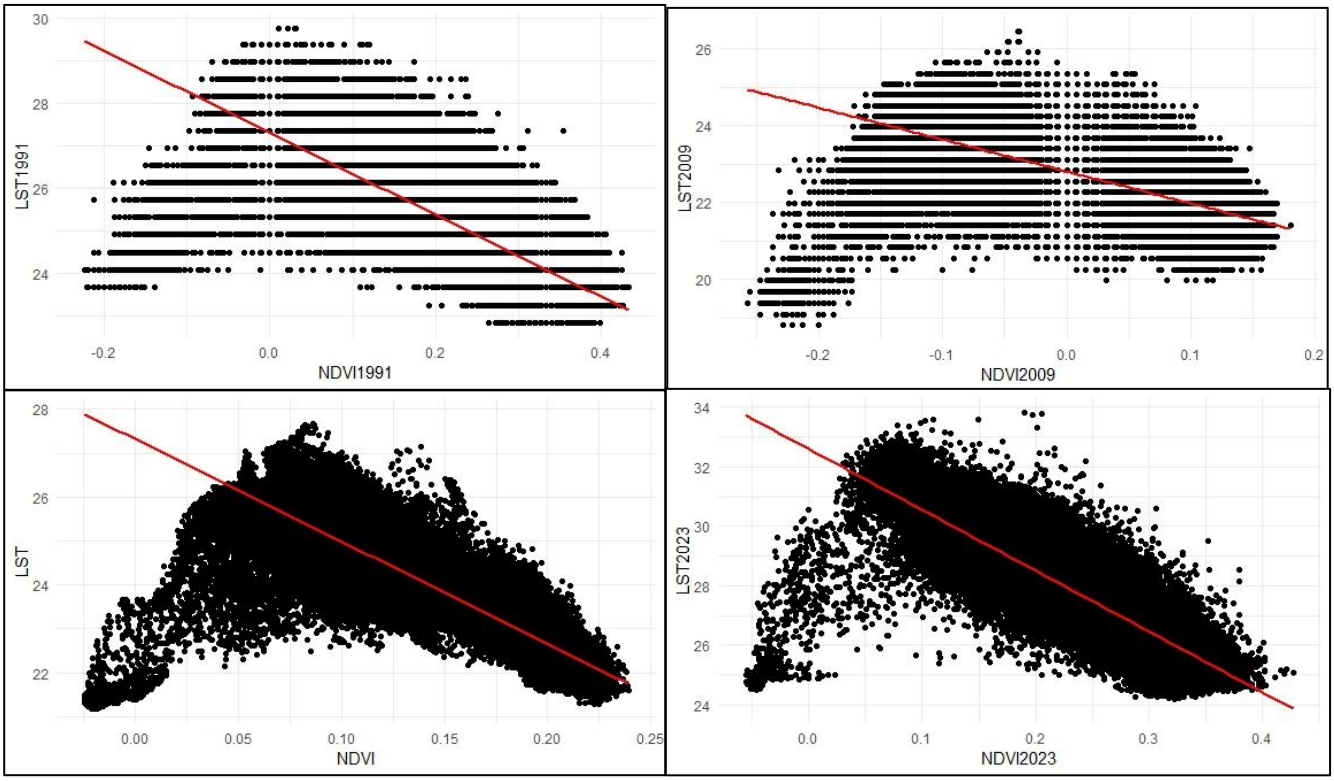

Figure 5.12: correlation between LST and NDVI.

5.4.9 Regression Analysis

5.4.9.1 Ordinary Least Square Regression (OLS)

The OLS regression indicated that the joint F-statistic, joint Wald statistic, and Koenker statistic were all statistically significant. The Jarque-Bera statistic indicated that the model was unbiased, as the residuals had a normal distribution (Table 5.9). The Variance Inflation Factor (VIF) scores were all below 7.5, indicating the absence of multicollinearity issues. The coefficients demonstrated the strength and correlation between the explanatory factors (NDBI and NDVI) and the dependent variable (LST). NDBI exerted a more significant influence owing to its higher coefficient value. The adjusted R-squared values for the years indicated a good model performance. According to the Corrected Akaike Information Criterion (AICc), the model for LST in 2009 had superior performance, evidenced by its lowest values (Table 5.9).

Table 5.9: Results of OLS Results

Year	Joint F statistics	Joint Wald statistic	Koenker Statistic	VIF (C)	Adjusted R-squared	AICc	Coefficient
1991	291788.16	362952.33	51007.26	2.43	0.73	369102.63	26.60
2009	249253.95	425335.12	15279.53	3.28	0.70	302280.27	23.40
2016	381164.06	810389.88	18338.27	4.55	0.78	370573.42	23.86
2023	472822.61	1191292.28	39831.30	5.46	0.82	543021.37	29.83

The OLS regression equations yielded positive intercept values across study years. Nonetheless, the NDVI coefficients yielded negative values contrary to the positive coefficients of the NDBI produced throughout the study period (Equation 5.13- 5.16).

$$LST_{1991} = 26.60 - 4.60NDVI_{1991} + 5.78NDBI_{1991} + E \quad (5.13)$$

$$LST_{2009} = 23.40 - 1.37NDVI_{2009} + 10.66NDBI_{2009} + E \quad (5.14)$$

$$LST_{2016} = 23.86 - 1.41NDVI_{2016} + 9.06NDBI_{2016} + E \quad (5.15)$$

$$LST_{2023} = 29.83 - 6.24NDVI_{2023} + 8.54NDBI_{2023} + E \quad (5.16)$$

Where E is the error term

5.4.9.2 Geographically Weighted Regression

For the GWR model (Table 5.10), the bandwidth was consistent across all the years. Since smaller sigma values indicate better model performance, the lowest sigma value in 2016 revealed the most accurate prediction of the model. The 2016 AICc value also indicated the best balance between goodness-of-fit and model complexity while the Adjusted R^2 value of the model performed exceptionally in 2023.

Table 5.10: Result of GWR -Model variables.

Year	Bandwidth	Residual Square	Sigma Values	AICc	Adjusted R-squared	Coefficient
1991	211	11432.99	0.35	71743.73	0.94	26.60
2009	211	19185.19	0.31	100040.70	0.89	23.40
2016	211	8113.10	0.23	19114.44	0.96	23.86
2023	211	14540.17	0.38	94200.83	0.97	29.83

5.4.9.3 Comparison of OLS and GWR

The evaluation of model diagnostics is widely recognized as a critical approach to gauging the effectiveness of statistical models. In this context, OLS and GWR models were subjected to a comparative analysis based on their respective adjusted R-squared and Corrected Akaike Information Criterion (AICc) values. This comparative assessment was undertaken to determine the relative performance of the two models in explaining the observed data and to identify the model that offers the most parsimonious fit to the data. As shown in Table 5.11, GWR yielded higher adjusted R-squared values and lower AICc values compared to OLS regression. The GWR model surpassed the OLS in performance. Research by Nazarian (2022), Zhao et al. (2018), and Luo & Peng (2016,) highlighted the superiority of Geographically Weighted Regression (GWR) over Ordinary Least Squares (OLS) in modeling spatially varying coefficients. Similarly, a study by Liu et al (2021) applied both OLS and GWR models to explore the relationship between Land Surface Temperature (LST) and environmental factors such as land use, population density, and elevation in Beijing, China. The results indicated that GWR outperformed OLS in terms of model fit and spatial autocorrelation. In a related study, Liu & Murayama (2021) employed both regression models to analyze the relationship between LST and environmental factors, with GWR demonstrating superior model performance. Furthermore, research by Rahaman et al. (2022) compared OLS and GWR in examining LST-land use/land cover (LULC) relationships, concluding that GWR offers distinct advantages by effectively capturing the spatial heterogeneity of LST.

Table 5.11: Comparison of OLS and GWR based on model diagnostics

Parameter	LST_{1991}		LST_{2009}		LST_{2016}		LST_{2023}	
	OLS	GWR	OLS	GWR	OLS	GWR	OLS	GWR
Adjusted R^2	0.73	0.94	0.70	0.88	0.78	0.96	0.82	0.97
AICc	369102	71743	302280	100040	370573	19114	543021	94200

5.8 LST AND LULC

Land use land cover constitutes another significant parameter employed to examine the correlation between urbanization and its effects on the climate (Choudhury et al., 2023). From Table 5.12, the average LST of each of the LULC increased over the study period. Water recorded the lowest LST while built-up had the highest LST.

Table 5.12: LST values over different LULC categories.

LULC	LST (°C)											
	1991			2009			2016			2023		
	Mean	Min	Max	Mean	Min	Max	Mean	Min	Max	Mean	Min	Max
Water	25.67	23.67	28.98	21.36	18.81	24.81	20.94	19.94	24.71	26.44	24.48	32.90
Vegetation	24.47	22.84	28.98	22.24	19.97	26.47	22.54	20.17	26.47	26.48	24.19	32.63
Built-up	27.13	24.09	29.77	23.62	19.69	25.92	24.21	19.95	26.42	29.77	25.12	33.94

LULC	Change in LST(°C)					
	1991-2009	2009-2016	2016-2023	1991-2023	Yearly increase	Decadal increase
Water	-4.31	-0.42	5.50	0.76	0.02	0.24
Vegetation	-2.23	0.30	3.94	2.02	0.06	0.63
Built-up	-3.52	0.60	5.56	2.64	0.08	0.82

Moreover, from 1991 to 2023 temperature increased at the rate of 0.76 °C for water, 2.02 °C for vegetation, and 2.64 °C for built-up (Table 5.12). These temperature values for each land cover class reveal that the LST of the metropolis is significantly influenced by built-up. This finding is in agreement with the work of Shen et al. (2022) where the highest LST was predominantly found in built-up areas while waterbodies and vegetation exhibited lower LST due to cooling effects. Mahmoodi et al. (2019) observed that in the semi-arid regions, higher surface temperatures were

exhibited in built-up areas compared to other classes. Also, similar results have been found by Mukherjee & Singh (2020) in Surat and Bharuch cities in India and by Huda & Al, (2021) in Chattogram City India where built-up class was identified as having the highest temperature as water experienced the lowest temperature. In Ghana, Wemegah et al. (2020) found that LST in the greater Accra region exhibited higher values in built-up areas compared to areas covered by vegetation and water. Varied land cover types exhibit distinct biophysical characteristics, which influence their respective responses to solar radiation energy (Shen et al., 2022). For instance, the absence of vegetation coupled with an increase in non-permeable surfaces leads to diminished latent heat fluxes and heightened sensible heat, resulting in a noticeable warming effect. Waterbodies and vegetation have been discovered to significantly mitigate urban heat islands, therefore, incorporating them into urban planning and design of the metropolis can effectively regulate the thermal environment of the metropolis.

5.9 Significance of spatial factor effect on LST

In this analysis, Land Surface Temperature (LST) is considered the dependent variable, while the spatial variables serve as covariates. According to Tables 5.13 and 5.14, the spatial factors are statistically significant (p-value < 2e-16) and accounted for 89.9% of the variation in LST (Table 5.13). This finding indicates that the spatial factors possess a robust capacity to explain the distribution of LST. The high EDF values suggest complex, nonlinear relationships between the predictors and LST, which are well-captured by the GAM.

Table 5.13: Generalized additive model (GAM)

	Estimate Std.	Error	t value	Pr(>|t|)	R-sq.(adj)	Deviance explained	REML
(intercept)	106202.0	42.3	2510	2e-16***	0.899	89.9%	2.379e+06

Significant codes: 0 ‘***’ 0.001 ‘**’ 0.01 ‘*’ 0.05 ‘.’ 0.1 ‘’ 1

Table 5.14: The effect of predictor variables on LST

Variables	edf	Ref.df	F	p-value	Interpretation
S(NDWI)	8.890	8.997	597.3	<2e-16***	NDWI has a significant effect on LST.
S(NDBI)	8.583	8.954	738.2	<2e-16 ***	NDBI also significantly affects LST, indicating the importance of built-up intensity.
S(NDVI)	8.009	8.761	694.6	<2e-16 ***	NDVI has a strong relationship with LST, reflecting the cooling effect of vegetation.
S(DEM)	8.820	8.990	862.3	<2e-16 ***	DEM (elevation) significantly influences LST, likely due to altitude-temperature relationships.
S(Prox_water)	8.897	8.995	20807.9	<2e-16***	Proximity to waterbodies strongly impacts LST, likely due to the cooling effects of water bodies.
S(Prox_Road)	8.966	9.000	19667.9	<2e-16***	Proximity to roads significantly affects LST, possibly due to heat retention of paved surfaces.
S(Prox_CBD)	8.983	9.000	1498.2	<2e-16***	Proximity to the Central Business District (CBD) strongly affects LST, highlighting urban heat island effects.

Significant. codes: 0 '***' 0.001 '**' 0.01 '*' 0.05 '.' 0.1 ' ' 1

5.10 Spatial distribution and characterization of the archetypes or classes

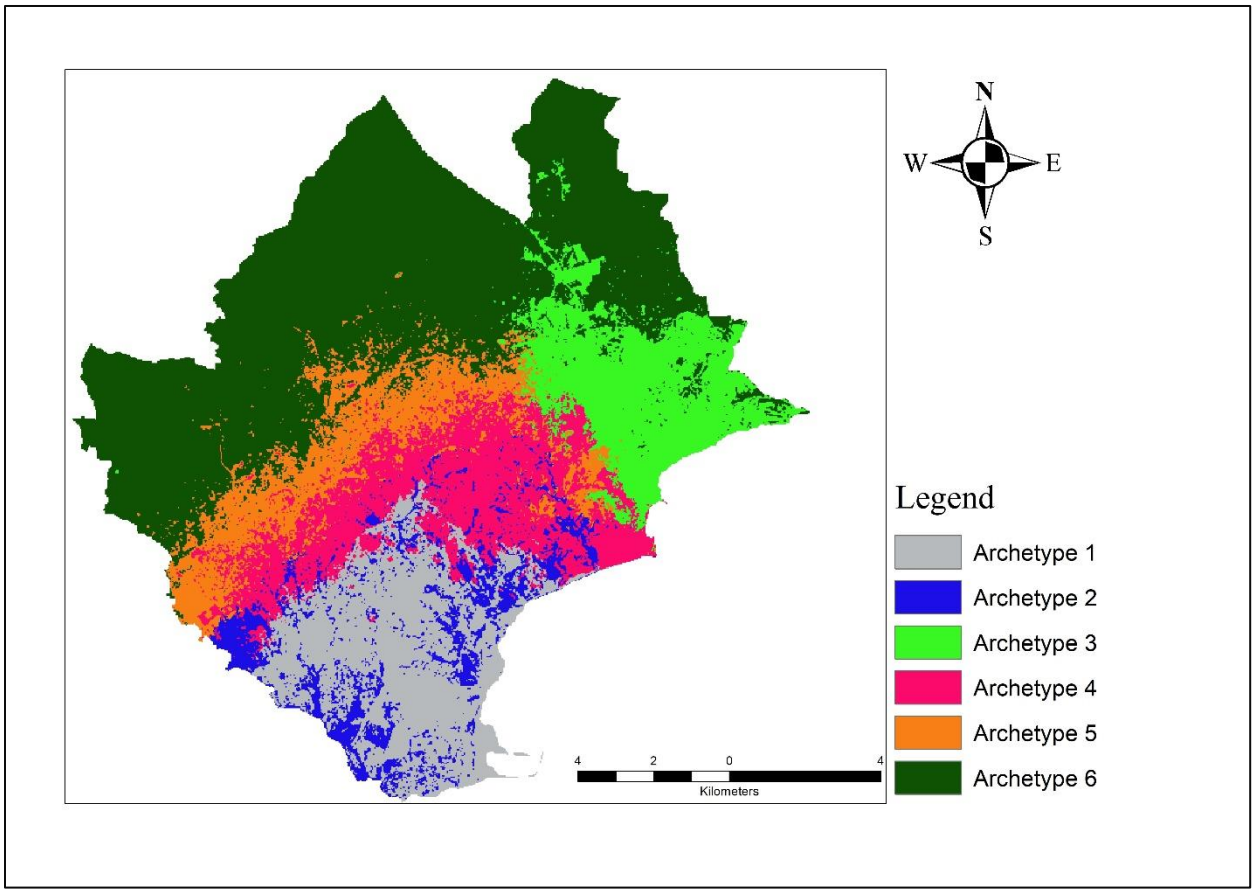

Figure 5.13: Urban Archetypes Map.

Figure 5.13 illustrates the spatial distribution of six archetypes defined by a combination of spatial variables characterized in Table 5.15. Archetype 1, which covers an area of 27.37 km^2 is located primarily in the southwestern part of the study area. and is characterized by moderate NDWI, high NDBI, low NDVI, and low elevation. It is also in close proximity to waterbodies, main roads, and the CBD, suggesting it represents urban areas with significant built-up surfaces, limited vegetation, and accessible infrastructure. Also, concentrated in the southwestern part of the study area and irregularly spread within Archetype 1 is Archetype 2. This archetype, covering an area of 11.93 km^2 is defined by moderate NDWI, moderate NDBI, moderate NDVI, and low elevation. It is also close to waterbodies, roads, and the CBD, indicating transitional zones between urban and rural areas with moderate vegetation and development. Archetype 3 is dominantly located in the eastern part of the study area at a size of 22.05 km^2 and is characterized by low NDWI, moderate NDBI, moderate NDVI, and high elevation. It is far from waterbodies and the CBD but close to main roads, reflecting rural or semi-natural areas at higher altitudes with moderate vegetation and

minimal water access. Concentrated in the central part of the study area is Archetype 4, covering an area of 26.89 km^2. This class exhibits low NDWI, high NDBI, low NDVI, and moderate elevation. It is moderately distant from waterbodies and the CBD but close to main roads, suggesting areas influenced by urbanization but with limited vegetation and intermediate topography. Archetype 5 surrounds Archetype 4 at a coverage of 20.04 km^2. This archetype has low NDWI, moderate NDBI, high NDVI, and moderate elevation. It is moderately distant from waterbodies, roads, and the CBD, indicating semi-natural or mixed-use landscapes with significant vegetation cover and balanced accessibility. Lastly, at 83.39 km^2, Archetype 6 dominates the far northern and western parts of the study area and is characterized by high NDWI, low NDBI, high NDVI, and high elevation. It is far from waterbodies, roads, and the CBD, reflecting a natural zone with abundant vegetation, water resources, and minimal urban influence. These spatial patterns highlight the diverse land characteristics and provide a foundation for targeted land use planning, conservation strategies, and infrastructure development in the study area.

Table 5.15: characterization of urban archetypes or classes

Class/ Archetype	NDWI	NDBI	NDVI	DEM	Proximity to waterbodies	Proximity to Main Road	Proximity to CBD
1	Moderate	High	Low	Low	Close	Close	Close
2	Moderate	Moderate	Moderate	Low	Close	Close	Close
3	Low	Moderate	Moderate	High	Far	Close	Far
4	Low	High	Low	Moderate	Moderate	Close	Moderate
5	Low	Moderate	High	Moderate	Moderate	Moderate	Moderate
6	High	Low	High	High	Far	Far	Far

The characterization of the archetypes has significant implications for land surface temperature (LST) as they highlight the influence of vegetation, urbanization, water bodies, and elevation on thermal dynamics. High NDVI in Classes 5 and 6 indicate dense vegetation, suggesting lower LST due to the cooling effects of evapotranspiration and shading, whereas low NDVI in Classes 1 and 4 may contribute to higher LST due to reduced vegetation cover and increased heat absorption. Research indicates that areas with high NDVI values tend to have lower LST, whereas regions

with low NDVI values generally exhibit higher LST within various parts of a city (Al-khakani, 2023; Guha et al., 2018; Mansourmoghaddam et al., 2023; Moisa & Gemeda, 2022; Moisa & Gemeda, 2022; Wahyu et al., 2019). Similarly, high NDBI in Classes 1 and 4, reflect significant urbanization, likely leading to elevated temperature through the urban heat island effect, while low NDBI in Class 6 indicates less built-up areas with lower heat retention. The presence of water, as indicated by high NDWI in Class 6, helps moderate LST through latent heat flux, whereas lower NDWI in Classes 3, 4, and 5 suggests reduced moisture availability and higher susceptibility to heat. Nath et al. (2020) identified reduced vegetation cover and diminished water coverage as significant contributing factors to the rising surface temperature in Mumbai. Elevation also plays a critical role with high-altitude areas in Classes 3 and 6 experiencing cooler temperatures due to natural thermal gradients, while lower elevations in Classes 1 and 2 are more prone to heat accumulation. For instance, a study by Eshetie (2024) observed that LST values decreased as elevation increased. Proximity to waterbodies and roads further influences LST, with areas near rivers (Classes 1 and 2) benefiting from natural cooling, whereas those farther from rivers (Classes 3 and 6) may experience higher temperatures Similarly, areas close to roads (Classes 1, 2, and 4) and close to CBD (Class 1 and 2) may experience elevated LST due to heat emissions from traffic and infrastructure. The thermal properties of roads such as concrete and asphalt material mostly make areas near roads experience higher surface temperatures. However, the results from Jaipur and Guwahati revealed a negative relationship which was attributed to the presence of roadside greenery (Nath et al. 2020), This means the existence of green surfaces can significantly influence and reduce surface temperature, even in areas typically expected to experience higher heat levels.

Also, Feng et al. (2019) assert that the central business district has higher temperatures compared to the fringes of the city. These findings underscore the importance of vegetation conservation, water resource management, and sustainable urban planning to mitigate LST and its associated impacts.

5.11. Statistical significance of the surface temperature differences between the archetypes

In determining the statistical significance difference among the mapped temperatures within the archetypes, a boxplot (Figure 5.14) was first conducted to provide a visual summary of the distribution and variability of temperature data across these classes. From Figure 5.14 LST_F1 represent archetype 1, LST_F3 is archetype 2, and LST_F5 is archetype 5. The median

temperatures exhibit a clear decreasing trend from class 1 to 6, reflecting spatial heterogeneity in surface temperature across the study area. The median LST for archetype 1 is the highest indicating that this class experiences significantly higher surface temperatures. In contrast, archetype 6 shows the lowest median temperature, suggesting cooler surface conditions in this class.

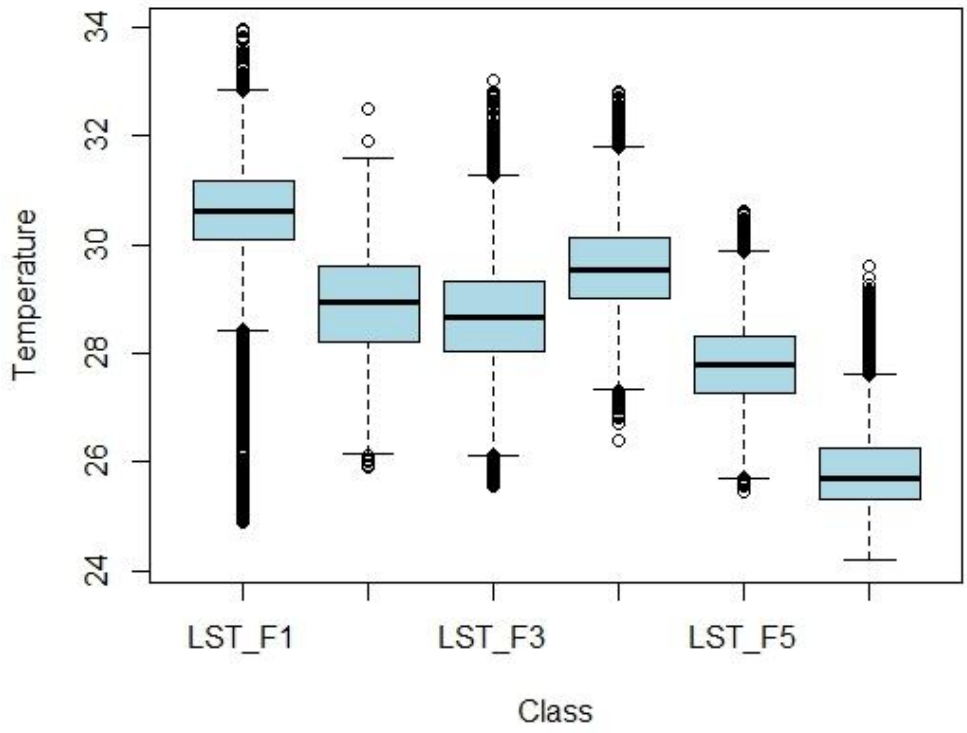

Figure 5.14: Boxplot of temperature values by class.

The normality of the dataset was checked using the Kolmogorov-Smirnov test. This test has a null hypothesis (**H_0**) which states that the sample data comes from the specified theoretical distribution (Normal distribution) and an alternative hypothesis (H_1) which states that the sample data does not come from the specified theoretical distribution (Normal distribution).

Table 5.16.: Normality test using Kolmogorov-Smirnov test.

Class	D value	P-value	Alternative Hypothesis
1	0.026	1.666e-08	two-sided
2	0.029	6.401e-10	two-sided
3	0.022	6.438e-06	two-sided
4	0.021	1.984e-05	two-sided
5	0.012	0.020	two-sided
6	0.084	2.2e-16	two-sided

From Table 5.16, the p-value calculated for each class was less than the alpha value of 0.05. This showed that the classes were all statistically significant and also signifies that the null hypothesis can be rejected. This also shows that the dataset used is non-parametric. Therefore, the Kruskal-Wallis test was further used to test the significance of the surface temperature among the classes or archetypes. Like other test methods, the null hypothesis (H_0) of Kruskal Wallis states that the distribution of a variable is the same across all groups while the alternative hypothesis (H_a) states that at least one group has a different distribution. From Table 5.17, the Kruskal-Wallis chi-squared value indicated greater differences between the classes while the p-value provided strong evidence against the null hypothesis. Hence, the results showed a significant difference in the distributions across the different classes.

Table 5.17: Kruskal-Wallis test

Kruskal-Wallis chi-squared	Df	p-value
58117	5	2.2e-16

Following the significant results shown by the Kruskal-Wallis test, Dunn's Test (Post-Hoc Pairwise Comparisons) was used to show which classes are statistically significant from each other.

Table 5.18**:** Dunn's Test (Post-Hoc Pairwise Comparisons)

COL MEAN-ROW MEAN	**LST_C1**	**LST_C2**	**LST_C3**	**LST_C4**	**LST_C5**
LST_C2	95.216 0.000*				
LST_C3	91.970 0.000*	-3.246 0.000*			
LST_C4	47.946 0.000*	-47.270 0.000*	-44.025 0.000*		
LST_C5	151.218 0.000*	56.002 0.000*	59.248 0.000*	103.272 0.000*	
LST_C6	216.790 0.000*	121.574 0.000*	124.820 0.000*	168.845 0.000*	65.572 0.0000*

The Dunn's test results reveal significant differences in mean ranks of surface temperature across all pairwise comparisons of the six groups (LST_C1 to LST_C6), as indicated by the adjusted p-values of 0.0000 (Table 5.18). The largest difference is between LST_C1 and LST_C6 (216.7903), where LST_C1 consistently shows higher mean ranks, while LST_C6 exhibits the lowest ranks. Conversely, the smallest difference is observed between LST_C3 and LST_C2 (-3.245647), where LST_C3 ranks slightly lower than LST_C2. These results highlight a gradient in LST values, with LST_C1 being distinctly higher and LST_C6 significantly lower compared to the other groups. The systematic variation in LST across the groups reflects diverse spatial or environmental conditions within the study area, emphasizing the heterogeneity of temperature distribution.

5.12 Analysis of Surface Temperature Variation within the Archetypes

The mean surface temperature values presented in Table 5.19, when considered alongside the characterization in Table 5.15, provided insights into the variations of temperature influenced by the spatial variables in each archetype. From Table 5.19, Archetype 1 had the highest mean temperature which according to its characterization (Table 5.19), suggests that the high urbanization and low vegetation in this archetype significantly contribute to the increased temperature with limited cooling influence from water and vegetation. Though Archetype 2 shared some similarities with Archetype 1, the mean LST of Archetype 2 was lower compared to Archetype 1. This can be attributed to the less pronounced urban footprint as seen in Table 5.19. Hence, resulting in a slightly reduced temperature compared to Archetype 1. The high elevation and moderate NDVI and NDBI likely mitigate the effects of low water availability, resulting in a lower temperature in Archetype 3 compared to Archetype 2 and 1. However, the mean temperature was high in Archetype 4 potentially due to the combination of significant urbanization and limited water and vegetation cover despite the moderate cooling effect of elevation and moderate proximity to main roads, CBD, and rivers. Contrastingly, Archetype 5 recorded a lower mean temperature likely attributable to the high vegetation cover and moderate elevation. Archetype 6 recorded the lowest mean temperature due to being characterized by high NDWI, low NDBI, high NDVI, and high elevation, as well as being far from waterbodies, main roads, and the CBD. The combination of abundant water availability, dense vegetation, and high elevation creates optimal conditions for reducing LST, making this archetype the coolest and most ecologically stable.

Table 5.19: Mean, minimum, and maximum LST of the urban archetype

Class/Archetype	Min	Mean	Max
1	24.887	30.590	33.942
2	25.897	28.868	32.494
3	25.554	28.697	33.002
4	26.397	29.584	32.795
5	25.444	27.794	30.598
6	24.189	25.830	29.593

5.5 Discussion

The rapid population growth in recent decades has led to excessive use of natural resources worldwide, especially in developing countries (Shamsudeen et al., 2022). As a result, the earth's natural resources are depleting, particularly in countries heavily reliant on them. (Molotoks et al. 2018). Ghana depends greatly on natural resources, and its population has increased from 5 million in 1970 to 32 million people per the 2021 census report (Ghana Statistical Service, 2021; Ghana Statistical Service, 2014). This surge in Ghana's population is reflected in the urbanization of Sekondi-Takoradi, making it the third most populous and urbanized metropolis in the country (Aduah et al., 2020b; STMA, 2022). Regrettably, this burgeoning population brings escalating demands, and considerable pressure is being exerted on its natural resources to meet the increasing needs of the metropolis.

Over the three-decade study period, land use land cover (LULC) changes in Sekondi-Takoradi indicated substantial expansion in built-up by 32.91%, while water and vegetation areas decreased by 1.09% and 31.82%, respectively. The core of the metropolis was mostly covered by built-up while a discernible concentration of vegetation existed mostly in the northern part of the study. The drastic decline in vegetation and water at the increasing expense of built-up aligns with the findings of Mensah et al. (2019) and Siddique et al. (2023). As stated by Biney et al. (2024) and Danso et al. (2024), the rapid urban expansion in Sekondi-Takoradi is a consequence of the three-fold population increase over the past thirty years. Unfortunately, this trend is anticipated to persist, with the United Nations projecting Sekondi-Takoradi's population to reach 1.3 million by 2030. Similar rapid population growth has been observed in the cities of Accra, and Kumasi which is parallel to the increased conversion of vegetation into built-up (Albert & Yiran, 2021). Additionally, many cities around the world including Morogoro in Tanzania (Sumari et al., 2020), Wuhan in China (Chen et al., 2021), Lagos in Nigeria (Al-khakani, 2023), and Bahir Dar in

Ethiopia (Getu & Bhat, 2021) have experienced rapid population growth and corresponding urban expansion. In line with the above-highlighted works, this study identifies the escalating population as a primary driver of land use land cover change in the region. Kleemann et al. (2017) assert that an array of factors contributes to the alterations in land use and land cover within a region. Economic development and rapid population growth have emerged as pivotal factors influencing land use changes in the Sekondi-Takoradi metropolis (Mensah et al., 2018a), as also documented by Chen et al. (2020). However, Shamsudeen et al., (2022), assert that urban sprawl is a significant factor influencing landscape conversion.

When cities are expanding, natural covers are predominantly transformed into built-up areas, which leads to the reduction of natural landscapes. The depletion of natural land cover, particularly vegetation, not only modifies the land cover composition but also has a discernible impact on the LST. This makes Rahaman et al. (2022) assert that global warming is one of the primary consequences of urbanization as it increases the earth's temperature. The first study on surface temperature conducted by Howard proved that urban expansion correlates with the formation of LST and UHI. For this reason, it has prompted similar research in several nations to evaluate the impact of urbanization on UHI (Kikon et al., 2023; Moisa & Gemeda, 2022; Mondal et al., 2021; Wahyu et al., 2019). LST in Sekondi-Takoradi consistently recorded high temperatures over built-up areas. These areas further exhibited large patches of UHI over densely populated areas and industrial zones. Similar research by Taloor et al. (2024) and Huang et al. (2024) have highlighted high-temperature trends over built-up in Chandigarh and Jammu District respectively. A study by Kwang et al. (2023) also observed an increase in LST in the Greater Accra region but attributed it to the significant built-up growth and climate change. Nigeria, Ethiopia, India, China, and several European nations have demonstrated that urban development and changes in land use significantly impact the LST (Cevik & Cetin, 2023; Guha, 2021). The direct correlation between NDBI and LST (Figure 11) aligns with the recognized concept that built-up areas contribute to elevated surface temperatures (Huang et al., 2024). Though the built-up areas exhibited high temperatures, the influence of spatial factors contributed to temperature variations within the urban setting. The significant effect of the spatial factors as inferred from Table 5.14 aligns with the findings of Feng et al., (2019), who identified land use indices and proximity factors as critical influences on LST. Similarly, studies by Song et al. (2021) and Nath et al. (2020) established positive correlations

between urban heat islands, low elevation, road networks, and city centers. In contrast, research by Traore et al. (2021), Chen et al. (2021), and Thapa, (2017) reported negative correlations between LST and factors such as NDVI, high elevation, and water. Furthermore, Eshetie, (2024) emphasized that vegetation cover, water bodies, built-up areas, and topography significantly influence LST. Specifically, areas with high elevation, extensive vegetation and water coverage, and low built-up density tend to record lower temperatures, whereas urban areas characterized by sparse vegetation and water, coupled with high built-up density, being far from rivers, main roads, and the CBD experience elevated temperatures(Feng et al., 2019; Nath et al., 2020). These observations align with the study's findings, particularly in explaining the lowest temperature recorded in Archetype 6. Despite temperature variations witnessed across the study area, the overall temperature patterns remain predominantly high. Unfortunately, the IPCC (2021) has substantiated a forecast indicating a temperature increase of 1.5-2.0 ºC in most urban centers by 2050. Given the surge in temperature witnessed in the metropolis, effective climate strategies are required. Jumari et al. (2023) established that a simple and effective means irrespective of other environmental factors in mitigating urban heat islands is by increasing the vegetation in an area as plants and trees contribute to a cooler environment through shading and evapotranspiration process (Taloor et al., 2024). The inverse relationship between NDVI and LST (Figure 10) supports this viewpoint. According to Gyimah et al. (2023), tree planting, the use of electric fans and air conditioners, and the opening of windows and doors were some strategies adopted in places with high LST in the Greater Accra region. Unfortunately, some of these strategies are inefficient as they add more problems to either the individual or the society. For instance, the strategy of opening windows and doors to allow air in also exposes people to mosquitoes. Hence, exposing them to Malaria. Also, the usage of air-conditioners directly increases electric bills and puts a high demand on energy. Therefore, in cases where demand is higher than supply, it results in power outages and rationing of electricity as observed many times in Ghana (Citinews, 2024; DW, 2024). In many urban centers across the Western world, efforts to mitigate the effects of the surface urban heat island have included various strategies such as utilizing lighter-colored construction materials, developing materials with higher reflectivity for roofs and pavements, planting more trees, establishing green roofs by growing vegetation on building tops (Filho et al., 2021; Viju et al., 2023). Other mitigating strategies involve optimizing wind flow through the strategic design of

building dimensions, forms, and alignments (Sarif et al., 2020). This makes living quarters more comfortable and less likely to cause heat waves or perspiration.

5.6 CONCLUSION

This study examined the influence of urban growth on urban heat islands from 1991 to 2023 and analyzed some spatial factors that contribute to temperature variations across the metropolis. LULC analysis revealed a significant shift in land use from natural and undeveloped spaces to artificial and urbanized areas. These shifts were primarily driven by population growth and urbanization. Likewise, the increasing LST trend emphasizes a warming environment primarily affected by urban expansion and declining vegetation. The correlation between LST, NDBI, and NDVI unveiled the connection between urban expansion and increasing LST. Notably, the influence of built-up on temperature changes surpassed that of vegetation, emphasizing the crucial role of urbanization in temperature rise. Moreover, across the urban space, temperature variations exist due to the influence or contribution of some spatial factors within the metropolis. These factors provided valuable insight into the intensification of LST and UHI in the metropolis. Further, the UHI effect analysis showed that the city core and high-density areas registered higher temperatures than the low-density areas. Although this study offers a valuable understanding of the evolving urbanization, rising temperatures, and increasing urban heat island effects, it also highlights certain shortcomings and inadequacies. These are:

1. The remote sensing data employed were not able to capture details at the smallest scale due to its medium spatial resolution.
2. The study did not explore the distinct functions of vegetation types and green infrastructures to mitigate the UHI effect.

These constraints not only highlight the necessity for careful interpretation of the results but also suggest potential avenues for future research. Also, the implementation of strategies such as rooftop gardening, green infrastructure, planned afforestation, and sustainability-focused policymaking and public awareness can help mitigate the impacts of UHI in the metropolis, thereby helping to achieve goal 11 of the sustainable development goals.

5.7 Publication:

The objective of this work has been published with the title below in the Scientific African Journal of Elsevier.

Scientific African 26 (2024) e02366

Contents lists available at ScienceDirect

Scientific African

journal homepage: www.elsevier.com/locate/sciaf

Analyzing the spatio-temporal pattern of urban growth and its influence on urban heat islands in the Sekondi-Takoradi metropolis, Ghana

Biney, E., Forkuo, E. K., Poku-Boansi, M., Hackman, K. O., Harris, E., Asare, Y. M., Yankey, D. B., Annan, E., & Agbenorhevi, A. E. (2024). Analyzing the spatio-temporal pattern of urban growth and its influence on urban heat islands in the Sekondi-Takoradi metropolis, Ghana. *Scientific African*, *26*(May), e02366. https://doi.org/10.1016/j.sciaf.2024.e02366

CHAPTER 6: GENERAL DISCUSSION AND SYNTHESIS

6.1 Discussion

The rapid population growth in recent decades has led to excessive use of natural resources worldwide, especially in developing countries (Shamsudeen et al., 2022). As a result, the earth's natural resources are depleting, particularly in countries heavily reliant on them (Molotoks et al. 2018). Ghana depends greatly on natural resources, and its population has increased from 5 million in 1970 to 32 million people per the 2021 census report (Ghana Statistical Service, 2021; Ghana Statistical Service, 2014)). This surge in Ghana's population is reflected in the urbanization of Sekondi-Takoradi, making it the third most populous and urbanized metropolis in the country (Aduah et al., 2020b; STMA, 2022). Regrettably, this burgeoning population brings escalating demands, and considerable pressure is being exerted on its natural resources to meet the increasing needs of the metropolis.

The categorization of LULC was done using the random forest algorithm and this aided in the production of LULC maps with higher accuracies; above 80%, which is a standard criterion for determining the reliability of image classification results. Despite the spatial resolution of the Landsat images employed in this study, a high agreement was obtained between the classified images and the referenced data. In comparison with studies of Kumi-Boateng & Stemn (2015) and Mensah et al. (2019) that used maximum likelihood for image classification, the accuracies of this study were higher. This can be attributed to the classifier's robustness to outliers and inherent design capabilities. Therefore, it is urged that attention should be given to its use in image classification. The land use land cover results revealed a significant transformation in the land cover types of the metropolis to built-up. Specifically, built-up consistently expanded at the expense of water and vegetation and this aligns with the findings of Blakime et al. (2024), Mensah et al. (2019), and Siddique et al. (2023) where land cover classes such as natural vegetation, water, and forest experienced a significant decline at the substantial increase in built-up. In most Ghanaian societies including the metropolis, horizontal expansion of buildings is a predominant architectural style instead of the vertical expansion of houses which does not claim much space (Frimpong et al., 2023). Also, house ownership is viewed as a higher social status and prominence people seek to attain, therefore, it has become a significant factor fueling the expansion of built-up besides the demand for housing (Frimpong et al., 2023). The core of the metropolis was mostly

covered by built-up while a discernible concentration of vegetation existed mostly in the northern part of the study (Figure 3.4). Although the expansion of built-up areas significantly affects vegetation as pointed out by (Roy et al., 2021) and evidenced in this study (Table 3.4), the rapid loss of vegetation will affect the urban thermal characteristics and health (Rahaman et al., 2022), reduce the carbon sinks, reduce ecosystem services (Kafy et al., 2022), and increase the vulnerability of the study area to flooding (Kwame et al., 2021) which is currently on the ascendancy. These negative implications will make the metropolis unsafe, not resilient, and unsustainable which is contrary to goal 11 of the sustainable development goal that Ghana seeks to achieve.

Kleemann et al. (2017) assert that an array of factors contributes to the alterations in land use and land cover within a region. Rapid population growth and economic development have emerged as pivotal factors influencing land use changes in the metropolis (Mensah et al., 2018a). This finding is also documented by Chen et al. (2020) and Baidoo et al., (2023) for the cities of Shenzhen, and Atwima Nwabiagya North District respectively. According to the Ghana Statistical Service, (2021), the study area has experienced a significant influx of migrants since 1991. This population growth has exerted pressure on the available green spaces, leading to the conversion of lands within and beyond the urban fringe for various purposes by individuals and private estate developers. Also, Biney et al. (2024) and Danso et al. (2024), state that the rapid urban expansion in Sekondi-Takoradi is a consequence of the three-fold population increase over the past thirty years. For instance, following the oil discovery in 2007, the population of the metropolis increased from 359,363 in 2000 to 559, 548 in 2010 (Service, 2014). This increase was due to the surge in socio-economic activities brought on by the oil and gas industry and other companies drawn by the discovery (Fiave, 2017; STMA, 2022). A report by the Independent Oil and Gas Information Centre (2017) revealed that about 49,000 people working in the oil and banking sectors sought housing within the metropolis. Unfortunately, the population of Sekondi-Takoradi is expected to continue to increase. This would require proper and efficient strategies to ensure a sustainable balance to prevent further degradation of the environment. Similar rapid population growth has been observed in the cities of Accra, and Kumasi which is parallel to the increased conversion of vegetation into built-up (Albert & Yiran, 2021). Additionally, many cities around the world including Morogoro in Tanzania (Sumari et al., 2020), Wuhan in China (L. Chen et al., 2021), Lagos in Nigeria (Al-khakani, 2023), and Bahir Dar in Ethiopia (Getu & Bhat, 2021) have

experienced rapid population growth and corresponding urban expansion. However, Shamsudeen et al. (2022) assert that urban sprawl is a significant factor influencing landscape conversion. An outlook of how the urban growth in the metropolis will be in 2030 further revealed an increase in built-up while vegetation and water would continue to decrease. This projection provides insightful information and guidance to urban planners and city authorities on where to expect built-up expansion, as the western and north-western part of the study area is projected to experience the majority of the urban expansion. With this, stakeholders of urban development in the metropolis can effectively prioritize areas in terms of provisions of social amenities and recreational facilities, neighbourhood design, and planning. Similar studies by Frimpong et al. (2023b) for the cities of Kumasi and Accra. Addae (2019) for Greater Accra in Ghana, Tian et al. (2023) for Nanjing city in China, Ullah et al. (2024) for Kabul in Afghanistan, and Baqa et al. (2021) Karachi in Pakistan have also projected a rise in built-up and a decrease in water and vegetation. Forecasting urban growth or expansion should be patronized or employed in the planning and formation of policies for urban areas as land use models serve as effective tools for analyzing scenarios (Pradhan, 2017; Ramadan & Effat, 2021). This will reduce uncertainties as scenarios create different scenes of the future, which is essential for creating a robust decision-making framework needed by urban planners and decision-makers for effective management of future urban growth.

The depletion of natural land cover, particularly vegetation, not only modifies the land cover composition but also has a discernible impact on the LST. This makes Rahaman et al. (2022) assert that global warming is one of the primary consequences of urbanization as it increases the earth's temperature. The first study on surface temperature conducted by Howard proved that urban expansion correlates with the formation of LST and UHI. For this reason, it has prompted similar research in several nations to evaluate the impact of urbanization on UHI (Kikon et al., 2023; Moisa & Gemeda, 2022; Mondal et al., 2021; Wahyu et al., 2019). LST in Sekondi-Takoradi consistently recorded high temperatures over built-up areas. These areas further exhibited large patches of UHI over densely populated areas and industrial zones. Similar research by Taloor et al. (2024) and Huang et al. (2024) have highlighted high-temperature trends over built-up in Chandigarh and Jammu District respectively. A study by Kwang et al. (2023) also observed an increase in LST in the Greater Accra region but attributed it to the significant built-up growth and climate change. Nigeria, Ethiopia, India, China, and several European nations have demonstrated that urban development and changes in land use significantly impact the LST (Cevik & Cetin,

2023; Guha, 2021). The direct correlation between NDBI and LST aligns with the recognized concept that built-up areas contribute to elevated surface temperatures. This is attributable to the dark building materials with high heat absorption properties (Huang et al., 2024). Though the built-up areas exhibited high temperatures, the influence of spatial factors contributed to temperature variations within the urban setting. The significant effect of the spatial factors as inferred from Table 5.14 aligns with the findings of Feng et al., (2019), who identified land use indices and proximity factors as critical influences on temperature. Similarly, studies by Song et al. (2021) and Nath et al. (2020) established positive correlations between urban heat islands, low elevation, road networks, and city centers. In contrast, research by Traore et al. (2021), Chen et al. (2021), and Thapa, (2017) reported negative correlations between LST and factors such as NDVI, high elevation, and water. Furthermore, Eshetie, (2024) emphasized that vegetation cover, water bodies, built-up areas, and topography significantly influence LST. Specifically, areas with high elevation, extensive vegetation and water coverage, and low built-up density tend to record lower temperatures, whereas urban areas characterized by sparse vegetation and water, coupled with high built-up density, being far from rivers, main roads, and the CBD experience elevated temperatures(Feng et al., 2019; Nath et al., 2020). These observations align with the study's findings, particularly in explaining the lowest temperature recorded in Archetype 6. Despite temperature variations witnessed across the study area, the overall temperature patterns remain predominantly high. Unfortunately, the IPCC (2021) has substantiated a forecast indicating a temperature increase of 1.5-2.0 ºC in most urban centers by 2050. Given the surge in temperature witnessed in the metropolis, effective climate strategies are required. Jumari et al. (2023) establish that a simple and effective means irrespective of other environmental factors in mitigating urban heat islands is by increasing the vegetation in an area as plants and trees contribute to a cooler environment through shading and evapotranspiration process (Taloor et al., 2024). The inverse relationship between NDVI and LST supports this viewpoint. According to Gyimah et al. (2023), tree planting, the use of electric fans and air conditioners, and the opening of windows and doors were some strategies adopted in places with high LST in the Greater Accra region. Unfortunately, some of these strategies are inefficient as they add more problems to either the individual or the society. For instance, the strategy of opening windows and doors to allow air in also exposes people to mosquitoes. Hence, exposing them to Malaria. Also, the usage of air-conditioners directly increases electric bills and creates a high energy demand. Therefore, in cases where demand is

higher than supply, it results in power outages and rationing of electricity as observed many times in Ghana (Citinews, 2024; DW, 2024). In many urban centers across the Western world, efforts to alleviate the effects of heat warming have included various strategies such as utilizing lighter-colored construction materials, developing materials with higher reflectivity for roofs and pavements, planting more trees, establishing green roofs by growing vegetation on building tops (Aflaki et al., 2017; Chen et al., 2022; Kuang et al., 2015). Other mitigating strategies involve optimizing wind flow through the strategic design of building dimensions, forms, and alignments (Sarif et al., 2020)**.** This makes living quarters more comfortable and less likely to cause heat waves or perspiration.

6.2 Adverse Implications of urban growth and urban heat islands on the metropolis

Across various parts of the world, urban growth transforms the urban environment. Unfortunately, these transformations come with numerous adverse implications which have made urban growth gain international attention (Buo et al., 2021). According to Blay & Abunyuwah, (2024), the implications of urban growth stem from the excessive and extensive use of natural resources by human actions and the improper or unproportionate proper planning and monitoring of urban growth, a situation mostly consistent with developing countries. The finding of the study revealed significant reduction in vegetation and water at the increasing expense of built-up and a rise in heat islands in the metropolis. This has adverse implications for the metropolis if urgent and decisive action is not taken by the city authorities and urban planners of the metropolis.

Vegetation offers vital functions such as carbon capture and storage, urban cooling, reduced runoff, and high infiltration (Pandey & Ghosh, 2023). These functions are important for building a sustainable and resilient urban environment. Therefore, reducing its coverage makes the urban environment less resilient and unsustainable which is not good for ecological life (Dehghani et al., 2022). The depletion of vegetation in the metropolis and its replacement by built-up has contributed to the emergence of flooding issues. For instance, from 31 May to 1 June 2019, many parts of Sekondi-Takoradi suffered severe flooding during the several hours of heavy downpours. This led to a total power outage, killing 10 people and the destruction of many properties. On 24th April 2020 parts of Sekondi-Takoradi got flooded following a downpour. The floodwaters broke into homes, stores, and offices, destroying properties and leaving many stranded (Peacefm, 2020). On 27th February 2021, a heavy downpour witnessed in the Sekondi-Takoradi Metropolis wreaked

havoc on school properties, homes, and stores, and blocked a lot of asphalt roads in the metropolis (Ghana Web, 2021). This annual successive occurrence of floods and its severe destructions highlighted above used to be rare in Sekondi-Takoradi, unlike Accra, which is known for its yearly flooding issues. This shows that the metropolis is becoming susceptible to frequent flooding. Unfortunately, a majority of the population in the metropolis resides in the suburbs and commutes to the business center daily (Fiave, 2017). The road network and quite recently, the rail network constitute the lifeline of the city, transporting thousands into the business center (STMA, 2022). So, any disruption owing to flooding results in economic and social disruption – loss of livelihood to the individuals and loss of business to commerce and industry. Since the establishment of the Takoradi harbour, Sekondi-Takoradi has been the center for business process outsourcing (BPO) or business hub for major local, national, and international organizations (STMA, 2022). Therefore, any disaster in Sekondi-Takoradi has a roll-over effect on the national economy and to some extent the global economy. According to Afriyie et al. (2020), the livelihood of urban dwellers may be affected by changes in urban areas. Therefore, inappropriate handling of urban growth would result in social, economic, and environmental tragedies and consequently destroy the sustainable development of urban lands.

Further, as water is vital for human sustenance, its reduction comes with far-reaching implications. The provision of fresh water for domestic and industrial use in the metropolis would reduce, exacerbating water scarcity in areas already facing water stress (Emile et al., 2022) This can lead to potential conflicts over water resources as occurred in Lamu, Kenya (Manigey et al., 2022). Presently, some areas of the metropolis such as the Central Business District, Adientam, Bankyease, Kweikuma, and Race Course are experiencing water rationing (Arhinful, 2024). Also, communities like Essipon, Essei, New Takoradi, Adakope, and Kokompe respectively depend on waterbodies such as Anankwari River, Essei Lagoon Butuah Lagoon, and Whin Estuary for activities such as fishing, tourism, and other economic activities. The decrease in water bodies would lead to loss of income and displacement of people in these communities whose livelihoods depend on the water bodies. For instance, as the Urmia Lake in Iran began to shrink, the farmers and those in the tourism industry lost their jobs and many people moved to other towns and cities in search of jobs and other income opportunities (Schmidt, Gonda & Transiskus, 2021). The metropolis, especially people whose livelihood depends on the waterbodies would suffer the same fate. Furthermore, water bodies often have recreational and cultural significance (Venohr et al.,

2018). The loss of them can reduce opportunities for leisure activities such as swimming, boating, and picnicking. The Aqua Makarios and riverside resorts in the metropolis offer the opportunity for people to swim, enjoy boat rides, and picnic there. This significance would diminish with time as water bodies keep reducing. Apart from vegetation, water also helps to regulate local microclimates by providing cooling effects (Erell & Zhou, 2022). Hence the observed decline in water would contribute to the intensification of the Urban Heat Island (UHI) effect (Zhu, Zhou & Cheng, 2022) and its increasing reliance on electronic cooling appliances like air conditioners which contribute to a greater carbon footprint and higher energy consumption. Valdés-Pineda et al. (2021) opine that waterbodies act as natural buffers, absorbing and retaining excess rainfall. Therefore, when they are reduced or replaced by impervious built-up areas, their capacity for natural water retention diminishes, leading to higher surface runoff and an increased risk of urban flooding which is currently the situation in the metropolis.

Lastly, in developing countries like Ghana, electric fans and air conditioners are mostly relied on to combat or mitigate thermal discomfort. Unfortunately, the usage of air conditioners is a privilege and luxury only a few affluent can afford (Buo et al., 2021) due to the high price and electricity bills associated with its usage. Ghana is already challenged with persistent power outages which have profoundly affected its economy in the form of collapse of businesses, loss of revenues, and laying off of workers due to low productivity and revenue (Mensah, 2024). In light of this, relying on electric fans and air-conditioners to mitigate UHI would worsen the existing power supply challenges, leading to more frequent and prolonged outages. Additionally, when power is unreliable, residents and businesses are compelled to use diesel generators, which contribute to local air pollution and release additional greenhouse gases (Kabeyi & Olanrewaju, 2023), thereby reinforcing the UHI effect. This cycle of rising temperatures and increasing power demand stresses the energy infrastructure and amplifies economic losses, particularly in urban areas where the concentration of people and infrastructure suffers most acutely from both UHIs and power shortages.

CHAPTER 7: CONCLUSIONS AND RECOMMENDATIONS

7.0 Introduction

This chapter provides a summary of the research findings, addresses the limitations of the study, and offers recommendations as well as suggests consideration for future research.

7.1 Conclusions

I. The LULC trend over the study period revealed a rapid growth in built-up areas by 63.08 km^2 (32.91 %) whereas vegetation and water decreased by 60.99 km^2 (31.82 %) and 2.08 km^2 (1.09 %) respectively. Notably, the most significant class conversion observed during the period was the depletion of vegetation, with a substantial portion of 60.99 km^2 converted into built-up land. Also, the projection for 2030 indicated further changes with water areas declining to 1.21 km^2 (0.63%), vegetation reducing to 95.31 km^2 (49.73%), and built-up areas expanding to 95.14 km^2 (49.64%). This indicates a notable transition shift towards urbanized areas and highlights the accelerating urbanization trend which is modifying the metropolis' land cover composition and potentially impeding the achievement of Sustainable Development Goal 11. Therefore, there is an urgent need for intensive monitoring and controlled urban expansion to alleviate possible adverse effects.

II. The urban expansion indices revealed that the metropolis expanded from a slow speed to a very high speed which indicates a high susceptibility of the metropolis to experiencing urban sprawl. Using Shannon's and relative entropy to quantify the degree of dispersion and compaction, it was evident that all the years had values greater than the thresholds that denote dispersion taking place in all the years. The extent of sprawl primarily increased from the city center towards the northeast and northwest directions leading to the annexation of adjacent communities. Moreover, the analysis of the landscape metrics revealed an increasing fragmentation, complexity, and an irregular pattern in the landscape potentially due to dispersed urban development. This dispersion can be attributed to factors such as ineffective and under-resourced planning agencies, challenges related to land title acquisition, and the complexities of the land tenure system which are key drivers of urban sprawl in Ghana. Also, laxity in zoning regulations, and the desire for people to live outside the city center as a result of high rent costs, heavy traffic, and increased pollution have

influenced the dispersed distribution of the metropolis. Moreover, the zonal gradient analysis revealed that throughout the study period, significant land development occurred mostly in the NE part of the study while low land development occurred in the SE part of the metropolis. The zonal gradient analysis revealed that throughout the study period, significant land development occurred mostly in the NE part of the study while low land development occurred in the SE part of the metropolis.

III. The significant shift in land use from natural and undeveloped spaces to artificial and urbanized areas led to a 3.1°C rise in mean LST. This indicates a warming environment primarily affected by urban expansion and declining vegetation. Also, through the correlation analysis, the influence of built-up on temperature changes surpassed that of vegetation and water, emphasizing the crucial role of urbanization in temperature rise. Moreover, temperature variations across the urban space were influenced by some spatial factors characterizing the metropolis. Areas characterized by high NDWI, low NDBI, high NDVI, and high elevation, as well as being far from rivers, main roads, and the CBD create optimal conditions for low temperatures. These factors provided valuable insight into the intensification of LST and UHI in the metropolis. Furthermore, the UHI effect analysis showed that the city core and high-density areas registered higher temperatures than the low-density areas. Areas affected by the UHI effect increased by 19.38 km^2 while the UTFVI analysis further indicated a 33.63 km^2 increase in the worst ecological zone due to the temperature rise. This shows that the study area is progressively becoming susceptible to severe thermal conditions which is not good for ecological life. The study equips city authorities and planners with the fundamental knowledge needed to prepare a sustainable development plan that alleviates adverse effects of urban growth and elevated temperature-related issues. Also, the findings contribute to global efforts to promote more livable and climate-resilient urban environments.

7.2 Recommendations

In line with the study objectives and conclusions, the following are recommended for policy and institutional actions.

7.2.1 Recommendations for Policy (Urban Planners and City Authorities)

I. Built-up restrictions and planned controls should be enforced to prevent the indiscriminate conversion of waterbodies and undeveloped green spaces into built-up areas.

II. Emphasis on the compact city model (vertical construction) should be encouraged to prevent the horizontal wastage of land. This will aid in limiting the number of green areas being converted into urban areas.

III. The physical planning unit of the metropolis should regularly sensitize and educate the general public or the metropolis on the local and structured plans of the metropolis. Also, as stated in the law [Act 925, part 16 section 66], a public data room or exhibition room should be created to display the spatial plans of the metropolis. This would not only create awareness of them but would aid in their conformity.

IV. The city authorities should enact by-laws that effectively integrate green spaces into built-up areas, increase tree planting, and also select and plant the right species in suitable locations.

V. Green roofs have been confirmed by studies as an effective strategy for the reduction of environmental temperature and energy consumption therefore city authorities should implement or incorporate their use in the metropolis.

VI. The city authorities should redirect/relocate heat-creating activities from the city center and densely populated areas to cooler and less populated locations.

VII. The industrial areas of the metropolis should be interspersed with vegetation and each industry should be charged with the responsibility of keeping an eco-friendly environment.

7.2.2 Recommendation for Future Research

I. Object-based image classification may be considered, or a comparison between both pixel-based and object-based techniques can be explored. This analysis will contribute to the state-of-the-art methods in classifying satellite images, particularly in Ghana.

II. Diverse spectral indices on vegetation and built-up exist but only one index of vegetation and built-up were employed in this study. Though detailed information was obtained from these indices, applying more than one index from each class could provide an in-depth understanding of the patterns of vegetation and built-up in the natural environment or metropolis.

III. Landsat-derived LST can be done by using devised methods such as split window and single channel. These techniques would enhance better comparison and provide essential information essential to the management and safeguarding of the metropolis.

IV. The analysis of temperature did not factor in the prediction of temperature which is essential for future planning. Forecasting of temperature will offer an in-depth understanding for planners and city authorities in Ghana; therefore, future studies should incorporate the prediction of temperature as part of their analysis.

V. Unlike traditional imagery that uses few spectral bands, hyperspectral imagery uses a wide range of spectral bands which allows for more precise identification and differentiation of land cover types. hence, hyperspectral may be considered for LULC studies.

7.3 Contribution to Knowledge

By analyzing direction-wise urban growth patterns, this research provides new insights into the spatial variability of urban expansion and its local drivers, a dimension previously unexplored in the metropolis. Also, the research extends the temporal scope of UHI studies in the metropolis, incorporating the Urban Thermal Field Variance Index (UTFVI) to assess thermal comfort levels—a novel application in Ghana. Moreover, the inclusion of spatial factors to characterize the metropolis into archetypes and assess their influence on temperature variations within the study area extended the approach and understanding of what is already known about the UHI. Additionally, the dual application of Ordinary Least Squares (OLS) and Geographically Weighted Regression (GWR) to model LST relationships with NDVI and NDBI introduces a spatially sensitive framework that advances the understanding of urban heat dynamics in tropical regions. These contributions not only address significant research gaps but also offer practical tools for sustainable urban development and environmental management in rapidly urbanizing areas. The innovative methodologies and localized insights set a strong foundation for future research in Ghana and similar contexts worldwide.

REFERENCES

Abass, K., Adanu, S. K., & Gyasi, R. M. (2018). Urban sprawl and land use / land-cover transition probabilities in peri-urban Kumasi , Ghana. *West African Journal of Applied Ecology*, *26*, 118–132.

Abass, K., Buor, D., Afriyie, K., Dumedah, G., Yao, A., Guodaar, L., Kofi, E., Adu-gyamfi, S., Forkuor, D., Ofosu, A., Mohammed, A., & Gyasi, R. M. (2020). Urban sprawl and green space depletion : Implications for flood incidence in. *International Journal of Disaster Risk Reduction*, *51*(March), 101915. https://doi.org/10.1016/j.ijdrr.2020.101915

Abass, K., Dumedah, G., Frempong, F., Muntaka, A. S., Appiah, D. O., Garsonu, E. K., & Gyasi, R. M. (2022). Rising incidence and risks of floods in urban Ghana : Is climate change to blame ? *Cities*, *121*(September 2021), 103495. https://doi.org/10.1016/j.cities.2021.103495

Abdul-kareem, R., Gnansounou, S. C., & Adongo, R. (2021). Effects of the oil-find on land management in the Sekondi-Takoradi Metropolis , Western Coast of Ghana. *Journal of Land Use Science*, *16*(4), 398–412. https://doi.org/10.1080/1747423X.2021.1991018

Abdullahi, S., & Pradhan, B. (2010). *Urban Expansion and Change Detection Analysis*. https://doi.org/10.1007/978-3-319-54217-1

Abudu, D., Azo, R., & Andogah, G. (2019). Spatial assessment of urban sprawl in Arua Municipality , Uganda. *The Egyptian Journal of Remote Sensing and Space Sciences*, *22*(3), 315–322. https://doi.org/10.1016/j.ejrs.2018.01.008

Adarkwa, K. K. (2012). The changing face of Ghanaian towns. *African review of economics and finance*, *4*(1), 1-29.

Addae, B. (2019). *Land-Use / Land-Cover Change Analysis and Urban Growth Modelling in the Greater Accra Metropolitan Area (GAMA), Ghana*. https://doi.org/10.3390/urbansci3010026

Aduah, M. S., & Baffoe, P. E. (2013). *Remote Sensing for Mapping Land-Use / Cover Changes and Urban Sprawl in Sekondi-Takoradi , Western Region of Ghana*. 66–73.

Aduah, M. S., & Mantey, S. (2023). Assessment of Land Use Efficiencies of Ghanaian Cities: Case Study of Sekondi-Takoradi Metropolis. *South African Journal of Geomatics*, *12*(1), 86–97. https://doi.org/10.4314/sajg.v12i1.6

Aduah, M. S., Mantey, S., & Area, T. M. (2020a). *Modelling Potential Future Urban Land Use Changes in the Sekondi-Takoradi Metropolitan Area of Ghana. 2*.

Aduah, M. S., Mantey, S., & Area, T. M. (2020b). *Modelling Potential Future Urban Land Use Changes in the Sekondi-Takoradi Metropolitan Area of Ghana *. 2*.

Aflaki, A., Mirnezhad, M., Ghaffarianhoseini, A., Ghaffarianhoseini, A., Omrany, H., Wang, Z. H., & Akbari, H. (2017). Urban heat island mitigation strategies: A state-of-the-art review

on Kuala Lumpur, Singapore and Hong Kong. *Cities*, *62*, 131–145. https://doi.org/10.1016/j.cities.2016.09.003

Africapolis. (2023). Ghana country report. Retrieved from https://africapolis.org/en/country-report/Ghana.

Afriyanie, D., Julian, M. M., Nugraha, H. A., Wanabakti, M. J., & Susilo, C. R. (2018). *Urban growth pattern with urban flood and temperature vulnerability using AI : a case study of Delhi Urban growth pattern with urban flood and temperature vulnerability using AI : a case study of Delhi*.

Agenda, D. (2013). *MEDIUM-TERM NATIONAL DEVELOPMENT POLICY FRAMEWORK : VOLUME I : POLICY FRAMEWORK*. *I*, 2010–2013.

Ahmed, C. F., & Kranthi, N. (2018). *Flood Vulnerability Assessment using Geospatial Techniques : Chennai ,*. *March*. https://doi.org/10.17485/ijst/2018/v11i6/110831

Akubia, J. E. K., & Bruns, A. (2019). *Unravelling the Frontiers of Urban Growth : Spatio-Temporal Dynamics of Land-Use Change and Urban Expansion in Greater Accra Metropolitan Area, Ghana*. 1–23.

Al kafy, A., Rahman, M. S., Faisal, A.-, Hasan, M. M., & Islam, M. (2020). Modelling future land use land cover changes and their impacts on land surface temperatures in Rajshahi , Bangladesh. *Remote Sensing Applications: Society and Environment*, *18*(February), 100314. https://doi.org/10.1016/j.rsase.2020.100314

Alam, I., Nahar, K., & Morshed, M. M. (2023). Measuring urban expansion pattern using spatial matrices in Khulna City, Bangladesh. *Heliyon*, *9*(2), e13193. https://doi.org/10.1016/j.heliyon.2023.e13193

Albert, G., & Yiran, B. (2021). *Urban sprawl and sustainability : A comparative Analysis of Accra and Kumasi urban regions Urban sprawl and sustainability : A comparative Analysis of Accra and Kumasi*. *June 2020*.

Alijani, Z., Hosseinali, F., & Biswas, A. (2020). Spatio-temporal evolution of agricultural land use change drivers: A case study from Chalous region, Iran. *Journal of Environmental Management*, *262*(June 2019), 110326. https://doi.org/10.1016/j.jenvman.2020.110326

Al-Kafy, A., Rahman, S., Faisal, A.-A., Hassan, M. M., & Islam, M. (2020). Modelling future land use land cover changes and their impacts on land surface temperatures in Rajshahi , Bangladesh. *Remote Sensing Applications: Society and Environment*, *18*(April), 100314. https://doi.org/10.1016/j.rsase.2020.100314

Al-khakani, E. T. (2023). *Land Surface Temperature Dynamics in Response to Changes in Land Cover in Land Surface Temperature Dynamics in Response to Changes in Land Cover in An-Najaf Province , Iraq*. *July*. https://doi.org/10.7780/kjrs.2023.39.1.7

Alqadhi, S., Mallick, J., Talukdar, S., Bindajam, A. A., & Shohan, A. A. A. (2021).

Quantification of Urban Sprawl for Past-To-Future in Abha City , Saudi Arabia Quantification of Urban Sprawl for Past-To-Future in Abha City ,. August. https://doi.org/10.32604/cmes.2021.016640

Alqattan, N., Acheampong, M., Jaward, F. M., Vijayakumar, N., Ebude, L., & Enomah, D. (2019). Evaluation of the potential hydrological impacts of land use / cover change dynamics in Ghana ' s oil city. *Environment, Development and Sustainability*, *0123456789*. https://doi.org/10.1007/s10668-019-00507-0

Amponsah, O., Blija, D. K., Ayambire, R. A., Takyi, S. A., Mensah, H., & Braimah, I. (2022). Global urban sprawl containment strategies and their implications for rapidly urbanising cities in Ghana. *Land Use Policy*, *114*(January), 105979. https://doi.org/10.1016/j.landusepol.2022.105979

Anande, D. M., & Park, M. (2021). *Impacts of Projected Urban Expansion on Rainfall and Temperature during Rainy Season in the Middle-Eastern Region in Tanzania*.

Andersson, K., Dickin, S., & Rosemarin, A. (2016). Towards " Sustainable " Sanitation : Challenges and Opportunities in Urban Areas. *Sustainability, MDPI*. https://doi.org/10.3390/su8121289

Antipova, A., & Antipova, A. (2018). City Structure and Spatial Patterns. *Urban Environment, Travel Behavior, Health, and Resident Satisfaction*, 153-204.

Anwar, M., Asming, A., Ibrahim, A. M., & Abir, I. M. (2022). Processing and classification of landsat and sentinel images for oil palm plantation detection. *Remote Sensing Applications: Society and Environment*, *26*(April), 100747. https://doi.org/10.1016/j.rsase.2022.100747

Appiah, D. O. (2016). *Geoinformation Modelling of Peri-Urban Land Use and Land Cover Dynamics for Climate Variability and Climate Change in the Bosomtwe District, Ghana*.

Asare, Y. M., Selby, I., Ashiagbor, G., & Asante, C. Y. (2023). *Analysis and prediction of land use land cover dynamics in the Kpeshie Lagoon Basin of Ghana using satellite remote sensing*.

Asibey, M. O., Osei, D. A., Doe, B., & Agyei, F. (2024). Rethinking the implications of sprawl for sustainable urban development: Insights from the Ejisu Municipality of Ghana between 2003 and 2023. *Habitat International*, *152*(August), 103161. https://doi.org/10.1016/j.habitatint.2024.103161

Asibey, M.O., Osei, D.A., Doe, B. and Agyei, F., 2024. Rethinking the implications of sprawl for sustainable urban development: Insights from the Ejisu Municipality of Ghana between 2003 and 2023. *Habitat International*, *152*, p.103161.

Asif, M., Kazmi, J. H., Tariq, A., Zhao, N., Guluzade, R., Soufan, W., Almutairi, K. F., Sabagh, A. El, Aslam, M., Asif, M., Kazmi, J. H., Tariq, A., Zhao, N., & Guluzade, R. (2023). Modelling of land use and land cover changes and prediction using CA-Markov and Random Forest. *Geocarto International*, *38*(1).

https://doi.org/10.1080/10106049.2023.2210532

Ayambire, R.A., Amponsah, O., Peprah, C. and Takyi, S.A., 2019. A review of practices for sustaining urban and peri-urban agriculture: Implications for land use planning in rapidly urbanising Ghanaian cities. *Land Use Policy*, *84*, pp.260-277.

Badasa, M., Temesgen, B., Busha, L., Niguse, I., & Obsi, D. (2022a). Analysis of land surface temperature using Geospatial technologies in Gida Kiremu , Limu , and Amuru District , Western Ethiopia. *Artificial Intelligence in Agriculture*, *6*, 90–99. https://doi.org/10.1016/j.aiia.2022.06.002

Badasa, M., Temesgen, B., Busha, L., Niguse, I., & Obsi, D. (2022b). Arti fi cial Intelligence in Agriculture Analysis of land surface temperature using Geospatial technologies in Gida Kiremu , Limu , and Amuru District , Western Ethiopia. *Artificial Intelligence in Agriculture*, *6*, 90–99. https://doi.org/10.1016/j.aiia.2022.06.002

Balew, A., & Korme, T. (2020). Monitoring land surface temperature in Bahir Dar city and its surrounding using Landsat images. *The Egyptian Journal of Remote Sensing and Space Sciences*, *23*(3), 371–386. https://doi.org/10.1016/j.ejrs.2020.02.001

Balha, A., Kumar, C., & Pandey, S. (2020). Remote Sensing Applications : Society and Environment Assessment of urban area dynamics in world ' s second largest megacity at sub-city (district) level during 1973 – 2016 along with regional planning. *Remote Sensing Applications: Society and Environment*, *20*(August), 100383. https://doi.org/10.1016/j.rsase.2020.100383

Baqa, M. F., Chen, F., Lu, L., Qureshi, S., Tariq, A., Wang, S., Jing, L., Hamza, S., & Li, Q. (2021). Monitoring and Modeling the Patterns and Trends of Urban Growth Using Urban Sprawl Matrix and CA-Markov Model : A case stuy of Karachi, Pakistan. *Land, MDPI*.

Barman, S., Roy, D., Sarkar, B. C., Almohamad, H., & Abdo, H. G. (2024). Assessment of urban growth in relation to urban sprawl using landscape metrics and Shannon ' s entropy model in Jalpaiguri urban agglomeration , West Bengal, India. *Geocarto International*, *39*(1). https://doi.org/10.1080/10106049.2024.2306258

Belenok, V., Noszczyk, T., Hebryn-baidy, L., & Kryachok, S. (2021). Investigating anthropogenically transformed landscapes with remote sensing. *Remote Sensing Applications: Society and Environment*, *24*(September), 100635. https://doi.org/10.1016/j.rsase.2021.100635

Bhatta, B. (2010). *Analysis of Urban Growth and Sprawl from Remote Sensing Data* (S. Balram & S. Dragicevic (eds.)). Springer. https://doi.org/DOI 10.1007/978-3-642-05299-6

Biney, E., & Boakye, E. (2021). Urban sprawl and its impact on land use land cover dynamics of Sekondi-Takoradi metropolitan assembly , Ghana. *Environmental Challenges*, *4*(April), 100168. https://doi.org/10.1016/j.envc.2021.100168

Biney, E., Biney, N., Dadzie, I., Harris, E., Ama, G., Mensah, Y., Bessah, E., & Kwabena, E.

(2022). Impact of mining on vegetation cover : A case study of Prestea Huni-Valley municipality. *Scientific African*, *17*, e01387. https://doi.org/10.1016/j.sciaf.2022.e01387

Biney, E., Forkuo, E. K., Poku-boansi, M., & Mensah, Y. (2024). Geospatial assessment of urban sprawl in Sekondi- Takoradi Metropolis , Ghana from 1991 to 2023. *African Geographical Review*, *00*(00), 1–18. https://doi.org/10.1080/19376812.2024.2334726

Biney, E., Forkuo, E. K., Poku-Boansi, M., Asare, Y. M., Hackman, K. O., Yankey, D. B., Agbenorhevi, A. E., & Annan, E. (2024). A comprehensive analysis and future projection of land use and land cover dynamics in a fast-growing city: A case study of Sekondi-Takoradi metropolis, Ghana. *Scientific African*, *24*(February), e02207. https://doi.org/10.1016/j.sciaf.2024.e02207

Blay, J. K., & Abunyuwah, I. (2024). Implications of land use and land cover change in Mampong municipality, Ghana. *Sustainable Environment*, *10*(1). https://doi.org/10.1080/27658511.2024.2345442

Boakye, E., Anyemedu, F. O. K., Quaye-ballard, J. A., & Donkor, E. A. (2019). *Spatio-temporal analysis of land use / cover changes in the Pra River Basin , Ghana*. *2008*.

Borges, L., Alencar, M. H., & Almeida, A. T. De. (2022). A novel spatiotemporal multi-attribute method for assessing flood risks in urban spaces under climate change and demographic scenarios. *Sustainable Cities and Society*, *76*(July 2021), 103501. https://doi.org/10.1016/j.scs.2021.103501

Buo, I., Sagris, V., Burdun, I., & Uuemaa, E. (2021). Estimating the expansion of urban areas and urban heat islands (UHI) in Ghana: a case study. *Natural Hazards*, *105*(2), 1299–1321. https://doi.org/10.1007/s11069-020-04355-4

Cengiz, S., Gormüs, S., & Oguz, D. (2022). Analysis of the urban growth pattern through spatial metrics ; Ankara City. *Land Use Policy*, *112*(January 2021). https://doi.org/10.1016/j.landusepol.2021.105812

Cengiz, S., Görmüş, S., & Oğuz, D. (2022). Analysis of the urban growth pattern through spatial metrics; Ankara City. *Land Use Policy*, *112*(September 2021). https://doi.org/10.1016/j.landusepol.2021.105812

Cevik, D. B., & Cetin, M. (2023). Evaluation of UTFVI index effect on climate change in terms of urbanization. *Environmental Science and Pollution Research*, *30*(30), 75273–75280. https://doi.org/10.1007/s11356-023-27613-x

Chanyal, P. and Purohit, S., 2024. A Geospatial analysis of Climate Change Impacts: Relationship of Normalized Difference Water Index (NDWI and Land Surface Temperature (LST) in Kumaun Himalaya.

Chatterjee, R. S., Singh, N., Thapa, S., Sharma, D., & Kumar, D. (2017). Retrieval of land surface temperature (LST) from landsat TM6 and TIRS data by single channel radiative

transfer algorithm using satellite and ground-based inputs. *International journal of applied earth observation and geoinformation*, *58*, 264-277.

Chatterjee, S., & Gupta, K. (2021). Exploring the spatial pattern of urban heat island formation in relation to land transformation : A study on a mining industrial region of West. *Remote Sensing Applications: Society and Environment*, *23*(July), 100581. https://doi.org/10.1016/j.rsase.2021.100581

Chen, L., Wang, X., Cai, X., Yang, C., & Lu, X. (2021). Seasonal variations of daytime land surface temperature and their underlying drivers over Wuhan, China. *Remote Sensing*, *13*(2), 1–22. https://doi.org/10.3390/rs13020323

Chen, L., Wang, X., Cai, X., Yang, C., & Lu, X. (2021). Seasonal variations of daytime land surface temperature and their underlying drivers over Wuhan, China. *Remote Sensing*, *13*(2), 1–22. https://doi.org/10.3390/rs13020323

Chen, S., Haase, D., Qureshi, S., & Firozjaei, M. K. (2022). Integrated Land Use and Urban Function Impacts on Land Surface Temperature: Implications on Urban Heat Mitigation in Berlin with Eight-Type Spaces. *Sustainable Cities and Society*, 103944. https://doi.org/10.1016/j.scs.2022.103944

Chettry, V. (2022). Peri - urban area delineation and urban sprawl quantification in Thiruvananthapuram Urban Agglomeration , India , from 2001 to 2021 using geoinformatics. *Applied Geomatics*, 639–652. https://doi.org/10.1007/s12518-022-00460-0

Chettry, V. (2023). A Critical Review of Urban Sprawl Studies. *Journal of Geovisualization and Spatial Analysis*, *7*(2), 1–13. https://doi.org/10.1007/s41651-023-00158-w

Cho, K. H., Lee, D., Kim, T., & Jang, G. (2021). *Measurement of 30-Year Urban Expansion Using Spatial Entropy in Changwon and Gimhae , Korea*. 1–12.

Choudhury, U., Singh, S. K., Kumar, A., Meraj, G., & Kumar, P. (2023). Assessing Land Use / Land Cover Changes and Urban Heat Island Intensification : A Case Study of Kamrup Metropolitan District , Northeast India (2000 – 2032). *Mdpi*, 503–521.

Cobbinah, P. B., & Erdiaw-Kwasie, M. O. (2018). Urbanization in Ghana: Insights and implications for urban governance. In *E-planning and collaboration: Concepts, methodologies, tools, and applications* (pp. 256-278). IGI Global.

Cobbinah, P. B., Asibey, M. O., Opoku-Gyamfi, M., & Peprah, C. (2019). Urban planning and climate change in Ghana. *Journal of Urban Management*, *8*(2), 261-271.

Daata, E., Kwabena, E., Biney, E., Harris, E., & Quaye-ballard, J. A. (2021). The impact of land use and land cover changes on socioeconomic factors and livelihood in the Atwima Nwabiagya district of the Ashanti region , Ghana. *Environmental Challenges*, *5*(July), 100226. https://doi.org/10.1016/j.envc.2021.100226

Dabie, K. P. (2015). *ASSESSING THE IMPACT OF URBAN SPRAWL ON AGRICULTURAL*

LAND USE AND FOOD SECURITY IN SHAI OSUDOKU DISTRICT. UNIVERSITY OF GHANA, LEGON.

Dadras, M., Shafri, H. Z. M., & Ahmad, N. (2015). Spatio-temporal analysis of urban growth from remote sensing data in Bandar Abbas city , Iran. *The Egyptian Journal of Remote Sensing and Space Sciences*, *18*(1), 35–52. https://doi.org/10.1016/j.ejrs.2015.03.005

Dadzie-paintsil, E., & Mensah, J. V. (2022). *Effects of urbanization on coastal wetlands in the Sekondi-Takoradi Metropolis , Ghana*. *6*(2), 94–105. https://doi.org/10.13057/oceanlife/o060205

Danniswari, D., Honjo, T. and Furuya, K., 2022. Analysis of Building Height Impact on Land Surface Temperature by Digital Building Height Model Obtained from AW3D30 and SRTM. *Geographies*, *2*(4), pp.563-576.

Danso, S. Y., & Addo, I. Y. (2016). *Coping strategies of households affected by flooding : A case study of Sekondi-Takoradi Metropolis in Ghana Coping strategies of households affected by flooding : A case study of*. *9006*(May). https://doi.org/10.1080/1573062X.2016.1176223

Danso, S. Y., & Addo, I. Y. (2018). Coping strategies of households affected by flooding : A case study of Sekondi-Takoradi Metropolis in Ghana. *Urban Water Journal*, *July*, 1–7. https://doi.org/10.1080/1573062X.2016.1176223

Danso, S. Y., Ma, Y., Dodzi, Y., Adjakloe, A., & Addo, I. Y. (n.d.). *Application of an Index-Based Approach in Geospatial Techniques for the Mapping of Flood Hazard Areas : A Case of Cape Coast Metropolis in Ghana*. 6–8.

Danso, S. Y., Ma, Y., Osman, A., & Addo, I. Y. (2024). Integrating multi-criteria analysis and geospatial applications for mapping flood hazards in Sekondi-Takoradi Metropolis, Ghana. *Journal of African Earth Sciences*, *209*(November 2023). https://doi.org/10.1016/j.jafrearsci.2023.105102

Danso-wiredu, E. Y., Darkwa, O. I., Bonful, E., Bismark, M., Mohammed, S., & Tuu, B. M. (2020). *Patterns of Land Use Activities in Ghana ' s Secondary Cities*. *12*(2), 84–107.

Darlington, T., Odindi, J., Dube, T., & Nyasha, T. (2017). Remote sensing applications in monitoring urban growth impacts on in-and- out door thermal conditions : A review. *Remote Sensing Applications: Society and Environment*, *8*(August), 83–93. https://doi.org/10.1016/j.rsase.2017.08.001

Das, S., & Angadi, D. P. (2020). Land use-land cover (LULC) transformation and its relation with land surface temperature changes : A case study of Barrackpore Subdivision ,. *Remote Sensing Applications: Society and Environment*, *19*(July 2019), 100322. https://doi.org/10.1016/j.rsase.2020.100322

Das, S., & Angadi, D. P. (2020). Land use-land cover (LULC) transformation and its relation with land surface temperature changes : A case study of Barrackpore Subdivision ,. *Remote*

Sensing Applications: Society and Environment, *19*(July 2019), 100322. https://doi.org/10.1016/j.rsase.2020.100322

Davis, K., & Golden, H. H. (2017). Urbanization and the development of pre-industrial areas. In *Kingsley Davis* (pp. 295-317). Routledge.

Deilami, K. (2017). *MODELLING THE URBAN HEAT ISLAND INTENSITIES OF ALTERNATIVE URBAN GROWTH MANAGEMENT POLICIES IN BRISBANE*.

Deribew, K. T. (2020a). Spatiotemporal analysis of urban growth on forest and agricultural land using geospatial techniques and Shannon entropy method in the satellite town of Ethiopia, the western fringe of Addis Ababa city. *Ecological Processes*, *9*(1). https://doi.org/10.1186/s13717-020-00248-3

Deribew, K. T. (2020b). *Spatiotemporal analysis of urban growth on forest and agricultural land using geospatial techniques and Shannon entropy method in the satellite town of Ethiopia , the western fringe of Addis Ababa city*. *September*. https://doi.org/10.1186/s13717-020-00248-3

Dewa, D. D., Buchori, I., & Sejati, A. W. (2022). Assessing land use / land cover change diversity and its relation with urban dispersion using Shannon Entropy in the Semarang Metropolitan Region , Indonesia. *Geocarto International*, *37*(26), 11151–11172. https://doi.org/10.1080/10106049.2022.2046871

Dhali, K., Chakraborty, M., & Sahana, M. (2019a). Assessing spatio-temporal growth of urban sub-centre using Shannon ' s entropy model and principle component analysis : A case from North 24. *The Egyptian Journal of Remote Sensing and Space Sciences*, *22*(1), 25–35. https://doi.org/10.1016/j.ejrs.2018.02.002

Dhali, K., Chakraborty, M., & Sahana, M. (2019b). Assessing spatio-temporal growth of urban sub-centre using Shannon ' s entropy model and principle component analysis : A case from North 24. *The Egyptian Journal of Remote Sensing and Space Sciences*, *22*(1), 25–35. https://doi.org/10.1016/j.ejrs.2018.02.002

Dhali, K., Chakraborty, M., & Sahana, M. (2019c). Assessing spatio-temporal growth of urban sub-centre using Shannon ' s entropy model and principle component analysis : A case from North 24 Parganas, lower Ganga River Basin, India. *The Egyptian Journal of Remote Sensing and Space Sciences*, *22*(1), 25–35. https://doi.org/10.1016/j.ejrs.2018.02.002

Dijkstra, L., Galic, A., & Brandmüller, T. (2022). *Measuring Sustainable Development Goals in cities , towns and rural areas : The new Degree*. *38*, 549–559. https://doi.org/10.3233/SJI-220020

Ding, Y., Shi, B., Su, G., Li, Q., Meng, J., Jiang, Y., Qin, Y., Dai, L., & Song, S. (2021). Assessing suitability of human settlements in high-altitude area using a comprehensive index method: A case study of Tibet, China. *Sustainability (Switzerland)*, *13*(3), 1–21. https://doi.org/10.3390/su13031485

Dissanayake, K. (2020). *Ecological Evaluation of Urban Heat Island Effect in Colombo City , Sri Lanka Based on Landsat 8 Satellite Data*. 531–536.

Doe, B., Amoako, C., & Adamtey, R. (2022). Spatial expansion and patterns of land use/land cover changes around Accra, Ghana – Emerging insights from Awutu Senya East Municipal Area. *Land Use Policy*, *112*(August 2021), 105796. https://doi.org/10.1016/j.landusepol.2021.105796

Dutta, D., Gupta, S., & Chakraborty, A. (2022). Effect of different land use land cover on surface heat budget – A case study from a tropical humid region of India. *Remote Sensing Applications: Society and Environment*, *25*(September 2021), 100675. https://doi.org/10.1016/j.rsase.2021.100675

Elagouz, M. H., Abou-shleel, S. M., Belal, A. A., & El-mohandes, M. A. O. (2020). Detection of land use / cover change in Egyptian Nile Delta using remote sensing. *The Egyptian Journal of Remote Sensing and Space Sciences*, *23*(1), 57–62. https://doi.org/10.1016/j.ejrs.2018.10.004

Eshetie, S. M. (2024). Exploring urban land surface temperature using spatial modelling techniques : a case study of Addis Ababa city , Ethiopia. *Scientific Reports*, 1–16. https://doi.org/10.1038/s41598-024-55121-6

F, W. L., Taciane, C., Antonio, C., Eduardo, P., Everaldo, C., Barros, E., & Machado, F. (2022). *The influence of urban expansion in the socio-economic , demographic , and environmental indicators in the City of*. *25*(September 2021). https://doi.org/10.1016/j.rsase.2021.100662

Faisal, A.-, Al, A., Al, A., Shaleha, K., Amir, D., Sikdar, S., Jahan, T., & Mallik, S. (2021). Assessing and predicting land use / land cover , land surface temperature and urban thermal field variance index using Landsat imagery for Dhaka Metropolitan area. *Environmental Challenges*, *4*(April), 100192. https://doi.org/10.1016/j.envc.2021.100192

Feng, Q., & Gauthier, P. (2021a). *Untangling Urban Sprawl and Climate Change : A Review of the Literature on Physical Planning and Transportation Drivers*.

Feng, Q., & Gauthier, P. (2021b). Untangling urban sprawl and climate change: A review of the literature on physical planning and transportation drivers. *Atmosphere*, *12*(5). https://doi.org/10.3390/atmos12050547

Feng, Y., Gao, C., Tong, X., Chen, S., Lei, Z., & Wang, J. (2019). Spatial Patterns of Land Surface Temperature and Their Influencing Factors : A Case Study in Suzhou, China.

Fiave, R. E. (2017). *Sekondi-Takoradi as an Oil City*. *37*(1), 61–79.

Filho, W. L., Wolf, F., Castro-d, R., Li, C., Ojeh, V. N., Guti, N., Nagy, G. J., & Savi, S. (2021). *Addressing the Urban Heat Islands Effect : A Cross-Country Assessment of the Role of Green Infrastructure*.

Foody, G. M. (2020). Explaining the unsuitability of the kappa coefficient in the assessment and

comparison of the accuracy of thematic maps obtained by image classification. *Remote Sensing of Environment*, *239*(August 2019), 111630. https://doi.org/10.1016/j.rse.2019.111630

Friedrich, H. K. (2021). *Satellite-Based Human Settlement Datasets Inadequately Detect Refugee Settlements : A Critical Assessment at Thirty Refugee Settlements in Uganda*. 15–17.

Frimpong, B. F. (2015). *Land Use and Cover Changes in the Mampong Municipality of the Ashanti Region*. Kwame Nkrumah University 0f Science and Technology, Kumasi.

Frimpong, B. F. (2022). *Analysis of the relationship between spatial urban expansion and temperature utilising remote sensing and GIS techniques in the Accra and Kumasi Metropolises in Ghana*. https://doi.org/10.26127/BTUOpen-6073

Frimpong, B. F., Koranteng, A., & Opoku, F. S. (2023). Analysis of urban expansion and its impact on temperature utilising remote sensing and GIS techniques in the Accra Metropolis in Ghana (1986–2022). *SN Applied Sciences*, *5*(8). https://doi.org/10.1007/s42452-023-05439-z

Frimpong, K., Eugene, D., & Etten, E. J. Van. (2022). Urban sprawl and microclimate in the Ga East municipality of Ghana. *Heliyon*, *8*(March), 09791. https://doi.org/10.1016/j.heliyon.2022.e09791

García-álvarez, D., Teresa, M., & Olmedo, C. (2022). *Land Use Cover Datasets and Validation Tools* (D. García-Álvarez, M. Paegelow, M. T. C. Olmedo, & J. F. Mas (eds.)). Springer International Publishing. https://doi.org/https://doi.org/10.1007/978-3-030-90998-7

Gašparović, M. (2020). *Urban growth pattern detection and analysis*. 35–48. https://doi.org/10.1016/B978-0-12-820730-7.00003-3

Gaur, S., & Rajendra, S. (2023). A Comprehensive Review on Land Use / Land Cover (LULC) Change Modeling for Urban Development : Current Status and Future Prospects. *MDPI*. https://doi.org/doi.org/10.3390/su15020903

Getu, K., & Bhat, H. G. (2021). Analysis of spatio-temporal dynamics of urban sprawl and growth pattern using geospatial technologies and landscape metrics in Bahir Dar, Northwest Ethiopia. *Land Use Policy*, *109*(August), 105676. https://doi.org/10.1016/j.landusepol.2021.105676

Ghaderi, D., & Rahbani, M. (2020). Shoreline change analysis along the coast of Bandar Abbas city, Iran using remote sensing images. *International Journal Of Coastal, Offshore And Environmental Engineering (ijcoe)*, *5*(2), 51-64.

Ghana Statistcal Service. (2021). *GHANA 2021 POPULATION AND HOUSING CENSUS*. 1–128.

Ghana Statistical Service. (2014). *2010 POPULATIONA & HOUSING CENSUS REPORT*.

Ghosh, A., Das, S., & Pahari, D. P. (2023). Determination of urban sprawl using Shannon Entropy Model in GIS: a study of Bardhaman City of West Bengal, India. In *Urban Commons, Future Smart cities and sustainability* (pp. 207-224). Cham: Springer International Publishing.

Gidey, E., Dikinya, O., Sebego, R., Segosebe, E., & Zenebe, A. (2017). Cellular automata and Markov Chain (CA _ Markov) model-based predictions of future land use and land cover scenarios (2015 – 2033) in Raya , northern Ethiopia. *Modeling Earth Systems and Environment*, *0*(0), 0. https://doi.org/10.1007/s40808-017-0397-6

Glaeser, E. L., & Kahn, M. E. (2004). Sprawl and urban growth. In *Handbook of regional and urban economics* (Vol. 4, pp. 2481-2527). Elsevier.

Golestani, Z., Borna, R., Ali, M., & Hosein, K. (2024). Impact of Urban Expansion on the Formation of Urban Heat Islands in Isfahan , Iran : A Satellite Base Analysis (1990 – 2019). *Journal of Geovisualization and Spatial Analysis*. https://doi.org/10.1007/s41651-024-00189-x

Guha, S. (2017). Dynamic analysis and ecological evaluation of urban heat islands in Raipur city, India. *Journal of Applied Remote Sensing*, *11*(03), 1. https://doi.org/10.1117/1.jrs.11.036020

Guha, S. (2021). Dynamic seasonal analysis on LST-NDVI relationship and ecological health of Raipur City, India. *Ecosystem Health and Sustainability*, *7*(1), 1–13. https://doi.org/10.1080/20964129.2021.1927852

Guha, S. and Govil, H., 2021. Relationship between land surface temperature and normalized difference water index on various land surfaces: A seasonal analysis. *International journal of engineering and geosciences*, *6*(3), pp.165-173.

Guha, S., Govil, H., Dey, A., & Gill, N. (2018). Analytical study of land surface temperature with NDVI and NDBI using Landsat 8 OLI and TIRS data in Florence and Naples city , Italy. *European Journal of Remote Sensing*, *51*(1), 667–678. https://doi.org/10.1080/22797254.2018.1474494

Gyimah, R. R., Kwang, C., Antwi, R. A., Morgan Attua, E., Owusu, A. B., & Doe, E. K. (2023). Trading greens for heated surfaces: Land surface temperature and perceived health risk in Greater Accra Metropolitan Area, Ghana. *Egyptian Journal of Remote Sensing and Space Science*, *26*(4), 861–880. https://doi.org/10.1016/j.ejrs.2023.09.004

Hackman, K. O., Li, X., Asenso-gyambibi, D., Emmanuella, A., & Nelson, I. D. (2020). Analysis of geo-spatiotemporal data using machine learning algorithms and reliability enhancement for urbanization decision support. *International Journal of Digital Earth*, *0*(0), 1–16. https://doi.org/10.1080/17538947.2020.1805036

Haldar, S., & Majumder, A. (2022b). Changing nature of Land surface temperature and transformation of vegetation cover and water bodies in the 2nd largest urban agglomeration of West Bengal , Eastern India. *Remote Sensing Applications: Society and Environment*,

27(August), 100811. https://doi.org/10.1016/j.rsase.2022.100811

Halder, B., & Bandyopadhyay, J. (2021). Evaluating the impact of climate change on urban environment using geospatial technologies in the planning area of Bilaspur , India. *Environmental Challenges*, *5*(September), 100286. https://doi.org/10.1016/j.envc.2021.100286

Han, H., Yang, C., & Song, J. (2015). *Scenario Simulation and the Prediction of Land Use and Land Cover Change in Beijing, China*. 4260–4279. https://doi.org/10.3390/su7044260

Hasan, M. M., Faisal, A.-, & Nipun, W. H. (2019). *Estimation of Urban Heat Islands Effect and Its Impact on Climate Change : A Remote Sensing and GIS-Based Approach in Rajshahi District Estimation of Urban Heat Islands Effect and Its Impact on Climate Change : A Remote Sensing and GIS-Based Approach in R*. *December*.

Hasan, M., Haque, R., & Rahman, M. (2023). Identifying the land use land cover (LULC) changes using remote sensing and GIS approach : A case study at Bhaluka in Mymensingh , Bangladesh. *Case Studies in Chemical and Environmental Engineering*, *7*(December 2022), 100293. https://doi.org/10.1016/j.cscee.2022.100293

Hasan, S. S., Zhen, L., Miah, M. G., Ahamed, T., & Samie, A. (2020). Impact of land use change on ecosystem services: A review. *Environmental Development*, *34*, 100527.

Hatab, A. A., Cavinato, M. E. R., Lindemer, A., & Lagerkvist, C. J. (2019). Urban sprawl, food security and agricultural systems in developing countries: A systematic review of the literature. *Cities*, *94*(May), 129–142. https://doi.org/10.1016/j.cities.2019.06.001

Hidalgo-García, D., & Arco-Díaz, J. (2022). Modeling the Surface Urban Heat Island (SUHI) to study of its relationship with variations in the thermal field and with the indices of land use in the metropolitan area of Granada (Spain). *Sustainable Cities and Society*, *87*(May). https://doi.org/10.1016/j.scs.2022.104166

Huang, J., Lu, X., & Wang, Y. (2024). Spatio − Temporal Changes and Key Driving Factors of Urban Green Space Configuration on Land Surface Temperature. *Mdpi*, 1–16.

Huda, N., & Al, A. (2021b). Assessment of urban thermal field variance index and defining the relationship between land cover and surface temperature in Chattogram city : A remote sensing and statistical approach. *Environmental Challenges*, *4*(April), 100107. https://doi.org/10.1016/j.envc.2021.100107

Hussain, S., Mubeen, M., & Karuppannan, S. (2022). Land use and land cover (LULC) change analysis using TM , ETM + and OLI Landsat images in district of Okara , Punjab , Pakistan. *Physics and Chemistry of the Earth*, *126*(February 2021), 103117. https://doi.org/10.1016/j.pce.2022.103117

Ibrahim, R. E., Taha, L. G., & Shalaby, A. (2019). *Urban Expansion and Pattern Analysis using Shannon ' s Entropy approach in ElMinya*. *13*, 637–646.

Ismael, H.M., 2021. Urban form study: the sprawling city—review of methods of studying urban sprawl. *GeoJournal*, *86*(4), pp.1785-1796.

Issiako, D., Soufiyanou, K., & Ismaila, T. I. (2022). Prospective Mapping of Land Cover and Land Use in The Classified Forest of The Upper Alibori Based on Satellite Imagery. *Journal of Geomatics and Planning*, *June*. https://doi.org/10.14710/geoplanning.8.2.115-126

Jaber, S. M. (2020). Is there a relationship between human population distribution and land surface temperature ? Global perspective in areas with different climatic classifications. *Remote Sensing Applications: Society and Environment*, *20*(June), 100435. https://doi.org/10.1016/j.rsase.2020.100435

Jahan, E., & Rahman, U. (2021). Simulation of future land surface temperature under the scenario of climate change using remote sensing & GIS techniques of northwestern Rajshahi district , Bangladesh. *Environmental Challenges*, *5*(October), 100365. https://doi.org/10.1016/j.envc.2021.100365

Jalayer, S., Sharifi, A., Abbasi-moghadam, D., Tariq, A., & Qin, S. (2022). *Modeling and Predicting Land Use Land Cover Spatiotemporal Changes : A Case Study in Chalus Watershed, Iran*. *July*. https://doi.org/10.1109/JSTARS.2022.3189528

Juma, A., Gudo, A., Deng, J., & Qureshi, A. S. (2022). *Analysis of Spatiotemporal Dynamics of Land Use / Cover Changes in Jubek State , South Sudan*.

Jumari, A. S. K. N., Kasniza, S., Najah, A., Feng, Y., Lin, J., Hoon, C., Lun, K., Sherif, M., & Elshafie, A. (2023). Analysis of urban heat islands with landsat satellite images and GIS in Kuala Lumpur Metropolitan City. *Heliyon*, *9*(8), e18424. https://doi.org/10.1016/j.heliyon.2023.e18424

Kafy, A. Al, Faisal, A. Al, Al Rakib, A., Fattah, M. A., Rahaman, Z. A., & Sattar, G. S. (2022). Impact of vegetation cover loss on surface temperature and carbon emission in a fastest-growing city, Cumilla, Bangladesh. *Building and Environment*, *208*(October 2021), 108573. https://doi.org/10.1016/j.buildenv.2021.108573

Kanani-sadat, Y., Arabsheibani, R., Karimipour, F., & Nasseri, M. (2019). A new approach to fl ood susceptibility assessment in data-scarce and ungauged regions based on GIS-based hybrid multi criteria decision-making method. *Journal of Hydrology*, *572*(January), 17–31. https://doi.org/10.1016/j.jhydrol.2019.02.034

Karakayaci, Zuhal. "The concept of urban sprawl and its causes." *Journal of International Social Research* 9, no. 45 (2016).

Khan, R., Li, H., Basir, M., & Lin, Y. (2022). Monitoring land use land cover changes and its impacts on land surface temperature over Mardan and Charsadda Districts , Khyber Pakhtunkhwa (KP), Pakistan. *Environmental Monitoring and Assessment*, *May*. https://doi.org/10.1007/s10661-022-10072-1

Khwarahm, N. R., Najmaddin, P. R., Ararat, K., & Qader, S. (2021). Past and future prediction of land cover land use change based on earth observation data by the CA – Markov model : a case study from Duhok governorate , Iraq. *Arabian Journal Geosciences, Springer*, 1–14.

Kikon, N., Kumar, D., & Ahmed, S. A. (2023). Quantitative assessment of land surface temperature and vegetation indices on a kilometer grid scale. *Environmental Science and Pollution Research*, *30*(49), 107236–107258. https://doi.org/10.1007/s11356-023-27418-y

Kleemann, J., Inkoom, J. N., Thiel, M., Shankar, S., Lautenbach, S., & Fürst, C. (2017). Peri-urban land use pattern and its relation to land use planning in Ghana, West Africa. *Landscape and Urban Planning*, *165*, 280–294. https://doi.org/10.1016/j.landurbplan.2017.02.004

Kleemann, J., Nana, J., Thiel, M., Shankar, S., Lautenbach, S., & Fürst, C. (2017). Peri-urban land use pattern and its relation to land use planning in. *Landscape and Urban Planning*, *165*, 280–294. https://doi.org/10.1016/j.landurbplan.2017.02.004

Kombate, A., Folega, F., Atakpama, W., Dourma, M., Wala, K., & Goïta, K. (2022). *Characterization of Land-Cover Changes and Forest-Cover Dynamics in Togo between 1985 and 2020 from Landsat Images Using Google Earth Engine*. 1–34.

Korah, A., Koch, J.A. and Wimberly, M.C., 2024. Understanding urban growth modeling in Africa: Dynamics, drivers, and challenges. *Cities*, *146*, p.104734.

Kowalczyk, A. (2020). Theories and concepts related to gastronomy in urban space. *Gastronomy and Urban Space: Changes and Challenges in Geographical Perspective*, 53-90.

Kpienbaareh, D., Appiah, J. O., & Kpienbaareh, D. (2019). A geospatial approach to assessing land change in the built-up landscape of Wa Municipality of Ghana A geospatial approach to assessing land change in the built-up landscape of Wa Municipality of Ghana. *Geografisk Tidsskrift-Danish Journal of Geography*, *119*(2), 121–135. https://doi.org/10.1080/00167223.2019.1587307

Krishnaveni, K. S., & Anil kumar, P. P. (2022). Spatio-temporal dynamics of urban sprawl in a rapidly urbanizing city using machine learning classification. *Geocarto International*, *37*(27), 17403–17434. https://doi.org/10.1080/10106049.2022.2129817

Kuang, W., Liu, Y., Dou, Y., Chi, W., Chen, G., Gao, C., Yang, T., Liu, J., & Zhang, R. (2015). What are hot and what are not in an urban landscape: quantifying and explaining the land surface temperature pattern in Beijing, China. *Landscape Ecology*, *30*(2), 357–373. https://doi.org/10.1007/s10980-014-0128-6

Kumar, P., Tokas, J., Kumar, N., Lal, M., & Singal, H. R. (2018). Climate change consequences and its impact on agriculture and food security. *International Journal of chemical studies*, *6*(6), 124-133.

Kumi-boateng, B., & Stemn, E. (2015b). Effect of Urban Growth on Urban Thermal Environment : A Case Study of Sekondi-Takoradi Metropolis of Ghana. *Journal of*

ENVIRONMENT AND EARTH SCIENCE, *5*(2), 32–42.

Kuria, E., Kimani, S., & Mindila, A. (2019). A framework for web GIS development: a review. *International Journal of Computer Applications*, *178*(16), 6-10.

Kursah, M. B. (2023). Urban Climate Satellite image analysis of thermal comfort for a sustainable urban ecology of Winneba , Ghana. *Urban Climate*, *52*(January), 101685. https://doi.org/10.1016/j.uclim.2023.101685

Kwame, B., Ahenkorah, I., Ewusi, A., & Bani, E. (2021). Assessment of flood prone zones in the Tarkwa mining area of Ghana using a GIS-based approach. *Environmental Challenges*, *3*(January), 100028. https://doi.org/10.1016/j.envc.2021.100028

Larbi, I. (2023). Land use-land cover change in the Tano basin , Ghana and the implications on sustainable development goals. *Heliyon*, *9*(4), e14859. https://doi.org/10.1016/j.heliyon.2023.e14859

Leal Filho, Walter, Franziska Wolf, Ricardo Castro-Díaz, Chunlan Li, Vincent N. Ojeh, Nestor Gutiérrez, Gustavo J. Nagy et al. "Addressing the urban heat islands effect: A cross-country assessment of the role of green infrastructure." *Sustainability* 13, no. 2 (2021): 753.

Lima, G. N. De, Orlando, V., & Rueda, M. (2018). The urban growth of the metropolitan area of Sao Paulo and its impact on the climate. *Weather and Climate Extremes*, *21*(January), 17–26. https://doi.org/10.1016/j.wace.2018.05.002

Liu, F., Zhang, X., & Murayama, Y. (2020). *Impacts of Land Cover / Use on the Urban Thermal Environment : A Comparative Study of 10 Megacities in China*. 1–31.

Lu, Q., Chang, N., Joyce, J., Chen, A. S., Savic, D. A., & Djordjevic, S. (2017). *Exploring the potential climate change impact on urban growth in London by a cellular automata-based Markov chain model*. *November*. https://doi.org/10.1016/j.compenvurbsys.2017.11.006

M. Guha, S., Govil, H., Dey, A., & Gill, N. (2018). Analytical study of land surface temperature with NDVI and NDBI using Landsat 8 OLI and TIRS data in Florence and Naples city , Italy. *European Journal of Remote Sensing*, *51*(1), 667–678. https://doi.org/10.1080/22797254.2018.1474494

Manesha, E. P. P., Jayasinghe, A., & Nawod, H. (2021). Measuring urban sprawl of small and medium towns using GIS and remote sensing techniques : A case study of Sri Lanka. *The Egyptian Journal of Remote Sensing and Space Sciences*, *24*(3), 1051–1060. https://doi.org/10.1016/j.ejrs.2021.11.001

Mansour, K., Alkhuzamy, M., Hashim, S., & Effat, H. (2022a). Impact of anthropogenic activities on urban heat islands in major cities of El-Minya Governorate, Egypt. *The Egyptian Journal of Remote Sensing and Space Sciences*, *25*(2), 609–620. https://doi.org/10.1016/j.ejrs.2022.03.014

Mensah, C. A., Eshun, J. K., Asamoah, Y., & Ofori, E. (2019). Changing land use / cover of

Ghana ’ s oil city (Sekondi-Takoradi Metropolis): implications for sustainable urban development. *International Journal of Urban Sustainable Development*, *11*(2), 223–233. https://doi.org/10.1080/19463138.2019.1615492

Mensah, C. A., Gough, K. V., & Simon, D. (2018a). Urban green spaces in growing oil cities: The case of Sekondi-Takoradi Metropolis, Ghana. *International Development Planning Review*, *40*(4), 371–395. https://doi.org/10.3828/idpr.2018.16

Mirchooli, F., Hamidreza, S., Prof, S., & Darvishan, A. K. (2020). Analyzing spatial variations of relationships between Land Surface Temperature and some remotely sensed indices in different land uses. *Remote Sensing Applications: Society and Environment*, *19*(February), 100359. https://doi.org/10.1016/j.rsase.2020.100359

Mohammad, P., Goswami, A., Chauhan, S., & Nayak, S. (2022). Urban Climate Machine learning algorithm based prediction of land use land cover and land surface temperature changes to characterize the surface urban heat island phenomena over Ahmedabad city , India. *Urban Climate*, *42*(July 2021), 101116. https://doi.org/10.1016/j.uclim.2022.101116

Mohammadian, H., Tavakoli, J., & Khani, H. (2017). Monitoring land use change and measuring urban sprawl based on its spatial forms The case of Qom city. *The Egyptian Journal of Remote Sensing and Space Sciences*, *20*(1), 103–116. https://doi.org/10.1016/j.ejrs.2016.08.002

Mohan, M. (2023). Remote Sensing of Urban Development and Environmental Landscape: a Study of Green Cover Lungs of Delhi and Surrounding City Regions. *The International Archives of the Photogrammetry, Remote Sensing and Spatial Information Sciences*, *48*, 463-470.

Mohanta, K., & Sharma, L. K. (2017). Assessing the impacts of urbanization on the thermal environment of Ranchi City (India) using geospatial technology. *Remote Sensing Applications: Society and Environment*, *8*(August 2016), 54–63. https://doi.org/10.1016/j.rsase.2017.07.008

Moisa, B. M., & Gemeda, O. D. (2022). Assessment of urban thermal fi eld variance index and thermal comfort level of Addis Ababa metropolitan city , Ethiopia. *Heliyon*, *8*(August), e10185. https://doi.org/10.1016/j.heliyon.2022.e10185

Mondal, A., Guha, S., & Kundu, S. (2021). Dynamic status of land surface temperature and spectral indices in Imphal city, India from 1991 to 2021. *Geomatics, Natural Hazards and Risk*, *12*(1), 3265–3286. https://doi.org/10.1080/19475705.2021.2008023

Mondal, S., & Gavsker, K. K. (2024). Unraveling the spatio-temporal trajectories of urban growth in Asansol city , West Bengal : A geospatial exploration of the emerging urban landscape. *Remote Sensing Applications: Society and Environment*, *36*(August), 101386. https://doi.org/10.1016/j.rsase.2024.101386

Mukherjee, F., & Singh, D. (2020). Assessing Land Use – Land Cover Change and Its Impact on Land Surface Temperature Using LANDSAT Data : A Comparison of Two Urban Areas in

India. *Earth Systems and Environment*, *0123456789*. https://doi.org/10.1007/s41748-020-00155-9

Naim, N., & Kafy, A. (2021). Assessment of urban thermal field variance index and defining the relationship between land cover and surface temperature in Chattogram city : A remote sensing and statistical approach. *Environmental Challenges*, *4*(April), 100107. https://doi.org/10.1016/j.envc.2021.100107

Nath, D., Chakraborti, S., Saha, G., Banerjee, A., & Singh, D. (2020). Analysing the dynamic relationship of land surface temperature and landuse pattern : A city level analysis of two climatic regions in India. *City and Environment Interactions*, *8*, 100046. https://doi.org/10.1016/j.cacint.2020.100046

Nath, N., Sahariah, D., Meraj, G., Debnath, J., & Kumar, P. (2023). *Land Use and Land Cover Change Monitoring and Prediction of a UNESCO World Heritage Site : Kaziranga Eco-Sensitive*.

Negesse, D. M., Hishe, S., & Getahun, K. (2024). Urban Land Use Land Cover Change. *Discover Environment*, 175–189. https://doi.org/10.1007/978-981-10-5927-8_9

Nickerson, C., 2024. Concentric Zone Model by Ernest Burgess. *Retrieved on*, *3*(04), p.2024.

Nieves, J. J., Bondarenko, M., Sorichetta, A., Steele, J. E., Kerr, D., Carioli, A., Stevens, F. R., Gaughan, A. E., & Tatem, A. J. (2020). Predicting near-future built-settlement expansion using relative changes in small area populations. *Remote Sensing*, *12*(10), 1–26. https://doi.org/10.3390/rs12101545

Nimish, G., Bharath, H. A., & Lalitha, A. (2020). Exploring temperature indices by deriving relationship between land surface temperature and urban landscape. *Remote Sensing Applications: Society and Environment*, *18*(November 2019), 100299. https://doi.org/10.1016/j.rsase.2020.100299

Njoku, E.A. and Tenenbaum, D.E., 2022. Quantitative assessment of the relationship between land use/land cover (LULC), topographic elevation and land surface temperature (LST) in Ilorin, Nigeria. *Remote Sensing Applications: Society and Environment*, *27*, p.100780.

Nyamekye, C., Kwofie, S., Ghansah, B., Agyapong, E., & Appiah, L. (2020a). Assessing urban growth in Ghana using machine learning and intensity analysis : A case study of the New Juaben Municipality. *Land Use Policy*, *99*(August), 105057. https://doi.org/10.1016/j.landusepol.2020.105057

Nyamekye, C., Kwofie, S., Ghansah, B., Agyapong, E., & Appiah, L. (2020b). Assessing urban growth in Ghana using machine learning and intensity analysis : A case study of the New Juaben Municipality. *Land Use Policy*, *99*(September), 105057. https://doi.org/10.1016/j.landusepol.2020.105057

Obeng, K., Forkuo, E. K., Asare, Y. M., Opoku, P., & Obeng, A. S. (2023). *Land Use Land Cover Changes in the Densu River Basin of Ghana From 1991 To 2020*. *41*(1), 1–18.

Obodai, J., Amaning, K., Nii, S., & Lumor, M. (2019). Land use / land cover dynamics using landsat data in a gold mining basin-the. *Remote Sensing Applications: Society and Environment*, *13*(October 2018), 247–256. https://doi.org/10.1016/j.rsase.2018.10.007

Offong, S.E., 2020. Rural Urbanization in Itu Local Government Area of Akwa Ibom State: Antecedents, Requirements, and Prospects. *Ibom Journal of Social Issues*, *10*(1), pp.69-69.

Ofori, P. (2020). *HOUSING POVERTY IN DEVELOPING COUNTRIES : CHALLENGES AND IMPLICATIONS FOR DECENT ACCOMMODATION IN SWEDRU, GHANA*. https://doi.org/http://dx.doi. org/10.18820/24150487/as27i2.3

Osawe, A. I., & Ojeifo, M. O. (2019). *Unregulated Urbanization and Challenge of Environmental Security in Africa*. *4*, 1–10.

Osei, J. D., Damoah-Afari, P., Yevugah, L. L., Mensah, C., & Prempeh, N. A. (2023). Impact of land use and land cover dynamics on urban heat island in the Sunyani Municipality using satellite remote sensing. *Journal of the Ghana Institution of Engineering (JGhIE)*, *23*(2), 6–16. https://doi.org/10.56049/jghie.v23i2.61

Østby, G. (2016). Rural–urban migration, inequality and urban social disorder: Evidence from African and Asian cities. *Conflict Management and Peace Science*, *33*(5), 491–515. https://doi.org/10.1177/0738894215581315

Othow, O. O., Gebre, S. L., & Gemeda, D. (2017). *Analyzing the Rate of Land Use and Land Cover Change and Determining the Journal of Remote Sensing & GIS Analyzing the Rate of Land Use and Land Cover Change and Determining the Causes of Forest Cover Change in Gog District , Gambella Regional*. *January*. https://doi.org/10.4172/2469-4134.1000219

Owusu, G. (2015). Decentralized development planning and fragmentation of metropolitan regions: The case of the Greater Accra Metropolitan Area, Ghana. *Ghana Journal of Geography*, *7*(1), 1-24.

Owusu, G., & Yankson, P. W. (2017). Urbanization in Ghana. *The economy of Ghana Sixty years after independence*, 23-38.

Owusu, G., & Yankson, P. W. (2017). Urbanization in Ghana. *The economy of Ghana Sixty years after independence*, 23-38.

Oztruk, D. (2017). ASSESSMENT OF URBAN SPRAWL USING SHANNON'S ENTROPY AND FRACTAL ANALYSIS : A CASE STUDY OF ATAKUM , ILKADIM AND CANIK (SAMSUN, TURKEY). *JOURNAL OF ENVIRONMENTAL ENGINEERING AND LANDSCAPE MANAGEMENT*, *25*(03), 264–276. https://doi.org/10.3846/16486897.2012.721784

Pabi, O., Egyir, S., & Attua, E. M. (2021). Flood hazard response to scenarios of rainfall dynamics and land use and land cover change in an urbanized river basin in Accra, Ghana. *City and Environment Interactions*, *12*, 100075. https://doi.org/10.1016/j.cacint.2021.100075

Phong, L. T. (2004). *Analysis of Forest Cover Dynamics and Their Driving Forces in Bach Ma National Park and Its Buffer Zone Using Remote Sensing and GIS*. International Institute fro Geo-information and Earth Observation, Enschede, The Netherlands.

Piracha, A., & Chaudhary, M. T. (2022). Urban air pollution, urban heat island and human health: a review of the literature. *Sustainability*, *14*(15), 9234.

Pradhan, B. (2017). *Spatial Modeling and Assessment of Urban Form*.

Pradhan, R.P., Arvin, M.B. and Nair, M., 2021. Urbanization, transportation infrastructure, ICT, and economic growth: A temporal causal analysis. *Cities*, *115*, p.103213.

Rahaman, Z. A., Kafy, A. Al, Saha, M., Rahim, A. A., Almulhim, A. I., Rahaman, S. N., Fattah, M. A., Rahman, M. T., S, K., Faisal, A. Al, & Al Rakib, A. (2022). Assessing the impacts of vegetation cover loss on surface temperature, urban heat island and carbon emission in Penang city, Malaysia. In *Building and Environment* (Vol. 222). https://doi.org/10.1016/j.buildenv.2022.109335

Rainey, J. L., Brody, S. D., Galloway, G. E., Highfield, W. E., Rainey, J. L., Brody, S. D., Galloway, G. E., & Highfield, W. E. (2021). Assessment of the growing threat of urban flooding : a case study of a national survey Assessment of the growing threat of urban flooding : a case study of a national survey ABSTRACT. *Urban Water Journal*, *00*(00), 1–7. https://doi.org/10.1080/1573062X.2021.1893356

Ramachandra, T. V, Bharath, A. H., & Sowmyashree, M. V. (2015). Monitoring urbanization and its implications in a mega city from space : Spatiotemporal patterns and its indicators. *Journal of Environmental Management*, *148*, 67–81. https://doi.org/10.1016/j.jenvman.2014.02.015

Ramadan, M. S., & Effat, H. A. (2021). Geospatial modeling for a sustainable urban development zoning map using AHP in Ismailia Governorate , Egypt. *The Egyptian Journal of Remote Sensing and Space Sciences*, *24*(2), 191–202. https://doi.org/10.1016/j.ejrs.2021.01.003

Rami, S., Alhaddad, M., Al-fugara, A., Al-hawwari, L., Al-hawwari, M., Omoush, A., & Arar, M. (2023). Modeling the impact of urban land cover features and changes on the land surface temperature (LST): The case of Jordan. *Ain Shams Engineering Journal*, *May*, 102359. https://doi.org/10.1016/j.asej.2023.102359

Rana, S., & Sarkar, S. (2021). Prediction of urban expansion by using land cover change detection approach. *Heliyon*, *7*(August), e08437. https://doi.org/10.1016/j.heliyon.2021.e08437

Rangarajan, S. (2022). *Predicting the Future Land Use and Land Cover Changes for Bhavani Basin , Tamil Nadu , India Using QGIS MOLUSCE Plugin*.

Renard, F., Alonso, L., Fitts, Y., Hadjiosif, A., Comby, J., Lyon, M., Cnrs, U. M. R., & City, E. (2019). *Evaluation of the Effect of Urban Redevelopment on Surface Urban Heat Islands*.

https://doi.org/10.3390/rs11030299

Roberts, N. (2019). How humans changed the face of Earth. *Science*, *365*(6456), 865-866.

Roy, B., & Kasemi, N. (2021). Monitoring urban growth dynamics using remote sensing and GIS techniques of Raiganj Urban Agglomeration , India. *The Egyptian Journal of Remote Sensing and Space Sciences*, *24*(2), 221–230. https://doi.org/10.1016/j.ejrs.2021.02.001

Roy, B., & Kasemi, N. (2022). Quantification of urban expansion in Siliguri urban agglomeration (UA): a model-based approach. *GeoJournal*, *87*(March 2022), 869–884. https://doi.org/10.1007/s10708-022-10628-1

Roy, B., Bari, E., Jahan, N., & Afrin, S. (2021). Comparison of temporal changes in urban settlements and land surface temperature in Rangpur and Gazipur Sadar , Bangladesh after the establishment of city corporation. *Remote Sensing Applications: Society and Environment*, *23*(April), 100587. https://doi.org/10.1016/j.rsase.2021.100587

Rui, Y. (2013). *Urban Growth Modeling Based on Land-use Changes and Road Network Expansion*.

Saha, S., Saha, A., Das, M., Saha, A., Sarkar, R., & Das, A. (2021b). Analyzing spatial relationship between land use / land cover (LULC) and land surface temperature (LST) of three urban agglomerations (UAs) of Eastern India. *Remote Sensing Applications: Society and Environment*, *22*(April), 100507. https://doi.org/10.1016/j.rsase.2021.100507

Sahak, A. S. (2022). *Evaluating the Impact of Land Use / Land Cover Changes on the Surface Urban Heat Island intensity : The case study of Kabul city , Afghanistan*.

Saleem, H., Ahmed, R., Mushtaq, S., & Saleem, S. (2024). Remote sensing-based analysis of land use , land cover , and land surface temperature changes in Jammu District , India. *International Journal of River Basin Management*, *March*, 1–16. https://doi.org/10.1080/15715124.2024.2327493

Salimi, M., & Al-ghamdi, S. G. (2020). Climate change impacts on critical urban infrastructure and urban resiliency strategies for the Middle East. *Sustainable Cities and Society*, *54*(November 2019), 101948. https://doi.org/10.1016/j.scs.2019.101948

Saraiva, M. and Pinho, P., 2017. Spatial modelling of commercial spaces in medium-sized cities. *GeoJournal*, *82*(3), pp.433-454.

Sarica, G. M., & Zhu, T. (2021). *Spatio-temporal dynamics of flood exposure in Shenzhen from present to future*. *48*(5), 1011–1024. https://doi.org/10.1177/2399808321991540

Sarif, O., Rimal, B., & Stork, E. N. (2020). Assessment of Changes in Land Use / Land Cover and Land Surface Temperatures and Their Impact on Surface Urban Heat Island Phenomena in the Kathmandu Valley (1988 – 2018). *Mdpi*, 29.

Satterthwaite, D., Archer, D., Colenbrander, S., Dodman, D., Hardoy, J., Mitlin, D., & Patel, S.

(2020). Building Resilience to Climate Change in Informal Settlements. *One Earth*, *2*(2), 143–156. https://doi.org/10.1016/j.oneear.2020.02.002

Satya, B. A. (2020). *Future land use land cover scenario simulation using open source GIS for the city of Warangal , Telangana , India*. *2011*.

Satya, B. A., Shashi, M., & Pratap, D. (2020). Future land use land cover scenario simulation using open source GIS for the city of Warangal , Telangana , India. *Applied Geomatics, Springer*, *2011*. https://doi.org/https://doi.org/10.1007/s12518-020-00298-4

Sekertekin, A., & Bonafoni, S. (2020). Land Surface Temperature Retrieval from Landsat 5 , 7 , and 8 over Rural Areas : Assessment of Di ff erent Retrieval Algorithms and Emissivity Models and Toolbox Implementation. *Remote Sensing*.

Service, G. S. (2014). *2010 Population and housing census report, Ghana Statistical Service*.

Service, G. S. (2021). *Ghana 2021 Population and Housing Census*.

Shamsudeen, M., Padmanaban, R., Cabral, P., & Morgado, P. (2022). Spatio-Temporal Analysis of the Impact of Landscape Changes on Vegetation and Land Surface Temperature over Tamil Nadu. *MDPI*, *3*, 614–638.

Shao, Z., Sumari, N. S., Portnov, A., Ujoh, F., & Mandela, P. J. (2021). Geo-spatial Information Science Urban sprawl and its impact on sustainable urban development : a combination of remote sensing and social media data. *Geo-Spatial Information Science*, *24*(2), 241–255. https://doi.org/10.1080/10095020.2020.1787800

Shen, C., Hou, H., Zheng, Y., Murayama, Y., Wang, R., & Hu, T. (2022). Prediction of the future urban heat island intensity and distribution based on landscape composition and configuration: A case study in Hangzhou. *Sustainable Cities and Society*, *83*(2318), 103992. https://doi.org/10.1016/j.scs.2022.103992

Shen, C., Hou, H., Zheng, Y., Murayama, Y., Wang, R., & Hu, T. (2022). Prediction of the future urban heat island intensity and distribution based on landscape composition and configuration: A case study in Hangzhou. *Sustainable Cities and Society*, *83*(2318), 103992. https://doi.org/10.1016/j.scs.2022.103992

Shikary, C., & Rudra, S. (2020). Measuring Urban Land Use Change and Sprawl Using Geospatial Techniques : Measuring Urban Land Use Change and Sprawl Using Geospatial Techniques : A Study on Purulia Municipality , West Bengal , India. *Journal of the Indian Society of Remote Sensing*, *November*. https://doi.org/10.1007/s12524-020-01212-6

Shu, X., Han, H., Huang, C. and Li, L., 2020. Defining functional polycentricity from a geographical perspective. *Geographical Analysis*, *52*(2), pp.169-189.

Siddique, A. M., Boqing, F., & Dongyun, L. (2023). Modeling the Impact and Risk Assessment of Urbanization on Urban Heat Island and Thermal Comfort Level of Beijing City, China (2005–2020). *Sustainability (Switzerland)*, *15*(7). https://doi.org/10.3390/su15076043

Siddiqui, A., Siddiqui, A., Maithani, S., Jha, A. K., Kumar, P., & Srivastav, S. K. (2018). Urban growth dynamics of an Indian metropolitan using CA Markov and Logistic Regression. *The Egyptian Journal of Remote Sensing and Space Sciences*, *21*(3), 229–236. https://doi.org/10.1016/j.ejrs.2017.11.006

Sinha, S.K., 2018. Causes of urban sprawl: A comparative study of developed and developing world cities. *Res. Rev. Int. J. Multidiscip*, *3*, pp.1-5.

Song, Z., Yang, H., Huang, X., Yu, W., Huang, J., & Ma, M. (2021). The spatiotemporal pattern and influencing factors of land surface temperature change in China from 2003 to 2019. *International Journal of Applied Earth Observation and Geoinformation*, *104*, 102537. https://doi.org/10.1016/j.jag.2021.102537

Songsore, J. (2020). The urban transition in Ghana: Urbanization, national development and poverty reduction. *Ghana Social Science Journal*, *17*(2), 57-57.

Stemn, E., & Agyapong, E. (2014). *Assessment of Urban Expansion in the Sekondi-Takoradi Metropolis of Ghana Using Remote-Sensing and GIS Approach*. *3*(8).

Stemn, E., & Kumi, B. (2020). Modelling of land surface temperature changes as determinant of urban heat island and risk of heat - related conditions in the Wassa West Mining Area of Ghana. *Modeling Earth Systems and Environment*, *0123456789*. https://doi.org/10.1007/s40808-020-00786-x

Steurer, M., & Bayr, C. (2020a). Measuring urban sprawl using land use data. *Land Use Policy*, *97*(May), 104799. https://doi.org/10.1016/j.landusepol.2020.104799

Steurer, M., & Bayr, C. (2020b). Measuring urban sprawl using land use data. *Land Use Policy*, *97*(December 2019), 104799. https://doi.org/10.1016/j.landusepol.2020.104799

STMA. (2022). *SEKONDI-TAKORADI METROPOLITAN ASSEMBLY MEDIUM-TERM DEVELOPMENT PLAN*. *June 2021*.

Sui, C. and Lu, W., 2021. Study on the urban fringe based on the expansion–shrinking dynamic pattern. *Sustainability*, *13*(10), p.5718.

Sumari, S. N., Cobbinah, B. P., Ujoh, F., & Xu, G. (2020). On the absurdity of rapid urbanization : Spatio-temporal analysis of land-use changes in Morogoro , Tanzania. *Cities*, *107*(July), 102876. https://doi.org/10.1016/j.cities.2020.102876

Surawar, M., & Kotharkar, R. (2017). *Assessment of Urban Heat Island through Remote Sensing in Nagpur Urban Area Using Landsat 7 ETM + Satellite Images*. *11*(7), 868–874.

Surya, B., Salim, A., Hernita, H., Suriana, S., Menne, F., & Rasyidi, S. E. (2021). Land Use Change, Urban Agglomeration, and Urban Sprawl: A Sustainable Development Perspective of Makassar City, Indonesia. *MDPI*.

Talkhabi, H., & Jafarpour, K. (2022). Ecological Informatics Spatial and temporal population

change in the Tehran Metropolitan Region and its consequences on urban decline and sprawl. *Ecological Informatics*, *70*(March), 101731. https://doi.org/10.1016/j.ecoinf.2022.101731

Taloor, A. K., Parsad, G., Jabeen, S. F., Sharma, M., Choudhary, R., & Kumar, A. (2024). Analytical study of land surface temperature for evaluation of UHI and UHS in the city of Chandigarh India. *Remote Sensing Applications: Society and Environment*, *35*(April), 101206. https://doi.org/10.1016/j.rsase.2024.101206

Taloor, A.K., Manhas, D.S. and Kothyari, G.C., 2021. Retrieval of land surface temperature, normalized difference moisture index, normalized difference water index of the Ravi basin using Landsat data. *Applied Computing and Geosciences*, *9*, p.100051

Tarawally, M., Wenbo, X., Weiming, H., Darlington, T., & Biniyam, M. (2019). Land use / land cover change evaluation using land change modeller : A comparative analysis between two main cities in Sierra Leone. *Remote Sensing Applications: Society and Environment*, *16*(September), 100262. https://doi.org/10.1016/j.rsase.2019.100262

Tariq, A., Mumtaz, F., Zeng, X., Yousuf, M., & Baloch, J. (2022). Spatio-temporal variation of seasonal heat islands mapping of Pakistan during 2000 – 2019 , using day-time and night-time land surface temperatures MODIS and meteorological stations data. *Remote Sensing Applications: Society and Environment*, *27*(May), 100779. https://doi.org/10.1016/j.rsase.2022.100779

Tariq, A., Yan, J., & Mumtaz, F. (2022). Land change modeler and CA-Markov chain analysis for land use land cover change using satellite data of Peshawar , Pakistan. *Physics and Chemistry of the Earth*, *128*(October), 103286. https://doi.org/10.1016/j.pce.2022.103286

Tasantab, J. (2019). *Beyond the plan : How land use control practices influence flood risk in Sekondi-Takoradi*. 1–9.

Tassi, A., & Vizzari, M. (2020). Object-oriented lulc classification in google earth engine combining snic, glcm, and machine learning algorithms. *Remote Sensing*, *12*(22), 1–17. https://doi.org/10.3390/rs12223776

Thambawita, T. K. C. N., Munasinghe, D. S., & Yapa, L. K. K. (2023). Identification of Urban Heat Island Effect on Land Use Land Cover Changes. *Journal of Geospatial Surveying*, *3*(2), 43–53. https://doi.org/10.4038/jgs.v3i2.50

Thapa, S. (2017). *EXPLORING THE IMPACT OF URBAN GROWTH ON LAND SURFACE TEMPERATURE OF KATHMANDU VALLEY , NEPAL*.

Tian, L., Tao, Y., Li, M., Qian, C., Li, T., Wu, Y., & Ren, F. (2023). Prediction of Land Surface Temperature Considering Future Land Use Change Effects under Climate Change Scenarios in Nanjing City, China. *Remote Sensing*, *15*(11). https://doi.org/10.3390/rs15112914

Traore, M., Son, M., Rasul, A., & Balew, A. (2021). Assessment of land use / land cover changes and their impacts on land surface temperature in Bangui (the capital of Central

African Republic *Environmental Challenges*, *4*(April), 100114. https://doi.org/10.1016/j.envc.2021.100114

Ullah, N., Siddique, A. M., Ding, M., Grigoryan, S., Zhang, T., & Hu, Y. (2022). Spatiotemporal Impact of Urbanization on Urban Heat Island. *Buildings, MPDI*, 21–23.

Ullah, S., Abbas, M., & Qiao, X. (2024). Impact assessment of land-use alteration on land surface temperature in Kabul using machine learning algorithm. *Journal of Spatial Science*, *00*(00), 1–23. https://doi.org/10.1080/14498596.2024.2364283

Varghese, N., & Singh, N. P. (2016). Land Use Policy Linkages between land use changes , desertification and human development in the Thar Desert Region of India. *Land Use Policy*, *51*, 18–25. https://doi.org/10.1016/j.landusepol.2015.11.001

Verma, S., Agrawal, S., Dutta, K., Temperature, L. S., & Entropy, S. (2021). *SATELLITE IMAGERY DRIVEN ASSESSMENT OF LAND USE LAND COVER , URBANIZATION AND SURFACE TEMPERATURE PATTERN DYNAMICS OVER*. *XLVI*(November), 17–19.

Viana, C. M., Oliveira, S., Oliveira, S. C., & Rocha, J. (2019). Land Use/Land Cover Change Detection and Urban Sprawl Analysis. In *Spatial Modeling in GIS and R for Earth and Environmental Sciences*. Elsevier Inc. https://doi.org/10.1016/b978-0-12-815226-3.00029-6

Viju, T., Firoz, M., & Krishnan, S. (2023). *Assessment of Land Surface Temperature Variations and Implications of Land Use/Land Cover Changes: A Case of Malappuram Urban Agglomeration Region, Kerala, India*. *10*(3), 13–36. https://doi.org/10.11113/ijbes.v10.n3.1102

Vinh, T., & Nguyen, D. (2019). *Transcalar Urban Governance : Planning and Development in the " Oil-City " of Sekondi-Takoradi , Ghana. September*.

Wahyu, S. A., Buchori, I., & Rudiarto, I. (2019). The spatio-temporal trends of urban growth and surface urban heat islands over two decades in the Semarang Metropolitan Region. *Sustainable Cities and Society*, *46*(July 2018), 101432. https://doi.org/10.1016/j.scs.2019.101432

Wangyel, S., Munkhnasan, L., & Lee, W. (2021). *Land use and land cover change detection and prediction in Bhutan ' s high altitude city of Thimphu , using cellular automata and Markov chain*. *2*(November 2020). https://doi.org/10.1016/j.envc.2020.100017

Wei, Y. D., & Ewing, R. (2018). Urban expansion, sprawl and inequality. *Landscape and urban planning*, *177*, 259-265.

Wemegah, C. S., Yamba, E. I., Aryee, J. N. A., Sam, F., & Amekudzi, L. K. (2020). Assessment of urban heat island warming in the greater accra region. *Scientific African*, *8*, e00426. https://doi.org/10.1016/j.sciaf.2020.e00426

Wondmagegn, B. Y., Xiang, J., Williams, S., Pisaniello, D., & Bi, P. (2019). What do we know about the healthcare costs of extreme heat exposure? A comprehensive literature review. *Science of the total environment*, *657*, 608-618.

Worku, G., Teferi, E., & Bantider, A. (2021). Assessing the effects of vegetation change on urban land surface temperature using remote sensing data : The case of Addis Ababa city , Ethiopia. *Remote Sensing Applications: Society and Environment*, *22*(April), 100520. https://doi.org/10.1016/j.rsase.2021.100520

Xiang, X., Qiu, C., Hu, J., Shi, Y., Wang, Y., Schmitt, M., & Taubenb, H. (2022). *The urban morphology on our planet – Global perspectives from space*. *269*(September 2021), 1–11. https://doi.org/10.1016/j.rse.2021.112794

Yankson, P. W. K., Gough, K. V, Esson, J., & Ebenezer, F. (2017). Spatial and social transformations in a secondary city : the role of mobility in Sekondi-Takoradi , Ghana. *Geografisk Tidsskrift-Danish Journal of Geography*, *7223*, 1–11. https://doi.org/10.1080/00167223.2017.1343672

Younes, A., Ahmad, A., Hanjagi, A. D., & Nair, A. M. (2023). *Understanding Dynamics of Land Use & Land Cover Change Using GIS & Change Detection Techniques in Tartous , Syria*. *14*(3), 20–41. https://doi.org/10.48088/ejg.a.you.14.3.020.041

Yu, Z., Yao, Y., Yang, G., Wang, X. and Vejre, H., 2019. Spatiotemporal patterns and characteristics of remotely sensed region heat islands during the rapid urbanization (1995–2015) of Southern China. *Science of the Total Environment*, *674*, pp.242-254.

Zaki, A., Buchori, I., Wahyu, A., & Liu, Y. (2022). An object-based image analysis in QGIS for image classification and assessment of coastal spatial planning q. *The Egyptian Journal of Remote Sensing and Space Sciences*, *25*(2), 349–359. https://doi.org/10.1016/j.ejrs.2022.03.002

Zhao, M., Cai, H., Qiao, Z., & Xu, X. (2016). Influence of urban expansion on the urban heat island effect in Shanghai. *International Journal of Geographical Information Science*, *30*(12), 2421–2441. https://doi.org/10.1080/13658816.2016.1178389

Zhou, M., Lu, L., Guo, H., Weng, Q., Cao, S., Zhang, S., & Li, Q. (2021). *Urban Sprawl and Changes in Land-Use Efficiency in the Beijing – Tianjin – Hebei Region , China from 2000 to 2020 : A Spatiotemporal Analysis Using Earth Observation Data*.

APPENDICES

Appendix 1: UTFVI maps

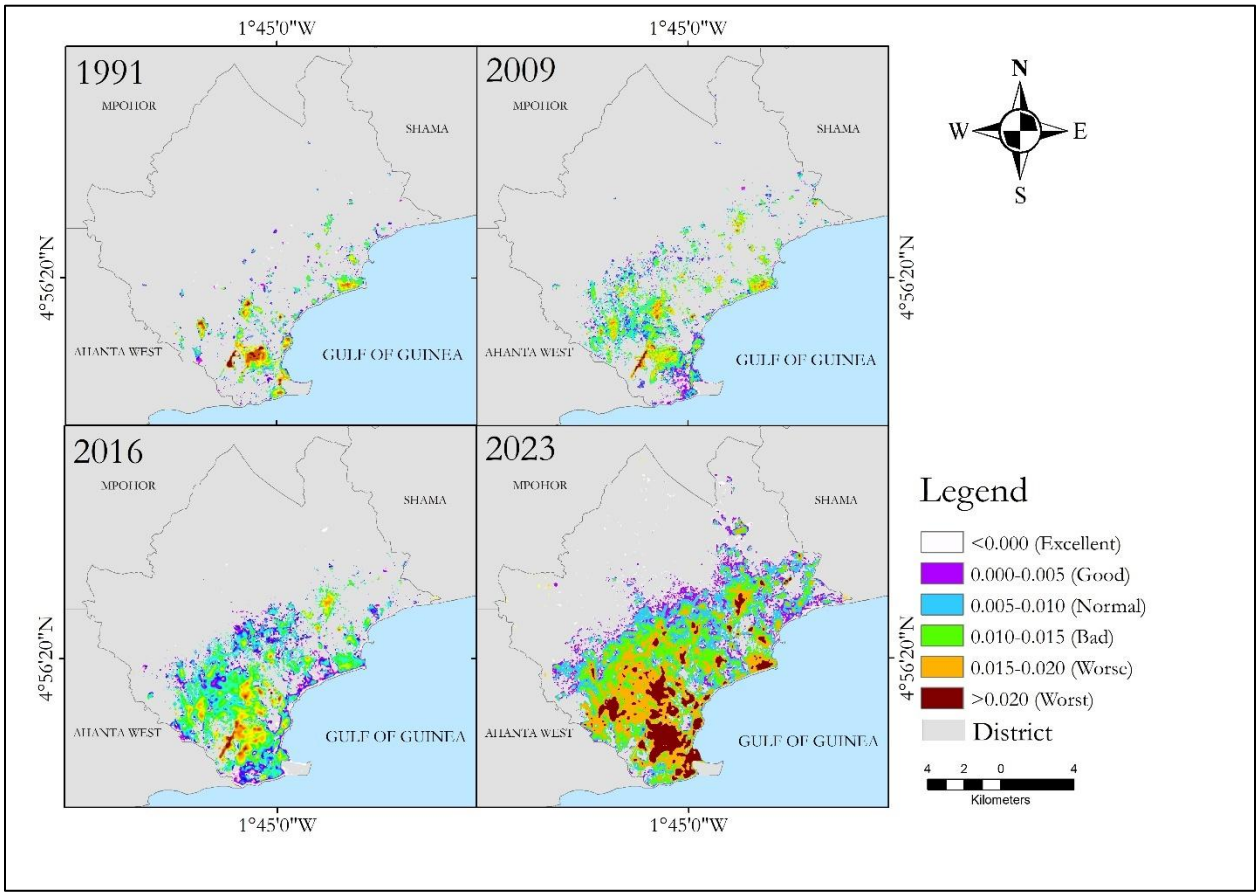

Appendix 2a: Summary of OLS Results from 1991 to 2023 - Model Variables

Variable	Coefficient	StdError	t-Statistic	Probability	Robust_SE	Robust_t	Robust_Pr	VIF
$Intercept_{1991}$	26.60	0.00	5910.16	0.00*	0.01	2407.44	0.00*	----
$NDBI_{1991}$	5.78	0.02	300.55	0.00*	0.04	148.61	0.00*	2.43
$NDVI_{1991}$	-4.60	0.02	-219.50	0.00*	0.05	-87.78	0.00*	2.43
$Intercept_{2009}$	23.40	0.00	12378.34	0.00*	0.00	9962.22	0.00*	----
$NDBI_{2009}$	10.66	0.02	431.30	0.00*	0.04	244.43	0.00*	3.28
$NDVI_{2009}$	-1.37	0.03	-50.66	0.00*	0.05	-26.22	0.00*	3.28
$Intercept_{2016}$	23.86	0.00	13307.40	0.00*	0.00	9657.20	0.00*	----
$NDBI_{2016}$	9.06	0.03	358.02	0.00*	0.06	156.34	0.00*	4.55
$NDVI_{2016}$	-1.41	0.02	56.96	0.00*	0.06	-23.16	0.00*	4.55
$Intercept_{2023}$	29.83	0.01	2864.15	0.00*	0.03	997.52	0.00*	----
$NDBI_{2023}$	8.54	0.03	301.63	0.00*	0.07	116.56	0.00*	5.46
$NDVI_{2023}$	-6.24	0.05	-122.96	0.00*	0.14	-43.13	0.00*	5.46

Appendix 2b: Efficiency criteria explanation for OLS and GWR

Parameters/Criteria	Explanation
Coefficient	Represents the strength and type of relationship between each explanatory variable and the dependent variable.
Probability and Robust Probability (Robust_Pr)	Asterisk (*) indicates a coefficient is statistically significant ($p < 0.01$); if the Koenker (BP) Statistic [f] is statistically significant, use the Robust Probability column (Robust_Pr) to determine coefficient significance.
Variance Inflation Factor (VIF)	Large Variance Inflation Factor (VIF) values (> 7.5) indicate redundancy among explanatory variables
R-Squared and Akaike's Information Criterion (AICc)	Measures of model fit/performance.
Joint F and Wald Statistics	Asterisk (*) indicates overall model significance ($p < 0.01$); if the Koenker (BP) Statistic [f] is statistically significant, use the Wald Statistic to determine overall model significance.
Koenker (BP) Statistic	When this test is statistically significant ($p < 0.01$), the relationships modeled are not consistent (either due to non-stationarity or heteroskedasticity). You should rely on the Robust Probabilities (Robust_Pr) to determine coefficient significance and on the Wald Statistic to determine overall model significance
Jarque-Bera Statistic	: When this test is statistically significant ($p < 0.01$) model predictions are biased (the residuals are not normally distributed)
* An asterisk next to a number	indicates a statistically significant p-value ($p < 0.01$).

Appendix 3: Transition area matrices of LULC from 1991 to 2023.

		2009		
	LULC Class	**Non-built-up (km^2)**	**Built-up (km^2)**	**Total of 1991**
	Non-built-up	168.07	13.03	**181.10**
1991	**Built-up**	1.46	**9.10**	**10.56**
	Total of 2009	**169.53**	**22.13**	**191.66**
Net change		***-11.57***	***11.57***	
Total unchanged		***177.17 (92.44%)***		

		2016		
	LULC Class	**Non-built-up (km^2)**	**Built-up (km^2)**	**Total of 2009**
	Non-built-up	**150.85**	18.68	**169.53**
2009	**Built-up**	1.83	**20.30**	**22.13**
	Total of 2016	**152.68**	**38.98**	
Net change		***-16.85***	***16.85***	
Total unchanged		***171.15 (89.30%)***		

		2023		
	LULC Class	**Non-built-up (km^2)**	**Built-up (km^2)**	**Total of 2016**
	Non-built-up	**117.10**	**35.58**	**152.68**
2016	**Built-up**	0.93	**38.05**	**38.98**
	Total of 2023	**118.03**	**73.63**	
Net change		***-34.65***	***34.65***	
Total unchanged		***155.15 (80.98%)***		

		2023		
	LULC Class	Non-built-up **(km^2)**	**Built-up (km^2)**	**Total of 1991**

	Non-built-up	**117.77**	**63.33**	**181.10**
1991	**Built-up**	0.26	**10.30**	**10.56**
	Total of 2023	**118.03**	**73.63**	
Net change		***-63.07***	***63.07***	
Total unchanged		***128.07(66.83%)***		

Appendix 5: Transition maps.